

**PHYSICAL AND MATHEMATICAL MODELING OF TOLUENE  
DIFFUSION AND BIODEGRADATION  
IN UNSATURATED SANDY SOIL**

Liannha Sa

B.S., Chemical Engineering, Chulalongkorn University, 1982

M.S., Chemical Engineering, Louisiana State University, 1986

A dissertation submitted to the faculty of the  
Oregon Graduate Institute of Science & Technology  
in partial fulfillment of the requirements for the degree  
Doctor of Philosophy  
in  
Environmental Science and Engineering

October 1994

The dissertation "Physical and Mathematical Modeling of Toluene Diffusion and Biodegradation in Unsaturated Sandy Soil" by Lianna Sa has been examined and approved by the following examination committee:

---

Richard A. Johnson, Thesis Advisor  
Associate Professor

---

David R. Boone  
Professor

---

Wesley M. Farrell  
Professor

---

Michelle M. Allen-King  
Assistant Professor  
Washington State University

## **DEDICATION**

To my father who was awarded a graduate scholarship from University of Minnesota many years ago, but had to give up due to financial difficulty.

## ACKNOWLEDGEMENTS

I wish to express my gratitude and appreciation to my advisor, Dr. Richard L. Johnson, for everything. His wit, advice, and financial support helped this project succeed. He is a great boss, and I am glad to have worked for him. I am also grateful to Dr. David R. Boone for his patience and expertise in microbiology. Appreciation is also extended to Dr. Wesley M. Jarrell and Dr. Richelle M. Allen-King for serving on my examining committee.

Many thanks go to the library staff for being the nicest personnel I have ever encountered. Their patience and enthusiasm in helping others deserve recognition. Thanks are also due to Doug Davis and his assistants in the machine shop for their technical support.

There are many colleagues and friends that have made these past years a fun learning experience for me. I am grateful to them all, in particular, Kathy McCarthy, Leah Matheson, and Patty Toccalino for their past and continuing moral support and friendship. Judi Irvine, Lorne Isabelle, Matt Perrott, Pam Locke, and Allan Ryall are thanked for their valuable advice (both technical and non-technical) and friendship.

Finally, I owe a great deal to my husband, Don Buchholz, for making my life as a graduate student endurable, for checking my mathematics, and for helping with computer problems. He also deserves credits for those good-looking Freelance plots. Above all, I am indebted to my parents who have given me a good life and taught me to be the person that I am today.

## TABLE OF CONTENTS

DEDICATION .....	iii
ACKNOWLEDGEMENTS .....	iv
TABLE OF CONTENTS .....	v
LIST OF TABLES .....	viii
LIST OF FIGURES .....	ix
ABSTRACT .....	xiii
1. INTRODUCTION .....	2
1.1 PROBLEM STATEMENT .....	2
1.2 GASOLINE RETENTION AND MIGRATION .....	3
1.3 RESEARCH OBJECTIVES .....	6
1.4 REFERENCES .....	8
2. DIFFUSION AND BIODEGRADATION OF TOLUENE IN AN UNSATURATED SANDY SOIL .....	12
2.1 INTRODUCTION .....	12
2.2 PROCESSES AFFECTING TRANSPORT AND FATE .....	14
2.2.1 Vapor-Phase Diffusion .....	14
2.2.2 Aerobic Biodegradation .....	19
2.3 EXPERIMENTAL METHODS .....	24
2.3.1 Experimental Design .....	24
2.3.2 Sampling and Analytical Procedure .....	26
2.4 RESULTS AND DISCUSSIONS .....	27
2.4.1 Column Soil Characterization .....	30

2.5 CONCLUSIONS	31
2.6 REFERENCES:	33
3. AEROBIC BIODEGRADATION KINETICS OF TOLUENE	
IN AN UNSATURATED SANDY SOIL	55
3.1 INTRODUCTION	55
3.2 THEORETICAL BACKGROUND	57
3.2.1 Growth Kinetics	58
3.2.2 Biodegradation Kinetics	60
3.2.3 Factors Affecting Biodegradation	64
3.3 EXPERIMENTAL METHODS	66
3.3.1 Experimental Design	66
3.3.2 Sampling and Analysis Procedure	67
3.3.3 Data Analysis	69
3.4 RESULTS AND DISCUSSIONS	69
3.4.1 Biodegradation Kinetics	69
3.4.2 Respike Assays	71
3.4.3 Biodegradation Stoichiometry	74
3.5 CONCLUSIONS	75
3.6 REFERENCES	77
4. NUMERICAL MODELING OF TOLUENE TRANSPORT AND	
FATE IN UNSATURATED SANDY MEDIA	99
4.1 INTRODUCTION	99
4.1.1 Literature Review	100
4.1.2 Biodegradation Kinetics Concept	104
4.2 MODEL DEVELOPMENT	106
4.2.1 Physical Bases and Mathematical Formulae	107
4.2.2 Numerical Verification	114

4.3	MODEL EVALUATIONS .....	117
4.3.1	Simulation Results .....	118
4.3.2	Sensitivity Analyses .....	120
4.4	CONCLUSIONS .....	126
4.5	REFERENCES .....	128
5.	SUMMARY AND CONCLUSIONS .....	156
5.1	OVERALL RESEARCH .....	156
5.1.1	Soil Column Experiments .....	157
5.1.2	Batch Kinetics Experiments .....	158
5.1.3	Numerical Modeling .....	159
5.2	GENERAL CONCLUSIONS .....	160
5.3	APPLICATIONS AND FUTURE STUDIES .....	161
5.4	REFERENCES .....	164
APPENDIX A.	.....	166
APPENDIX B.	.....	193
APPENDIX C.	.....	198
APPENDIX D.	.....	230
APPENDIX E.	.....	234
VITA	.....	269

## LIST OF TABLES

Table 2.1. Characteristics of unamended Columbia River soil. . . . .	41
Table 2.2. Nitrate contents measured in soil samples from column 2. . . . .	42
Table 3.1. Monod coefficients for aerobic biodegradation of toluene. . . . .	82
Table 3.2. Values of kinetic coefficients fitted to equation (3.6). . . . .	83
Table 4.1. Boundary and initial conditions and other parameter inputs used in majority of modeling. . . . .	134
Table 4.2. Physical and chemical properties of toluene at 10 and 15°C. . . . .	135
Table 4.3. Parameter ranges used for sensitivity analyses. . . . .	136

## LIST OF FIGURES

Figure 2.1.	Schematic diagram of soil columns. . . . .	43
Figure 2.2.	Process flow chart of soil column experiments. . . . .	44
Figure 2.3a.	Diagram of six-port valve used for toluene analyses. . . . .	45
Figure 2.3b.	Diagram of multi-port valve used for respiration-gas analyses. . . . .	45
Figure 2.4.	Toluene profiles in Column 1 at selected sampling times. . . . .	46
Figure 2.5.	O <sub>2</sub> profiles in Column 1 at selected sampling times. . . . .	47
Figure 2.6.	CO <sub>2</sub> profiles in Column 1 at selected sampling times. . . . .	48
Figure 2.7.	Toluene profiles in Column 2 at selected sampling times. . . . .	49
Figure 2.8.	O <sub>2</sub> profiles in Column 2 at selected sampling times. . . . .	50
Figure 2.9.	CO <sub>2</sub> profiles in Column 2 at selected sampling times. . . . .	51
Figure 2.10.	Toluene profiles in Column 3 at selected sampling times. . . . .	52
Figure 2.11.	O <sub>2</sub> profiles in Column 3 at selected sampling times. . . . .	53
Figure 2.12.	CO <sub>2</sub> profiles in Column 3 at selected sampling times. . . . .	54
Figure 3.1.	Typical growth curve for a microbial population. . . . .	84
Figure 3.2a.	Relationship between substrate concentration, growth rate, and total growth. . . . .	85
Figure 3.2b.	Effect of substrate concentration on growth rate. . . . .	85
Figure 3.3.	Disappearance curves for chemicals that are mineralized by different kinetics. . . . .	86

Figure 3.4.	Diagram of canisters used for batch experiments. . . . .	87
Figure 3.5a.	Diagram of eight-port valve used for toluene analyses. . . . .	88
Figure 3.5b.	Diagram of fourteen-port valve used for respiration-gas analyses. . . . .	88
Figure 3.6.	Toluene disappearance curves at low initial concentrations (Batch Experiment #6). . . . .	89
Figure 3.7.	Toluene degradation resembles logarithmic-growth kinetics (Batch Experiment #6). . . . .	90
Figure 3.8.	Toluene disappearance curves at different initial concentrations (Batch Experiment #5). . . . .	91
Figure 3.9.	Curves fit to toluene degradation data from individual canisters. Symbols are experimental data. . . . .	92
Figure 3.10.	Toluene disappearance curves at higher initial concentrations (Batch Experiment #4). . . . .	93
Figure 3.11.	Absence of detectable sorption or degradation of toluene in controls. . . . .	94
Figure 3.12.	Effect of N concentration on toluene biodegradation. Soil depicted by filled symbols contained ~4 times as much N as soil with open symbols. . . . .	95
Figure 3.13a.	Canisters receiving low initial doses of toluene (a) exhibited faster degradation rates when more toluene was added (b). The rates eventually decreased (c) unless more N was added (d). . . . .	96
Figure 3.13b.	Effects of additional toluene (b) and bioavailable N (c) on biodegradation in canisters with high initial doses of toluene (a). . . . .	96
Figure 3.14.	Absence of toluene inhibition over the concentration range investigated. . . . .	97
Figure 3.15.	Extrapolation of toluene data (Batch Experiment #6) to time zero for an estimation of the initial population. Larger uncertainty in measurements of these data can be seen at early times. . . . .	98
Figure 4.1.	Flow chart of numerical scheme. . . . .	136

Figure 4.2.	Diffusion profiles of toluene over time. Solid lines depict analytical solutions. Open ( $\alpha=1$ ) and closed ( $\alpha=0.5$ ) symbols depict model results using $\Delta z = 5$ cm and $\Delta t = 0.5$ hour. . . . .	137
Figure 4.3.	Decrease in numerical error with time for diffusion solutions at different $\alpha$ (time-weighting schemes). $\Delta z = 5$ cm and $\Delta t = 5$ hour. . . . .	138
Figure 4.4.	Rates of convergence with respect to $1/\Delta z$ ( $\Delta z = 5$ cm and $\Delta t = 0.5$ hour). . . . .	139
Figure 4.5.	Rates of convergence with respect to $1/\Delta t$ ( $\Delta z = 5$ cm and $\Delta t = 0.5$ hour). Simulation time = 21 days. . . . .	140
Figure 4.6.	Biodegradation of toluene (model and analytical solutions). . . . .	141
Figure 4.7.	Model simulations (solid lines) of toluene migration in Column 1. Symbols are data; dashed lines are diffusion profiles generated by model. . . . .	142
Figure 4.8.	Model simulations (solid lines) of toluene migration in Column 2. Symbols are experimental data. . . . .	143
Figure 4.9.	Simulated (a) and measured (b) $\text{CO}_2$ profiles in Column 2 as a function of time. . . . .	144
Figure 4.10.	Model simulations of cell concentrations in Column 2 over time. . . . .	145
Figure 4.11.	Effects of $\mu_{\max}$ on toluene concentration profiles in Column 1 (model sensitivity analyses). . . . .	146
Figure 4.12.	Effects of $\mu_{\max}$ on toluene concentration profiles in Column 2 (model sensitivity analyses). . . . .	147
Figure 4.13.	Effects of $X_0$ on toluene concentration profiles in Column 1 (model sensitivity analyses). . . . .	148
Figure 4.14.	Effects of $X_0$ on toluene concentration profiles in Column 2 (model sensitivity analyses). . . . .	149
Figure 4.15.	Effects of $X_N$ on toluene concentration profiles in Column 1 (model sensitivity analyses). . . . .	150

Figure 4.16. Effect of $X_N$ on toluene concentration profiles in Column 2 (model sensitivity analyses). . . . .	151
Figure 4.17. Effects of $K_{oc}$ on toluene concentration profiles in Column 2 (model sensitivity analyses). . . . .	152
Figure 4.18. Effects of $K_{oc}$ on toluene diffusion profiles in Column 2 (model sensitivity analyses). . . . .	153
Figure 4.19. Model simulations of toluene, $O_2$ , and X profiles in Column 2 at ~75% water saturation. Simulation time = 300 days. . . . .	154
Figure 4.20. Model simulations of toluene, $O_2$ , and X profiles in Column 2 at 50% water saturation. Simulation time = 300 days. . . . .	155

**ABSTRACT**

**PHYSICAL AND MATHEMATICAL MODELING OF TOLUENE  
DIFFUSION AND BIODEGRADATION  
IN UNSATURATED SANDY SOIL**

Liannha Sa

Oregon Graduate Institute of Science & Technology, 1994

Supervising Professor: Richard L. Johnson

The unsaturated zone provides a natural remediation pathway for subsurface hydrocarbon contamination. Vapor-phase diffusion and biodegradation are important processes affecting transport in the unsaturated zone, and their effects on toluene migration in sandy soil are examined here. This research was conducted by using a combination of column diffusion experiments, batch biodegradation experiments, and numerical modeling.

The diffusion experiments were conducted in 0.1-m diameter by 1.6-m long stainless-steel cylinders filled with sandy soil at uniform residual water content. Toluene vapor from a constant-concentration source diffused across the column at the same time as O<sub>2</sub> diffused from the opposite direction. Concentrations of these constituents and CO<sub>2</sub> in soil air were periodically monitored within the column. Three column experiments were conducted at two different source concentrations.

The batch biodegradation experiments were conducted in 0.8-L stainless-steel canisters with 55 g of sand under similar conditions to those in the column experiments. Toluene disappearance was monitored with time over a range of initial concentrations.

These batch experiments provided information on rate kinetics and factors limiting the extent of biodegradation. Degradation patterns reflecting a logarithmic growth of toluene degraders were observed. Kinetic coefficients were determined by nonlinear regression.

A one-dimensional multi-phase transport model which incorporated diffusion, biodegradation, linear sorption, and air-water partitioning was developed. The model is capable of describing toluene movement in the column experiments using input parameters derived from batch experiments and the literature. The numerical model confirmed that biodegradation in the column experiments was most sensitive to nitrogen bioavailability.

Results from this research are: 1) in an unsaturated sandy soil environment near an immiscible contaminant source, vapor diffusion is significant and biodegradation is often inhibited; 2) when conditions for microbial growth are unlimited, microbial parameters such as the initial population and the maximum growth rate control the transport; and 3) nutrient bioavailability may often limit microbial removal of volatile aromatic hydrocarbons.

# CHAPTER 1

## INTRODUCTION

### 1.1 PROBLEM STATEMENT

The release of gasoline and other petroleum products near land surface has led to widespread contamination of soil and groundwater. When a lighter-than-water nonaqueous-phase liquid (LNAPL) such as gasoline enters the subsurface, it migrates downward through the unsaturated zone under the influence of gravity. Depending on the geological setting of the site and the volume of the spill, a pool of gasoline may form in the vicinity of the water table. When the bulk movement of gasoline has stopped, subsequent contaminant migration may occur via solute transport in the groundwater. An alternate route of contaminant migration may occur via vapor-phase transport. Vapor transport is generally an important process for gasoline compounds in the unsaturated zone. Contaminant vapors may migrate into the atmosphere as well as to groundwater (Baehr, 1987). For instance, in a location where the aquifer is very deep and receives small amount of rainfall, volatilization and subsequent diffusion of the LNAPL in the unsaturated zone may be the key means by which the groundwater becomes contaminated (Falta et al., 1989).

Gasoline is a complex mixture of several hundred refined petroleum hydrocarbons. Of all constituents, the monoaromatic hydrocarbons are generally of greatest environmental concern due to their significant proportion, aqueous solubilities, and toxicity. Benzene, toluene, ethylbenzene and xylenes (BTEX) are commonly found at fuel spill sites and their presence at low concentrations in groundwater makes it unsuitable as a drinking water supply. The current U.S. drinking-water standard for benzene is 5  $\mu\text{g/L}$  (Fetter, 1993), and typical concentrations of benzene at gasoline spill

sites range from 1 to 10 mg/L (Barker and Mayfield, 1988). Fortunately, dissolved BTEX may undergo complete transformation to nontoxic substances when environmental conditions are appropriate for microbial degradation.

Subsurface biodegradation has been increasingly the subject of research because it has great potential for *in situ* remediation (Lee and Swindoll, 1993; Hincbee et al., 1991; Lee et al., 1988; Lee and Ward, 1985). Most biodegradation studies have focused on the saturated zone. In many of these cases, degradation has been limited by oxygen (O<sub>2</sub>) supply (Chiang et al., 1989; Jamison et al., 1975). In the unsaturated zone, the rate of O<sub>2</sub> diffusion is less likely to limit biodegradation (Hult, 1987). This is particularly true for shallow sandy or gravelly aquifers, where the impact of gasoline spill is likely to be most serious as well.

The saturated zone has been studied more extensively than the overlying unsaturated zone since it is typically the greatest source of human exposure. However, the significance of the unsaturated zone should not be ignored, for it is the region through which liquid and gaseous species are exchanged between the soil surface and water table. In addition, the unsaturated zone may provide a natural remedial pathway for contaminants of volatile or gaseous compounds. Hult (1987) reported almost complete removal of nearly all the volatile hydrocarbons from a shallow aquifer before reaching land surface owing to microbial degradation in the unsaturated zone. Furthermore, the extent of hydrocarbon removal by microbially induced reactions in soil water or groundwater may in part depend on the diffusivity of O<sub>2</sub> in the unsaturated zone. The research presented here examines the importance of transport and degradation in the unsaturated zone and provides a quantitative understanding of how physical, chemical, and biological processes interact in a shallow sandy soil.

## 1.2 GASOLINE RETENTION AND MIGRATION

Gasoline infiltrates downward in the unsaturated zone as a separate nonaqueous phase under the influence of gravity. As long as there is a sufficient volume of LNAPL,

the spill will tend to spread downward with some degree of lateral spreading due to capillary effects and the spatial variability of the soil. As the LNAPL migrates, a fraction of its volume becomes trapped within pore spaces by capillary forces. In the unsaturated zone, the immobilized gasoline exists as a discontinuous phase in the forms of pendular rings and small blobs (Wilson and Conrad, 1984). The entrapped volume of the discontinuous LNAPL per unit volume of pore space is called the residual saturation. The residual saturation of gasoline in the unsaturated medium is controlled by the characteristics of the soil, the viscosity of gasoline, and the soil moisture content. Residual saturation measurements involving various LNAPLs and media typically range from .10-.20 in the unsaturated zone (Mercer and Cohen, 1990). If the volume of gasoline spilled is small, the spill will be contained in the unsaturated zone in a state of residual saturation. [The ability of the vadose zone to trap LNAPL is sometimes measured and reported as the volumetric retention capacity, of which the unit is liters of residual LNAPL per cubic meter of medium (Mercer and Cohen, 1990; Wilson and Conrad, 1984)]. If the volume of the spill is sufficiently large, the petroleum product will reach the capillary zone and spread laterally along the capillary fringe. As in the unsaturated zone, LNAPL within the saturated zone will also become immobilized as blobs by capillary forces. Values of residual saturation in saturated media typically range from .15-.50 (Mercer and Cohen, 1990; Wilson et al., 1988). In many places, water table fluctuations occur seasonally or due to pumping. As the water table rises and falls, free-phase gasoline is redistributed ("smearing"), causing a broader area contaminated by residual hydrocarbon. Detailed descriptions of nonaqueous-phase migration in porous media can be found elsewhere (Mercer and Cohen, 1990; Abdul, 1988; Hoag and Marley, 1986; Schwille, 1984).

Common physical remedial actions (e.g., product skimming, soil excavation, etc.) are unable to remove all the residual LNAPL. The residual gasoline will remain trapped in the subsurface for an indefinite time period, allowing further contamination via several routes. Soluble components in the residual gasoline trapped below the water table will dissolve into the groundwater forming a solute plume. As the water table drops, the

residual LNAPL below the water table becomes exposed to air. Volatile components will vaporize and diffuse into the overlying unsaturated region. These hydrocarbon vapors may partition into the unsaturated medium or be scavenged by infiltrating rainwater before they finally reach the ground surface. Moreover, the residual gasoline in the upper vadose zone is susceptible to leaching by infiltrating rainwater as well as to volatilization and subsequent emission into the atmosphere. Consequently, the residual LNAPL will serve as a continual source to contamination of groundwater and soil vapor.

In addition to above physical processes, sorption and biodegradation may also be important mechanisms influencing the transport and fate of gasoline compounds in the unsaturated zone. Sorption of extremely hydrophobic compounds to organic phase of soil particles can severely restrict the migration of contaminants. BTEX, however, are moderately hydrophobic and usually only mildly retarded by porous media. The extent to which BTEX partition between the bulk gasoline, soil organic matter, pore water, and soil air is determined by their physicochemical properties and the subsurface environment. All processes mentioned above affect the mobility of pollutant compounds released into the environment to different extent.

Biodegradation of gasoline hydrocarbons has been demonstrated to occur naturally at contaminated sites in groundwater (Borden et al., 1994; Armstrong et al., 1991; Chiang et al., 1989; Baedecker et al., 1987; Wilson et al., 1986), in unsaturated zone (Caldwell et al., 1992; Ostendorf and Kampbell, 1991; Hult and Grabbe, 1985) and in surface soil, i.e., landfarming experiments (Reynolds et al., 1994; Raymond et al., 1976). In the saturated zone, the availability of dissolved  $O_2$  is often found to be the limiting factor controlling the extent of biodegradation (Chiang et al., 1989; Barker et al., 1987; Wilson et al., 1986; Jamison et al., 1975). Most contaminant plumes develop anoxic conditions rapidly as a result of an excessive  $O_2$  demand by aerobes and the low availability of  $O_2$  in the aquifer. Biotransformation in the absence of  $O_2$  may proceed at a much slower rate, resulting in contaminant persistence and further plume migration. In contrast, gaseous  $O_2$  transport in the unsaturated zone may be fast with respect to  $O_2$  demands by microbes in soil water. As a result, aerobic conditions often exist in the unsaturated zone

(O'Leary et al., 1993; Caldwell et al., 1992; Ostendorf and Kampbell, 1991; Hult and Grabbe, 1985). Therefore, the biodegradation potential in the unsaturated media may be significant because O<sub>2</sub> is usually not limiting.

It can be deduced from the preceding discussion that the subsurface migration of contaminants is governed by complex interactions of many environmental and biological parameters. Much effort has already been devoted to investigating the transport and fate of gasoline in the subsurface. However, the variability of subsurface properties (e.g., permeability, organic carbon content, pH, etc.) and their effects on the interaction of various physical, chemical, and biological processes give rise to extremely complex problems. In order to quantify the movement of organic contaminants in subsurface, it is important to determine the relative importance of these processes and their interacting effects upon the transport and fate of the compounds. Only a few studies in the past involved quantification of the interacting effect of both abiotic and biotic processes upon transport and fate in the unsaturated zone. In addition, many past investigations have been "site-specific", and therefore information obtained is limited to that particular case study. As a result, there is a need for continued research to acquire better understanding and quantification of the contaminant transport and fate, so that better risk estimates, site characterization, and remediation plans can be made.

### **1.3 RESEARCH OBJECTIVES**

The objective of this research was to examine and to identify key processes in controlling the transport and fate of hydrocarbon compounds in an unsaturated medium. Since *in situ* biodegradation is a potentially important means of attenuating pollutants in the subsurface, factors affecting biodegradation were emphasized in this study. Since vapor-phase diffusion is often the dominant transport mechanism in the unsaturated medium, the relative importance of biodegradation and diffusion of a monoaromatic hydrocarbon and their effects upon the contaminant migration were investigated. Due to variability of field conditions, the studies were conducted in well-controlled laboratory

columns. The column models were constructed to represent contaminant transport within an unsaturated medium bounded at the bottom by a residual source of gasoline and at the top by the land surface. Precipitation was not considered here.

Due to their mobility and potential to contaminate groundwater, the BTEX compounds are the focus of this research. Toluene was chosen to be representative of BTEX compounds for three reasons. First, as a component in many types of petroleum fuel, toluene was commonly found in soil and groundwater at sites contaminated by petroleum fuels (Aelion and Bradley, 1991; Chiang et al., 1989; Downey, et al., 1988; Wilson et al., 1986). Trace levels of toluene were also found in groundwater impacted by landfill leachate (Armstrong et al., 1991; Barker et al., 1986; Reinhard et al., 1984; Khare and Dondero, 1977). Second, toluene is considered to be a serious threat to the groundwater quality due to a low drinking-water standard (1 mg/L) (Fetter, 1993) and a relatively high aqueous solubility (~500 mg/L at 25°C, MacKay et al., 1992). Third, its physical and chemical properties are well documented. Sandy soil was used because it permits rapid diffusion of toluene and O<sub>2</sub>. In addition, it often has low contents of organic carbon and inorganic nutrients, allowing minimal effects of sorption and biodegradation. Hence, the experimental conditions represent a "worst case" scenario of petroleum contamination.

An integrated approach of physical experiments and numerical modeling was used to provide a comprehensive study of toluene migration through the unsaturated soil. The overall study has three principal components:

#### *Sand column experiments.*

The study of toluene vapor-phase transport was performed in large-scale columns packed with Columbia River sand at a uniform residual water content. Three column experiments were carried out at two distinctly different source concentrations. Biodegradation was observed by monitoring the levels of toluene, O<sub>2</sub>, and carbon dioxide with time. These experiments are discussed in Chapter 2.

*Biodegradation batch experiments.*

Data from column experiments suggested that biodegradation was significant and that the kinetics were not first order. As a result, a series of batch experiments was conducted to examine biodegradation kinetics under the same conditions as those in the column experiments. Toluene removal rates were monitored over a range of initial concentrations. These experiments are discussed in Chapter 3.

*Numerical modelling.*

A one-dimensional mathematical model was developed and solved numerically by the finite-element method. The model was used as a tool to investigate the effects of various processes on volatile hydrocarbon transport and fate in unsaturated soil. Processes of importance include air- and aqueous-phase diffusion, linear sorption, and aerobic biodegradation/microbial growth. Several factors affecting biodegradation rate were also accounted for. Simulations of column experiments were conducted by using model variables obtained from literature and batch experiments. Model simulation results were compared to column experimental data. Sensitivity analyses were also performed. The development and the performance of the model is discussed in Chapter 4.

## 1.4 REFERENCES

- Abdul, A. S., Migration of petroleum products through sandy hydrogeologic systems, in *Proceedings of the Second National Outdoor Action Conference on Aquifer Restoration Groundwater Monitoring and Geophysical Methods*, National Water Well Association, Dublin, Ohio, pp. 1533-1550, 1988.
- Aelion, C. M., and P. M. Bradley, Aerobic biodegradation potential of subsurface microorganisms from a jet fuel-contaminated aquifer, *Appl. Environ. Microbiol.*, *57*, 57-63, 1991.
- Armstrong, A. Q., R. E. Hodson, H. M. Hwang, and D. L. Lewis, Environmental factors affecting toluene degradation in ground water at a hazardous waste site, *Environ. Toxicol. Chem.*, *10*, 147-158, 1991.
- Baedecker, M. J., I. M. Cozzarelli, and J. A. Hopple, The composition and fate of hydrocarbons in a shallow glacial-outwash aquifer, in U.S. Geological Survey Program on Toxic Waste--Ground-Water Contamination, edited by B. J. Franks, Proceedings of the Third Technical Meeting, Pensacola, Florida, March 23-27, 1987, *U.S. Geol. Surv. Open File Rep. 87-109*, pp. C23-C24, 1987.
- Baehr, A. L., Selective transport of hydrocarbons in the unsaturated zone due to aqueous and vapor phase partitioning, *Water Resour. Res.*, *23*, 1926-1938, 1987.
- Barker, J. F., G. C. Patrick, and D. Major, Natural attenuation of aromatic hydrocarbons in a shallow sand aquifer, *Ground Water Monitoring Review*, *7*, 64-71, 1987.
- Barker, J. F., and C. I. Mayfield, The persistence of aromatic hydrocarbons in various ground water environments, in *Proceedings of the Conference on Petroleum Hydrocarbons and Organic Chemicals in Groundwater: Prevention, Detection, and Restoration*, National Water Well Association, Dublin, Ohio, pp. 649-667, 1988.
- Barker, J. F., J. S. Tessman, P. E. Plotz, and M. Reinhard, The organic geochemistry of a sanitary landfill leachate plume, *J. Contam. Hydrol.*, *1*, 171-189, 1986.
- Borden, R. C., C. A. Gomez, and M. T. Becker, Natural bioremediation of a gasoline spill, in *Hydrocarbon Bioremediation*, edited by Hinchee, R. E., B. C., Alleman, R. E. Hoepfel, R. N. Miller, Lewis Publishers, Ann Arbor, pp. 290-295, 1994.
- Caldwell, K. R., D. L. Tarbox, K. D. Barr, S. Fiorenza, L. E. Dunlap, and S. B. Thomas, Assessment of natural bioremediation as an alternative to traditional active remediation at selected Amoco oil company sites, florida, in *Proceedings of the Conference on*

*Petroleum Hydrocarbons and Organic Chemicals in Ground Water: Prevention, Detection, and Restoration*, Ground Water Management, Dublin, Ohio, pp. 509-525, 1992.

Chiang, C. Y., J. P. Salanitro., E. Y. Chai, J. D. Colthart, and C. L. Klein, Aerobic biodegradation of benzene, toluene, and xylene in a sandy aquifer - Data analysis and computer modeling, *Ground Water*, 27, 823-834, 1989.

Downey, D. C., R. E. Hinchee, M. S. Westray, and J. K. Slaughter, Combined biological and physical treatment of a jet fuel-contaminated aquifer, in *Proceedings of the Conference on Petroleum Hydrocarbons and Organic Chemicals in Ground Water: Prevention, Detection, and Restoration*, National Water Well Association, Dublin, Ohio, pp. 627-645, 1988.

Falta, R. W., I. Javandel, K. Pruess, and P. A. Witherspoon, Density-driven flow of gas in the unsaturated zone due to the evaporation of volatile organic compounds, *Water Resour. Res.*, 25, 2159-2169, 1989.

Fetter, C. W., *Contaminant Hydrogeology*, Macmillan Publishing Company, New York, 1993.

Hinchee, R. E., D. C. Downey, R. R. Dupont, P. Aggarwal, R. E. Miller, Enhancing biodegradation of petroleum hydrocarbons through soil venting, *J. Hazardous Mater.*, 28, 3-11, 1991

Hoag, G. E., and M. C. Marley, Gasoline residual saturation in unsaturated uniform aquifer materials, *J. Environ. Eng.*, 112, 586-604, 1986.

Hult, M. F., Microbial oxidation of petroleum vapors in the unsaturated zone, in U.S. Geological Survey Program on Toxic Waste--Ground-Water Contamination, edited by B. J. Franks, Proceedings of the Third Technical Meeting, Pensacola, Florida, March 23-27, 1987, *U.S. Geol. Surv. Open File Rep.*, 87-109, pp. C25-C26, 1987.

Hult, M. F., and R. R. Grabbe, Permanent gases and hydrocarbon vapors in the unsaturated zone, in U.S. Geological Survey Program on Toxic Waste--Ground-Water Contamination, edited by S. E. Ragone, Proceedings of the Second Technical Meeting, Cape Cod, Massachusetts, Oct. 21-25, 1985, *U.S. Geol. Surv. Open File Rep.*, 86-481, pp. C21-C25, 1986.

Jamison, V. M., R. L. Raymond, and J. O. Hudson, Jr., Biodegradation of high-octane gasoline in groundwater, *Dev. Ind. Microbiol.*, 16, 305-312, 1975.

Khare, M., and N. C. Dondero, Fractionation and concentration from water of volatiles and organics on high vacuum system: Examination of sanitary landfill leachate, *Environ. Sci. Technol.*, 11, 814-819, 1977.

Lee, M. D., and C. M. Swindoll, Bioventing for *in situ* remediation, *Hydrological Sciences J.*, 38, 273-282, 1993.

Lee, M. D., J. M. Thomas, R. C. Borden, P. B. Bedient, C. H. Ward, J. T. Wilson, Bioremediation of aquifers contaminated with organic compounds, *CRC Crit. Rev. Environ. Control*, 18, 29-89, 1988.

Lee, M. D., and C. H. Ward, Biological methods for the restoration of contaminated aquifers, *Environ. Toxicol. Chem.*, 4, 743-750, 1985.

Mackay, D. M., W. Y. Shiu, K. C. Ma, *Illustrated Handbook of Physical-Chemical Properties and Environmental Fate for Organic Chemicals*, Vol. I, II, III, Lewis Publishers, Ann Arbor, 1992.

Mercer, J. W., and R. M. Cohen, A review of immiscible fluids in the subsurface: Properties, models, characterization and remediation, *J. Contam. Hydrol.*, 6, 107-163, 1990.

O'Leary, K. E., J. F. Barker, R. W. Gillham, Surface application, of dissolved BTEX: A prototype field experiment, in *Proceedings of the Conference on Petroleum Hydrocarbons and Organic Chemicals in Ground Water: Prevention, Detection, and Restoration*, Ground Water Management, Dublin, Ohio, pp. 149-160, 1993.

Ostendorf, D. W., and D. H. Kampbell, Biodegradation of hydrocarbon vapors in the unsaturated zone, *Water Resour. Res.*, 27, 453-462, 1991.

Raymond, R. L., J. O. Hudson, and V. W. Jamison, Oil degradation in soil, *Appl. Environ. Microbiol.*, 31, 522-535, 1976.

Reinhard, M., N. L. Goodman, and J. F. Barker, Occurrence and distribution of hazardous organic chemicals in the leachate plumes of two sanitary landfills, *Environ. Sci. Technol.*, 18, 953-961, 1984.

Reynolds, C. M., M. D. Travis, W. A. Braley, and R. J. Scholze, Applying field-experiment bioreactors and landfarming in alaska climates, in *Hydrocarbon Bioremediation*, edited by Hinchee, R. E., B. C., Alleman, R. E. Hoeppel, R. N. Miller, Lewis Publishers, Ann Arbor, pp. 100-106, 1994.

Schwille, F., Migration of organic fluids immiscible with water in the unsaturated zone, in *Pollutants in Porous Media*, edited by Yaron B., G. Dagan, and J. Goldshmid, Springer-Verlag, New York, pp. 27-45, 1984.

Wilson, B. H., B. E. Bledsoe, D. H. Kampbell, J. T. Wilson, J. M. Armstrong, J. H. Sammons, Biological fate of hydrocarbons at an aviation gasoline spill site, in *Proceedings of the NWWA/API Conference on Petroleum Hydrocarbons and Organic Chemicals in Ground Water: Prevention, Detection, and Restoration*, National Water Well Association, Dublin, Ohio, pp. 78-90, 1986.

Wilson, J. L., and S. H. Conrad, Is physical displacement of residual hydrocarbons a realistic possibility in aquifer restoration?, in *Proceedings of the NWWA/API Conference on Petroleum Hydrocarbons and Organic Chemicals in Ground Water*, National Water Well Association, Worthington, Ohio, pp. 274-298, 1984.

Wilson, J. L., S. H. Conrad, E. Hagan, W. R. Mason, and W. Peplinski, The pore level spatial distribution and saturation of organic liquids in porous media, in *Proceedings of the Conference on Petroleum Hydrocarbons and Organic Chemicals in Ground Water: Prevention, Detection, and Restoration*, National Water Well Association, Dublin, Ohio, pp. 107-133, 1988.

## **CHAPTER 2**

### **DIFFUSION AND BIODEGRADATION OF TOLUENE IN AN UNSATURATED SANDY SOIL**

#### **2.1 INTRODUCTION**

Vapor-phase diffusion is often considered to be the main transport mechanism within the unsaturated subsurface (Ostendorf and Kampbell, 1991; Bruell and Hoag, 1986; Abriola and Pinder, 1985). For instance, in a location where the aquifer is very deep and receives small amount of rainfall, volatilization and subsequent diffusion of the residual LNAPL in the unsaturated zone may be the key means by which the groundwater becomes contaminated (Falta et al., 1989). Additionally, vapor-phase advection may be significant due to barometric pressure changes or vapor-density gradients. However, Buckingham (1904) showed that the effects of barometric fluctuations are small, and vapor-phase advection is small unless there is deep infiltration or rapidly fluctuating water table (Kreamer et al., 1988). In coarse soils, density driven flow can be important. Falta et al. (1989) performed simulation analyses to illustrate the effect of density-driven flow on gas phase transport of toluene in a simple hypothetical field situation. Simulation results showed that the effect of density gradient upon toluene diffusion under high gas-phase permeability is insignificant. Therefore, vapor-phase diffusion is expected to be the dominant transport process for gasoline hydrocarbons in a highly permeable, shallow unsaturated zone. Retardation of vapor-phase transport may occur by the processes of aqueous-phase partitioning and sorption. Volatile aromatics may partition between the different phases of the unsaturated soil: soil organic matter, pore water, and pore air.

Biodegradation has been shown to be an important mechanism for the attenuation of hydrocarbons in the subsurface. Biodegradation of hydrocarbon vapors in the unsaturated zone above a sandy aquifer can minimize the escape of contaminants to the atmosphere (Ostendorf and Kampbell, 1991; Chiang et al., 1989; Hult, 1987). Hult and Grabbe (1985) reported that the vertical profile of hydrocarbon concentrations in the unsaturated zone varied more than 10,000 fold within 15 feet due to the effect of biodegradation. Similar findings were also observed by other investigators (Diem and Ross, 1988; Evans and Thomson, 1986). Like diffusion, biodegradation is likely to be important in the unsaturated zone of a highly permeable shallow aquifer, where sufficient O<sub>2</sub> supply often exists.

The relative importance of each of the above processes depends upon the properties of the contaminant and the soil as well as other environmental conditions. In order to quantify the subsurface movement of hydrocarbon pollutants, it is important to determine the relative importance and the interaction of these physical, chemical, and biological processes. Relatively little information exists in the literature on quantitative evaluations of the degree to which these coupled processes influence the transport. Therefore, the goal of this study was to investigate the influence of various processes upon transport and fate of a volatile hydrocarbon in a highly permeable unsaturated soil using a comprehensive approach of physical experiments and numerical modeling.

The physical experiments conducted here were designed to simulate vapor-phase transport of toluene from a continuous source above the water table through a sandy soil. Toluene was chosen to represent the class of single-ring aromatic hydrocarbons which are generally considered to pose the greatest threat to groundwater. Significant levels of toluene are commonly found in soils and groundwater at sites contaminated by petroleum-fuel spills (Borden et al., 1994; Downey, et al., 1988; Hult, 1987). Toluene is also present at low levels in groundwater impacted by landfill leachate (Armstrong et al., 1991; Wilson et al., 1986; Reinhard et al., 1984) and at river infiltration sites (Schwarzenbach et al., 1983). Because vapor-phase diffusion is relatively rapid, a 1.6-m long column was used. To simplify interpretation of the experiments, a homogeneous

sandy soil was chosen and soil columns were operated under isothermal conditions. The temperature was controlled by setting the entire experiment unit in a constant temperature cold room. Soil moisture was controlled to produce a uniform residual water content. As a result, there was no liquid water movement. The experimental methods and results will be described in greater detail in subsequent sections.

## 2.2 PROCESSES AFFECTING TRANSPORT AND FATE

### 2.2.1 Vapor-Phase Diffusion

Vapor-phase diffusion in porous media has been studied for nearly a century. Bruell (1987) and Sallam et al. (1984) provide reviews of these studies. Diffusion in soil is usually described by Fick's first law:

$$J_k = -D_k \nabla G_k \quad (2.1)$$

where  $k$  is compound index;  $J$  is the vapor flux through the soil;  $D_k$  is the apparent diffusion coefficient in soil gas; and  $\nabla G$  is the vapor concentration gradient. The apparent diffusion coefficient is used to account for impedance arising from the reduction in the open fraction of a porous medium, and the increased diffusion length of tortuous soil pores. Buckingham (1904) proposed a relation of the following form for the apparent diffusion coefficient:

$$D_k = \theta_a \tau d_k \quad (2.2)$$

where  $\theta_a$  is the air-filled porosity;  $\tau$  is the tortuosity factor; and  $d_k$  is the diffusion coefficient in the free fluid phase. Air-filled porosity is a soil parameter determined by subtracting volumetric water content from the total soil porosity. The tortuosity factor is generally derived by fitting experimental data to equation (2.2). These parameters are interrelated to other soil characteristics such as bulk density, the water saturation level, pore size distribution, pore geometry, and pore continuity. A number of empirical

equations for tortuosity factors have been developed from laboratory data using easily determined parameters such as total and air-filled porosities. However, these equations are usually intended to work over finite ranges of water content. To avoid the limitation of using experimentally derived relations, some investigators have proposed tortuosity equations based on theoretical models of soil pores and their geometry (Nielson et al., 1984; Marshall, 1959; Millington, 1959). Among these, the model of Millington (1959) has been implemented most successfully (McCarthy and Johnson, 1994; Karimi et al., 1987; Bruell and Hoag, 1986; Sallam et al., 1984; Farmer et al., 1980; Shearer et al. 1973). Weeks et al. (1982) list a number of formulae that relate the tortuosity factor to total porosity and air-filled porosity.

There is a large body of information in the literature on diffusion of compounds which normally are gaseous at ambient conditions or exhibit very low vapor pressures (e.g., pesticides). Studies also have been reported on the influence of soil characteristics upon vapor-phase transport of low molecular-weight hydrocarbon compounds (Karimi et al., 1987; Bruell and Hoag, 1986). Bruell and Hoag (1986) investigated a variety of physical and chemical factors affecting the diffusion of gasoline hydrocarbons within porous media. Vapor diffusion of benzene, toluene, hexane, and isooctane were measured in dry soil columns. Benzene was also measured under various moist soil conditions. Experimental data of both dry and wet soils were best described by the equation of Millington (1959). They concluded that soil tortuosity was a result of the physical characteristics of the soil such as air-filled porosity but independent of soil temperature and hydrocarbon component type. Furthermore, they found that vapor diffusion is a significant process in the movement of gasoline hydrocarbons within unsaturated soil. Karimi et al. (1987) evaluated soil properties, such as bulk density and soil-water content, for their influence on the steady-state vapor diffusion of benzene in a soil cover under isothermal conditions. The diffusive flux of benzene in soil was greatly reduced by increased soil bulk density and increased soil-water content. Farmer et al. (1980) observed similar effects of soil bulk density and soil-water content on hexachlorobenzene volatilization. Increasing soil bulk density decreased the total soil

porosity whereas increasing soil-water content decreased the pore space available for vapor diffusion. Since the effects of soil bulk density and soil-water content can be attributed to the effect on the air-filled porosity, they concluded that air-filled porosity is the major soil parameter controlling diffusion through soil.

Under steady-state diffusion conditions, the presence of water in soil results in not only physically blocking of the pores, but also modification of the pore geometry and the length of gas passage (Currie, 1960). Sallam et al. (1984) compared the applicability of several tortuosity models to a wide range of saturation levels. Good agreement among the models was found at air-filled porosities above 0.30. At higher saturation levels, Sallam et al. (1984) measured gas diffusion coefficients of an inert gas in Yolo silt loam with air-filled porosities ranging from 0.05 to 0.15, and found the equation of Millington (1959) was far superior to the others. The same equation was fairly well applied to both air- and liquid-phase diffusion of trichloroethylene in varying water-content sand columns (McCarthy and Johnson, 1994). Other factors that could affect vapor-phase transport are heterogeneities of the medium and ground-surface conditions (Tanner, 1964), but they are beyond the scope of this study.

The partitioning of hydrocarbon vapors to the aqueous phase reduces their gas-phase diffusion coefficients in porous media. The extent to which partitioning occurs is determined by the relative values of the compound solubility and vapor pressure. Compounds with high solubilities tend to present in pore water whereas those of high vapor pressures tend to be in the gas phase. There are several ways of expressing aqueous-phase partitioning at equilibrium. For dilute aqueous-phase solutions, the water-air partition coefficient can be described by a reciprocal of Henry's constant:

$$H_k \equiv \frac{C_k}{p_k} = \frac{1}{h_k} \quad (2.3)$$

where  $H_k$  is the water-air partition coefficient;  $C_k$  and  $p_k$  are the aqueous concentration and the partial pressure, respectively; and  $h_k$  is the Henry's constant at system temperature. Values of Henry's constant have been tabulated for a wide range of compounds, including all of the EPA priority pollutants (Mackay et al., 1992;

Verschueren, 1983; Mabey et al., 1982). Studies have shown that this relationship is valid at saturation concentrations for many substances (Spencer and Cliath, 1970). Consequently, partitioning constants can also be estimated from vapor pressure and solubility data (Mackay and Paterson, 1981).

The relative importance of vapor- and aqueous-phase diffusion is determined by the magnitudes of the compound concentrations in the air and solution phases (Letey and Farmer, 1974; Goring, 1962). Chemicals with  $H_k$  less than  $10^4$  diffuse mainly in the vapor phase, and those with  $H_k$  greater than  $10^4$  diffuse primarily in the solution phase. For example, benzene would be expected to diffuse primarily in the vapor phase. This was experimentally confirmed by Karimi et al. (1987).

Several researchers studied the influence of water/air partitioning on vapor-phase diffusion of gasoline hydrocarbons in soils (Baehr, 1987; Bruell, 1987; Karimi et al., 1987; Robbins, 1987). These studies indicate that aqueous-phase partitioning results in a decrease in the apparent vapor-phase diffusion of BTEX in soil. Robbins (1987) found that the diffusion coefficients of BTEX decreased nonlinearly with increasing moisture content. Baehr (1987) performed a numerical simulation of vapor-phase diffusion of various hydrocarbons from a hypothetical mixture, accounting for differences in aqueous-phase partitioning. The relative rates of vapor diffusion among hydrocarbon constituents have led to species dependent profiles, as vapors migrate through the unsaturated zone.

Sorption of BTEX compounds to soil materials also reduces vapor-phase diffusion. Sorption between nonionic, hydrophobic organic compounds and natural materials is relatively weak, and often affected by the hydrophobicity of the compound and the organic fraction of the soil. At a constant temperature and pressure, sorption at equilibrium can be described by an isotherm, a functional relationship between adsorbed and aqueous concentrations. Over the past 30 years, various theoretical and empirical isotherm models have been developed. However, a linear Freundlich isotherm is the most commonly used,

$$S_k = K_d C_k \quad (2.4)$$

In this expression,  $S_k$  is the concentration of compound  $k$  sorbed to soil phase,  $C_k$  is the concentration dissolved in water, and  $K_d$  is the distribution coefficient which is a function of temperature and total system pressure. Linear sorption was reported by a number of researchers (Schwarzenbach and Westall, 1981; Chiou et al., 1979; Karickhoff et al., 1979) for dilute solutions of nonpolar organics and soils with organic carbon (C) content greater than 0.1% (wt/wt). These researchers have attributed linear sorption of nonpolar organic solutes to the organic C content in the soils. Chiou et al. (1982) postulated that sorption of nonionic organic compounds from water on soil organic matter is a partitioning process similar to that between an organic solvent phase and water. Values of  $K_d$  is usually experimentally determined by curve-fitting equation (2.4) to equilibrium batch data.

Because values of  $K_d$  vary significantly with soil types, also because they strongly correlate with organic content, a coefficient of organic C sorption can be defined by normalizing  $K_d$  with respect to soil organic C content,

$$K_{oc} = \frac{K_d}{f_{oc}} \quad (2.5)$$

where  $f_{oc}$  is the organic C fraction in soil (wt/wt). Although  $K_{oc}$  is highly sediment/soil independent, measured  $K_{oc}$  values of toluene from a few studies are differed by a factor of 4 (Kan and Tomson, 1987; Kemplowski, et al., 1987; Jury et al., 1990).

Deviation from linear isotherm was also reported for soils with  $f_{oc}$  less than 0.1% (Schwarzenbach and Westall, 1981; Karickhoff, 1981; Karickhoff et al., 1979) and for dry soils in which moisture content is below a monomolecular layer (English and Loehr, 1991; Chiou and Shoup, 1985; Spencer and Cliath, 1970). English and Loehr (1991) observed linear sorption of benzene to a sandy loam soil with a moisture content of 80% field capacity. Sorption became nonlinear below this level. In a typical field situation, the water content of the subsoil is usually above this critical level, so that gasoline vapors will partition into the aqueous phase before sorbing onto soil organics.

Several experiments have shown that BTEX sorption on surface soils or aquifer materials is linear and reversible (Fan and Scow, 1993; Kan and Tomson, 1987; Kemblowski, et al., 1987). Kan and Tomson (1987) assessed the effect of aqueous flow rate on the mobility of benzene and toluene in columns packed with sandy soil containing 0.3% (wt/wt) organic C. They found that linear equilibrium sorption was attained for toluene within the range of flow-rates investigated. They also found that the  $K_{oc}$  correlation of Karickhoff et al. (1979) gave higher sorption coefficients than the experimental by a factor of seven. Kemblowski et al. (1987) determined sorption for BTX on sandy soils with organic C ranging from 0.12-1.08% (wt/wt). Batch results were adequately described by linear isotherms for low equilibrium aqueous concentrations. Measured  $K_{oc}$  of toluene ranges from 57 to 194 ml/g.

### **2.2.2 Aerobic Biodegradation**

Gasoline hydrocarbons that enter the subsurface environment can undergo both aerobic and anaerobic biodegradation. There have been numerous field demonstrations of aerobic biodegradation of gasoline hydrocarbons in surface soil (Reynolds et al., 1994; Raymond et al., 1976), in the unsaturated zone (O'Leary et al., 1993; Caldwell et al., 1992; Ostendorf and Kampbell, 1991; Hult and Grabbe, 1985), and in groundwater (Armstrong et al., 1991; Chiang et al., 1989; Jamison et al., 1975). In the absence of  $O_2$ , monoaromatic hydrocarbons have been demonstrated to bacterially degrade in both field (Barbaro et al., 1992; Piet and Smeenk, 1985; Reinhard et al., 1984; Schwarzenbach et al., 1983) and laboratory (Barbaro et al., 1992; Kuhn et al., 1988; Major et al., 1988; Wilson et al., 1986; Zeyer et al., 1986; Kuhn et al., 1985) studies of saturated systems. Two widely observed anaerobic degradation pathways of toluene are those under denitrifying (Barbaro et al., 1992; Kuhn et al., 1988; Major et al., 1988; Zeyer et al., 1986) and under methanogenic conditions (Grbic-Galic and Vogel, 1987; Wilson et al., 1986). Anaerobic reactions generally proceed at much slower rates than aerobic processes, especially those under strongly reducing conditions. Since the activity of

anaerobes is generally suppressed when O<sub>2</sub> is present, the discussion here will be limited to aerobic biodegradation. Similarly, abiotic degradation processes such as hydrolysis and chemical oxidation/reduction of these compounds are not expected to be significant (Barker and Mayfield, 1988; Mabey et al., 1982).

The aerobic biodegradation of aromatic hydrocarbons in soil is well documented (Dagley, 1984; Gibson and Subramanian, 1984). Toluene and xylene, for instance, are initially converted via alcohols and aldehydes to benzoate and toluate, respectively (Kuhn et al., 1988). The rate of microbial degradation is limited by the number and activity of microorganisms which, in turn, is affected by the geochemistry of subsurface environment. Important environmental factors include soil temperature, pH, and moisture content, hydrocarbon concentration, dissolved O<sub>2</sub>, nutrient bioavailability, and the presence of other substrates or toxins. At present, the relative importance and interaction of these chemical and biological factors are not well understood. With wide variability of subsurface hydrogeological properties, it is no surprise that wide range of biodegradation rates have been reported in the literature. The following sections address potential factors affecting biodegradation rates in unsaturated sandy soils.

#### *Hydrocarbon-degrading organisms*

Significant microbial communities of diverse species inhabit the subsurface environment. Since the subsurface generally has low nutrient concentrations and high specific surface area, most microorganisms form small localized colonies fixed on the surface of soil particles (Bouwer and McCarty, 1984). Because soil aggregates provides discrete microhabitats, the microbial cells are distributed nonuniformly (Hattori, 1973).

Hydrocarbon-utilizers are widely distributed in virtually all arable, pasture, and forest soils (Schlegel, 1986). Wilson et al. (1983) reported that bacteria predominate the microbial communities in the deeper region, whereas more higher organisms such as fungi, yeasts, and protozoa are present in river sands and gravels. For uncontaminated aquifers, the numbers of hydrocarbon degraders are on the order of 10<sup>6</sup> per 1 g of dry soil (Thomas et al., 1990; Balkwill and Ghiorse, 1985; Webster et al., 1985; Wilson et

al., 1983). Soils taken from petroleum-contaminated subsurface generally contain a higher number of hydrocarbon oxidizers (Leahy and Colwell, 1990; McKee et al., 1972). Thus, the entry of petroleum compounds can stimulate the growth of soil microbes. In most uncontaminated subsurface, the stringent oligotrophic (low substrate and nutrient) conditions exist. Therefore, most microorganisms that can utilize hydrocarbons as the sole source of C are capable of growing in simple mineral salts medium without growth factors such as vitamins and amino acids (Jamison et al., 1975).

#### *Soil Moisture Content*

Microorganisms are physiologically restricted by the availability of water, which is needed to support their growth and enzymatic activities. Generally, the microbial activity in soil is optimal at field capacity (Alexander, 1977). Lower values of soil moisture inhibit microbial activities due to inadequate water activity. At higher soil moisture contents, the aeration is poor and results in low microbial activities. However, a number of studies have also shown that water content less than field capacity can yield faster degradation rates (English and Loehr, 1991; Rao et al., 1983; Dibble and Bartha, 1979). In addition, soil water can affect microbial activity by restricting the metabolism of established colonies through nutrient deficiencies (Griffin, 1981).

#### *Hydrocarbon Concentration*

The rate of biodegradation in soil is affected by the hydrocarbon concentration. Dibble and Bartha (1979) observed increases in biodegradation in soil with increased hydrocarbon concentration up to a threshold level. Higher concentrations of applied hydrocarbon resulted in a decrease in biodegradation. The inhibition of biodegradation at high hydrocarbon concentrations was perhaps due to microbial toxicity, O<sub>2</sub> depletion, or nutrient limitation. Alvarez et al. (1991) studied aerobic degradation of benzene and toluene in batches using aquifer materials saturated with basal media. For over a month, no benzene or toluene was degraded when the initial substrate concentration was present at 250 mg/L, suggesting that the concentration was too high for the microbial survival.

In the same study, toluene biodegradation was also inhibited at aqueous concentrations above 100 mg/L.

### *O<sub>2</sub> Availability*

O<sub>2</sub> is needed for aerobic degradation as a terminal electron acceptor in respiratory reactions and as a reactant in oxidation reactions of saturated and aromatic hydrocarbons. In major aerobic degradative pathways for aromatic hydrocarbons, molecular O<sub>2</sub> is added onto the aromatic ring by microbial enzymes called oxygenases.

Biodegradation within the contaminant plumes in the saturated zone is often limited by O<sub>2</sub> supply because microbes consume O<sub>2</sub> faster than it can be replenished. When measured O<sub>2</sub> concentrations drop below 1-2 mg/L, hydrocarbon degradation rates are reduced (Chiang et al., 1989; Barker and Mayfield, 1988).

Aerobic conditions generally exist throughout a sandy unsaturated zone, at least in the macropores. Anoxic conditions may be found in localized micro-environments of soil aggregates, in water-logged soils, or near a contaminant source. Hult and Grabbe (1985) reported the partial pressure of O<sub>2</sub> in soil air to be less than 0.01 immediately above the floating oil, and 0.16 near the water table at the edge of the floating oil. This may suggest that the rate of O<sub>2</sub> diffusion through the unsaturated zone is not limiting the microbial oxidation of hydrocarbons except in the immediate vicinity of the source. The relationship between hydrocarbon and O<sub>2</sub> in a biodegradation process is rather complex. In the case of BTEX in groundwater, Barker and Mayfield (1988) generally noticed much more O<sub>2</sub> was utilized than that predicted by the stoichiometry of chemical oxidation reaction.

### *Mineral Nutrients*

Mineral nutrients are essential substances for microbial metabolism and usually are present at low concentrations in soils. Nitrogen (N) and phosphorus (P) are two major nutrients since they are required in large amounts for synthesis of proteins, DNA, RNA, and ATP. In an enriched medium, microbial growth is fast and has a maximum specific

growth rate, which is an inherent characteristic of the organism subject to nutrient balance, culture history, and environmental conditions. In addition, both biomass and RNA content per cell are large. In a medium that contains all but one of the essential nutrients in excess, both growth rate and microbial density then depend on the concentration of this limiting nutrient. As the microbial density increases and the nutrient becomes limiting, the growth rate will slow down and the amounts of nutrients incorporated as cell constituents decrease. This is known as the cell quota concept. When the cell quota approaches some minimum value, the net growth rate reduces to zero. However, cells may still be able to oxidize hydrocarbons for maintenance-energy production (Pirt, 1975). However, the consumption of hydrocarbons is reduced when compared to that required for a growing microbial population. At this point, population turnover allows for recycling of the limiting mineral nutrient (Hattori, 1973).

Most petroleum fuels contain little or no mineral nutrients. As a result, the bioavailability of N and P in the contaminated area may limit the extent of hydrocarbon biodegradation after major oil spills (Atlas, 1981). Several field studies have shown that the addition of N and/or P stimulated aerobic biodegradation in subsurface (O'Leary et al., 1993; Jamison et al., 1975) and surface soils (Raymond et al., 1976).

The effects of N on propane and butane biodegradation in the unsaturated sandy soil used for the current study were examined by Toccalino et al. (1993). Batch experiments showed that N supplements initially stimulated both propane and butane degraders. After the initial available inorganic N was utilized, propane-amended soil became N-limited, whereas butane degradation rate later increased regardless of whether more N was added. They suggested that butane-oxidizing soil overcame N limitation by fixing  $N_2$ .

Several investigators conducted batch degradation experiments of BTX using either soil and/or groundwater samples from field sites (Allen-King et al., 1994; Aelion and Bradley, 1991; Armstrong et al., 1991). In all studies, enhanced biodegradation of these compounds was observed following N addition.

Dibble and Bartha (1979) conducted batch biodegradation of oil sludge in soils and obtained optimal C:N and C:P ratios of 60:1 and 800:1, respectively. However, lower ratios of C:N and C:P (15:1 and 200:1) did not accelerate sludge biodegradation. Baker et al. (1994) reported a decrease in toluene mineralization after adding nitrate-N to a certain level (40 mg-N per kg of unsaturated soil). The inhibition of hydrocarbon mineralization at higher levels of N was also reported by Morgan and Watkinson (1992). Swindoll et al. (1988) showed that amending toluene-treated samples with N, P, or both did not significantly alter the total amount of toluene mineralized after 60 days. However, the addition of P did increase the rate of mineralization during the initial 10 days. Other studies of nutrient additions resulted in no apparent effects on BTEX biodegradation (Thomas et al., 1990). Lee and Ward (1985) noted a considerable variation in nutritional requirements of microorganisms among different aquifers. The variation in nutrient requirements may be attributed to the variable composition of soils, N reserves, and the presence of N-fixing bacteria (Leahy and Colwell, 1990). These findings suggest that nutrient addition to enhance biodegradation of hydrocarbons is site-specific, and must be determined experimentally for each contaminated area (Dibble and Bartha, 1979).

## **2.3 EXPERIMENTAL METHODS**

### **2.3.1 Experimental Design**

A schematic diagram of the sand columns used in these studies is shown in Fig. 2.1. The columns consisted of cylindrical stainless-steel (SS) tubes, one end of which was connected to a reservoir and the other to an end cap. A liquid source containing toluene was stored in the reservoir to provide a continuous vapor source for diffusion. The end cap was made of cast aluminum and functioned as a flow channel. A perforated SS plate was placed at the connections of both ends to hold up the sand. A number of vapor-sampling ports were located at 10-cm intervals along the column axis. The

sampling ports were 16-gauge SS luerlock hypodermic needles with Swagelok fittings positioned such that the needles extended about 5 cm into the column.

An uncontaminated medium sand taken from the Columbia River near Scappoose, OR, was used in this study. Properties of this soil are listed in Table 2.1. The soil was packed into a two-section column joined together with a dresser coupler (Sure-Flo Fittings, Ann Arbor, MI). The two-section column setup was used to allow the entire upper section to reach residual water saturation. The coupled column was saturated from the bottom with deionized, tap-water either unamended or amended with  $\text{NH}_4\text{NO}_3$  (reagent grade, Aldrich Chemical Co., Inc., Milwaukee, WI). It was subsequently drained by gravity to obtain residual saturation in the upper section. Finally, the column halves were carefully separated, and the upper section was assembled to the end pieces previously described.

Two source concentrations were studied: (1) 65 mg/L vapor (i.e., the saturated-vapor concentration of pure toluene at 10°C) and (2) 10 mg/L vapor (produced by equilibration with an aqueous solution of toluene at 15°C). For the saturated-vapor experiment, pure liquid toluene (spectrophotometric grade, Aldrich Chemical Co., Inc., Milwaukee, WI) was added in the reservoir periodically to provide a continual vapor source. For the low-concentration column experiments, a source-circulating system was used to provide a constant concentration of toluene in the reservoir (see Fig. 2.1). A peristaltic pump delivered an aqueous solution of toluene from a 27-L glass jar to the reservoir at 13 ml/min. A constant head was maintained in the reservoir, and the overflow solution was drained back to the glass jar by gravity. Small amount of liquid toluene was added weekly into the glass jar to replenish mass loss to the column.

A process flow chart of the column experiments is depicted in Fig. 2.2. An air stream from a compressed air cylinder (Air Products and Chemicals, Allentown, PA) flushed through the end cap to provide a zero-concentration boundary condition. The air stream was saturated with water prior to entry to minimize water-vapor loss from the columns. The humidified air was regulated by a needle valve with a calibrated rotameter

at 50 ml/min. The entire experimental apparatus except the compressed air cylinder was placed in a temperature-controlled room at 10 or 15°C.

### 2.3.2 Sampling and Analysis Procedures

Vapor samples were collected from the columns using a gas-tight syringe (Hamilton Co., Reno, NV) and analyzed immediately by using gas chromatography (GC). A 1-ml of vapor was drawn through the syringe to purge the sampling ports before a 1.5 ml of sample was collected. Half of the sample was analyzed for toluene and the other half for O<sub>2</sub>, CO<sub>2</sub>, and CH<sub>4</sub> (respiration gases). The column was initially sampled 1 to 3 times a day for first few days. Subsequent sampling was then reduced to every other day for two weeks. When the system became more stable, weekly sampling was performed.

Toluene was analyzed by using an HP-5890 GC (Hewlett Packard, Avondale, Pa) equipped with a flame-ionization detector (FID). A six-port valve (Carle Instruments, Inc., Loveland, CO) with a fixed volume sample loop (100- $\mu$ l) heated to 100°C was used for sample injection (see Fig. 2.3a). A 0.53 mm I.D., 25 m long fused-silica capillary column (Chrompack International, The Netherlands) was used to separate toluene from other gases. The column and FID temperatures were at 120 and 170°C, respectively. Flow rates of He, air, and H<sub>2</sub> were 4, 400, and 35 cm<sup>3</sup>/min, respectively. N<sub>2</sub> was used as makeup gas at a rate of 30 cm<sup>3</sup>/min.

Respiration gas analyses were performed by using an HP5890 GC equipped with a multi-port valve (Valco Instruments Co., Inc., Houston, TX). The valve (see Fig. 2.3b) contained two fixed-volume sample loops used for sample injection. The content of each sample loop was flushed by He onto separate packed columns. O<sub>2</sub> was separated by using a 6.4 mm O.D., 48.3 cm long SS column packed with 60/80 mesh molecular sieve 5A (Altech Associates, Inc., Deerfield, IL) and analyzed by a thermal-conductivity detector (TCD). CO<sub>2</sub> and CH<sub>4</sub> were separated by using a 3.2 mm O.D., 40.6 cm long SS column packed with 100/200 mesh Spherocarb (Analabs, Norwalk, CT). The oven temperature was programmed at an initial temperature of 40°C for 1 min, increased at

a rate of 30°C/min to a final temperature of 80°C, and held at 80°C for 3 min. After separation, CO<sub>2</sub> was reduced to CH<sub>4</sub> in a catalyst column (Ni) heated at 500°C. Both gases were then analyzed by FID. The TCD and FID temperatures were at 105 and 225°C, respectively. The carrier gas (He) to each detector was at 30 ml/min, and the reference gas for TCD (He) was at 30 ml/min. The air flow rate for FID was 400 ml/min. H<sub>2</sub> (30 ml/min) was used as a reductant in the catalytic reaction of CO<sub>2</sub> to CH<sub>4</sub>.

Standards were analyzed at the beginning of all sampling sessions and selected standards were reanalyzed at the end of most sampling sessions. The gas-phase standards were used in quantifying respiration gases. They were prepared in a 0.8-L SS canisters equipped with SS bellows valves (Whitey Co., Highland Heights, OH). Pure gases (Air Products and Chemicals, Allentown, PA) were added in sequence and diluted with N<sub>2</sub> to obtain a multi-component standard.

Aqueous-phase standards were used to quantify toluene. They were prepared in 40-ml glass vials fitted with Teflon Mininert valves (Pierce, Rockford, IL). A known volume of deionized water was placed into each vial, which was sealed afterwards. A known volume of toluene-saturated aqueous stock solution was then injected through the valve into the water. The vial was then shaken vigorously and stored inverted. The standards were allowed to equilibrate for a minimum of 24 hours before use, and were prepared weekly. All aqueous- and gas-phase standards were stored in a temperature-controlled room.

The valves and data acquisition were controlled by a Nelson Analytical 760 Series Interface (Nelson Analytical, Cupertino, CA). All peak areas were quantified by comparison with external standards as described above.

## 2.4 RESULTS AND DISCUSSIONS

In all experiments, O<sub>2</sub> concentrations showed only minor changes from atmospheric. This is because the rate of O<sub>2</sub> diffusion was sufficiently rapid relative to the rate of O<sub>2</sub> consumption. Although no enumeration of toluene degraders was

performed, biodegradation was assessed by measurements of toluene and O<sub>2</sub> consumptions and CO<sub>2</sub> production. Under aerobic conditions, toluene is mineralized to CO<sub>2</sub> in a microbial respiration process where O<sub>2</sub> is the electron acceptor. This process sustains energy requirements for cell functions. Therefore, the production of CO<sub>2</sub> is indicative of aerobic biodegradation.

In the saturated-vapor experiment (Column 1), toluene vapor was allowed to diffuse from a constant-concentration source of saturated vapor at 10°C. Concentrations of toluene, O<sub>2</sub>, and CO<sub>2</sub> in soil air along the column length at selected times are shown in Figures 2.4(a,b), 2.5, and 2.6, respectively. Both toluene and CO<sub>2</sub> profiles suggested that the vapor diffusion of toluene overwhelmed biodegradation. As seen in Fig. 2.4(a,b), toluene migrated swiftly throughout the column. At 220 hours, trace concentrations of toluene were qualitatively detected in the effluent flushed air. CO<sub>2</sub> profiles indicated that the microbial activity was insignificant until 320 hours, at which time the concentration of CO<sub>2</sub> slightly increased near the cap end. The CO<sub>2</sub> concentrations in the column suggested that biodegradation in all but the last ~40 cm of the column was inhibited due to substrate toxicity. This result agrees with previous studies which showed aerobic biodegradation of toluene is inhibited at concentrations above 16 mg/L vapor (equivalent to an aqueous concentration of 100 mg/L) (Alvarez et al., 1991). The inhibition by substrate toxicity was demonstrated by low CO<sub>2</sub> productions in most part of the column where toluene concentrations were above the inhibitory level. Despite the microbial activity in the vicinity of the cap, the overall removal rate of toluene by biodegradation was low compared to the supply rate by diffusion, and hence no effect of biodegradation on toluene profiles was seen. After 1560 hours, toluene biodegradation decreased as indicated by a decrease in the CO<sub>2</sub> level. This was probably because N became limiting.

Two column experiments were conducted with a source concentration of 10 mg/L vapor at 15°C. These two columns are hereafter referred to as Column 2 and 3. In order to promote the microbial activity in these experiments, water added to these columns was amended with NH<sub>4</sub>NO<sub>3</sub> (~22 mg-N/L aqueous).

Selected profiles of toluene, O<sub>2</sub>, and CO<sub>2</sub> of Column 2 at various sampling times are shown in Figures 2.7(a,b), 2.8, and 2.9, respectively. As evident in Fig. 2.7(a,b), the diffusive gradient of toluene was much less than in Column 1. Since the source concentration was below the inhibitory level, biodegradation was possible along the entire column as long as there was toluene mass present. The biodegradation rate was initially low, and within 43 hours, toluene vapor was detected at a distance as far as 130 cm from the source. At 73 hours, the effect of biodegradation was apparent, for toluene was no longer detectable in the portion of the column between 60 to 80 cm (the detection limit = 0.014 mg/L vapor). This was followed by the disappearance of toluene from 50 cm and above, resulting in a retreat of toluene vapor front to a distance of 50 cm from the source. Subsequently, the vapor front of toluene gradually moved across the column with time. At 1896 hours, toluene travelled to a distance of 120 cm (Data not shown).

CO<sub>2</sub> profiles also delineated the pattern of the moving front as the peak of the profiles shifted away from the source with time. The initial low concentrations of CO<sub>2</sub> near the source end were caused by dissolution of CO<sub>2</sub> into the aqueous source of toluene in the reservoir. As the aqueous source became saturated with CO<sub>2</sub>, the level of CO<sub>2</sub> in the column near the source end started to rise, and by 1676 hours, a zero-flux boundary condition was developed.

The shifting of vapor front may be explained as follows. Biodegradation was initially low, presumably due to a small initial microbial population (see Chapter 3). The biodegradation rate then increased until it was greater than the diffusion rate, causing a shift of the vapor front back towards the source. With a continual supply of toluene and O<sub>2</sub>, biodegradation in the source region continued until N was exhausted. As soils in the source area became depleted with respect to N, the rate of biodegradation decreased, and toluene moved away from the source under the influence of diffusion. The rate of toluene transport across the column was therefore controlled by the bioavailability of N in the soil and the rates of diffusion and biodegradation. During this time, it was postulated that most biodegradation occurred in a thin zone around the vapor front; however, the width of this zone was not quantifiable with our sampling design.

The source concentration of Column 2 was raised to 15 mg/L vapor at 1968 hours, and concentrations of the constituents were monitored for an additional 1104 hours. Toluene vapor diffused through the column by 2688 hours. These data can be found in Appendix A.

The effect of biodegradation on toluene vapor transport was confirmed in column 3. Selected data from Column 3 are plotted in Figures 2.10(a,b), 2.11, and 2.12 for toluene, O<sub>2</sub>, and CO<sub>2</sub>, respectively. The effect of biodegradation was readily demonstrated in Fig. 2.10a. After 20 hours, toluene vapor diffused somewhat less distance in Column 3 than in Column 2 (50 vs. 90 cm). In addition, the effect of biodegradation (as indicated by the retreat of the vapor front) was shown at an earlier time than that in Column 2. Toluene vapor front was moved closer to the source, thus establishing a steeper gradient, than in the case of Column 2. Subsequently, the vapor front moved slowly across the column, and trace toluene was detected in the effluent air after 5 months. Overall, the trends obtained from Column 3 results were similar to those of Column 2.

#### **2.4.1 Column Soil Characterization**

Following the cessation of the experiment, soil cores were taken from column 2, and soil characteristics were analyzed gravimetrically. In general, water content was exceedingly uniform along the entire column, while the total and air-filled porosities showed greater variation. Table A.1 in Appendix A contains quantitative analyses of these properties. The average values (in volume fraction) of porosity, water, and air content were  $.41 \pm .03$ ,  $.11 \pm .01$ , and  $.30 \pm .04$ , respectively.

Nitrate remaining in the soil in Column 2 was determined by specific ion chromatography. These concentration results are summarized in Table 2.2. Very little nitrate was left in most parts of the column where degradation had been active. Under the column conditions, the process of nitrification was very likely, and the ammonium ions present may have been converted to nitrate. With such assumptions, up to 91% of

nitrate available in the column soil was gone. This information supports the hypothesis that the bioavailable N in the soil became limiting due to biodegradation of toluene.

## 2.5 CONCLUSIONS

Three soil-column experiments were carried out to evaluate the importance of diffusion and biodegradation of toluene in an unsaturated sandy soil. The soil column experiments modeled processes occurring in the unsaturated region bounded by a planar contaminated source above the capillary fringe and the ground surface. In all experiments, O<sub>2</sub> monitoring confirmed that grossly aerobic conditions existed in the columns at all times. In the "high source" column (i.e., 65 mg/L vapor) the diffusive flux was strong, and the movement of toluene through the column greatly exceeded the rate of biodegradation. CO<sub>2</sub> measurements indicated low microbial activity. The high diffusive flux and the substrate toxicity effect were responsible for the relative unimportance of biodegradation compared to diffusion.

Both low-concentration column studies (10 mg/L vapor) showed that microbial degradation appeared to be a significant attenuation mechanism. The utilization of toluene as the sole C and energy source was carried out by the ubiquitous native microflora present in the uncontaminated soil. The effect of biodegradation was apparent shortly after toluene was introduced, since source concentrations were below the inhibitory level. CO<sub>2</sub> concentrations in the column increased from an ambient concentration by 20 fold. This evidence suggested that biodegradation was significant under low-flux conditions, and therefore toluene transport was slower in these cases. However, as the soil in a region became limited with respect to N, the biodegradation rate decreased, and toluene moved away from the source under the influence of diffusion. Nitrate analyses of column soils support this hypothesis.

The dynamics of toluene migration in the unsaturated sandy soil as well as the influence of diffusion and biodegradation were qualitatively evaluated here. This study showed that under the conditions tested aerobic biodegradation was important, and

transport was controlled by diffusion, biodegradation, and N bioavailability. It was also demonstrated that these processes affected mobility of the contaminant compound to different degrees depending on various conditions. Because these processes all interacted, the results from column experiments were best evaluated by using a simulation model. Therefore, a mathematical model was developed which included diffusion, water-air partitioning, sorption, and biodegradation. To quantify biodegradation, batch experiments were conducted to characterize toluene biodegradation kinetics and its rate parameters. Additional experiments were also carried out to substantiate the effects of N nutrient and substrate toxicity on the biodegradation. The batch studies and findings are discussed in Chapter 3. The mathematical model and the quantitative evaluations of column data are presented in Chapter 4.

## 2.6 REFERENCES

Abriola, L. M., and G. F. Pinder, A multiphase approach to the modeling of porous media contamination by organic compounds, 2, Numerical simulation, *Water Resour. Res.*, 21, 19-26, 1985.

Aelion, C. M., and P. M. Bradley, Aerobic biodegradation potential of subsurface microorganisms from a jet fuel-contaminated aquifer, *Appl. Environ. Microbiol.*, 57, 57-63, 1991.

Alexander, M., *Introduction of Soil Microbiology*, 2nd ed., John Wiley & Sons, Inc., New York, 1977.

Allen-King, R. M., J. F. Barker, R. W. Gillham, and B. K. Jensen, Substrate- and nutrient-limited toluene biotransformation in sandy soil, *Environ. Toxicol. Chem.*, 13, 693-705, 1994.

Alvarez, P. J. J., P. J. Anid, and T. M. Vogel, Kinetics of aerobic biodegradation of benzene and toluene in sandy aquifer material, *Biodegradation*, 2, 43-51, 1991.

Armstrong, A. Q., R. E. Hodson, H. M. Hwang, and D. L. Lewis, Environmental factors affecting toluene degradation in ground water at a hazardous waste site, *Environ. Toxicol. Chem.*, 10, 147-158, 1991.

Atlas, R. M., Microbial degradation of petroleum hydrocarbons: An environmental perspective, *Microbiol. Rev.*, 45, 180-209, 1981.

Baehr, A. L., Selective transport of hydrocarbons in the unsaturated zone due to aqueous and vapor phase partitioning, *Water Resour. Res.*, 23, 1926-1938, 1987.

Balkwill, D. L., and W. C. Ghiorse, Characterization of subsurface bacteria associated with two shallow aquifers in Oklahoma, *Appl. Environ. Microbiol.*, 50, 580-588, 1985.

Baker, R. S., J. Ghaemghami, S. Simkins, and L. M. Mallory, A vadose column treatability test for bioventing applications, in *Hydrocarbon Bioremediation*, edited by Hinchee, R. E., B. C., Alleman, R. E. Hoeppe, R. N. Miller, Lewis Publishers, Ann Arbor, pp. 32-29, 1994.

Barker, J. F., and C. I. Mayfield, The persistence of aromatic hydrocarbons in various ground water environments, in *Proceedings of the Conference on Petroleum Hydrocarbons and Organic Chemicals in Groundwater: Prevention, Detection, and Restoration*, National Water Well Association, Dublin, Ohio, pp. 649-667, 1988.

Barbaro, J. R., J. F. Barker, L. A. Lemon, and C. I. Mayfield, Biotransformation of BTEX under anaerobic, denitrifying conditions: Field and laboratory observations, *J. Contam. Hydrol.*, 11, 245-272, 1992.

Borden, R. C., C. A. Gomez, and M. T. Becker, Natural bioremediation of a gasoline spill, in *Hydrocarbon Bioremediation*, edited by Hinchee, R. E., B. C., Alleman, R. E. Hoepfel, R. N. Miller, Lewis Publishers, Ann Arbor, pp. 290-295, 1994.

Bouwer, E. J., and P. L. McCarty, Modeling of trace organics biotransformation in the subsurface, *Ground Water*, 22, 433-440, 1984.

Brady, N. C., *The Nature and Properties of Soils*, 8th ed., Macmillan Publishing Co., Inc., New York, 1974.

Bruell, C. J., *The Diffusion of Gasoline-Range Hydrocarbon Vapors in Porous Media*, Ph.D. diss., University of Connecticut, Department of Civil Engineering, Storrs, 1987.

Bruell, C. J., and G. E. Hoag, The diffusion of gasoline-range hydrocarbon vapors in porous media, experimental methodologies, in *Proceedings of the NWWA/API Conference on Petroleum Hydrocarbons and Organic Chemicals in Groundwater: Prevention, Detection, and Restoration*, National Water Well Association, Dublin, Ohio, pp. 420-443, 1986.

Buckingham, E., Contribution to our knowledge of the aeration of soils, *U.S. Dep. of Agric. Bureau of Soils Bull.*, 25, 5-52, 1904.

Caldwell, K. R., D. L. Tarbox, K. D. Barr, S. Fiorenza, L. E. Dunlap, and S. B. Thomas, Assessment of natural bioremediation as an alternative to traditional active remediation at selected Amoco oil company sites, florida, in *Proceedings of the Conference on Petroleum Hydrocarbons and Organic Chemicals in Ground Water: Prevention, Detection, and Restoration*, Ground Water Management, Dublin, Ohio, pp. 509-525, 1992.

Chiang, C. Y., J. P. Salanitro., E. Y. Chai, J. D. Colthart, and C. L. Klein, Aerobic biodegradation of benzene, toluene, and xylene in a sandy aquifer - Data analysis and computer modeling, *Ground Water*, 27, 823-834, 1989.

Chiou, C. T., L. J. Peters, and V. H. Freed, A physical concept of soil-water equilibria for nonionic organic compounds, *Science*, 206, 831-832, 1979.

Chiou, C. T., D. W. Schmedding, M. Manes, Partitioning of organic compounds in octanol-water systems, *Environ. Sci. Technol.*, 16, 4-10, 1982.

Chiou, C. T., and T. D. Shoup, Soil sorption of organic vapors and effects of humidity on sorptive mechanism and capacity, *Environ. Sci. Technol.*, *19*, 1196-1200, 1985.

Currie, J. A., Gaseous diffusion in porous media: Part 3, Wet granular materials, *Br. J. Appl. Phys.*, *12*, 275-281, 1960.

Dagley, S., Microbial degradation of aromatic compounds, *Dev. Ind. Microbiol.*, *25*, 53-65, 1984.

Dibble, J. T., and R. Bartha, Effect of environmental parameters on the biodegradation of oil sludge, *Appl. Environ. Microbiol.*, *37*, 729-739, 1979.

Diem, D. A., and B. E. Ross, Field Evaluation of a soil-gas Analysis method for detection of subsurface diesel fuel contamination, in *Proceedings of the Second National Outdoor Action Conference on Aquifer Restoration Groundwater Monitoring and Geophysical Methods*, National Water Well Association, Dublin, Ohio, pp. 1015-1030, 1988.

Downey, D. C., R. E. Hinchey, M. S. Westray, and J. K. Slaughter, Combined biological and physical treatment of a jet fuel-contaminated aquifer, in *Proceedings of the Conference on Petroleum Hydrocarbons and Organic Chemicals in Ground Water: Prevention, Detection, and Restoration*, National Water Well Association, Dublin, Ohio, pp. 627-645, 1988.

English, C. W., and R. C. Loehr, Degradation of organic vapors in unsaturated soils, *J. Hazardous Mater.*, *28*, 55-64, 1991.

Evans, O. D., and G. M. Thompson, Field and interpretation techniques for delineating subsurface petroleum hydrocarbon spills using soil gas analysis, in *Proceedings of the NWWA/API Conference on Petroleum Hydrocarbons and Organic Chemicals in Ground Water: Prevention, Detection, and Restoration*, National Water Well Association, Dublin, Ohio, pp. 444-455, 1986.

Falta, R. W., I. Javandel, K. Pruess, and P. A. Witherspoon, Density-driven flow of gas in the unsaturated zone due to the evaporation of volatile organic compounds, *Water Resour. Res.*, *25*, 2159-2169, 1989.

Fan, S., and K. M. Scow, Biodegradation of trichloroethylene and toluene by indigenous microbial populations in soil, *Appl. Environ. Microbiol.*, *59*, 1911-1918, 1993.

Farmer, W. J., M. S. Yang, J. Letey, and W. F. Spencer, Hexachlorobenzene: Its vapor pressure and vapor phase diffusion in soil, *Soil Sci. Soc. Am. Proc.*, *44*, 676-680, 1980.

Gibson, D. T., and V. Subramanian, Microbial degradation of aromatic hydrocarbons, in *Microbial Degradation of Organic Compounds*, edited by D. T. Gibson, Marcel Dekker, Inc., New York, pp. 181-252, 1984.

Goring, C. A. I., Theory and principles of soil fumigation, *Adv. Pest Control Res.*, 5, 47-84, 1962.

Grbic-Galic, D., and T. M. Vogel, Transformation of toluene and benzene by mixed methanogenic cultures, *Appl. Environ. Microbiol.*, 53, 254-260, 1987.

Griffin, D. M., Water potential as a selective factor in the microbial ecology of soils, in *Water Potential Relations in Soil Microbiology*, edited by J. F. Parr, W. R. Gardner, and L. F. Elliott, Soil Science Society of America, Madison, pp. 141-151, 1981.

Hattori, T., *Microbial Life in The Soil: An Introduction*, Marcel Dekker, Inc., New York, 1973.

Hult, M. F., Microbial oxidation of petroleum vapors in the unsaturated zone, in U.S. Geological Survey Program on Toxic Waste--Ground-Water Contamination, edited by B. J. Franks, Proceedings of the Third Technical Meeting, Pensacola, Florida, March 23-27, 1987, *U.S. Geol. Surv. Open File Rep.*, 87-109, pp. C25-C26, 1987.

Hult, M. F., and R. R. Grabbe, Permanent gases and hydrocarbon vapors in the unsaturated zone, in U.S. Geological Survey Program on Toxic Waste--Ground-Water Contamination, edited by S. E. Ragone, Proceedings of the Second Technical Meeting, Cape Cod, Massachusetts, Oct. 21-25, 1985, *U.S. Geol. Surv. Open File Rep.*, 86-481, pp. C21-C25, 1986.

Jamison, V. W., R. L. Raymond, and J. O. Hudson Jr., Biodegradation of high octane gasoline in groundwater, *Dev. Ind. Microbiol.*, 16, 305-312, 1975.

Jury, W. A., D. Russo, G. Streile, and H. E. Abd, Evaluation of volatilization by organic chemicals residing, *Water Resour. Res.*, 26, 13-20, 1990.

Kan, A. T., and M. B. Tomson, Sorption and migration of organic contaminants in soil column, in *Proceedings of the NWWA/API Conference on Petroleum Hydrocarbons and Organic Chemicals in Groundwater: Prevention, Detection, and Restoration*, National Water Well Association, Dublin, Ohio, pp. 397-407, 1987.

Karickhoff, S. W., Semi-empirical estimation of sorption of hydrophobic pollutants on natural sediments and soils, *Chemosphere*, 10, 833-846, 1981.

Karickhoff, S. W., D. S. Brown, and T. A. Scott, Sorption of hydrophobic pollutants on natural sediments, *Water Res.*, 13, 241-248, 1979.

Karimi, A. A., W. J. Farmer, and M. M. Cliath, Vapor-phase diffusion of benzene in soil, *J. Environ. Qual.*, *16*, 38-43, 1987.

Kemblowski, M. W., J. P. Salanitro, G. M. Deeley, and C. C. Stanley, Fate and transport of residual hydrocarbon in ground water, A case study, in *Proceedings of the NWWA/API Conference on Petroleum Hydrocarbons and Organic Chemicals in Groundwater: Prevention, Detection, and Restoration*, National Water Well Association, Dublin, Ohio, pp. 207-220, 1987.

Kreamer, D. K., E. P. Weeks, G. M. Thompson, A field technique to measure the tortuosity and sorption-affected porosity for gaseous diffusion of materials in the unsaturated zone with experimental results from near Barnwell, South Carolina, *Water Resour. Res.*, *24*, 331-341, 1988.

Kuhn E. P., P. J. Colberg, J. L. Schnoor, O. Wanner, A. J. B. Zehnder, and R. P. Schwarzenbach, Microbial transformations of substituted benzenes during infiltration of river water to groundwater: Laboratory column studies, *Environ. Sci. Technol.*, *19*, 961-968, 1985.

Kuhn E. P., J. Zeyer, P. Eicher, and R. P. Schwarzenbach, Anaerobic degradation of alkylated benzenes in denitrifying laboratory aquifer columns, *Appl. Environ. Microbiol.*, *54*, 490-496, 1988.

Leahy, J. G., and R. R. Colwell, Microbial degradation of hydrocarbons in the environment, *Microbiol. Rev.*, *54*, 305-315, 1990.

Lee, M. D., and C. H. Ward, Biological methods for the restoration of contaminated aquifers, *Environ. Toxicol. Chem.*, *4*, 743-750, 1985.

Letey, J., and W. J. Farmer, Movement of pesticides in soil, in *Pesticides in Soil and Water*, edited by W. D. Guenzi, Soil Science Society of America, Madison, pp. 67-97, 1974.

Mabey, W. R., J. H. Smith, R. T. Podoll, H. L. Johnson, T. Mill, T. W. Chou, J. Gates, I. W. Partridge, H. Jaber, and D. Vandenberg, *Aquatic Fate Process Data For Organic Priority Pollutants*, USEPA, Washington D.C., 1982. EPA/440/4-81-014.

MacPherson, J. R. Jr., *Gas Phase Diffusion of Organic Compounds in Porous Media: Physical and Numerical Modeling*, Ph.D. diss., Oregon Graduate Institute of Science & Technology, Department of Environmental Science and Engineering, Beaverton, 1991.

Mackay, D. M., and S. Paterson, Calculating fugacity, *Environ. Sci. Technol.*, *15*, 1006-1014, 1981.

Mackay, D. M., W. Y. Shiu, K. C. Ma, *Illustrated Handbook of Physical-Chemical Properties and Environmental Fate for Organic Chemicals*, Vol. I, II, III, Lewis Publishers, Ann Arbor, 1992.

Major, D. W., C. I. Mayfield, and J. F. Barker, Biotransformation of benzene by denitrification in aquifer sand, *Ground Water*, 26, 8-14, 1988.

Marshall, T. J., The diffusion of gases through porous media, *J. Soil Sci.*, 10, 79-82, 1959.

McCarthy, K. A., and R. L. Johnson, Measurements of TCE diffusion as a function of moisture content in sections of gravity-drained soil columns, *J. Environ. Qual.*, (submitted), 1994.

McKee, J. E., F. B. Laventy, and R. N. Hertel, Gasoline in groundwater, *J. Water Pollut. Control Fed.*, 44, 293-302, 1972.

Millington, R. J., Gas diffusion in porous media, *Science*, 130, 100-102, 1959.

Morgan, P., and R. J. Watkinson, Factors limiting the supply and efficiency of nutrient and oxygen supplements for the *in situ* biotreatment of contaminated soil and groundwater, *Water Res.*, 26, 73-78, 1992.

Nielson, K. K., V. C. Rogers, and G. W. Gee, Diffusion of radon through soils: A pore distribution model, *Soil Sci. Soc. Am. J.*, 48, 482-487, 1984.

O'Leary, K. E., J. F. Barker, R. W. Gillham, Surface application, of dissolved BTEX: A prototype field experiment, in *Proceedings of the Conference on Petroleum Hydrocarbons and Organic Chemicals in Ground Water: Prevention, Detection, and Restoration*, Ground Water Management, Dublin, Ohio, pp. 149-160, 1993.

Ostendorf, D. W., and D. H. Kampbell, Biodegradation of hydrocarbon vapors in the unsaturated zone, *Water Resour. Res.*, 27, 453-462, 1991.

Piet, G. J., and J. G. M. M. Smeenk, Behavior of organic pollutants in pretreated Rhine water during dune infiltration, in *Ground Water Quality*, edited by C. H. Ward, W. Giger, and P. L. McCarty, John Wiley & Sons, Inc., New York, pp. 122-144, 1985.

Pirt, S. J., *Principles of Microbe and Cell Cultivation*, John Wiley, New York, 1975.

Rao, P. S. C., V. E. Berkheiser, and L. T. Ou, *Estimation of Parameters for Modeling the Behavior of Selected Pesticides and Orthophosphate*, USEPA, Athens, Georgia, 1983. EPA/600/3-84-019.

Raymond, R. L., J. O. Hudson Jr., and V. W. Jamison, Oil degradation in soil, *Appl. Environ. Microbiol.*, 31, 522-535, 1976.

Reinhard, M., N. L. Goodman, and J. F. Barker, Occurrence and distribution of organic chemicals in two landfill leachate plumes, *Environ. Sci. Technol.*, 18, 953-961, 1984.

Reynolds, C. M., M. D. Travis, W. A. Braley, and R. J. Scholze, Applying field-experiment bioreactors and landfarming in alaska climates, in *Hydrocarbon Bioremediation*, edited by Hinchee, R. E., B. C., Alleman, R. E Hoeppe, R. N. Miller, Lewis Publishers, Ann Arbor, pp. 100-106, 1994.

Robbins, G. A., Influence of pore air/water exchange on the diffusion of volatile organic vapors in soil, in *Proceedings of the NWWA/API Conference on Petroleum Hydrocarbons and Organic Chemicals in Groundwater: Prevention, Detection, and Restoration*, National Water Well Association, Dublin, Ohio, pp. 509-520, 1987.

Sallam, A., W. A. Jury, and J. Letey, Measurement of gas diffusion coefficient under relatively low air-filled porosity, *Soil Sci. Soc. Am. J.*, 48, 3-6, 1984.

Schlegel, H. G., *General Microbiology*, 6th ed., Cambridge University Press, Cambridge, 1986.

Schwarzenbach, R. P., W. Giger, E. Hoehn, and J. K. Schneider, Behavior of organic compounds during infiltration of river water to groundwater. Field studies, *Environ. Sci. Technol.*, 17, 472-479, 1983.

Schwarzenbach, R. P., and J. Westall, Transport of nonpolar organic compounds from surface water to groundwater: Laboratory sorption studies, *Environ. Sci. Technol.*, 15, 1360-1367, 1981.

Shearer, R. C., J. Letey, W. J. Farmer, and A. Klute, Lindane diffusion in soil, *Soil Sci. Soc. Am. Proc.*, 37, 189-193, 1973.

Spencer, W. F., and M. M. Cliath, Desorption of lindane from soil as related vapor density, *Soil Sci. Soc. Am. Proc.*, 37, 574-578, 1970.

Swindoll, C. M., C. M. Aelion, and F. K. Pfaender, Influence, of inorganic and organic nutrients on aerobic biodegradation and on the adaptation response of subsurface microbial communities, *Appl. Environ. Microbiol.*, 54, 212-217, 1988.

Tanner, A., Radon migration in the ground: A review, in *The Natural Radiation Environment*, edited by J. Adams, and W. Lowder, U. of Chicago Press, Chicago, pp. 161-179, 1964.

Thomas, J. M., V. R. Gordy, S. Fiorenza, and C. H. Ward, Biodegradation of BTEX in subsurface materials contaminated with gasoline: Granger, Indiana, *Water Sci. Tech.*, 22, 53-62, 1990.

Toccalino, P. L., *Optimization of Hydrocarbon Biodegradation in a Sandy Soil*, Ph.D. diss., Oregon Graduate Institute of Science & Technology, Department of Environmental Science and Engineering, Beaverton, 1992.

Toccalino, P. L., R. L. Johnson, and D. R. Boone, Nitrogen limitation and nitrogen fixation during alkane biodegradation in a sandy soil, *Appl. Environ. Microbiol.*, 59, 2977-2983, 1993.

Verschuere, K., *Handbook of Environmental Data on Organic Chemicals*, 2nd ed., Van Nostrand Reinhold, New York, 1983.

Webster, J. J., G. J. Hampton, J. T. Wilson, W. C. Ghiorse, and F. R. Leach, Determination of microbial cell numbers in subsurface samples, *Ground Water*, 23, 17-25, 1985.

Weeks, E. P., D. E. Earp, and G. M. Thompson, Use of atmospheric fluorocarbons F-11 and F-12 to determine the diffusion parameters of the unsaturated zone in the southern high plains of Texas, *Water Resour. Res.*, 18, 1365-1378, 1982.

Wilson, J. T., J. F. McNabb, D. L. Balkwill, and W. C. Ghiorse, Enumeration and characterization of bacterial indigenous to a shallow water-table aquifer, *Ground Water*, 21, 134-142, 1983.

Wilson, B. H., G. B. Smith, and J. F. Rees, Biotransformations of selected alkylbenzenes and halogenated aliphatic hydrocarbons in methanogenic aquifer material: A microcosm study, *Environ. Sci. Technol.*, 20, 997-1002, 1986.

Zeyer, J., E. P. Kuhn, and R. P. Schwarzenbach, Rapid microbial mineralization of toluene and 1,3-dimethylbenzene in the absence of molecular oxygen, *Appl. Environ. Microbiol.*, 52, 944-947, 1986.

**Table 2.1. Characteristics of unamended Columbia River soil (after Toccalino, 1992).**

Characteristic		Value	Reference	
Total N		55 mg/kg soil	a	
NO <sub>3</sub> <sup>-</sup> - N		0.4 mb/kg soil	a	
NH <sub>4</sub> <sup>+</sup> - N		0.97 mg/kg soil	a	
Available N (NO <sub>3</sub> <sup>-</sup> - N + NH <sub>4</sub> <sup>+</sup> - N)		1.37 mg/kg soil	b	
Available phosphorus		2.7 mg/kg soil	b	
Iron		7.5 mg/kg soil	b	
Organic C content		0.3% (w/w)	b	
pH		6.56	b	
Bulk density		1.52 g/cm <sup>3</sup>	c	
porosity		0.41 (v/v)	c	
Gravimetric water content ( $\theta_a$ ) at field capacity		0.08 (v/v)	c	
Grain size fractions, mm	≥ 4.0	Gravel <sup>d</sup>	4%	c
	4.0 - 1.0	Very coarse sand, gravel	37%	
	1.0 - 0.71	Coarse sand	8%	
	0.71 - 0.5	Coarse sand	9%	
	0.5 - 0.246	Medium sand	26%	
	0.246 - 0.175	Fine sand	8%	
	0.175 - 0.043	Very fine and fine sand	7%	
	< 0.043	Silt	1%	

<sup>a</sup>Determined at Oregon State University's Soil Testing Laboratory.

<sup>b</sup>Determined by Toccalino (1992)

<sup>c</sup>Determined by MacPherson (1991)

<sup>d</sup>U.S. Department of Agriculture classification of soil particle sizes (Brady, 1984).

**Table 2.2. Nitrate contents measured in soil samples from Column 2.**

Column Distance (cm)	Nitrate Concentration (mg NO <sub>3</sub> <sup>-1</sup> /L) <sup>a</sup>	NO <sub>3</sub> -N content (mg N/g of sand) x10 <sup>4</sup>	% of N used (w/w) <sup>b</sup>
0 - 10	2.2	5.0	83
10 - 20	1.2	2.6	91
40 - 50	0.7	1.5	95
80 - 90	1.4	3.2	89
110 - 120	0.9	2.0	93
150 - 160	0.9	2.1	93

<sup>a</sup>10 g of soil samples was diluted with 10 ml of deionized water.

<sup>b</sup>Calculations were based on an initial concentration of 2.92x10<sup>-3</sup> mg-N per g of dry sand (Appendix A), assuming no NH<sub>3</sub> was left.

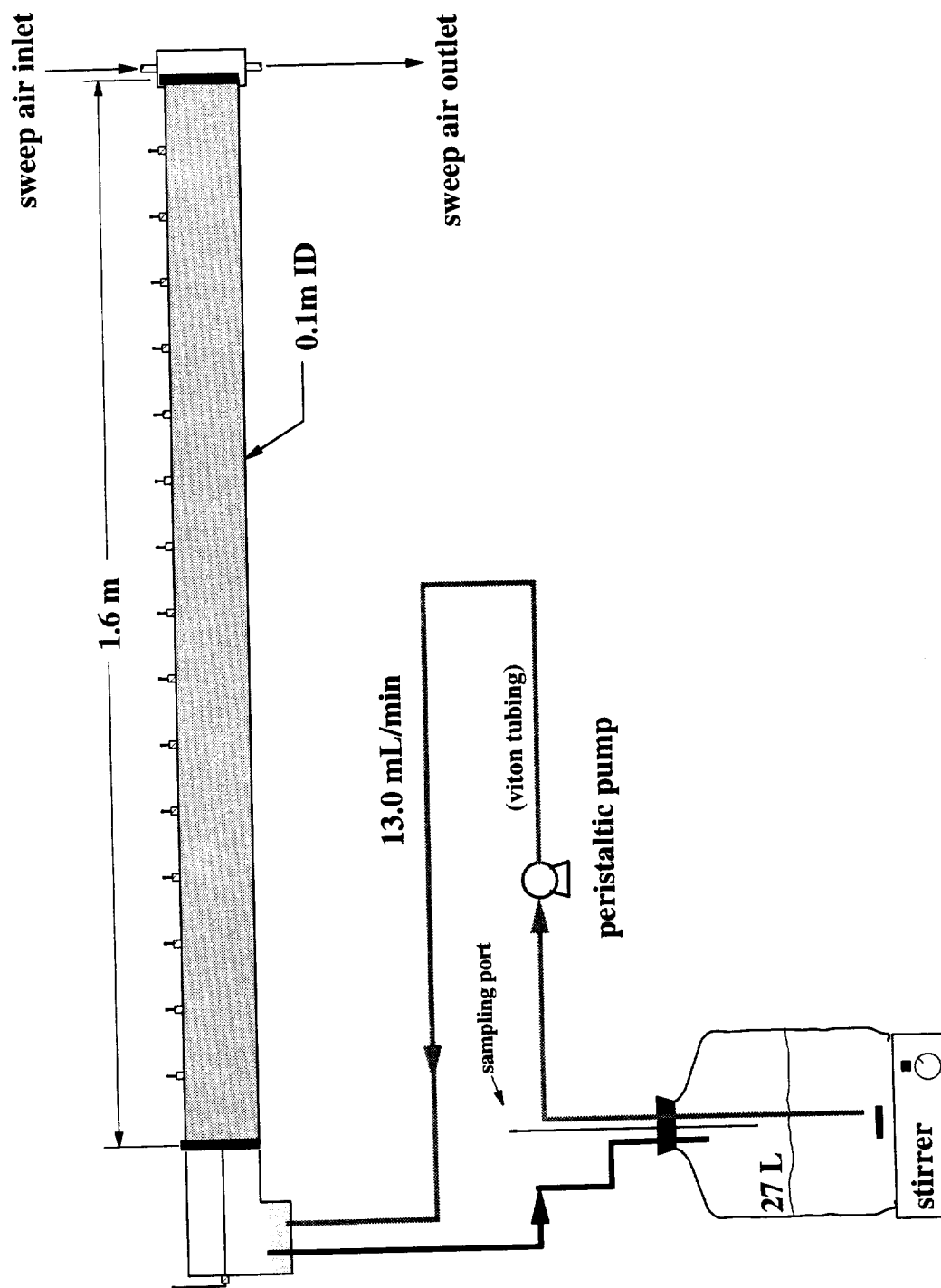


Figure 2.1. Schematic diagram of soil columns.

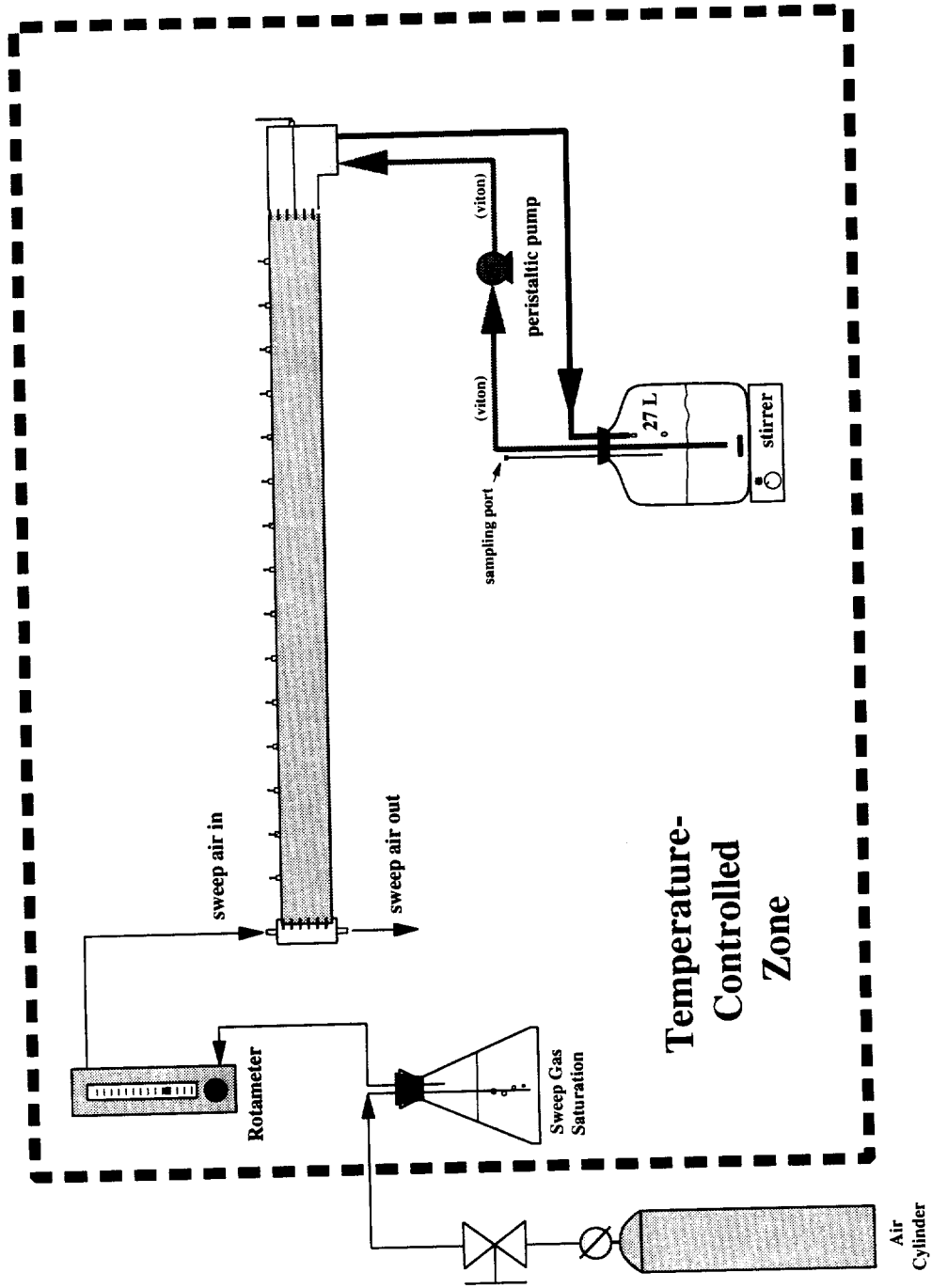
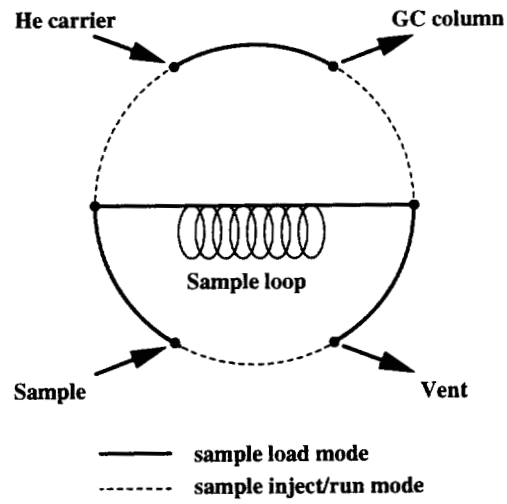
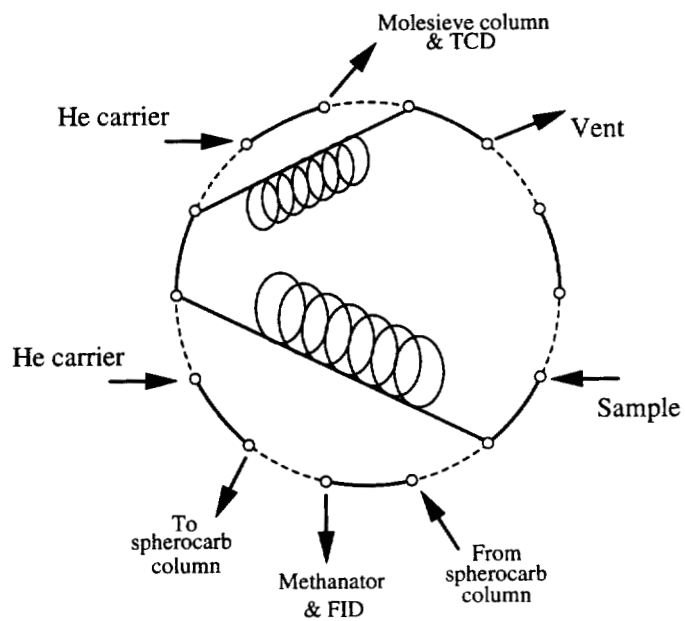


Figure 2.2. Process flow chart of soil column experiments.



**Figure 2.3a.** Diagram of six-port valve used for toluene analyses.



**Figure 2.3b.** Diagram of multi-port valve used for respiration-gas analyses.

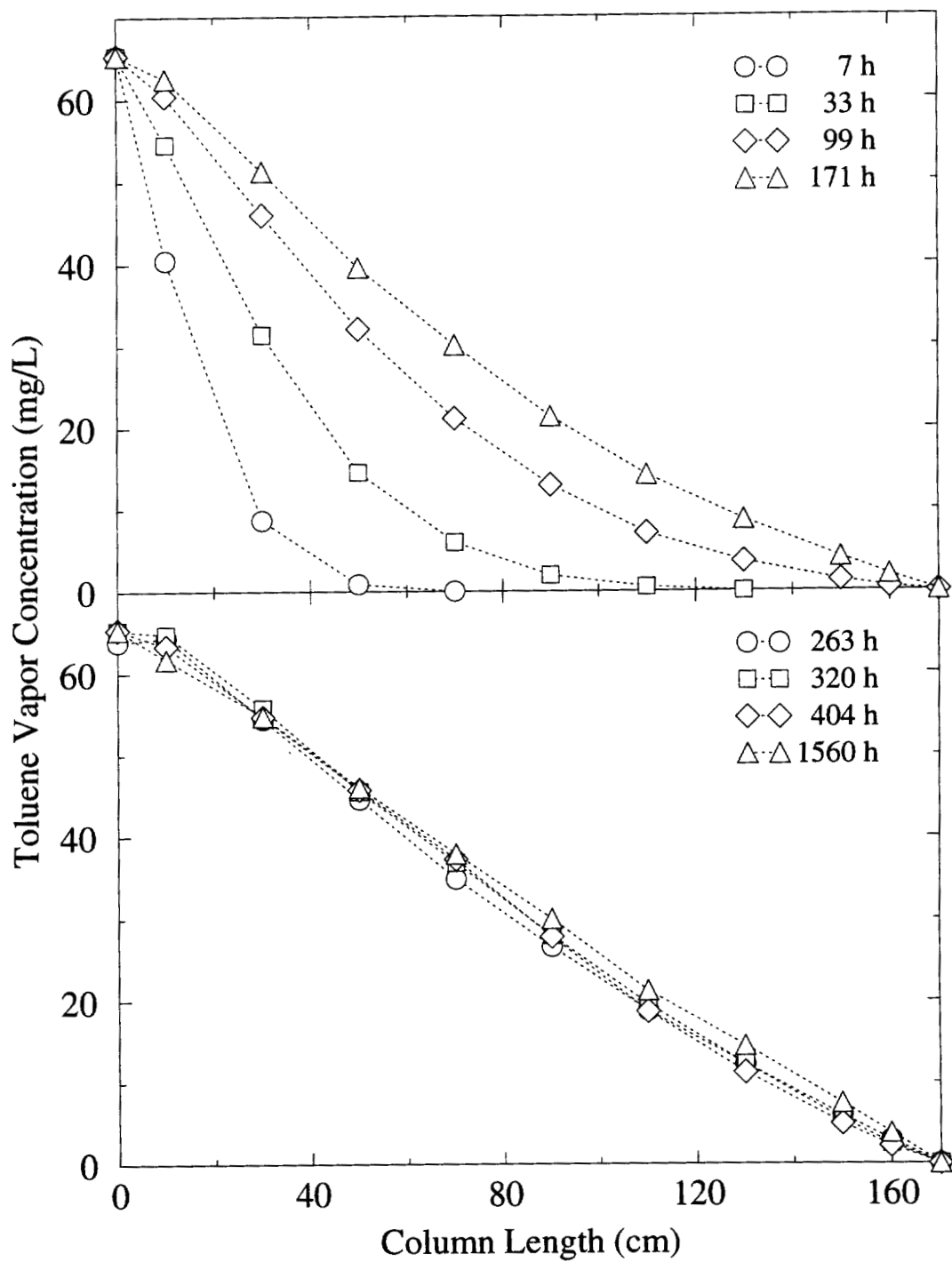


Figure 2.4. Toluene profiles in Column 1 at selected sampling times.

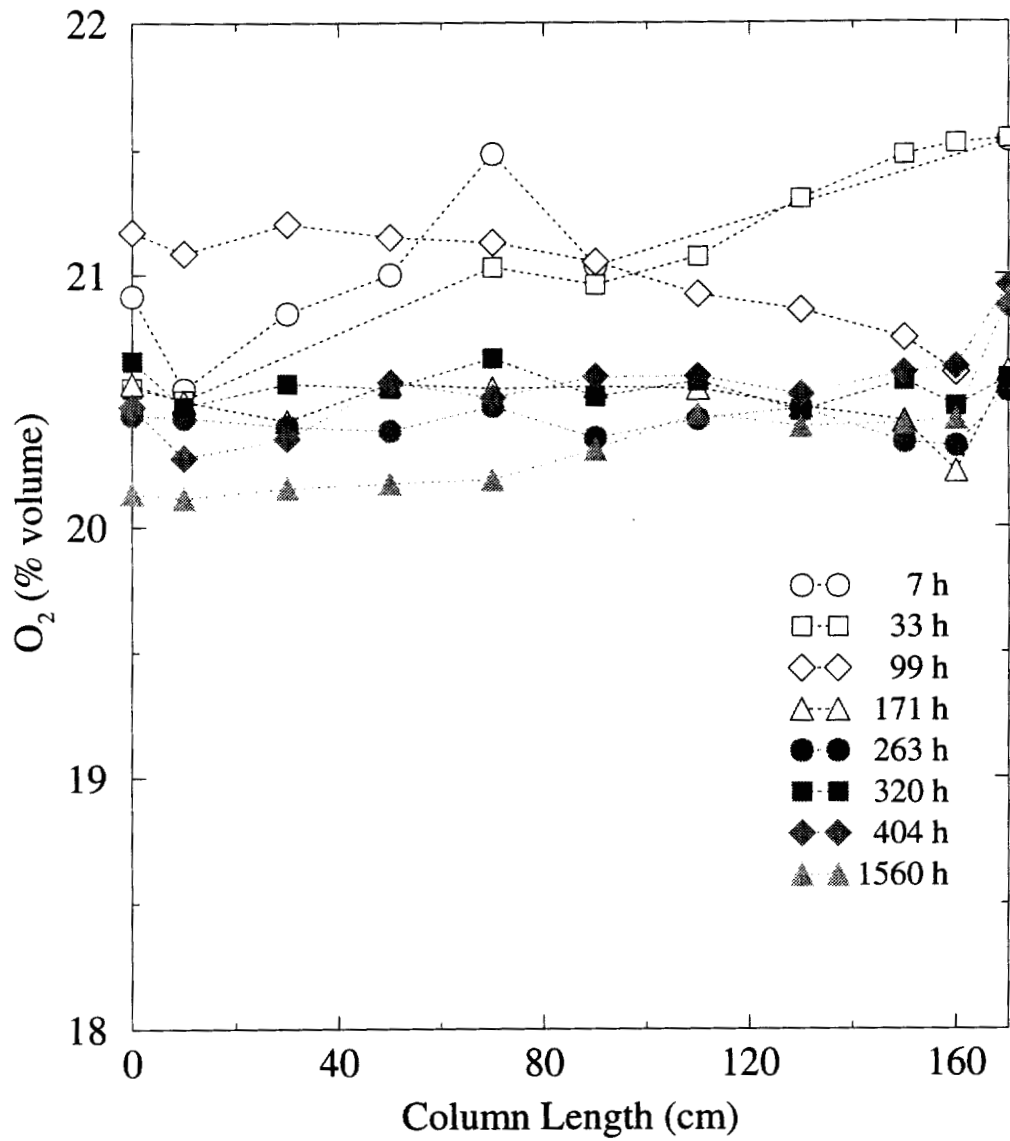


Figure 2.5. O<sub>2</sub> profiles in Column 1 at selected sampling times.

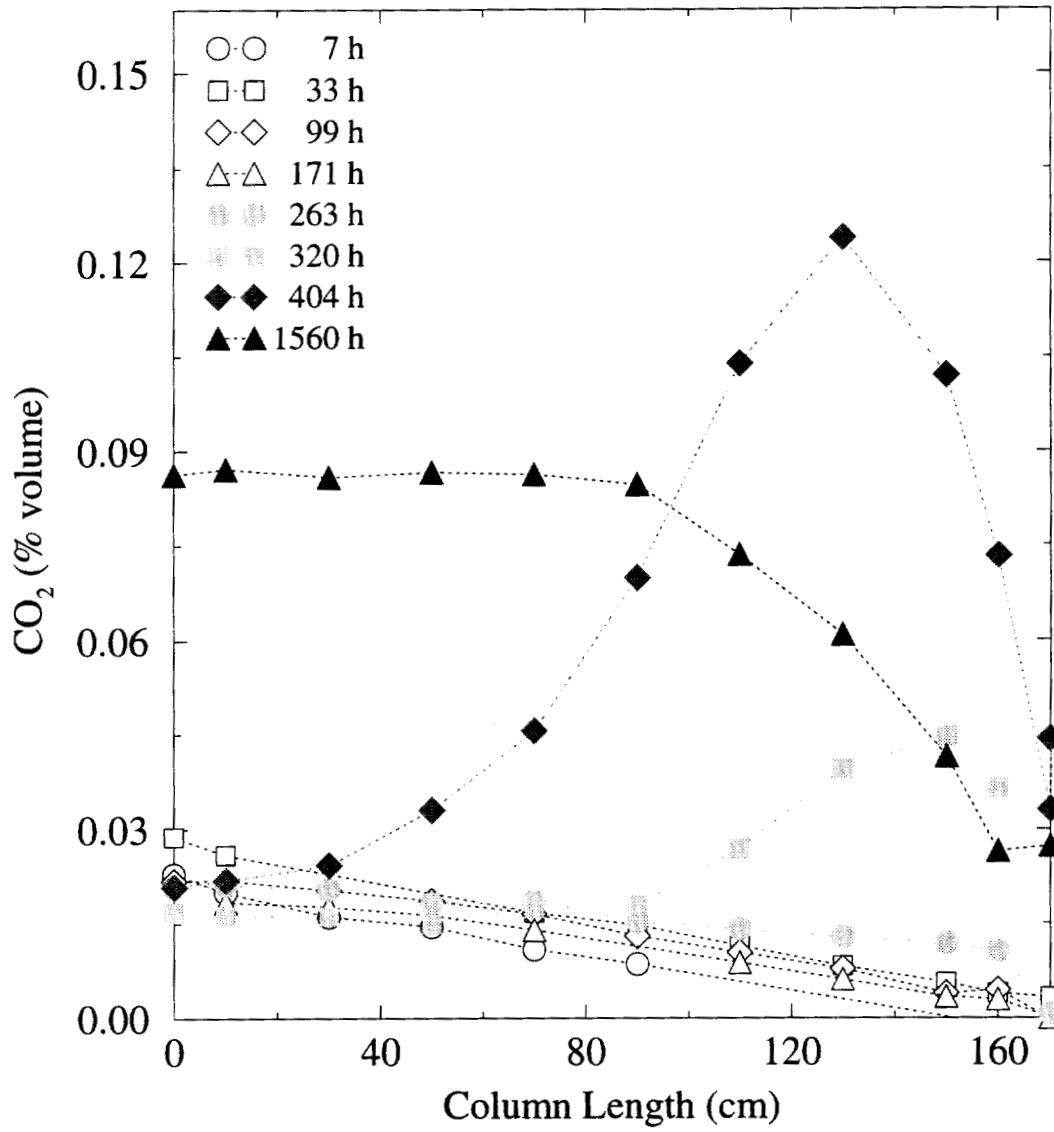


Figure 2.6. CO<sub>2</sub> profiles in Column 1 at selected sampling times.

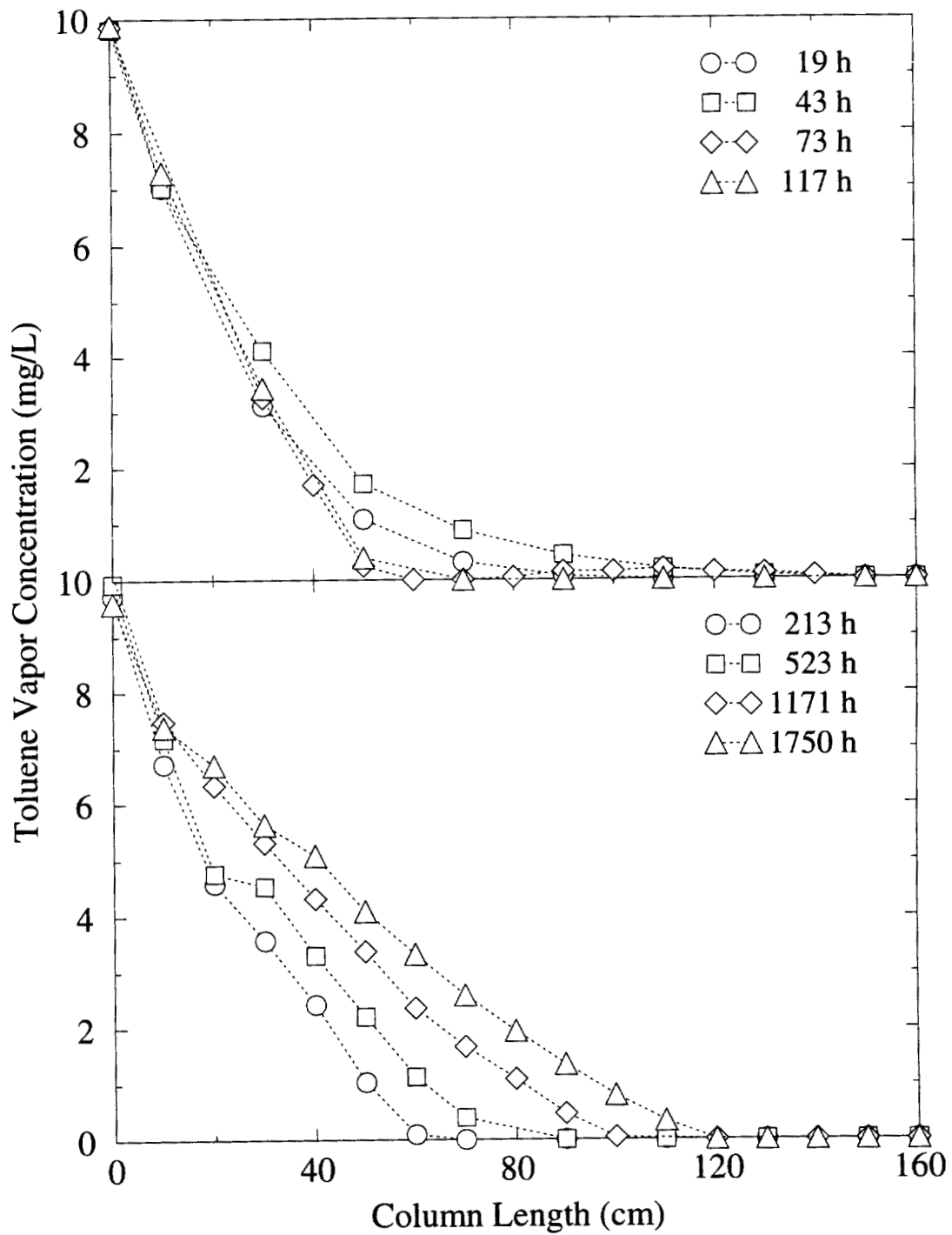


Figure 2.7. Toluene profiles in Column 2 at selected sampling times.

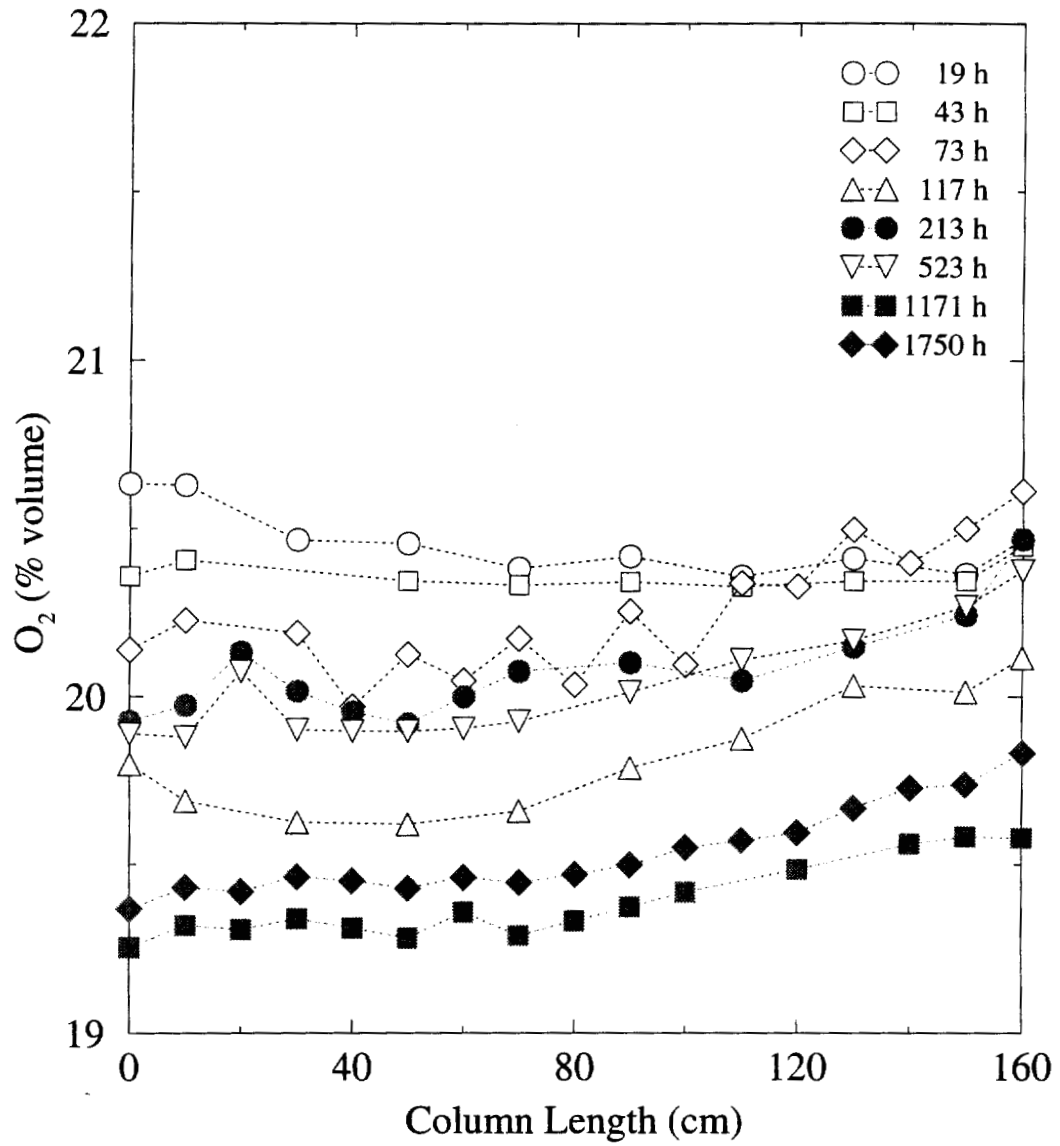


Figure 2.8. O<sub>2</sub> profiles in Column 2 at selected sampling times.

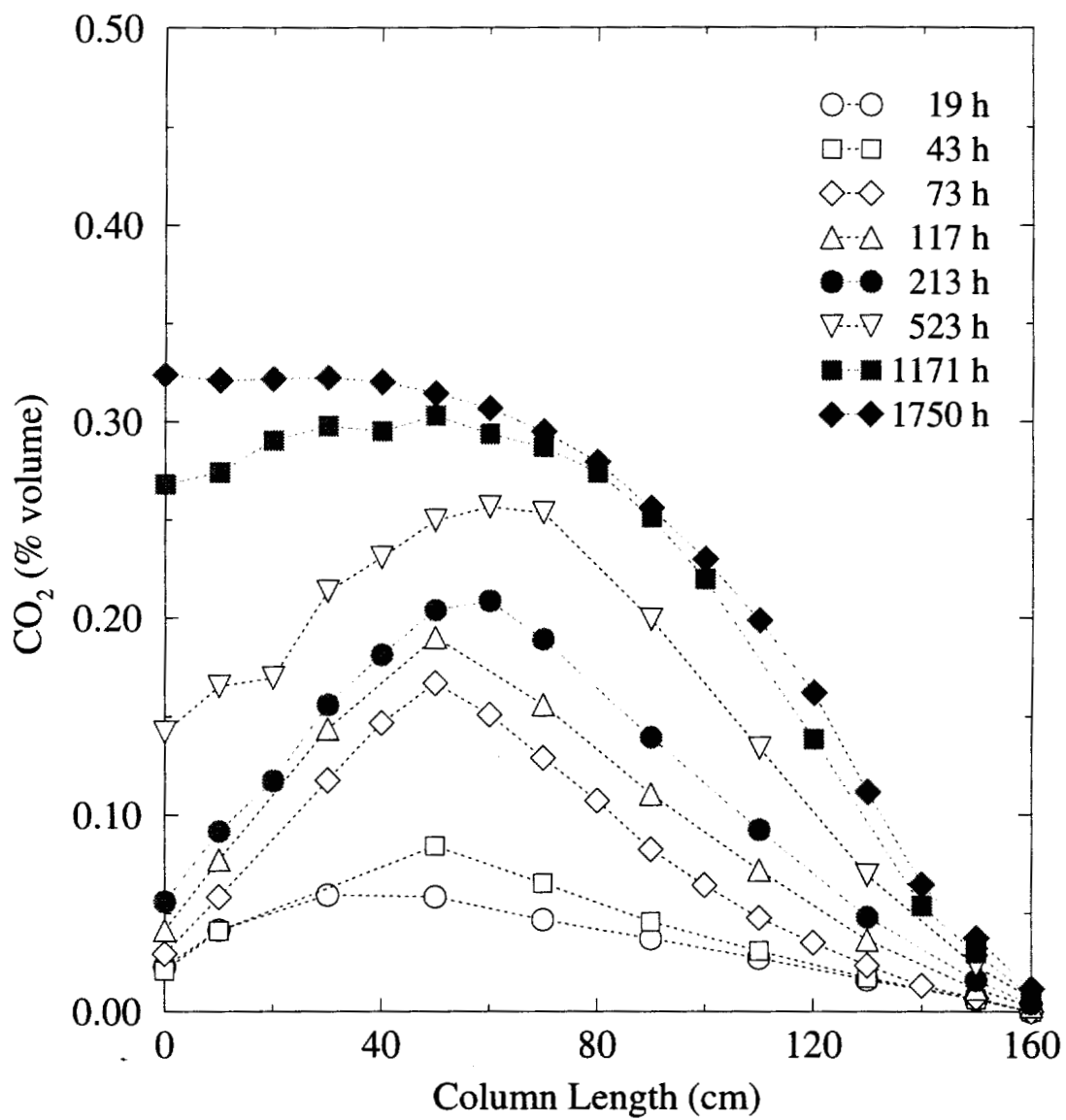


Figure 2.9. CO<sub>2</sub> profiles in Column 2 at selected sampling times.

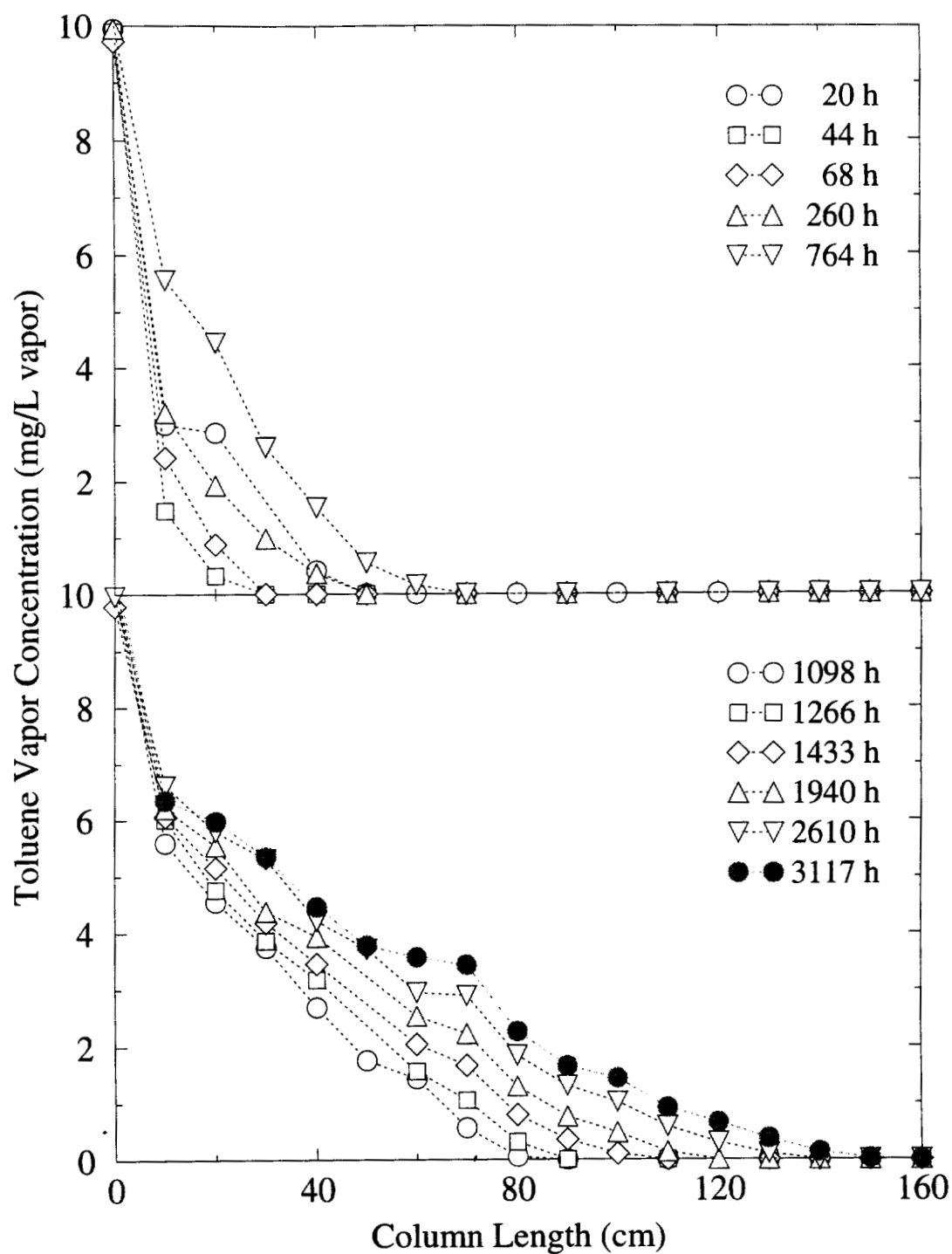


Figure 2.10. Toluene profiles in Column 3 at selected sampling times.

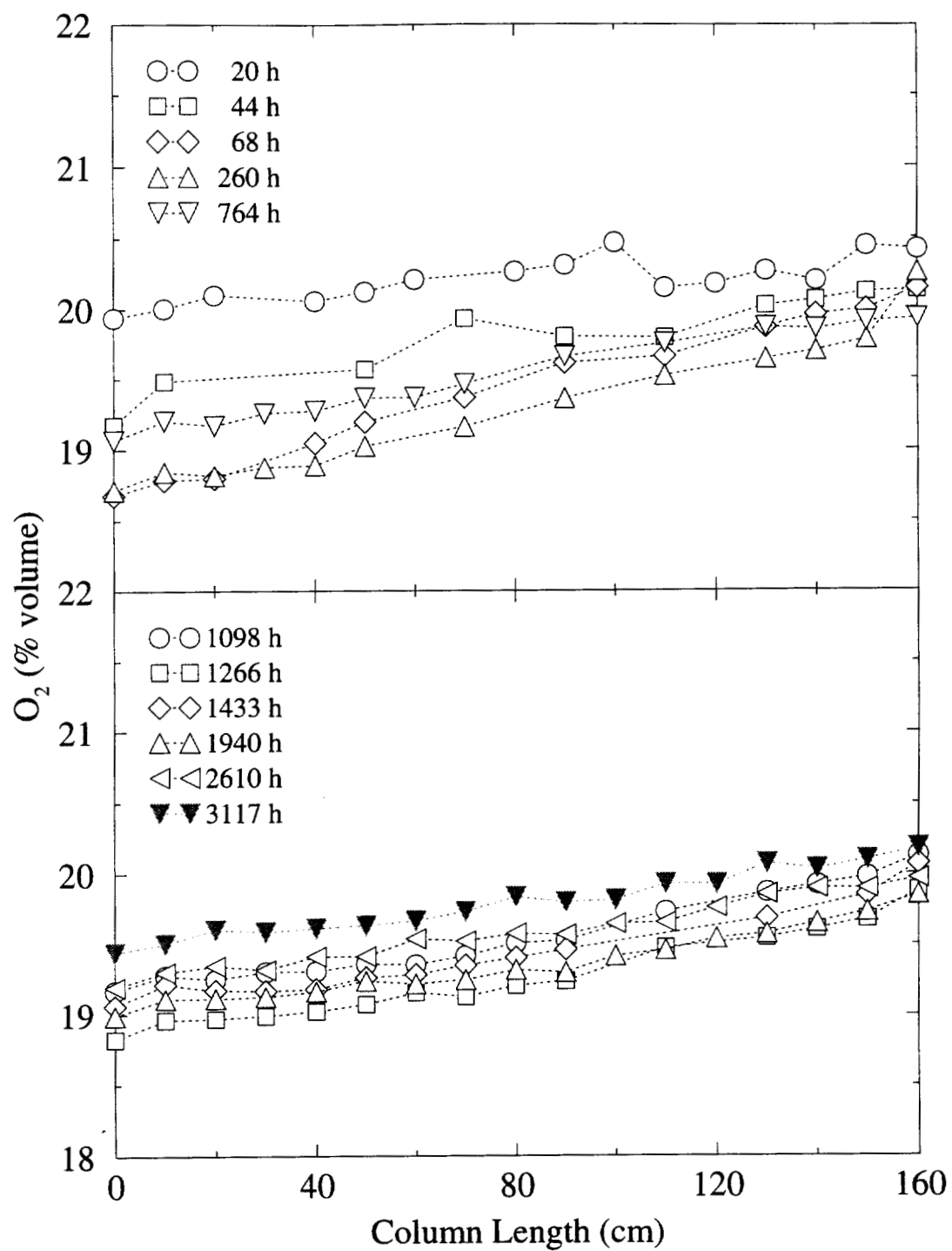


Figure 2.11.  $O_2$  profiles in Column 3 at selected sampling times.

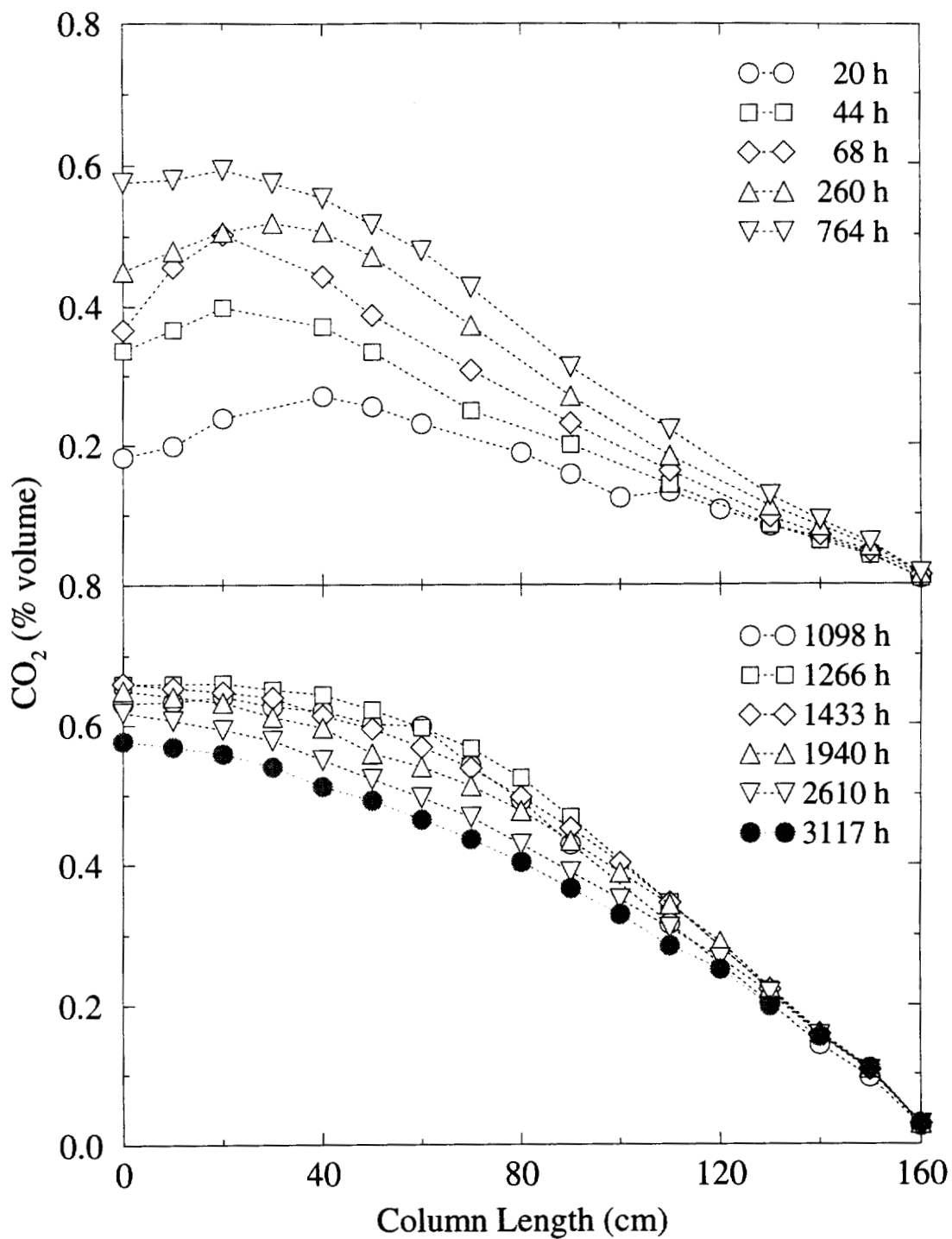


Figure 2.12. CO<sub>2</sub> profiles in Column 3 at selected sampling times.

## **CHAPTER 3**

### **AEROBIC DEGRADATION KINETICS OF TOLUENE IN AN UNSATURATED SANDY SOIL**

#### **3.1 INTRODUCTION**

Only in the last two decades, has it been noted that the subsurface supports a considerable microbial community with the ability to carry out biodegradation of contaminants (Wilson and McNabb, 1983). Due mainly to stringent oligotrophic conditions, rates of metabolism in subsurface communities are generally much slower than in aquatic or soil ecosystems (Federle et al., 1986; Wilson et al., 1985; Wilson and McNabb, 1983). Under aerobic conditions, subsurface microorganisms satisfy their energy requirements by oxidation of substrates using O<sub>2</sub> as an electron acceptor. In the absence of O<sub>2</sub>, other electron acceptors such as nitrate, sulfate, ferric ion, and CO<sub>2</sub> support diverse microbial communities. For light aromatic hydrocarbons such as BTEX, aerobic biodegradation is fast and has been widely demonstrated.

In contaminated groundwater, O<sub>2</sub> is often quickly depleted due to high demands by aerobes and slow replenishment rates. The depletion of O<sub>2</sub> generally leads to contaminant persistence in the saturated zone. On the contrary, aerobic biodegradation in the unsaturated zone may not be limited by O<sub>2</sub> availability because gas-phase diffusion is high. The removal of volatile hydrocarbons via biodegradation in the unsaturated zone has been demonstrated at many field sites. Most of the contaminant vapors have been removed before they reach ground surface (O'Leary et al., 1993; Ostendorf and Kampbell, 1991; Diem and Ross, 1988; Hult, 1987; Evans and Thomson, 1986).

The rate of biodegradation depends on the microbial population, the compound of interest, and a variety of environmental conditions. Due to variabilities of the

subsurface media and the microbial communities, the susceptibility of contaminants to degradation needs to be evaluated at each site. In order to quantitatively express biodegradation rates, a reaction-kinetics model is needed. Batch experiments provide a practical means for investigating biodegradation kinetics from which a rate expression and its coefficients can be determined. The biodegradation kinetics may then be incorporated into a contaminant transport/fate model. This chapter discusses batch studies of toluene biodegradation. The kinetic information obtained was then integrated into a mathematical model (Chapter 4), which was used in quantifying toluene migration observed in the column experiments reported earlier (see Chapter 2).

The purposes of batch studies were to examine the ability of natural microbial populations to aerobically degrade toluene as a sole C and energy source and to determine their biodegradation kinetics. In addition, studies were conducted to provide insight into the rate-limiting factors. Factors influencing biodegradation rates include the availability of inorganic nutrients and O<sub>2</sub>, substrate concentration and toxicity, predation, the presence of other substrates and metabolic toxins, and prior exposure. Toluene was chosen as the study compound to represent a group of potent aromatic compounds, BTEX, pervasively present at many petroleum-contaminated sites and waste-disposal landfills. Microbial degradation rates of toluene have been measured in laboratories by using culture media (Button, 1985; Robertson and Button, 1987) and natural microbial communities from subsurface (Allen-King et al., 1994; Alvarez et al., 1991; Chiang et al., 1989; Barker et al., 1987; Chang et al., 1985). The latter were often conducted in batch vessels using soil slurries at much more dilute concentrations than in natural environments. Spain et al. (1984) observed different results of biodegradation rates when different solid/water ratios were used. In order to estimate biodegradation kinetics in the columns, the batch studies conducted here were carried out under conditions which closely resembled those in the columns.

### 3.2 THEORETICAL BACKGROUND

Hydrocarbons entering an uncontaminated environment usually stimulate microbial growth (Leahy and Colwell, 1990; Atlas, 1981). Upon exposure to hydrocarbon contaminants, the otherwise oligotrophic microbial communities are selected based on their abilities to degrade the released chemicals. A typical growth curve for a microbial population in a particular culture medium is illustrated in Fig. 3.1. The growth curve can be divided into 4 distinct phases: lag, exponential, stationary, and death phases.

Microbial communities may not start growing immediately after exposure to a new substrate medium. An interval of time, called the *lag phase*, may be required for microbes to adapt to the new environment conditions. Adaptation may occur via three mechanisms: enzyme induction, gene transfer or mutation, and population changes. Often, the latter follows one of the first two (Spain et al., 1980). The time length for the latter depends on the growth rate of the microorganisms that degrade the material as well as the size of the initial population. It is usually in the order of days. The time required for enzyme induction is shorter, although longer time may be required at low substrate concentrations. Irreproducible lag periods among replicates are usually indicative of adaptation by mutation (Wiggins et al., 1987). For some compounds there appears to be a concentration threshold below which no adaptation could occur (Hutchins et al., 1983; Spain and Van Veld, 1983; Boethling and Alexander, 1979). Other possible explanations of the lag phase include preferential utilization of additional substrates, predation of the degrading organisms, and presence of metabolic inhibitors or toxins.

Most microorganisms proliferate by binary fission. As a consequence, cell number or cell mass in a population doubles during each generation time. The resulting pattern of population increase is referred to as *exponential growth*. Growth rate is defined to be a change in cell number or cell mass per unit time. The rate of exponential growth is influenced by inherent characteristics of the microbial species and external factors such as temperature and compositions of the culture medium. It is often difficult

to distinguish between lag and exponential growth of a small population. As a result, the period following exposure and prior to significant degradation, including both lag and early growth, are often operationally defined as the lag phase.

Growth rate in a closed system will reach a *stationary phase* due to a variety of causes, including (1) exhaustion of substrates or essential nutrients and (2) accumulation of waste or intermediate products. In the stationary phase, growth rates balance death rates, resulting in no net increase or decrease in cell number. In addition, cell metabolism continues at a minimal level for maintenance purpose. The duration of the stationary phase depends on the sensitivity of the specific organisms to the conditions of the medium.

Cells in a population may remain alive and continue to metabolize after a stationary phase is reached. However, cells in a closed environment often die, and the population is said to be in the *death phase*. During this death phase, death rates exceed rates of multiplication, and viable-cell count slowly drops with time. Sometimes cells lyse, leading to a decrease in both the total and viable counts.

### **3.2.1 Growth Kinetics**

In the following discussion, the simple case of a single-species microbial population growing on a single soluble organic compound as its sole C and energy source is considered. In addition, it is assumed that the chemical is nontoxic and that all the essential inorganic nutrients and growth factors needed by the microorganisms are abundant. The effect of organic concentration on total growth (difference between the initial and maximum cell density) and growth rate is shown in Fig. 3.2a. At very low organic concentrations, both the total growth and the growth rate are limited by the amount of substrate. Increasing organic concentration ultimately yields growth rates identical to the maximum growth rate. However, the total growth may still be limited by the substrate.

The concentration dependence between growth rate and the C source supporting the growth is shown in Fig. 3.2b. It has the shape of a hyperbolic curve and resembles such saturation processes as adsorption isotherm or Michaelis-Menton kinetics. Monod (1949) adopted a mathematical function similar to the Michaelis-Menton equation for describing growth kinetics

$$\mu = \frac{\mu_{\max} C}{K_s + C} \quad (3.1)$$

where  $\mu$  is the specific growth rate of the microbial population,  $\mu_{\max}$  is the maximum specific growth rate,  $C$  is the organic substrate concentration, and  $K_s$  is the organic concentration when the rate of growth is one-half of the maximum rate. The value for  $K_s$  represents the affinity of the microorganism for the growth-supporting compound. The lower the value, the greater is the affinity of the microorganism for the organic substrate. Both  $\mu_{\max}$  and  $K_s$  are characteristics of microbial species and the substrate used. Therefore, the specific growth rate,  $\mu$ , depends on the inherent character of the microorganisms and other external factors, for examples, the organic-substrate concentration and nutrient conditions. It is important to recognize that equation (3.1) was developed, assuming homogeneous environments for each cell with no barriers between the cells and substrate. Natural environmental systems comprise innumerable types of microorganisms in discrete habitats. Moreover, under most ecological conditions, a variety of factors may cooperate in limiting growth. Deviations from equation (3.1) are certainly expected in such heterogeneous unsaturated soils.  $K_s$  values for a given compound have been reported to be orders of magnitude larger in soils than in aquatic systems, due to a lower degree of contact in soil between the substrate and the microbes. In addition, larger values of  $K_s$  may be ascribed to lower bioavailability of the organic substrate as a result of sorption to aquifer material (Alexander and Scow, 1989).

When cells multiply exponentially in media containing a C source at concentrations far in excess of the  $K_s$ , the rate of growth can be expressed mathematically as

$$N = N_0 \exp^{kt} \quad (3.2)$$

where  $N$  and  $N_0$  are the cell numbers (or cell mass) at time  $t$  and  $t = 0$ , respectively. A semilogarithmic plot of  $N$  versus  $t$  of equation (3.2) results in a straight line. If it is assumed that each cell metabolizes the same amount of organic substrate during the exponential growth phase, a semilogarithmic plot of the amount of substrate metabolized versus time should also give a straight line. However, a semilogarithmic plot of substrate remaining versus time often does not give a straight line (Alexander and Scow, 1989). The shape of the curve that reflects logarithmic growth is depicted in Fig. 3.3. Because of a small initial population, most of the period during growth cycle occurs with little loss of the substrate level. Therefore, the initial rate of biodegradation is not markedly influenced by the concentration of substrate. During the period when nutrients are nonlimiting, the doubling of the population occurs at a constant time interval. As the population undergoes exponential growth, a sudden decline of the substrate level is shown. In fact, much of the disappearance of substrate often can be attributed to the last few doublings in population size.

### 3.2.2 Biodegradation Kinetics

Information on biodegradation kinetics is extremely important because it can be used to assess the concentration change of a chemical as a result of reactions at any time. A large volume of literature exists on the development of mathematical models for describing microbial transformation rates of toxic chemicals. Historically, the biodegradation-kinetics data have been fit by an empirical power-rate model (Alexander and Scow, 1989)

$$-\frac{dC}{dt} = kC^n \quad (3.3)$$

where  $t$  is time,  $k$  is the rate constant of the reaction, and  $n$  is a fitting parameter. When  $n = 1$ , the model is equivalent to first-order kinetics. First-order kinetics have been

described for many soil decomposition processes of nitrogenous species and mineralized carbonaceous wastes (Angelakis and Rolston, 1985), and for pesticide degradation in surface soils (Wagenet and Rao, 1985). First-order coefficients for toluene degradation in aquifer systems have also been reported (Chiang et al., 1989; Patrick et al., 1986; Zoetman et al., 1981). These coefficients often correspond to natural attenuations limited by the availability of  $O_2$ . Greater than first-order kinetics are commonly observed in soils (Alexander and Scow, 1989).

Simkins and Alexander (1984) derived kinetic models from Monod kinetics (equation 3.1) to describe biodegradation rates as a function of a limiting substrate concentration and population density. They assumed that cell quota (the reciprocal of cell yield) was invariant with time and substrate concentration, a sound approximation for a C substrate. The following is a general expression for concentration-dependent kinetics of biodegradation accompanied by microbial growth in a system of aqueous phase.

$$-\frac{dC}{dt} = \mu_{\max} C \frac{(C_0 + X_0 - C)}{K_s + C} \quad (3.4)$$

where  $C$  and  $C_0$  are the aqueous concentrations of the limiting substrate at time  $t$  and  $t = 0$ , respectively;  $X_0$  is the aqueous concentration of substrate required to produce the initial population. When  $C_0 \gg K_s$ , equation (3.4) may be reduced to

$$-\frac{dC}{dt} = \mu_{\max} (C_0 + X_0 - C) \quad (3.5)$$

Equation (3.5) represents logarithmic kinetics of substrate disappearance in a single-phase system. An analogous equation can be written for a multi-phase system (e.g., an unsaturated soil medium)

$$-\frac{dG}{dt} = \mu_{\max} \left( G_0 + \frac{\theta_w X_0}{a} - G \right) \quad ; \quad (3.6)$$

$$a = \theta_a + \theta_w H_{wa} + \rho_b K_d H_{wa}$$

where  $G$  and  $G_0$  are the air-phase concentrations of substrate at time  $t$  and  $t = 0$ , respectively;  $\theta_a$  and  $\theta_w$  are the respective volumetric contents of air and water phases;  $H_{wa}$  is the water-air partitioning coefficient;  $\rho_b$  is the bulk soil density;  $K_d$  is the distribution coefficient of the compound between soil and water phases. The derivation of equation (3.6) can be found in Appendix B. Equation (3.6) was used later in data analyses.

Published kinetic coefficients of toluene from several studies are compiled in Table 3.1. Clearly, there is some variation among the reported values. The incongruity may be attributed to the catabolic diversity of microbial populations and the different experimental conditions used in these studies. For instance, experiments conducted with pure cultures isolated from oligotrophic environments (Robertson and Button, 1987; Button, 1985) yield lower coefficient values than those by mixed cultures in nutrient-rich conditions (Alvarez et al., 1991). In addition, the discrepancy may also be caused by different methods in determining these parameters (i.e., continuous-flow vs. batch mode).

Barker et al. (1987) studied aerobic biodegradation of benzene, toluene, and *o*- and *m*-xylenes (BTX) in microcosms of saturated sandy aquifer material. The aqueous concentrations of BTX decreased from their initial values of 1,100-2,600  $\mu\text{g/L}$  to below 1-2  $\mu\text{g/L}$  within 78 days. The biodegradation kinetics were individually best described as zero-order reactions ranging from 33  $\mu\text{g/L/d}$  for benzene to 37  $\mu\text{g/L/d}$  for *o*-xylene. The dissolved  $\text{O}_2$  was never found to be less than 1  $\text{mg/L}$ . Zero-order kinetics were also used to represent mass loss rates of BTX at other initial concentrations. At lower initial concentrations, the mass loss rates of individual compounds were similar ( $\sim 43 \mu\text{g/L/d}$ ). At higher initial concentrations, the mass loss rates varied from about 27 to 52  $\mu\text{g/L/d}$ . An initial lag phase, when little mass loss occurred, ranged from 2-10 days. The incubation temperature was at  $10^\circ\text{C}$ . The observed rates of BTX loss were postulated to be controlled by the supply of  $\text{O}_2$  and not by the biotransformation kinetics. Neither  $\mu_{\text{max}}$  nor  $K_s$  was determined in their study.

MacQuarrie et al. (1990) obtained Monod coefficients for toluene degradation in aquifer sand from the University of Waterloo's research facility at the Canadian Forces

Base Borden by fitting a 1-D transport model to breakthrough data from a saturated flow-through column. The model considered advective transport, sorption, and decay of toluene, O<sub>2</sub>, and microbes, respectively. Microbial degradation was described by a dual-Monod type function which includes kinetics of toluene as well as O<sub>2</sub>. In addition to the Monod parameters, cell-yield and cell-decay coefficients were also obtained by fitting.

Alvarez et al. (1991) studied the kinetics of aerobic biodegradation of benzene and toluene in sandy aquifer material. Drained aquifer material and basal mineral media were added to serum bottles. The bottles were shaken and incubated at 25°C. Aerobic conditions were ensured throughout the entire experiment. A lag time of 1-2 days was observed. Aqueous concentrations higher than 100 mg/L were inhibitory. Batches with initial aqueous concentrations of benzene and toluene at 250 mg/L each exhibited no biodegradation for over a month. Initial biodegradation rates were measured for substrate concentrations ranging from 1-100 mg/L, and the Monod coefficients were obtained by Hanes linearization.

Soil from A, B, and C horizons of the unsaturated zone at Borden site was mixed with groundwater in microcosm studies for toluene biodegradation at 24°C (Allen-King et al., 1994). In most microcosms with soil previously exposed to toluene, aerobic biodegradation was initially controlled by substrate-limited growth, with a maximum growth rate of 2.0 d<sup>-1</sup> and a half-saturation constant of no greater than 100 µg/L in water. With repeated additions of toluene to the B- and C-horizon soils, transformation rates eventually declined to zero-order at 1.5 and 1.7 µg/g/d, respectively. Substrate-limited kinetics were not observed in the uncontaminated C-horizon soil, in which the rate of transformation was almost immeasurable.

In brief, the Monod-kinetics coefficients reflect complex interaction between inherent characteristics of the microbial species and their environmental conditions. Therefore, biodegradation experiments need to be a close representative of the study system to which the characterized kinetics will be applied. Since Monod coefficients may vary with the system conditions from which they are derived, environmental factors affecting biodegradation are the subject of next discussion.

### 3.2.3 Factors Affecting Biodegradation

In natural environments, a variety of factors influence the rate of biodegradation and, hence, the shape of the substrate disappearance curves. In addition to the chemical structure and concentration and the nature of the microbial communities, the rate and the extent of biodegradation are likely to be greatly influenced by various environmental factors. These factors include pH, temperature, the depletion of inorganic nutrients or growth factors, the availability of O<sub>2</sub>, the presence of other readily degradable substrates, inhibitors, or predators, the binding of the compound to colloidal matter, and prior exposure. In the unsaturated systems, the moisture content also plays an important role in controlling biodegradation.

Ridgway et al. (1990) investigated catabolic activity of gasoline-degrading bacteria by using groundwater and aquifer cores from a site contaminated by unleaded gasoline. The conditions at the site were characterized to be anoxic and depleted of inorganic nutrients such as N, and P. Of 15 gasoline hydrocarbons, toluene, *p*-xylene, and ethylbenzene were most frequently utilized by gasoline-degrading isolates. Unsubstituted aromatics such as benzene were less frequently used than most alkylated aromatics with the exception of *o*-xylene. The branched alkanes, such as 2,2,4-trimethylpentane, were the least frequently catabolized. Somewhat different findings were reported earlier by Jamison et al. (1975) in which gasoline-degrading isolates were obtained from groundwater following *in situ* injection of nutrients and O<sub>2</sub>. They reported that 2,2,4-trimethylpentane was the most frequently biodegraded compound and *p*-xylene was infrequently utilized. Toluene and ethylbenzene were among the most frequently used. These conflicting results may be due to different subsurface conditions of these two aquifers which may have enhanced the growth of microbial communities selectively (Ridgway et al., 1990).

The effects of inorganic nutrients and temperature on the biodegradation rates of crude oil and hexadecane were studied in a mixture of aquifer sediment and groundwater (Chang et al., 1985). Both crude oil and hexadecane exhibited a 2-day lag phase when

incubated at 12°C and 5-day at 2°C. O<sub>2</sub> uptake, hydrocarbon mineralization, and microbial growth were enhanced by increase in temperature, inorganic nutrients (N, P, and S), and O<sub>2</sub> availability. Nonetheless, the effect of temperature was relatively small when compared to those of O<sub>2</sub> and nutrients.

Biodegradation of 47 soluble hydrocarbons from gas oil were studied in groundwater batches by Kappeler and Wuhrmann (1978). After a lag phase of 5-6 days, individual hydrocarbon concentrations began to decrease at a measurable rate. They concluded that the lag phase preceding degradation was indicative of a small initial number of bacteria capable of oxidizing hydrocarbons. They also found that N and dissolved O<sub>2</sub> were two limiting factors in the complete degradation of these hydrocarbons in groundwater.

Several environmental factors affecting toluene degradation in groundwater under a chemical waste-disposal site were investigated (Armstrong et al., 1991). Toluene mineralization rate at 11°C was 36% of the rate at 25°C. Additions of P and potassium enhanced mineralization by twofold when compared to unamended samples. No effect of O<sub>2</sub> addition on toluene mineralization was observed.

The effect of inorganic nutrients on propane and butane degradation had been previously examined in the Columbia River sand studied here (Toccalino et al. 1993). N was shown to be the most limiting mineral nutrient in the sand. Butane degradation rates increased with increasing N concentrations and were not affected by the form of N added. All experiments were conducted with unsaturated soil at a water content of 4.0-4.5 ml of H<sub>2</sub>O per 100 g of dry soil. The incubation temperature was at 20°C.

The effect of N on toluene degradation kinetics was observed for A-, B-, and C-horizon soils from the unsaturated zone at Borden site (Allen-King et al., 1994). With repeated additions of toluene, soil of all horizons became limited with respect to N, resulting in a change in biodegradation kinetics. The addition of (NH<sub>4</sub>)<sub>2</sub>SO<sub>4</sub> relieved N-limiting conditions, and biodegradation kinetics were once again growth-limited. N was found more limiting in the B- and C-horizon soils. In the uncontaminated C-horizon soil, biodegradation was initially immeasurable. The addition of KNO<sub>3</sub> or NH<sub>4</sub>Cl accelerated

biodegradation, and growth-limited kinetics were observed. Because A-horizon soil contained more N than the others, more toluene was degraded in this horizon.

Despite its complexity, it is possible to characterize biodegradation kinetics empirically. More specifically, factors which most influence biotransformation may be determined, and functional relationships between these factors and substrate removal rates may be derived. In many instances, the rate of substrate disappearance may be described by concentration-dependent kinetics relating two variables: substrate and population concentrations (Simkins and Alexander, 1984). Without a full characterization of the relationships between all environmental variables, measured biodegradation parameters are system-specific. Therefore, caution should be taken when applying biodegradation-rate constants measured in one environment to another. As a consequence, it is necessary to conduct experiments for determining parameter values relevant to the system of interest. Such experiments are presented in the following sections.

### **3.3 EXPERIMENTAL METHODS**

#### **3.3.1 Experimental Design**

A schematic diagram of the vessels used in the batch experiments is shown in Fig. 3.4. The vessels were stainless-steel (SS) canisters (0.8-L) capped with a specially-designed low-dead-volume valve. Uncontaminated sandy soil from the Columbia River was air-dried, passed through a 2-mm sieve, before packed into a small column. The column was then saturated from the bottom with a  $\text{NH}_4\text{NO}_3$  (reagent grade, Aldrich Chemical Co., Inc., Milwaukee, WI) solution (22.2 mg-N/L) and subsequently drained to a residual moisture content by gravity. Approximately 55 g of moist sand was placed in each can. The headspace in the canister was to ensure a sufficient  $\text{O}_2$  supply throughout the experiment, as well as to prevent significant negative pressure developed due to frequent sampling. The latter effect was tested by sampling the autoclaved controls the same number of times as the active batches. A precalculated amount of pure

toluene (>99.9%, Aldrich Chemical Co., Inc., Milwaukee, WI) was injected with a 10- $\mu$ l syringe #1701 (Hamilton Co., Reno, NV) to give the desired initial concentration. The canister was then sealed, shaken, and incubated at 15°C for over night prior to the first sampling. Batch experiments were conducted in duplicate or triplicate. Sterile controls were prepared in the same manner, except that after their first samplings they were autoclaved at 121°C for 30 min on two consecutive days.

### 3.3.2 Sampling and Analysis Procedure

Toluene biodegradation kinetics were monitored by frequent measurements of headspace concentration with time. Each canister was shaken before it was analyzed. The experiments were terminated, when no toluene was detected in the headspace or when toluene disappearance rates became very slow. O<sub>2</sub>, CO<sub>2</sub>, and CH<sub>4</sub> were measured twice: once at the beginning and once more at the end of experiments.

Toluene concentration was analyzed by using a flame-ionization detector (FID) equipped on an HP-5890 gas chromatograph (Hewlett Packard, Avondale, Pa). An eight-port valve (Carle Instruments, Inc., Loveland, CO) with a 100- $\mu$ l sample loop heated to 100°C was used for sample injection. In the "injection" mode, the carrier gas (He) bypassed the valve via the dotted line (see Fig. 3.5a). A vacuum pump was connected to an "evacuation chamber". In the "load" mode, the "evacuation chamber" was connected to the canister which was opened just before the valve switched. The vapor from the canister (1.1 ml) was drawn to fill the sample loop and the chamber. As the valve switched back to the "injection" mode, the content of the sample loop was flushed by He to a 0.32 mm I.D., 30 cm long fused-silica capillary column (DB-1). The column temperature was at 150°C. Flow rates of He, air, and H<sub>2</sub> were 4, 400, and 35 cm<sup>3</sup>/min, respectively. N<sub>2</sub> was used as makeup gas at 30 cm<sup>3</sup>/min. The temperature of FID was at 200°C.

Respiration-gas analyses were performed by using an HP5890 GC equipped with a fourteen-port valve (Valco Instruments Co., Inc., Houston, TX) shown in Fig. 3.5b.

A 1.25-ml of vapor sample was drawn by vacuum to two sample loops on the valve. Each sample loop was connected to a packed column.  $O_2$  was separated on a 6.4 mm O.D., 48.3 cm long SS column packed with 60/80 mesh molecular sieve 5A (Altech Associates, Inc., Deerfield, ILL) and analyzed by a thermal-conductivity detector (TCD).  $CO_2$  and  $CH_4$  were separated on a 3.2 mm O.D., 40.6 cm long SS column filled with 100/120 mesh Spherocarb (Analabs, Norwalk, CT). The oven temperature was programmed at an initial temperature of  $40^\circ C$  for 1 min, then increased at  $30^\circ C/min$  to a final temperature of  $80^\circ C$ , and held at  $80^\circ C$  for 3 min. After separation,  $CO_2$  was reduced to  $CH_4$  in a catalyst column (Ni) heated at  $500^\circ C$ . Both gases were then analyzed by FID. The TCD and FID temperatures were at 105 and  $225^\circ C$ , respectively. He was used as the carrier gas to both detectors at 30 ml/min. He was also used as the reference gas for TCD at 30 ml/min. The air flow rate to FID was 400 ml/min.  $H_2$  (30 ml/min) was used as reductant in the catalytic reaction of  $CO_2$  to  $CH_4$ .

Gas-phase standards of toluene were used throughout these experiments. The standards were prepared in a 0.8-L SS canisters capped with SS-bellows valves (Whitey Co., Highland Heights, OH). A known quantity of pure liquid toluene was injected into each canister with a gas-tight syringe. Adequate time was allowed for toluene to vaporize before it was diluted with  $N_2$  to obtain the desired concentration. All canisters were stored in a cold room at  $15^\circ C$ , and their concentrations were corrected for the temperature effects. Respiration-gas standards were prepared in the same way as described earlier (Chapter 2).

Data acquisition and the valve were controlled by a Nelson Analytical 760 Series Interface (Nelson Analytical, Cupertino, CA). All peak areas were quantified by comparison with external standards as described above. The detection limits by these analytical methods were 0.014 mg/L for headspace toluene and 1 and 0.004% by volume for  $O_2$  and  $CO_2$ , respectively.

### 3.3.3 Data Analysis

Data from each batch were analyzed separately for  $\mu_{\max}$  and  $X_0$  by curve-fitting to the integrated form of equation (3.6). Nonlinear regression analyses were conducted by using Igor (WaveMetrics, Inc., Lake Oswego, OR), which employs the Levenberg-Marquardt algorithm (Press et al., 1988) in searching of the optimal fitting parameters. Values of individually fitted  $\mu_{\max}$  and  $X_0$  were then averaged among triplicates.

## 3.4 RESULTS AND DISCUSSIONS

### 3.4.1 Biodegradation Kinetics

A number of batch experiments were carried out with initial concentrations ranging from 0.6 mg/L to 9.0 mg/L. A period of 2-4 days elapsed before a decline of toluene vapor concentration was evident. The cause of this "lag" time was not investigated, although it was believed to occur because of small initial populations of toluene degraders. Once biodegradation became significant, toluene was completely consumed within 0.5-2 days. From this point on, the toluene concentration refers as to the vapor phase, unless otherwise stated.

Figure 3.6 shows measured headspace concentrations of toluene plotted with time for canisters at different initial concentrations ranging from 0.6-2.7 mg/L. These batches demonstrated a consistent pattern of degradation, which reflects logarithmic growth kinetics (see Fig. 3.3). Toluene concentrations remained unchanged for approximately 3 days before they rapidly reduced to below the detection limit. Figure 3.7 shows data from the same batch experiments in terms of toluene concentration being removed. These curves resemble growth kinetics occurring in the batch experiments, if it is assumed that the quantity of toluene degraded is proportional to the cell density produced. Here, the exponential growth and the "lag" time (the time elapsed before degradation was evident) were readily illustrated. All batches exhibited similar lag times

and growth rates. Table C.1 (Appendix C) summarizes the initial and final values of O<sub>2</sub> and CO<sub>2</sub> in these canisters. O<sub>2</sub> levels in all canisters were nearly unchanged and CO<sub>2</sub> levels increased approximately 17 fold from ambient concentrations. Additionally, no CH<sub>4</sub> was produced. These results indicated that aerobic conditions existed during the experiment. Since toluene was the only added C source, the evolution of CO<sub>2</sub> was an indicative of microbial degradation of toluene. Hence, these results suggested that the indigenous microorganisms in the study soil were capable of utilizing toluene as the sole C and energy source.

The change in concentration with time for batches with initial concentrations ranging from 2.5 to 5.1 mg/L are shown in Fig. 3.8. The depletion of toluene was apparent at ~2-3 days after toluene was introduced. The disappearance rate then increased exponentially until toluene was almost gone. A low concentration of toluene appeared to persist in some canisters.

The above data were analyzed by nonlinear regression in order to determine  $\mu_{\max}$  and  $X_0$ . Examples of curve fits are shown in Fig. 3.9, and fitted values of  $\mu_{\max}$  and  $X_0$  from individual curves are summarized in Table 3.2.

Batches incubated at higher initial concentrations (5.9-8.0 mg/L) are plotted in Fig. 3.10. Toluene disappearance rate was initially insignificant during a period of ~4 days, after which it increased, but later decreased. All autoclaved batches showed no significant changes of headspace toluene over 15 days (Fig. 3.11).

Biodegradation kinetics at initial concentrations of 5.3, 7.3, and 9.2 mg/L were conducted using same soil amended with higher content of N (96.6 mg-N/L). At all three concentrations, the biodegradation became evident in 2 days, and by day 4 little toluene was left (Fig. 3.12). Degradation kinetics of a batch at low N content (shown by open symbols) are included in the figure for comparison. The lag time was somewhat reduced in batches with higher N. However, the most distinct difference was that in the high N case, the biodegradation rate did not decline with time.

### 3.4.2 Respike Assays

After all toluene was exhausted, most canisters were respiked with toluene and degradation was monitored. Two different types of response were observed. In canisters that had previously received low toluene concentration ( $<3$  mg/L), degradation resumed at a much faster rate than what they had demonstrated earlier (see Fig. 3.13a). In contrast, degradation in those canisters that had previously received high toluene concentration ( $\geq 3$  mg/L) proceeded at a much slower rate. Further additions of toluene in the canisters with faster rates eventually resulted in a decline of the biodegradation rate. These results suggested that the bioavailable N in the soil was becoming depleted. The hypothesis was tested by adding 0.5 ml of 22.4 mg-N/L as  $\text{NaNO}_3$  (99.999%, Aldrich Chemical Co., Inc., Milwaukee, WI) to some canisters and 0.5 ml of NaCl solution with an equimolar concentration as  $\text{NaNO}_3$  solution to others. The results of selected canisters are shown in Fig. 3.13b. Canisters added with  $\text{NaNO}_3$  showed an abrupt drop of toluene level after one day whereas those of NaCl showed no change in their courses. The amounts of toluene needed to deplete the available N in soil were nearly the same in all canisters.

These kinetic and respike experiments have demonstrated that biodegradation in this system is growth related, and it follows a logarithmic rate until the bioavailable N becomes limited. Subsequently, the biodegradation rate is severely reduced. Data for the majority of these experiments are compiled in Appendix C.

#### *The Effect of Concentration*

When N was not limiting, exponential kinetics were observed for aerobic biodegradation of toluene at concentrations ranging from 0.6 to 8.0 mg/L. Even at the lowest initial concentration, the biodegradation kinetics were not affected by the concentration of toluene.  $K_s$  of this system was very low and could not be determined by the experimental method used. This pattern of toluene degradation kinetics was also observed by Allen-King et al. (1994).

Only those data showing complete removal of toluene were fitted to equation (3.6), and values of  $\mu_{\max}$  and  $X_0$  were obtained for each batch. Using weighted-mean values of  $\mu_{\max}$  and  $X_0$ , a maximum value of  $K_s$  was back-calculated from equation (B.7) (in Appendix B) to be 0.003 mg/L (equivalent to an aqueous concentration of 0.014 mg/L). These values of  $\mu_{\max}$  ( $0.103 \pm 0.002 \text{ h}^{-1}$ ) and  $K_s$  ( $\leq 0.003 \text{ mg/L}$ ) were much lower than those reported by Alvarez et al. (1991) but were consistent with those reported by Allen-King et al. (1994) and Robertson and Button (1987). Considerably lower  $K_s$  values were observed for oligotrophs (Robertson and Button, 1987) than eutrophs (Alvarez et al., 1991), presumably because oligotrophs need to strive for survival in nutrient-limiting conditions (Slater and Lovatt, 1984). Since the value of  $K_s$  was substantially lower than the concentration commonly found at a contaminated site,  $K_s$  was not environmentally relevant for this system. In brief, aerobic degradation of toluene in this unsaturated sandy soil conformed to equation (3.6) when N was not limiting, and the corresponding growth/degradation rate appeared more or less independent of toluene concentration.

Inhibition by toluene was not observed over the concentration range studied. Fig. 3.14 shows selected kinetic plots representing the entire concentration range. Except for some variation in the lag periods, the biodegradation kinetics were similar at different concentrations, suggesting that inhibition did not occur. This is consistent with results observed by Alvarez et al. (1991).

#### *The Effect of N*

The kinetic experiments conducted here demonstrated that N was the limiting inorganic nutrient in the soil studied here. N was previously determined to be the most limiting mineral nutrient in this soil for alkane degradation (Toccalino et al., 1993). The dependence of biodegradation on the presence of N suggested that the process was growth related. In addition, increases in toluene degradation rates with time suggested that the microbial-population size and thus the microbial activity might have increased over time. Other researchers also found faster removal rates of BTX when additional N was added (Allen-King et al., 1994; O'Leary et al., 1993; Aelion and Bradley, 1991).

### *The Effect of Lag*

No immediate decrease of toluene concentration was observed in any batch experiments when they were first introduced to toluene. These experiments repeatedly showed an operationally-defined lag period of 2-4 days, during which toluene disappearance was not measurable. Based on the available data, it was not possible to conclusively state what caused the observed lag period. However, the length of the lag time was too long to be caused by merely enzyme induction. In addition, the consistent lag time among triplicates did not suggest the possibility of gene transfer. Although no confirmation of which mechanisms causing the observed lag periods was sought in this study, it was suggested that the observed lag reflected the selection of toluene degraders from a small initial population. Other studies of toluene biodegradation showed that native microorganisms degrade toluene almost immediately, and that the apparent lag period in the biodegradation curve reflects the continuous growth of a small initial population (Swindoll et al., 1988; Barker et al., 1987). The Monod equation (equation 3.4) does not include the lag effect. Therefore, kinetic parameters obtained by fitting data to equation (3.6) presume the cause of lag was due to growth from a small initial population.

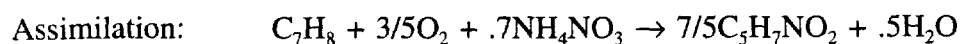
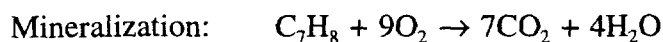
An estimate of the initial population of toluene degraders can be made by extrapolating a straight line through the data point to y-axis (Fig. 3.15). The intercept of this line (0.0062 mg/L) represents the amount of toluene that would be required to produce the initial cell concentration. The corresponding mass of toluene was calculated to be ~0.005 mg per 50 g of dry sand. Using a biomass yield of 0.5 (g of biomass per g of toluene degraded), the total cell mass of  $\sim 5 \times 10^{-5}$  mg-biomass per g of dry sand was obtained, which was converted to a cell number of  $\sim 5 \times 10^4$  cells per g of dry sand, assuming a cell weight of  $10^{-9}$  mg (Alvarez et al., 1991; Bouwer and McCarty, 1984). This number agrees with toluene degraders enumerated by the MPN method in Borden sand (Allen-King et al., 1994).

### 3.4.3 Biodegradation Stoichiometry

An equation of biodegradation reaction was predicted by using the extent of C assimilation and balanced equations representing an energy-yielding and a biomass-producing processes. The extent of C assimilation was calculated based on a C balance of CO<sub>2</sub> evolved and toluene degraded, assuming all toluene that was not mineralized was incorporated into biomass. Appendix C illustrates these calculations using initial and final concentrations of toluene and CO<sub>2</sub> from canisters that were not N-limited. The reason for using only canisters not depleted in N because during N- or C-limiting conditions, growth is suppressed, and more of the metabolite is expected to be mineralized for maintenance functions. A low percentage (29-43%) of toluene mineralized was found in every case. [The corresponding range of toluene assimilated was 57-71%]. As shown in Table C.4 (Appendix C), these measured values of percent mineralization were much lower than the range (50-60%) reported in the literature (Alexander, 1977; Porges et al., 1956).

The apparently low amount of CO<sub>2</sub> measured might have been due to incomplete mineralization of toluene, syntheses of extracellular materials, or accumulation of "storage" polymers (e.g., poly-β-hydroxybutyric acid and glycogen granules). Adsorption of CO<sub>2</sub> on goethite and hematite surfaces (see measured values of free irons in Table 2.1, Chapter 2) in the form of carbonates (van Geen et al., 1994) could not account for the low amount of CO<sub>2</sub> measured. Since soil pH (~6.5) did not change during the experiments, and since not much carbonates could be present at this pH (~7.5x10<sup>-10</sup> moles), precipitation of CO<sub>2</sub> with common divalent ions was not likely in this case. Hence, the low amount of CO<sub>2</sub> measured was probably resulted from biological causes mentioned above.

The following equations may be written for mineralization, assimilation, and overall metabolism, respectively, by taking into account the percentage of toluene mineralized and assimilated.



For the assimilative equation, an empirical biomass formula was used to represent the proportions of the major atoms present in the cell composition (Porges et al., 1956). A mean value of 61% was used to represent the extent of toluene assimilation. The overall metabolism equation predicted stoichiometric coefficients for  $NH_4NO_3$ ,  $O_2$ , and  $CO_2$  to be 0.5, 3.4, and 2.3, respectively. These coefficients could be used in predicting production rates of  $CO_2$  and removal rates of  $O_2$  and N.

Molar ratios of  $NH_4NO_3$  to toluene were estimated from data of those canisters indicating N limitation (see Tables C.5 and C.6 in Appendix C). An average value of these ratios was 0.16, which was comparable to the stoichiometric coefficient (0.5) predicted by the overall-metabolism equation. The quantity of N mass required to convert toluene C to biomass may also be estimated by using the extent of C assimilation and the C:N ratio found in cellular material. A value of 10:1 is widely accepted for C:N ratio for a mixed microbial population in soils (Atlas, 1981; Dibble and Bartha, 1979). Combining the value of C assimilation and the C:N ratio in cell mass, a C:N ratio of 15:1 was obtained for biodegradation. This was in good agreement with the value of 19:1 (Table C.5 and C.6) observed in the current experiments. The C:N ratio implies that a decomposition of 1 g of C from substrate toluene requires 0.06 g of N.

As seen in Tables C.1 and C.2, the degradation of toluene did not result in significant  $O_2$  depletion in any batches. As a consequence, a mass balance of  $O_2$  could not be constructed, and the molar ratio of  $O_2$  to toluene was unknown.

### 3.5 CONCLUSIONS

A series of batch studies for aerobic biodegradation of toluene was conducted using unsaturated Columbia River sand. The indigenous microorganisms were capable

of using toluene as the sole source of C and energy in the presence of  $O_2$ . This conclusion was supported by the disappearance of toluene, the production of  $CO_2$ , and the absence of  $CH_4$ .  $O_2$  levels in all canisters were nearly unchanged at the end of all experiments, confirming the existence of aerobic conditions. In all batches, a short lag was observed before biodegradation became apparent, after which toluene was rapidly removed. Furthermore, a degradation pattern that reflects exponential growth, of which the rate increased exponentially with time, was observed. However, after all bioavailable N was depleted, the degradation rate fell to a low level. When additional N was added, rapid degradation resumed, indicating that the extent of toluene degradation depended on the bioavailability of N. Batches amended with higher content of N permitted more toluene to be utilized than those with lower content. No effect of toluene concentration on the biodegradation rate was observed over the concentration range tested. The autoclaved controls showed no significant decrease in toluene concentrations for 15 days. Although there was no corresponding biomass measurements to confirm the association of biodegradation with growth, the fact that biodegradation was N-dependent provided indirect evidence.

Nonlinear regression analyses were used to estimate kinetic parameters from the substrate depletion curves. Mean values of  $\mu_{max}$  and  $X_0$  for toluene in this system were  $0.103 \text{ h}^{-1}$  and  $0.007 \text{ mg/L}$ , respectively.  $K_s$  was too low to be measured by the experimental and analytical procedures used in this study. Nevertheless, the maximum value of  $K_s$  was estimated to be no greater than  $0.003 \text{ mg/L}$ . These values of kinetic coefficients were assumed to represent biodegradation rates in the column experiments (Chapter 2). In the next chapter, the biodegradation kinetics as described by equation (3.6) will be incorporated into a mathematical model which includes other physical and chemical processes as well. The values of microbial parameters derived here and other independently-derived model inputs will be used in assessing the transport in the column experiments.

### 3.6 REFERENCES

- Aelion, C. M., and P. M. Bradley, Aerobic biodegradation potential of subsurface microorganisms from a jet fuel-contaminated aquifer, *Appl. Environ. Microbiol.*, *57*, 57-63, 1991.
- Angelakis, A. N., and D. E. Rolston, Transient movement and transformation of carbon species in soil during wastewater application, *Water Resour. Res.*, *21*, 1141-1148, 1985.
- Alexander, M., *Introduction of Soil Microbiology*, 2nd ed., John Wiley & Sons, Inc., New York, 1977.
- Alexander, M., and K. M. Scow, Kinetics of biodegradation in soil, in *Reactions and Movement of Organic Chemicals in Soils*, edited by B. L. Sawhney and K. Brown, SSSA Special Publication No. 22, Soil Science Society of America, Madison, pp. 243-269, 1989.
- Allen-King, R. M., J. F. Barker, R. W. Gillham, and B. K. Jensen, Substrate- and nutrient-limited toluene biotransformation in sandy soil, *Environ. Toxicol. Chem.*, *13*, 693-705, 1994.
- Alvarez, P. J. J., P. J. Anid, and T. M. Vogel, Kinetics of aerobic biodegradation of benzene and toluene in sandy aquifer material, *Biodegradation*, *2*, 43-51, 1991.
- Armstrong, A. Q., R. E. Hodson, H. M. Hwang, and D. L. Lewis, Environmental factors affecting toluene degradation in ground water at a hazardous waste site, *Environ. Toxicol. Chem.*, *10*, 147-158, 1991.
- Atlas, R. M., Microbial degradation of petroleum hydrocarbons: An environmental perspective, *Microbiol. Rev.*, *45*, 180-209, 1981.
- Barker, J. F., G. C. Patrick, and D. Major, Natural attenuation of aromatic hydrocarbons in a shallow sand aquifer, *Ground Water Monitoring Review*, *7*, 64-71, 1987.
- Boethling, R. S., and M. Alexander, Effects of concentration of organic chemicals on their biodegradation by natural microbial communities, *Appl. Environ. Microbiol.*, *37*, 1211-1216, 1979.
- Bouwer, E. J., and P. L. McCarty, Modeling of trace organics biotransformation in the subsurface, *Ground Water*, *22*, 433-440, 1984.

Brock, T. D., and M. T. Madigan, *Biology of Microorganisms*, 5th ed., Prentice-Hall, Inc., New Jersey, 1988.

Button, D. K., Kinetics of nutrient-limited transport and microbial growth, *Microbiol. Rev.*, 49, 270-297, 1985.

Chang, F. H., M. F. Hult, N. N. Noben, D. Brand, Microbial degradation of crude oil and some model hydrocarbons, in U.S. Geological Survey Program on Toxic Waste--Ground-Water Contamination, Proceedings of the Second Technical Meeting, Cape Cod, Massachusetts, Oct. 21-25, 1985, *U.S. Geol. Surv. Open File Rep. 86-481*, pp. C33-C42, 1988.

Chiang, C. Y., J. P. Salanitro., E. Y. Chai, J. D. Colthart, and C. L. Klein, Aerobic biodegradation of benzene, toluene, and xylene in a sandy aquifer - Data analysis and computer modeling, *Ground Water*, 27, 823-834, 1989.

Choi, Y., J. Lee, and H. Kim, A novel bioreactor for the biodegradation of inhibitory aromatic solvents: Experimental results and mathematical analysis, *Biotechnol. Bioeng.*, 40, 1403-1411, 1992.

Diem, D. A., and B. E. Ross, Field Evaluation of a soil-gas Analysis method for detection of subsurface diesel fuel contamination, in *Proceedings of the Second National Outdoor Action Conference on Aquifer Restoration Groundwater Monitoring and Geophysical Methods*, National Water Well Association, Dublin, Ohio, pp. 1015-1030, 1988.

Evans, O. D., and G. M. Thompson, Field and Interpretation Techniques for Delineating Subsurface Petroleum Hydrocarbon Spills Using Soil Gas Analysis, in *Proceedings of the NWWA/API Conference on Petroleum Hydrocarbons and Organic Chemicals in Ground Water: Prevention, Detection, and Restoration*, National Water Well Association, Dublin, Ohio, pp. 444-455, 1986.

Federle, T. W., D. C. Dobbins, J. R. Thornton-Manning, and D. D. Jones, Microbial biomass, activity, and community structure in subsurface soils, *Ground Water*, 24, 365-374, 1986.

Hult, M. F., Microbial oxidation of petroleum vapors in the unsaturated zone, in U.S. Geological Survey Program on Toxic Waste--Ground-Water Contamination, edited by B. J. Franks, Proceedings of the Third Technical Meeting, Pensacola, Florida, March 23-27, 1987, *U.S. Geol. Surv. Open File Rep.*, 87-109, pp. C25-C26, 1987.

Hutchins, S. R., S. B. Tomson, and C. H. Ward, Trace organic contamination of ground water from a rapid infiltration site: a laboratory-field coordinated study, *Environ. Toxicol. Chem.*, 2, 195-216, 1983.

Jamison, V. W., R. L. Raymond, and J. O. Hudson Jr., Biodegradation of high octane gasoline in groundwater, *Dev. Ind. Microbiol.*, 16, 305-312, 1975.

Kappeler, T. H., and K. Wuhrmann, Microbial degradation of the water-soluble fraction of gas oil. II. Bioassays with pure strains, *Water Res.*, 12, 335-342, 1978.

Leahy, J. G., and R. R. Colwell, Microbial degradation of hydrocarbons in the environment, *Microbiol. Rev.*, 54, 305-315, 1990.

MacQuarrie, K. T. B., E. A. Sudicky, and E. O. Frind, Simulation of biodegradable organic contaminants in groundwater, 1, Numerical formulation in principal directions, *Water Resour. Res.*, 26, 207-222, 1990.

Monod, J., The growth of bacterial cultures, *Ann. Rev. Microbiol.*, 371-393, 1949.

O'Leary, K. E., J. F. Barker, R. W. Gillham, Surface application, of dissolved BTEX: A prototype field experiment, in *Proceedings of the Conference on Petroleum Hydrocarbons and Organic Chemicals in Ground Water: Prevention, Detection, and Restoration*, Ground Water Management, Dublin, Ohio, pp. 149-160, 1993.

Ostendorf, D. W., and D. H. Kampbell, Biodegradation of hydrocarbon vapors in the unsaturated zone, *Water Resour. Res.*, 27, 453-462, 1991.

Patrick, G., J. F. Barker, R. W. Gillham, C. I. Mayfield, and D. Major, The behaviour of soluble petroleum product derived hydrocarbons in groundwater. Phase II. PACE Rept. No. 86-1, Petrol. Assoc. for Conservation Can. Environ., Ottawa, 1986.

Porges, N., L. Jasewicz, and S. R. Hoover, Principles of biological oxidation, In *Biological Treatment of Sewage and Industrial Wastes*, edited by McCabe B. J., and W. W. Eckenfelder, Reinhold, New York, pp. 35-48, 1956.

Press, W. H., B. P. Flannery, S. A. Teukolsky, and W. T. Vetterling, *Numerical Recipes in C*, Cambridge University Press, Cambridge, 1988.

Ridgway, H. F., J. Safarik, D. Phipps, P. Carl, and D. Clark, Identification and catabolic activity of well-derived gasoline-degrading bacteria from a contaminated aquifer, *Appl. Environ. Microbiol.*, 56, 3565-3575, 1990.

Robertson, B. R., and D. K. Button, Toluene induction and uptake kinetics and their inclusion in the specific-affinity relationships describing rates of hydrocarbon metabolism, *Appl. Environ. Microbiol.*, 53, 2193-2205, 1987.

Simkins, S., and M. Alexander, Models for mineralization kinetics with the variables of substrate concentration and population density, *Appl. Environ. Microbiol.*, 47, 1299-1306, 1984.

Slater, J. H., and D. Lovatt, Biodegradation and the significance of microbial communities, in *Microbial Degradation of Organic Pollutants*, edited by Gibson, D. T., Marcel Dekker, Inc., New York, pp. 439-485, 1984.

Spain, J. C., P. H. Pritchard, and A. W. Bourquin, Effects of adaptation on biodegradation rates in sediment/water cores from estuarine and freshwater environments, *Appl. Environ. Microbiol.*, 40, 726-734, 1980.

Spain, J. C., and P. A. Van Veld, Adaptation of natural microbial communities to degradation of xenobiotic compounds: Effects of concentration, exposure time, inoculum, and chemical structure, *Appl. Environ. Microbiol.*, 45, 428-435, 1983.

Spain, J. C., P. A. Van Veld, C. A. Monti, P. H. Pritchard, and C. R. Cripe, Comparison of *p*-nitrophenol biodegradation in field and laboratory test systems, *Appl. Environ. Microbiol.*, 48, 944-950, 1984.

Swindoll C. M., C. M. Aelion, and F. K. Pfaender, Influence of inorganic and organic nutrients on aerobic biodegradation and on the adaptation response of subsurface microbial communities, *Appl. Environ. Microbiol.*, 54, 212-217, 1988.

Toccalino, P. L., R. L. Johnson, and D. R. Boone, Nitrogen limitation and nitrogen fixation during alkane biodegradation in a sandy soil, *Appl. Environ. Microbiol.*, 59, 2977-2983, 1993.

van Geen, A., A. P. Robertson, and J. O. Leckie, Complexation of carbonate species at the goethite surface: Implications for adsorption of metal ions in natural waters, *Geochim. Cosmochim. Acta*, 58, 2073-2086, 1994.

Wagenet, R. J., and P. S. C. Rao, Basic concepts of modeling pesticide fate in the crop root zone, *Weed Sci.*, 33(Suppl. 2), 25-32, 1985.

Wiggins, B. A., S. H. Jones, and M. Alexander, Explanations for the acclimation period preceding the mineralization of organic chemicals in aquatic environments, *Appl. Environ. Microbiol.*, 53, 791-796, 1987.

Wilson, J. T., and J. F. McNabb, Biological transformation of organic pollutants in groundwater, *EOS*, 64, 505-506, 1983.

Wilson, J. T., J. F. McNabb, J. W. Cochran, T. H. Wang, M. B. Tomson, and P. B. Bedient, Influence of microbial adaptation on the fate of organic pollutants in ground water, *Environ. Toxicol. Chem.*, 4, 721-726, 1985.

Zoetman, B. C. J., E. De Greef, and F. J. J. Brikmann, Persistency of organic chemicals in groundwater, Lessons from soil pollution incidents in the Netherlands, *Science of the Total Environment*, 21, 187-202, 1981.

**Table 3.1. Monod coefficients for aerobic biodegradation of toluene (after Alvarez et al., 1991).**

k (g-compound per g-cells per day)	Y (g-cell per g-compound)	$\mu_m = k \cdot Y$ (d <sup>-1</sup> )	K <sub>s</sub> (mg/L)	Specific first- order coefficient (k/K <sub>s</sub> ) (L/mg/d)	Method of measurement	References
0.004	0.01	0.00004	0.33	0.01	Total <sup>14</sup> C-labeled product production, suspension of <i>Pseudomonas</i> sp. T2 (marine strain). Uninduced cells	Button (1985)
11	0.28	3.08	0.43	25.5	Total <sup>14</sup> C-labeled product production, suspension of <i>Pseudomonas</i> sp. T2 (marine strain). Induced cells	Button (1985)
0.013	0.1	0.0013	0.034	0.38	<sup>14</sup> CO <sub>2</sub> production, <i>Pseudomonas</i> sp. T2 (marine strain) Uninduced cells	Robertson & Button (1987)
0.33	0.17	0.056	0.044	7.7	<sup>14</sup> CO <sub>2</sub> production, <i>Pseudomonas</i> sp. T2 (marine strain) Induced cells	Robertson & Button (1987)
0.49	0.43	0.21	0.65	0.75	Computer model fit to data from flow through column packed with aquifer material	MacQuarrie et al. (1990)
9.9	0.5	2.16	17.4	0.57	Substrate disappearance in batch incubations with aquifer material in basal medium	Alvarez et al. (1991)
-	-	0.437	6	-	Optical density of the culture broth in batch incubations with induced <i>Pseudomonas Putida</i>	Choi et al. (1992)
-	0.5-1.5	2.0	<0.1	-	Substrate disappearance in microcosms of aquifer sand mixed with groundwater	Allen-King et al. (1994)

**Table 3.2. Values of kinetic coefficients fitted to equation (3.6).**

Can #	$X_0$ (mg/L)	Std Dev.	$\mu_{\max}$ (h <sup>-1</sup> )	Std Dev.
1	0.006	0.007	0.111	0.014
2	0.005	0.007	0.111	0.015
3	0.007	0.008	0.111	0.012
11	0.015	0.011	0.095	0.008
12	0.005	0.004	0.112	0.010
13	0.006	0.005	0.107	0.009
6	0.024	0.012	0.093	0.005
16	0.005	0.003	0.120	0.007
"c"	0.017	0.009	0.097	0.005
5	0.122	0.124	0.100	0.012
4	0.176	0.141	0.098	0.010
14	0.012	0.011	0.109	0.009
8	0.031	0.039	0.120	0.015
9	0.036	0.044	0.106	0.013
10	0.036	0.037	0.108	0.011
15	0.055	0.058	0.102	0.012
Average	0.007	0.002	0.103	0.002

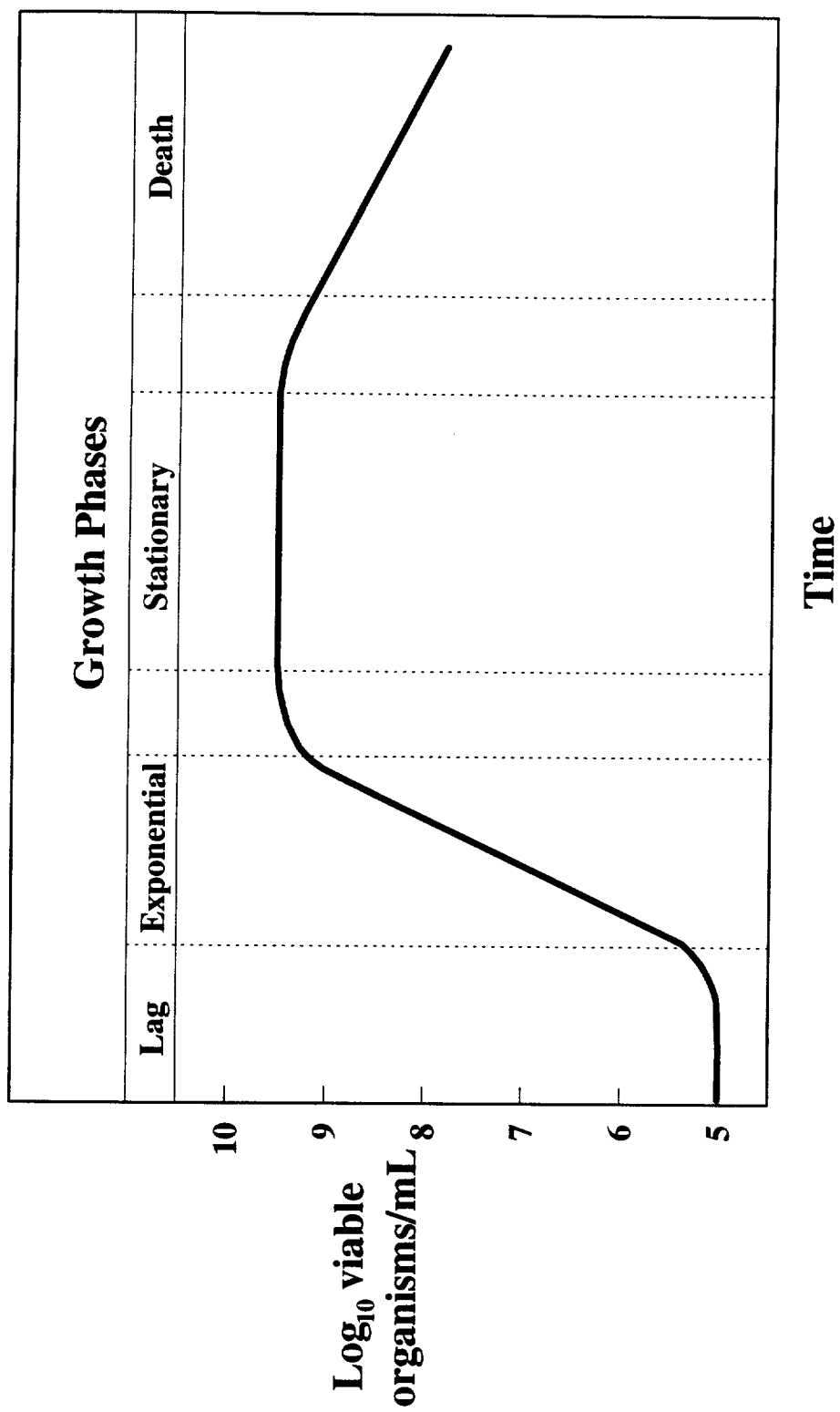
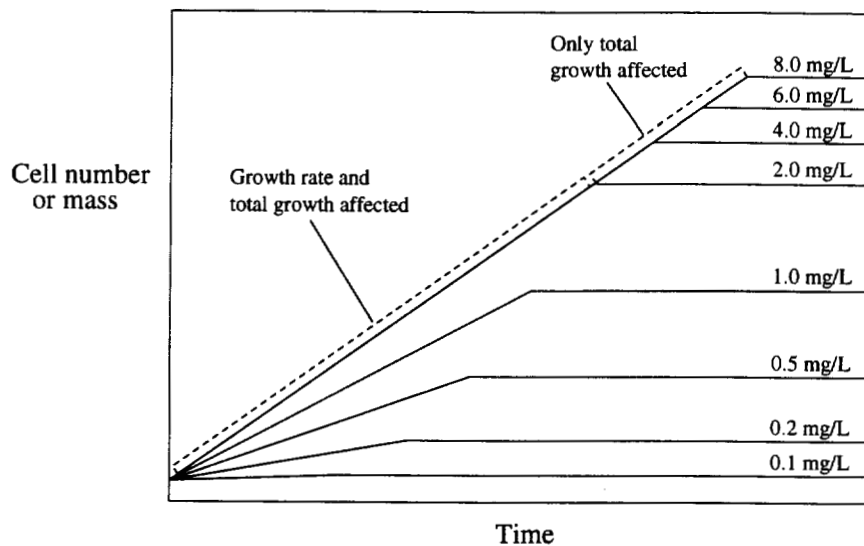
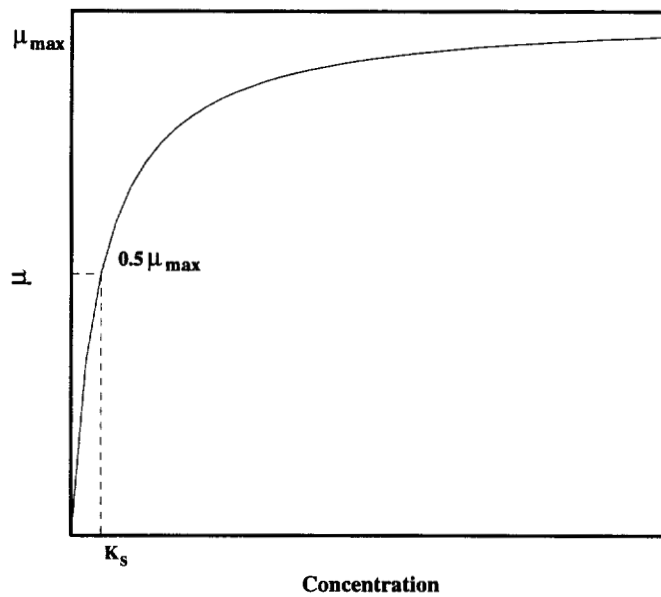


Figure 3.1. Typical growth curve for a microbial population (after Brock and Madigan, 1988).



**Figure 3.2a.** Relationship between substrate concentration, growth rate, and total growth (after Brock and Madigan, 1988).



**Figure 3.2b.** Effect of substrate concentration on growth rate (after Alexander and Scow, 1989).

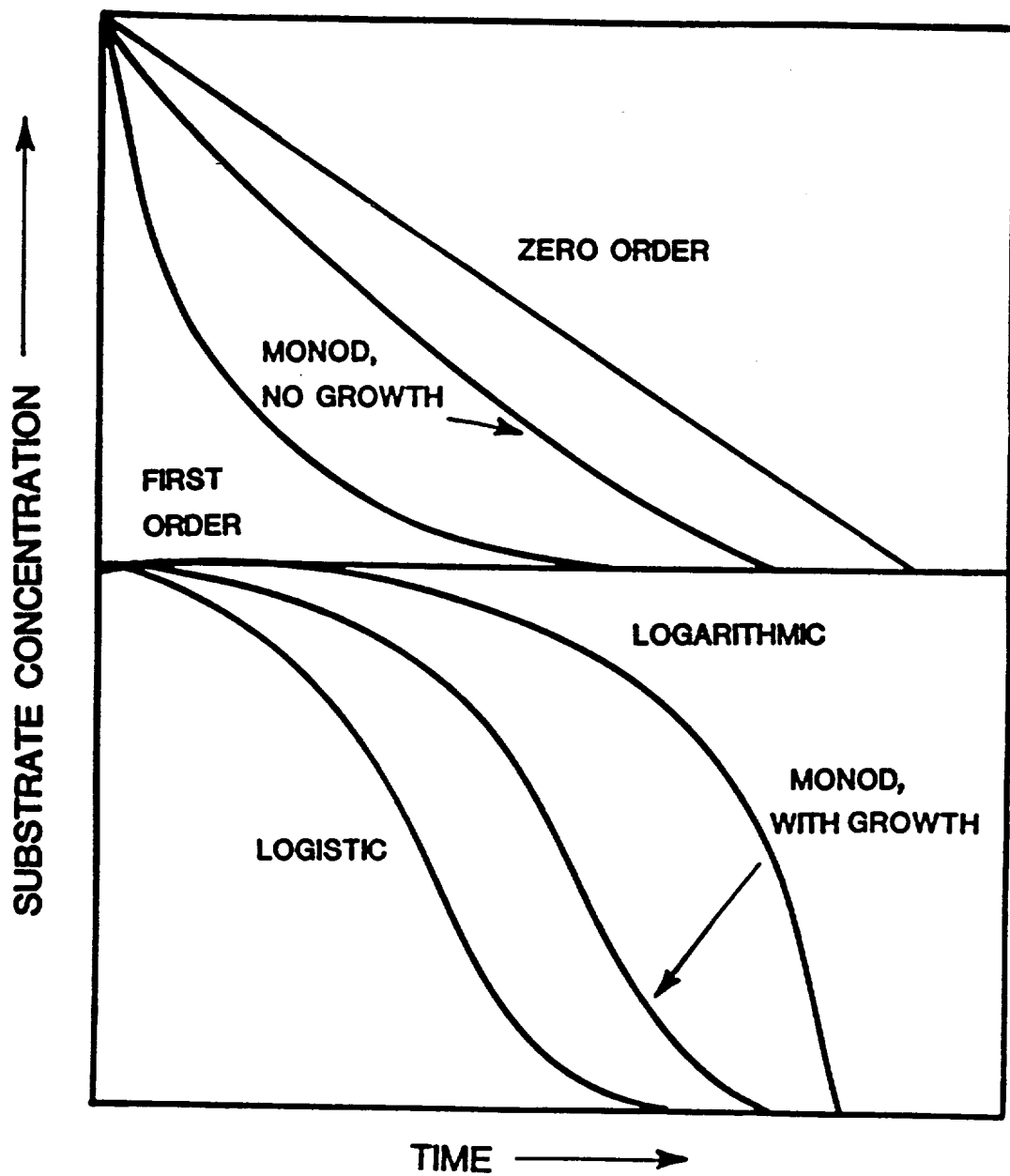
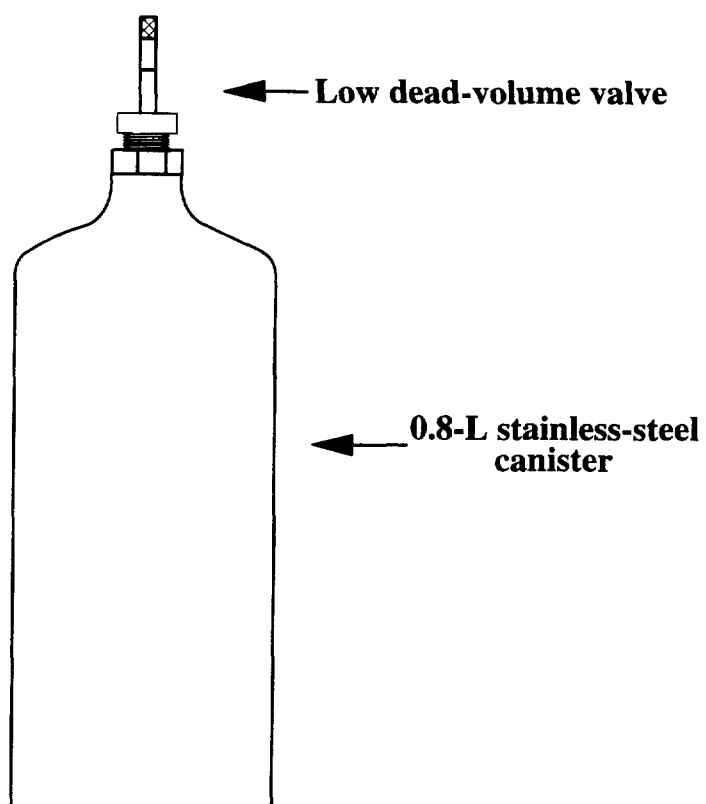
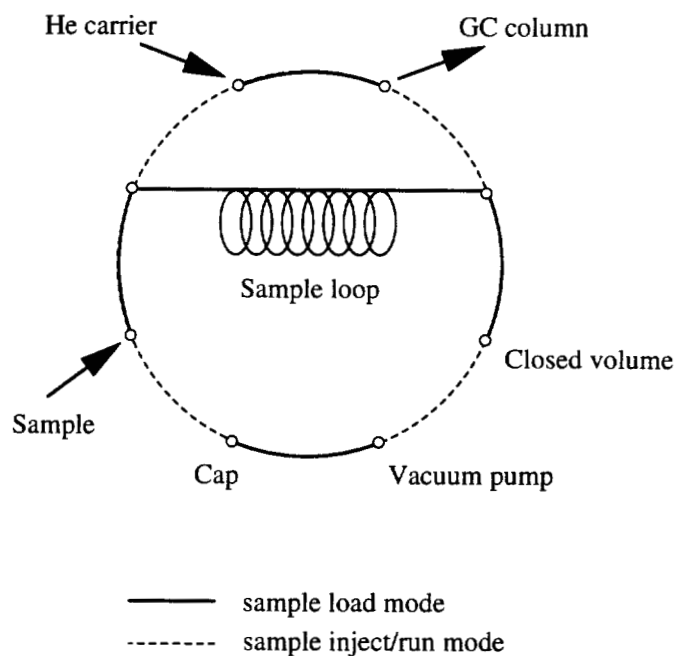


Figure 3.3. Disappearance curves for chemicals that are mineralized by different kinetics (Alexander and Scow, 1989).



**Figure 3.4.** Diagram of canisters used for batch experiments.



**Figure 3.5a. Diagram of eight-port valve used for toluene analyses.**

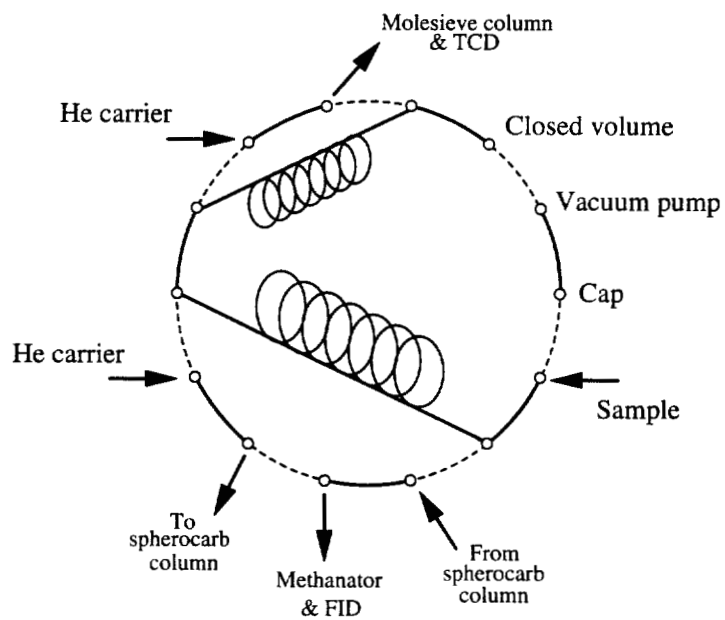


**Figure 3.5b. Diagram of fourteen-port valve used for respiration-gas analyses.**

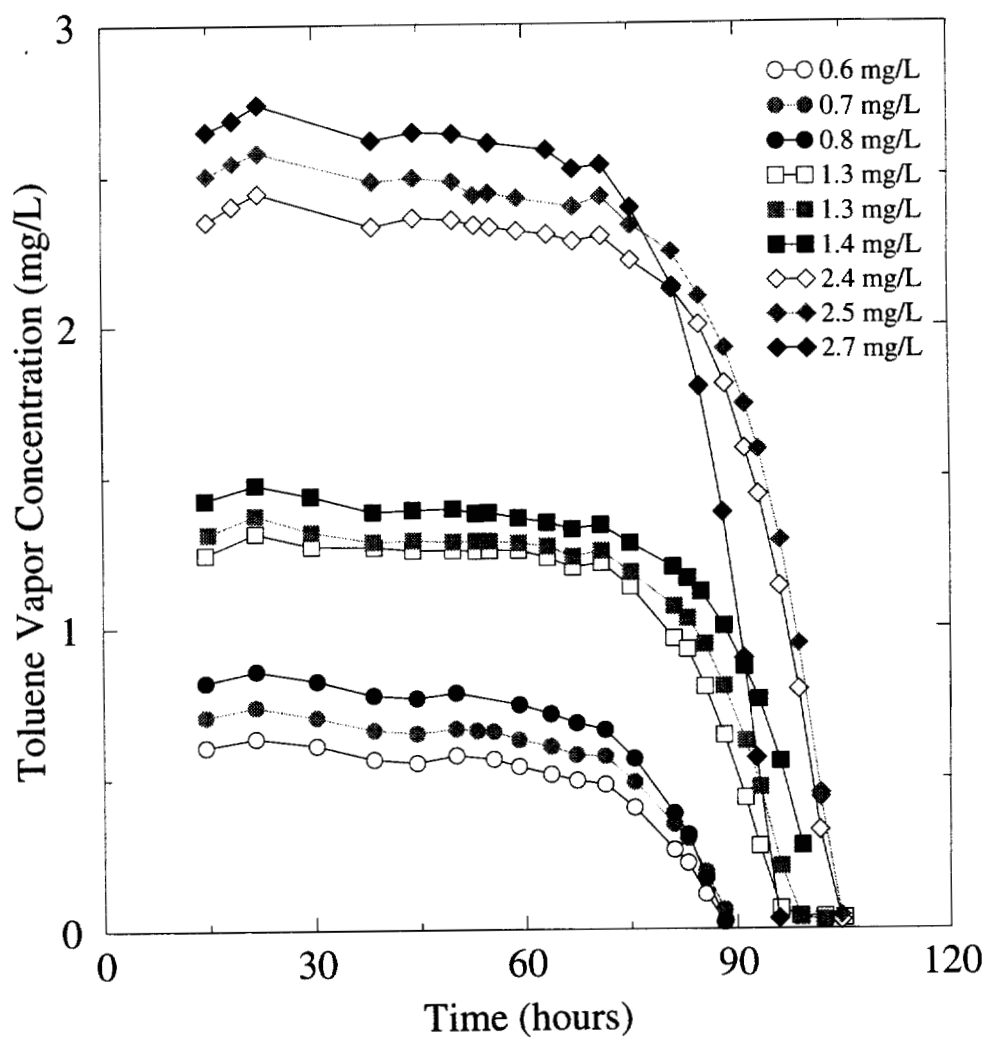
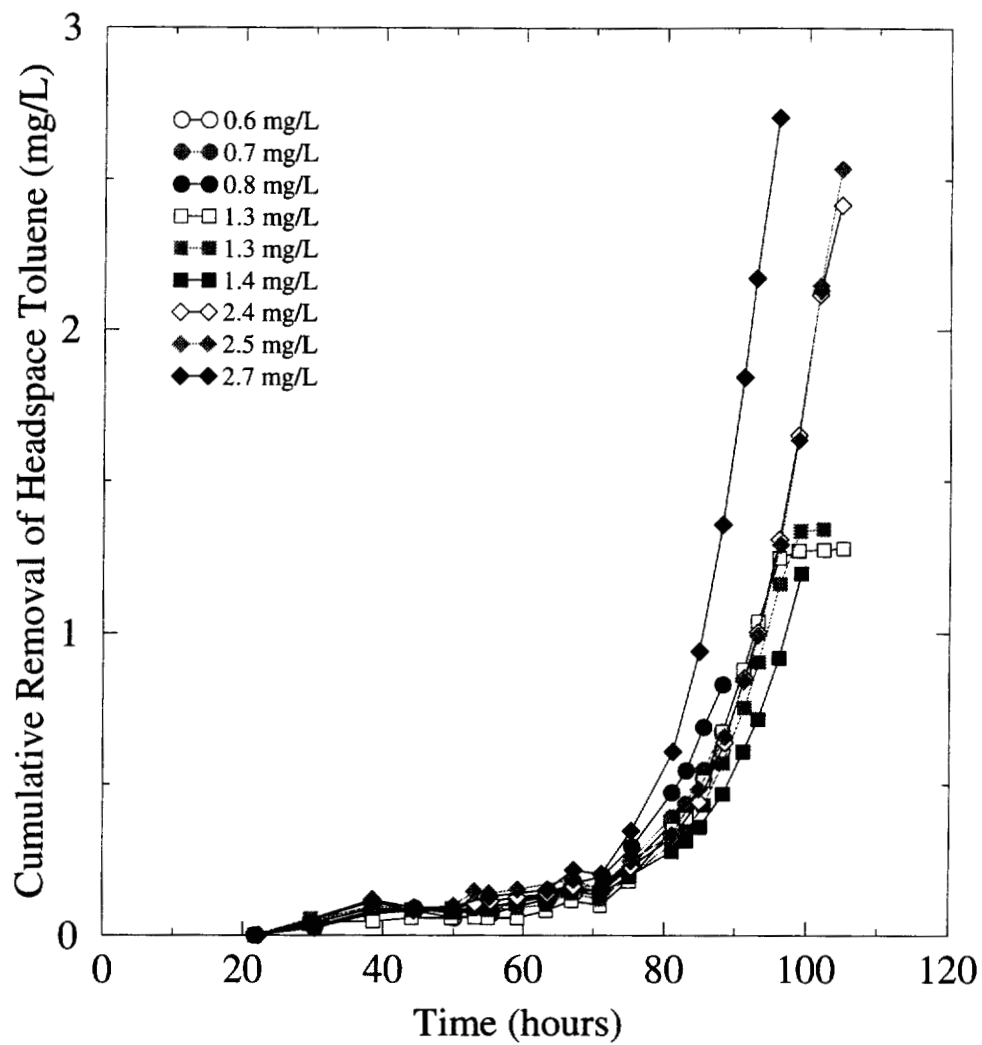


Figure 3.6. Toluene disappearance curves at low initial concentrations (Batch Experiment #6).



**Figure 3.7. Toluene degradation resembles logarithmic-growth kinetics (Batch Experiment #6).**

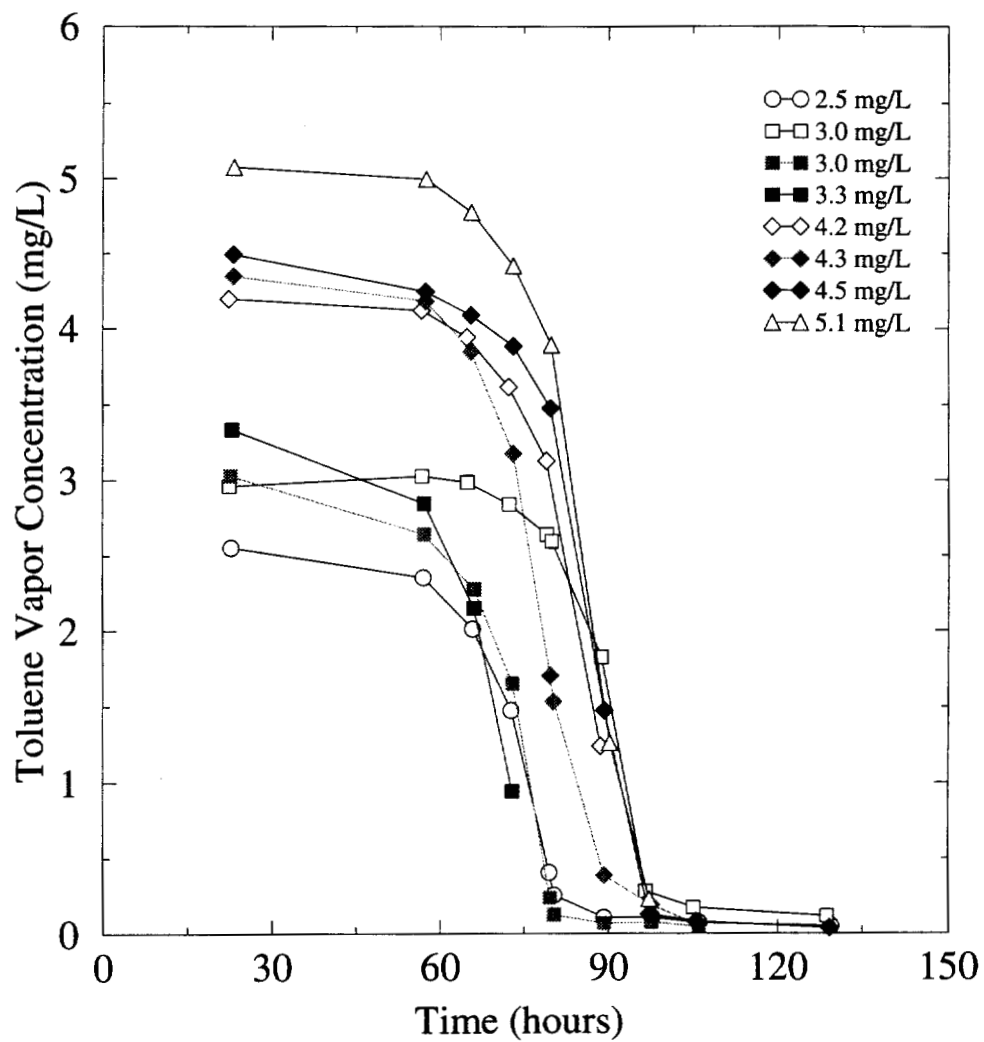


Figure 3.8. Toluene disappearance curves at different initial concentrations (Batch Experiment #5).

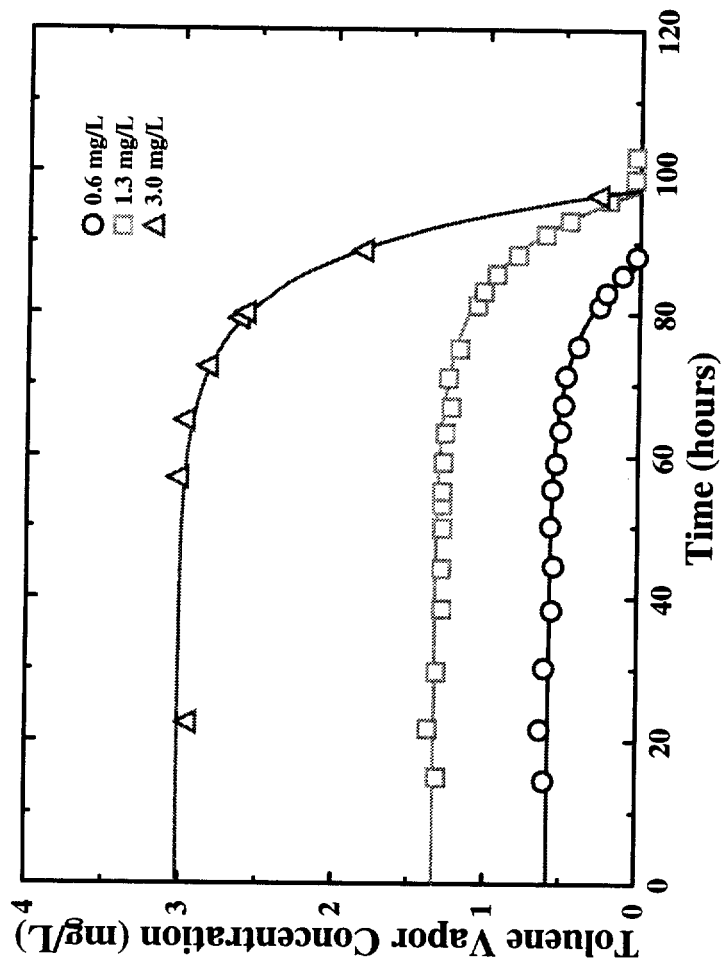
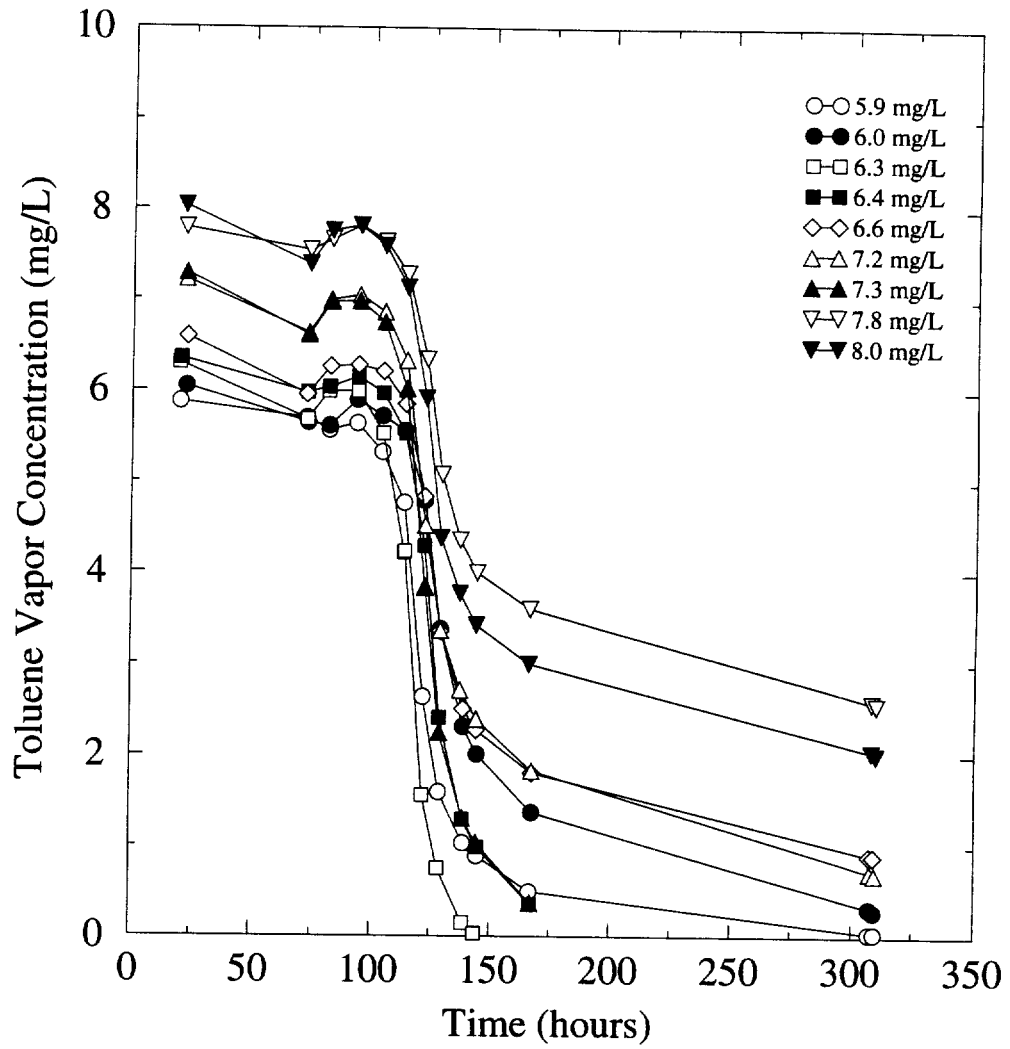
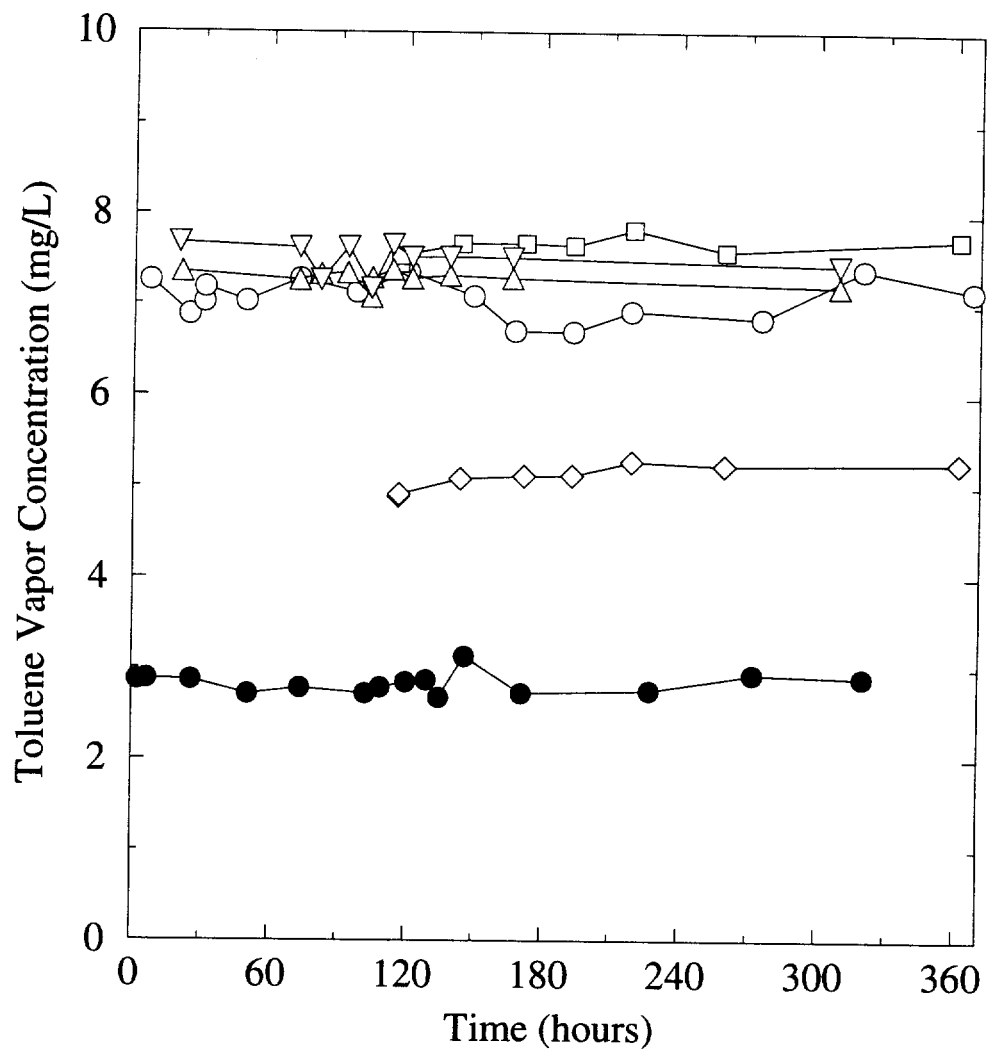


Figure 3.9. Curves fit to toluene degradation data from individual canisters. Symbols are experimental data.



**Figure 3.10. Toluene disappearance curves at higher initial concentrations (Batch Experiment #4).**



**Figure 3.11.** Absence of detectable sorption or degradation of toluene in controls.

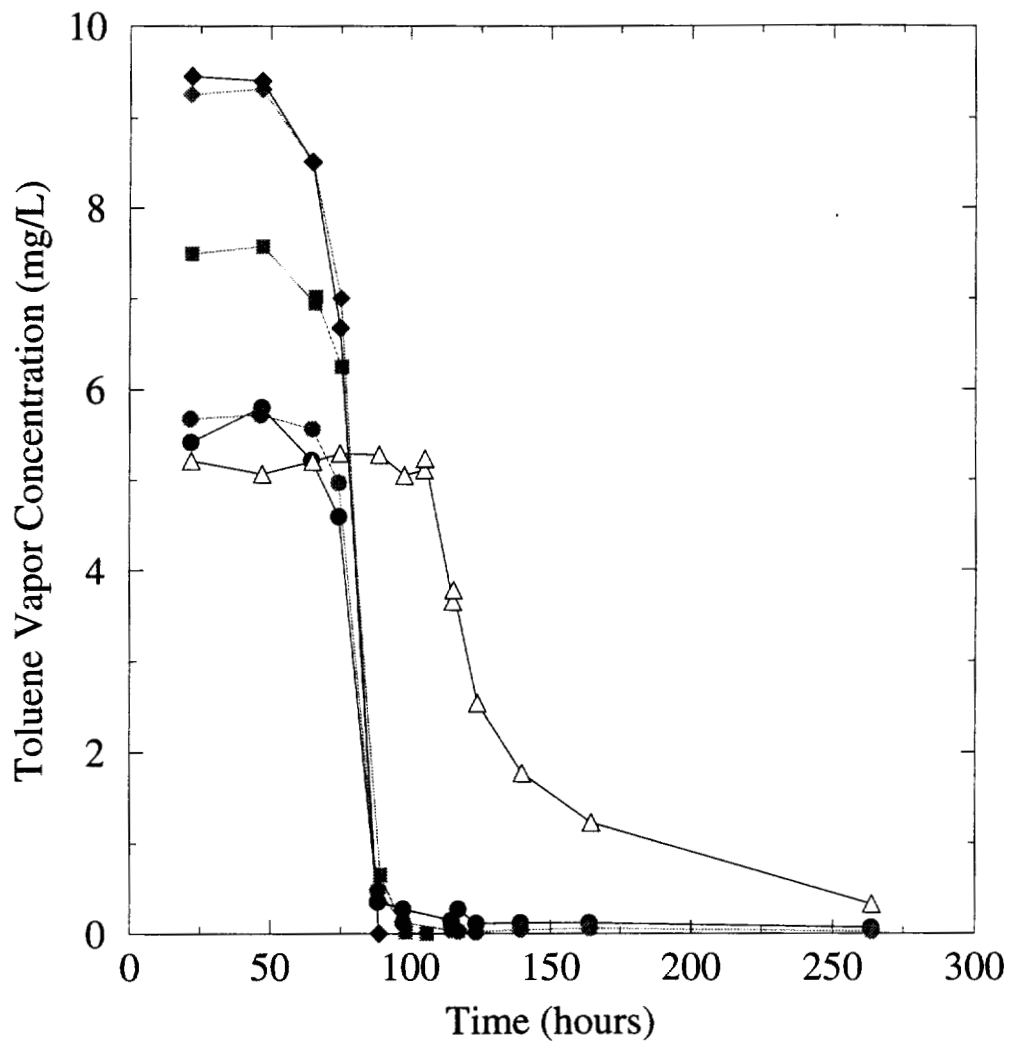


**Figure 3.12. Effect of N concentration on toluene biodegradation. Soil depicted by filled symbols contained ~4 times as much N as soil of open symbols.**

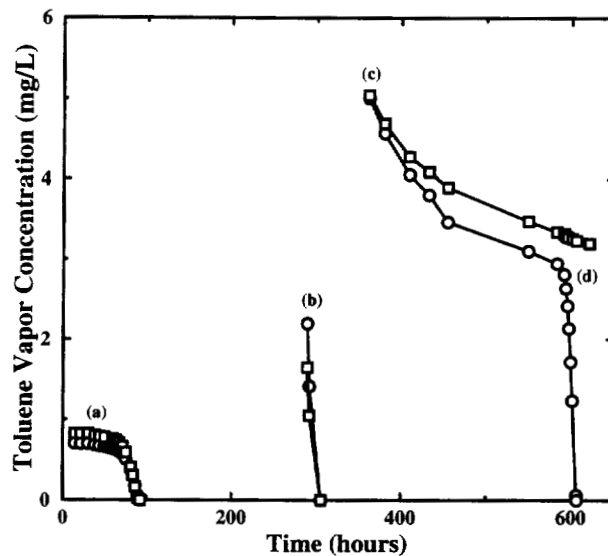


Figure 3.13a. Canisters receiving low initial doses of toluene (a) exhibited faster degradation rates when more toluene was added (b). The rates eventually decreased (c) unless more N was added (d).

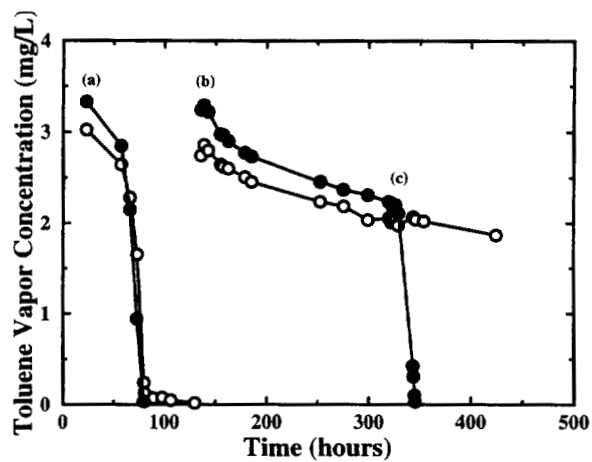
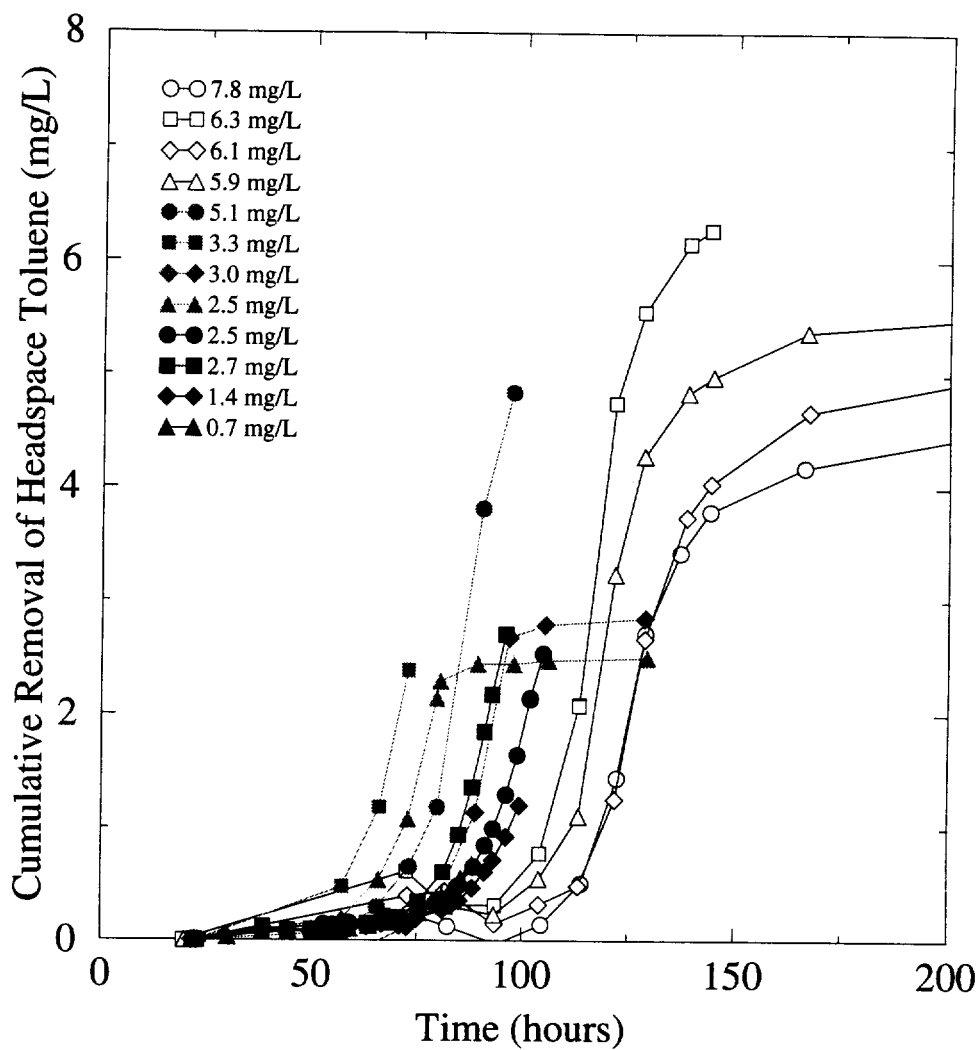
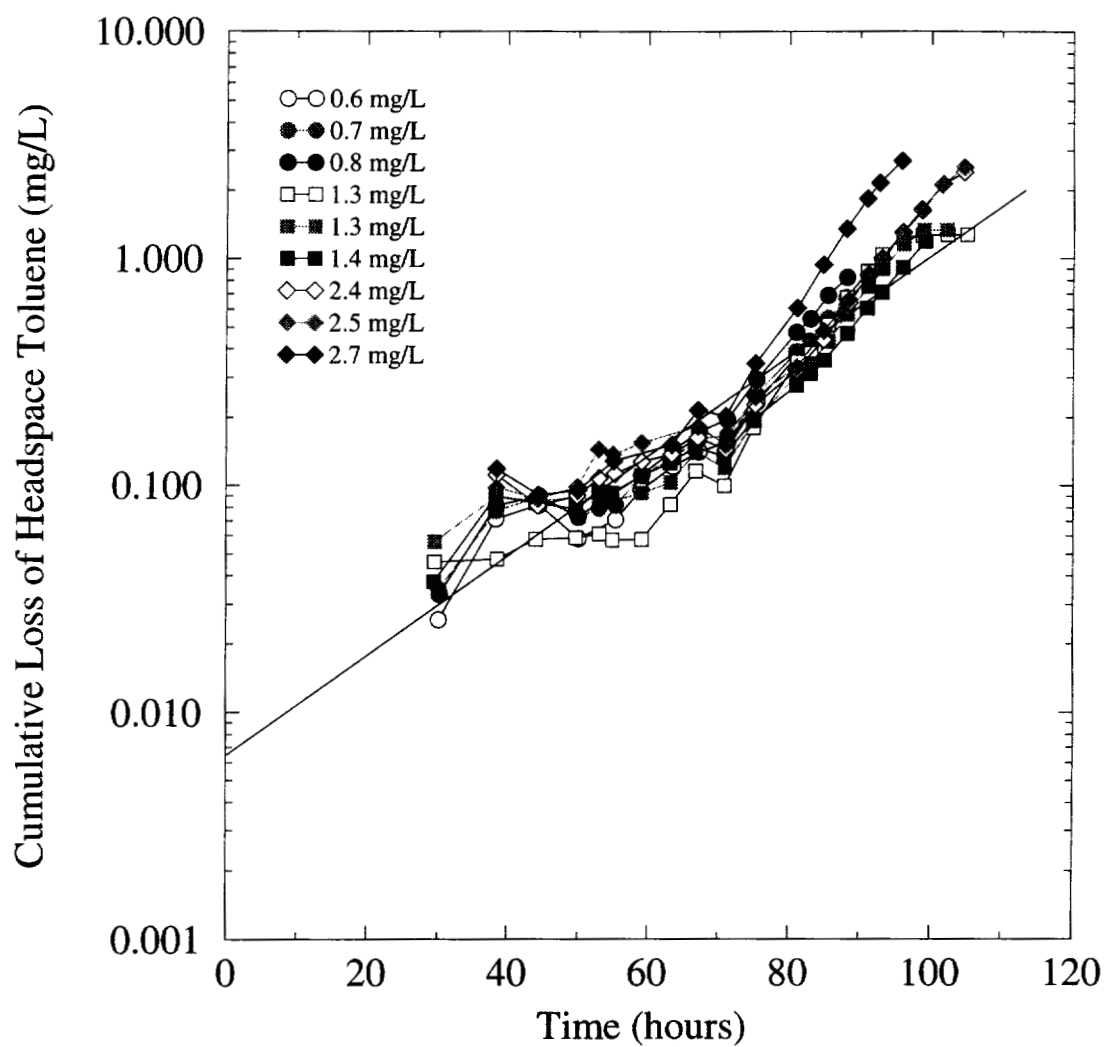


Figure 3.13b. Effects of additional toluene (b) and bioavailable N (c) on biodegradation in canisters with high initial doses of toluene (a).



**Figure 3.14.** Absence of toluene inhibition over the concentration range investigated.



**Figure 3.15.** Extrapolation of toluene data (Batch Experiment #6) to time zero for an estimation of the initial population. Larger uncertainty in measurements of these data can be seen at early times.

## **CHAPTER 4**

### **NUMERICAL MODELING OF TOLUENE TRANSPORT AND FATE IN UNSATURATED SANDY MEDIA**

#### **4.1 INTRODUCTION**

Simulation models provide a convenient and cost-effective way to analyze subsurface contaminant migration. However, it must be recognized that any transport model is merely a simplified representation of extremely complex phenomena resulting from combined effects of physical, chemical, and biological processes. Thus, the effectiveness of models relies on an understanding of the fundamental principles governing transport and fate and the accuracy of model input parameters. However, many complex models contain parameters that are difficult to estimate or measure. To overcome this limitation in the study reported here, an integrated approach of physical experiments and numerical modeling was conducted to gain insight into interactions between various processes responsible for the migration of contaminants in unsaturated sandy media. Using information from batch experiments reported earlier (Chapter 3), a relatively simple model was developed describing vapor diffusion and biodegradation of volatile hydrocarbons in a moist sandy soil. A one-dimensional (1-D) Galerkin finite-element solution was obtained and used in simulating column experiments discussed previously (Chapter 2). Model input data were obtained from either literature or independent laboratory measurements as presented in Chapter 2 and 3. Simulations were compared with experimental data to assess the degree of influence of various physical, chemical, and biological processes on the transport and fate of toluene in the unsaturated zone, as well as to confirm the conceptual model. This chapter deals with mathematical

formulation and numerical modeling of the physical model (soil columns). Subjects will be presented in the following order: a brief review of existing models, model development, model evaluations, and conclusions.

#### **4.1.1 Literature Review**

In the past few decades, a number of mathematical models were developed to describe the transport and fate of pollutants in the unsaturated zone. Some of these are for infinitely miscible polar compounds, inorganic or organic, of which transport processes are dominated by advection and hydrodynamic dispersion (Barnes, 1989; De Smedt and Wierenga, 1984; Rao et al., 1980; van Genuchten and Wierenga, 1976). These models have been applied to describe the transport of organic leachate in soil below sanitary landfills (van Genuchten et al., 1977). In general, the models are not well suited for immiscible organic compounds, which are moderately soluble and volatile at the same time.

Other models were developed to emphasize vapor-phase diffusion of pesticides in soil (Jury et al., 1990; Jury et al., 1983; Jury et al., 1980; Mayer et al., 1974). Most volatilization models neglect water phase and employ various assumptions which render to analytical solutions. Jury et al. (1983) integrated mass partitioning between air, water, and soil phases, leaching by soil solution at a constant velocity, volatilization, and degradation of first order into a 1-D analytical model. The model has been used to estimate pesticide losses by leaching or volatilization. These analytical models have limited use. The multi-phase partitioning approach was extended to two-dimensional (2-D) for vapor transport in the unsaturated zone (Silka, 1988; Striegl and Ishii, 1989). Silka (1988) performed simulations to investigate observations of soil-gas survey reported in the literature. However, biodegradation was not included in the analyses. Striegl and Ishii (1989) used a finite-difference model that includes a first-order reaction term to explain field data of methane adjacent to a buried waste-disposal site. Because no values

for methane consumption term was available, the model was calibrated to field data until a satisfactory fit was obtained.

Corapcioglu and Baehr (1987) proposed a multi-phase model incorporating an immiscible phase for describing subsurface movement of hydrocarbon mixtures such as gasoline. A 1-D finite-difference solution was derived for estimating contaminant fate of a hypothetical gasoline immobilized in the unsaturated zone (Baehr and Corapcioglu, 1987). O<sub>2</sub> transport was modeled to provide an upper bound estimate of aerobic degradation. Baehr (1987) provided sensitivity studies of a suite of gasoline hydrocarbon components with a broad range of air-water partitioning properties under the effects of sorption and diffusion. Model results showed that as these compounds evaporated and diffused towards ground surface, they were separated chromatographically due to partitioning into residual soil water at different degrees, leading to species-dependent profiles.

Vapor-phase transport of several volatile organics was examined for potential of density-driven flow due to volatilization. Sleep and Sykes (1989) presented a 2-D transport and flow model that incorporates water infiltration and gas-phase advection due to density effects. Mass transfer between phases was estimated by a first-order process; however, biodegradation was excluded. Both aqueous- and vapor-phase transport of trichloroethylene in variably saturated media were simulated under a variety of conditions. Falta et al. (1989) also conducted 2-D modeling analyses to illustrate the effect of density-gas flow on vapor diffusion of carbon tetrachloride and toluene under different gas-phase permeabilities. While both trichloroethylene and carbon tetrachloride were affected by density-driven flow, toluene, which has lower saturated-vapor pressure and smaller molecular weight, was not. Neither models were validated against field or laboratory data.

Recent models have focused on microbially mediated oxidation in the subsurface. Sykes et al. (1982) modeled the transport of organic leachate from a landfill in groundwater. The aqueous-phase transport was under the influence of advection, dispersion, and anaerobic degradation. Michaelis-Menten type function was used to

characterize the organic utilization rate in the zone just below landfill. At downgradient where the organic concentration was much less than the half-saturation constant, the organic consumption rate was simplified to first order. Model predictions were compared to limited field data.

O<sub>2</sub> depletion is often observed in hydrocarbon plumes. This has been interpreted to mean that the biodegradation reaction is rapid (i.e., "instantaneous") with respect to transport. Borden and Bedient (1986) presented a solute transport model for simulating degradation processes of dissolved hydrocarbons in groundwater low in O<sub>2</sub>. In addition to transport of O<sub>2</sub> and hydrocarbons, equations were developed for describing growth, decay, and transport of microorganisms. The transport of microorganisms was controlled by affinity of microorganisms for solid surfaces, and the exchange between suspended and attached microbes was assumed to be quantifiable with a microbial retardation factor. Modified Monod functions were used to characterize growth kinetics and removal of O<sub>2</sub> and hydrocarbon. Their sensitivity studies indicated that the model was insensitive to microbial parameters, especially in the body of the plume where O<sub>2</sub> was limited. In a companion paper, they modified an existing solute transport model (MOC, Konikow and Bredehoeft, 1978) to include instantaneous biodegradation of hydrocarbon and O<sub>2</sub>. The resulting model appeared to provide adequate description of both hydrocarbon and O<sub>2</sub> transport at a hazardous waste site (Borden et al., 1986). Following the approach of Borden et al. (1986), Rifai and Bedient (1987) expanded the model to include sorption, anaerobic decay, and the capability of simulating *in situ* bioremediation processes.

MacQuarrie et al. (1990) solved the set of equations presented by Borden and Bedient (1986) excluding the microbial growth on background organic C. Their 1-D model was fitted to toluene breakthrough data of a laboratory sand-packed column for determinations of microbial parameters. Fitted values of  $\mu_{\max}$  and  $K_s$  were  $.493 \pm .865$  day<sup>-1</sup> and  $0.655 \pm 2.87$  mg/L in aqueous concentration, respectively. Population density was predicted within a factor of ten of the results from bacterial plate counts. No independent experimental data were used to validate their model. Sensitivity analyses of the 2-D model showed that physical and chemical parameters were of primary

importance in controlling the rate of mass removal by aerobic degradation of a dissolved organic plume. For easily biodegradable compounds, the size of initial microbial population and the biodegradation kinetic constants had a secondary effect on organic plume behavior (MacQuarrie and Sudicky, 1990).

Molz et al. (1986) incorporated detailed characteristics of microbial populations at pore-scale view into the microbial kinetics concept used in their model development. The microbial population was assumed to grow as microcolonies in a cylindrical-plate shape, and microbial transport was excluded. In addition, a diffusion boundary layer existed between bulk pore-fluid and the surface of the microcolonies. A substrate utilization rate was quantified on the basis of each colony, and a dual-Monod growth function was used. They assumed that energy requirements for cell maintenance were satisfied through recycling internal substrate. A set of five coupled nonlinear equations was solved using the Eulerian-Lagrangian method. The 1-D model was tested for parameter sensitivity, however it was not evaluated with any field or experimental data. Widdowson et al. (1988) extended the transport model presented by Molz et al. (1986) to include transport of nitrate as an alternative electron acceptor and transport of ammonia-N as the inorganic nutrient necessary for growth. Utilization rates of all constituents considered in the model were in a form of triple-Monod kinetics. The resulting model, which consists of nine coupled nonlinear equations, was solved. Model simulations were illustrated for a hypothetical case of 1-D column experiment. Although the last model includes the effect of nutrient availability, it requires numerous input parameters, many of which are either difficult to obtain or not directly measurable.

Hydrocarbon transport and biodegradation in the unsaturated zone has not been modeled as extensively as the saturated zone. In soil science, degradation of pesticides in soil is usually represented by first-order kinetics (Wagenet and Rao, 1985; Jury et al., 1983; Mayer et al., 1974). Angelakis and Rolston (1985) proposed a 1-D model for simulating movements of dissolved C species in soil columns receiving wastewater effluent. Biotransformation were approximated by first-order kinetics. CO<sub>2</sub> production was modeled as a gas-phase diffusion process with constant gas solubility in soil water.

Numerical predictions of transient profiles of soluble C were more accurate in the early times than at later.

Ostendorf and Kampbell (1991) developed a steady-state analytical model featuring vapor-phase diffusion and Michaelis-Menton kinetics. The model was calibrated with field profiles of total hydrocarbon vapor and O<sub>2</sub> concentrations in the unsaturated zone above a capillary fringe contaminated by aviation gasoline. Using independently-derived site characteristics, maximum reaction rates and half-saturation constants, obtained by fitting, range from  $8.87 \times 10^{-9}$  to  $1.13 \times 10^{-8}$  and  $5.56 \times 10^{-4}$  to  $8.54 \times 10^{-4}$ , respectively. They concluded that a simple analytical model of gaseous diffusion and biodegradation was suitable for modeling hydrocarbon distribution in a geologically homogeneous vadose zone that has had prolonged exposure to hydrocarbon vapors. Results also indicated that little O<sub>2</sub> reached the water table because of the aerobic biodegradation process in the unsaturated zone.

Chen et al. (1992) applied the model by Widdowson et al. (1988) to describe multi-phase transport of hydrocarbon compounds in an unsaturated/saturated soil system by adding an immobile air phase. The 1-D model was evaluated by using data from continuous-flow saturated column experiments under either aerobic or denitrifying conditions. The columns were continuously fed with a mixture of BTX at an aqueous concentration of 20 mg/L per component, basal mineral medium, and the appropriate electron acceptor. Model parameters were determined independently from aquifer slurry studies, batch experiments, or literature. Simulated breakthrough curves of toluene and benzene were compared with the column data. Sensitivity analyses revealed that the predicted breakthrough curves were particularly sensitive to the initial biomass concentration, the maximum substrate-utilization rate, and the half-saturation coefficient.

#### **4.1.2 Biodegradation Kinetics Concept**

Several models have been proposed to represent biodegradation kinetics in soil. These range from the simple first-order rate equation to more complex models [e.g., the

three-halves-order kinetics model of Brunner and Focht (1984) or the two-compartment model of Scow et al., (1986)]. Prior column studies with a sandy soil (Chapter 2) demonstrated that aerobic biodegradation was an important process affecting hydrocarbon transport and fate under certain conditions. Batch experiments (Chapter 3) indicated that the indigenous microbial population grew at a logarithmic rate using toluene as the only C and energy source. Thus, zero-order Monod kinetics were selected to represent biodegradation kinetics in the transport model developed below.

When  $O_2$  supply is unlimited, biodegradation kinetics are the rate-controlling step, and the reaction rate of biodegradable hydrocarbon must be experimentally determined (Barker and Mayfield, 1988). This is because the transport process is fast relative to the time scale of biodegradation. Under balanced conditions, biodegradation may follow Michaelis-Menten kinetics for non-growing populations or Monod kinetics for small initial populations. In the former case, the rate is proportional to substrate concentration when substrate concentration is substantially below a half-saturation constant, and the reaction is thus first order with respect to substrate. Half lives of BTEX compounds of less than 20 days were observed when  $O_2$  was not limiting (Patrick et al., 1986). As the substrate concentration is increased, the reaction rate increases and is mixed-order. At high concentrations, the rate becomes constant and independent of substrate concentration. Similarly, for microorganisms follow Monod kinetics, their growth rates can be simplified to either first or zero order with respect to substrate. The corresponding biodegradation rates are second order (i.e., first order with respect to both substrate and biomass) and zero order with respect to substrate (i.e., substrate removal rate increases linearly with biomass concentration), respectively (Alexander and Scow, 1989).

When  $O_2$  becomes limiting, as in a water-logged soil, growth kinetics then depend on both substrate and  $O_2$  concentrations. The Monod function has been used extensively to model  $O_2$ -limited biodegradation in groundwater systems (Chen et al., 1992; MacQuarrie et al., 1988; Borden and Bedient, 1986; Molz et al., 1986). Borden and Bedient (1986) used dual-Monod kinetics with a half-saturation constant of  $O_2$  (0.1 mg/L

in aqueous concentration, Longmuir, 1954) to model the effect of O<sub>2</sub>-limited biodegradation on hydrocarbon transport in groundwater. The model showed that the transport rate of reacting species to microcolonies was slow with respect to degradation rate, and the system became transport-limited. As a consequence, biodegradation was assumed to be "instantaneous", and at any time the groundwater contained only O<sub>2</sub> or hydrocarbons, but not both. Hence, biodegradation rates of hydrocarbon and O<sub>2</sub> were approximated by reaction stoichiometry. Mass of hydrocarbon consumed was set equal to the total amount of hydrocarbon present or the stoichiometric equivalent of available O<sub>2</sub>, whichever was less. A mass ratio of 3.0-3.5 of O<sub>2</sub> to gasoline hydrocarbons is commonly used (Ostendorf and Kampbell, 1991; Rifai and Bedient, 1987; Corapcioglu and Baehr, 1987).

#### **4.2 MODEL DEVELOPMENT**

A 1-D contaminant diffusion/biodegradation model was developed. It consists of 3 distinct phases (air, water, and soil phases), in which toluene partitioning was assumed to be linear and at equilibrium. The model applied to a uniform spatial domain, at which the boundary was either Dirichlet (constant concentration) and/or Neuman (constant flux) types. A conceptual model of toluene biodegradation was formulated based on the batch kinetic experiments discussed earlier (Chapter 3): Toluene was used as the sole source of C and energy for microbial growth and cell maintenance. When environmental conditions are appropriate for growth, toluene utilization rate increased with time reflecting a logarithmic-growth pattern of microbial microorganisms. This increase in degradation rate was ultimately limited by the bioavailable N. Microbial growth was modeled by the Monod kinetics. Following N depletion, growth ceased, and the contaminant removal rate was reduced to a fixed rate, reflecting maintenance-energy requirements (Pirt, 1975). The maintenance-energy requirement for toluene was approximated using data from batch experiments (see Appendix C). No biodegradation took place when aqueous concentrations of toluene exceeded an inhibitory level.

O<sub>2</sub> is required for energy of synthesis as well as energy of maintenance (Pirt, 1975). Because the half-saturation constant of O<sub>2</sub> is 0.1 mg/L in aqueous phase (corresponding to a gaseous value of 2.6x10<sup>-3</sup> kg/m<sup>3</sup> or 0.2% by volume), the dependency of biodegradation rate on O<sub>2</sub> kinetics is not critical as long as the electron acceptor is in unlimited supply. In a shallow unsaturated sandy zone, O<sub>2</sub> is likely to be present far above this critical level. This was also the case in the column studies reported earlier (Chapter 2). Therefore, O<sub>2</sub> consumption rate was assumed to be proportional to toluene utilization rate during both periods of cell synthesis and maintenance.

No effect of pH, temperature, or accumulation of toxic products on the microbial dynamics were considered. Because microbes are enclosed within discontinuous droplets of residual water in the unsaturated zone, mass transport of microbial population can be neglected. All conditions imposed above gave rise to a system of three partial differential equations (PDE) and an exponential growth function, which was solved for transport and fate of toluene, O<sub>2</sub>, and CO<sub>2</sub> in unsaturated porous media.

#### 4.2.1 Physical Bases and Mathematical Formulae

An approach similar to that of Corapcioglu and Baehr (1987) was used in developing mass conservation equations for transport species in unsaturated porous media. A component mass-balance equation may be written for individual chemical species with respect to each constituent phase. For the fraction in the air phase

$$\frac{\partial}{\partial t} \theta_a G_k = \nabla \cdot J_{ka} + R_{k,vol} - R_{k,con} \quad (4.1)$$

For the fraction in the water phase

$$\frac{\partial}{\partial t} \theta_w C_k = \nabla \cdot J_{kw} + R_{k,con} - R_{k,vol} + R_{k,des} - R_{k,ads} + \theta_w R_{k,bio} \quad (4.2)$$

For the fraction adsorbed on the soil

$$\frac{\partial}{\partial t} \rho_b S_k = R_{k,ads} - R_{k,des} \quad (4.3)$$

The subscript  $k$  represents a hydrocarbon contaminant species;  $G_k$ ,  $C_k$ , and  $S_k$  are the concentrations of the species in the air, water, and solid phases, respectively;  $\theta_a$  and  $\theta_w$  are the volumetric contents of air and water, respectively;  $\rho_b$  is the bulk density of dry soil;  $J_{ka}$  and  $J_{kw}$  are the contaminant mass fluxes in the air and water phases, respectively;  $R_{k,con}$  and  $R_{k,vol}$  are the mass transfer rates of the contaminant from air to water phase (condensation) and from water to air phase (volatilization), respectively;  $R_{k,ads}$  and  $R_{k,des}$  are the rates of mass transfer of the species from water to adsorbed state (adsorption) and from adsorbed state to water phase (desorption), respectively;  $R_{k,bio}$  is the biodegradation rate of the compound in the water phase. It should be noted that while water and air concentrations are expressed per phase volume, the adsorbed concentration is per mass of solid. The volumetric contents and density are per total volume of the porous medium. The former is related to total porosity,  $\theta_T$ , as

$$\theta_a + \theta_w = \theta_T \quad (4.4)$$

By summing over the above equations, a total mass conservation of the contaminant can be written as

$$\frac{\partial}{\partial t} [\theta_a G_k + \theta_w C_k + \rho_b S_k] = \nabla \cdot [J_{ka} + J_{kw}] + \theta_w R_{k,bio} \quad (4.5)$$

Equation (4.5) assumes that abiotic transformations are insignificant (Corapcioglu and Baehr, 1987; others) and that microbially mediated oxidation occurs only in the water phase. Since microorganisms must exist in a water environment, they are assumed to be present as microcolonies enclosed within the discontinuous film of residual water in the unsaturated zone.

The soil air is assumed to be at uniform atmospheric pressure. No infiltration of rainwater is considered. In the absence of advection for either fluid phases,  $J_{ka}$  and  $J_{kw}$

are adequately quantified by molecular diffusion. According to Fick's first law, the mass fluxes in the air and water phases are

$$J_{ka} = -D_{ka} \nabla G_k \quad (4.6)$$

$$J_{kw} = -D_{kw} \nabla C_k \quad (4.7)$$

where  $D_{ka}$  and  $D_{kw}$  are the apparent diffusion coefficients in the air and water phases, respectively. The apparent diffusion coefficients are functions of the porous medium and the diffusive compound. In partially-saturated soil, the apparent diffusion coefficients in the air and water phases are usually expressed by

$$D_{ka} = d_{ka} \theta_a \tau_a \quad (4.8)$$

and

$$D_{kw} = d_{kw} \theta_w \tau_w \quad (4.9)$$

where  $d_{ka}$  and  $d_{kw}$  are the free air and free water diffusion coefficients, respectively;  $\tau_a$ , and  $\tau_w$  are the tortuosities for pore air and water, respectively. The Millington model (1959) for air-phase tortuosity has been shown by numerous investigators to be adequate for describing vapor-phase transport (Karimi et al., 1987; Bruell and Hoag, 1986; Farmer et al., 1980) and is employed here.

$$\tau_a = \frac{\theta_a^{7/3}}{\theta_T^2} \quad (4.10)$$

An analogous form to equation (4.10) can be applied to water-phase tortuosity.

$$\tau_w = \frac{\theta_w^{7/3}}{\theta_T^2} \quad (4.11)$$

Good agreement between equation (4.11) and experimental data over a wide range of moisture contents has been reported by McCarthy and Johnson (1994).

To further simplify the model, mass partitioning between phases is approximated by a linear equilibrium relationship. The assumption eliminates the need for solving mass conservative equations for specific phases. The two equilibrium partition coefficients are

$$H_{i,wa} = \frac{C_i}{G_i} \quad (4.12)$$

and

$$K_d = \frac{S_k}{C_k} \quad (4.13)$$

where  $H_{i,wa}$  is the dimensionless partition coefficient of a species between the water and air phases; and  $K_d$  is the distribution coefficient between the soil and water phases.  $K_d$  has a dimension of volume of water over mass of solid.  $H_{i,wa}$  can be derived by combination of Henry's constant and ideal gas laws; consequently, it varies with temperature. It also requires concentrations of solutes in the water phase to be dilute with respect to those compounds. The sparing solubilities of gasoline hydrocarbons fit the constraint. Likewise, equation (4.13) is generally applied well to uncharged organic compounds, such as hydrocarbons, at typical field moisture. Using the relationships given by equations (4.12) and (4.13), the equation of total mass conservation can be expressed in terms of one concentration only. In cartesian coordinates, equation (4.4) is now rewritten in terms of gas-phase concentration as follows:

$$\frac{\partial}{\partial t} G_k [\theta_a + \theta_w H_{k,wa} + \rho_b K_d H_{k,wa}] - \frac{\partial}{\partial z} \left[ D_{ka} \frac{\partial}{\partial z} G_k \right] - H_{k,wa} \frac{\partial}{\partial z} \left[ D_{kw} \frac{\partial}{\partial z} G_k \right] = \theta_w R_{k,bio} \quad (4.14)$$

The reaction term is given by

$$R_{k,bio} = -\mu_{\max} X \quad (4.15)$$

where  $\mu_{\max}$  is the maximum specific growth rate;  $X$  is the aqueous concentration of the microbial population expressed in terms of the concentration of the contaminant compound that is required to produce it (Simkins and Alexander, 1984). The derivation

of equation (4.15) can be found in Appendix B. Combining equations (4.14) and (4.15) yields the final formulation for hydrocarbon transport.

$$\frac{\partial}{\partial t} G_k [\theta_a + \theta_w H_{k,wa} + \rho_b K_d H_{k,wa}] - \frac{\partial}{\partial z} \left[ D_{ka} \frac{\partial}{\partial z} G_k \right] - H_{k,wa} \frac{\partial}{\partial z} \left[ D_{kw} \frac{\partial}{\partial z} G_k \right] = -\theta_w \mu_{\max} X \quad (4.16)$$

The parenthesis of the time derivative term will be referred to as the retardation factor. For a system of very small  $K_s$  (Chapter 3), the rate of microbial growth is logarithmic,

$$\frac{dX}{dt} = \mu_{\max} X \quad (4.17)$$

In a similar fashion, the following transport equations were obtained for  $O_2$  and  $CO_2$ , respectively.

$$\frac{\partial}{\partial t} G_{O_2} [\theta_a + \theta_w H_{O_2,wa}] - \frac{\partial}{\partial z} \left[ D_{O_2a} \frac{\partial}{\partial z} G_{O_2} \right] - H_{O_2,wa} \frac{\partial}{\partial z} \left[ D_{O_2w} \frac{\partial}{\partial z} G_{O_2} \right] = \theta_w R_{O_2,bio} \quad (4.18)$$

$$\frac{\partial}{\partial t} G_{CO_2} [\theta_a + \theta_w H_{CO_2,wa}] - \frac{\partial}{\partial z} \left[ D_{CO_2a} \frac{\partial}{\partial z} G_{CO_2} \right] - H_{CO_2,wa} \frac{\partial}{\partial z} \left[ D_{CO_2w} \frac{\partial}{\partial z} G_{CO_2} \right] = \theta_w R_{CO_2,bio} \quad (4.19)$$

where  $H_{O_2,wa}$  and  $H_{CO_2,wa}$  are the partition coefficients between the water and air phases for  $O_2$  and  $CO_2$ , respectively.  $G_{O_2}$  and  $G_{CO_2}$  are the gas-phase concentrations of  $O_2$  and  $CO_2$ , respectively.  $D_{O_2a}$  and  $D_{CO_2a}$  are the apparent diffusion coefficients in the air phase for  $O_2$  and  $CO_2$ , respectively. Similarly,  $D_{O_2w}$  and  $D_{CO_2w}$  are the apparent diffusion coefficients in the water phase for  $O_2$  and  $CO_2$ , and  $R_{bio,O_2}$  and  $R_{bio,CO_2}$  are the rates of  $O_2$  consumption and  $CO_2$  production in the water phase. Equations (4.18) and (4.19) state that  $O_2$  and  $CO_2$  partition between soil air and water according to the equilibrium assumption, and exclude the sorption of these gaseous compounds. The consumption of  $O_2$  and production of  $CO_2$  are attributed to biological processes only.

$R_{bio,O_2}$  and  $R_{bio,CO_2}$  are treated as known quantities and computed at each time step based on the rate of toluene degradation. Using stoichiometric ratios of  $O_2$  and  $CO_2$  to

toluene, respectively, the expressions for O<sub>2</sub> consumption and CO<sub>2</sub> production rates are

$$R_{O_2, bio} = -\mu_{\max} X \frac{v_{O_2} M_k}{v_k M_{O_2}} \quad (4.20)$$

$$R_{CO_2, bio} = \mu_{\max} X \frac{v_{CO_2} M_k}{v_k M_{CO_2}} \quad (4.21)$$

where  $v_k$ ,  $v_{O_2}$ , and  $v_{CO_2}$  are the stoichiometric coefficients of a balanced metabolic equation for hydrocarbon, O<sub>2</sub>, and CO<sub>2</sub>, respectively.  $M_k$ ,  $M_{O_2}$ , and  $M_{CO_2}$  are the molecular weights of hydrocarbon, O<sub>2</sub>, and CO<sub>2</sub>, respectively. An equation for toluene aerobic biodegradation, from which the stoichiometry was obtained, can be found in Chapter 3. Equations (4.20) and (4.21) assume the utilization and production rates of O<sub>2</sub> and CO<sub>2</sub> to be proportional to the rate of substrate degradation at each time step. This is appropriate for a system in which the biodegradation rate is not limited by O<sub>2</sub> supply.

With the assumption of an immobile microbial mass, an equation of microbial mass transport was omitted. Consequently, the transport equations (4.16, 4.18, and 4.19) together with the equation of logarithmic growth kinetics (equation 4.17) were solved for vapor-phase concentrations of toluene, O<sub>2</sub>, and CO<sub>2</sub> as a function of position in the column over time. Because these equations are uncoupled, owing to the logarithmic growth condition, they were solved sequentially at every time step. An outline of the numerical solving scheme is shown in Fig. 4.1. Equation (4.17) is independent of space, therefore no boundary conditions are required. Hence, it was solved analytically to give  $X$  at any point in the column with the following initial condition,

$$X = X_0 \quad ; (t=0) \quad (4.22)$$

where  $X_0$  is the initial concentration of microbial populations expressed in terms of the concentration of the metabolic compound that would be required to produce it. Equation (4.16) was solved numerically with the following initial and boundary conditions:

$$G_k(z,0) = G_{k0} \quad ; 0 \leq z \leq L \quad (4.23.a)$$

$$G_k(0,t) = G_k^\circ \quad ; t > 0 \quad (4.23.b)$$

$$G_k(L,t) = 0 \quad ; t > 0 \quad (4.23.c)$$

where  $G_{k0}$  is the initial concentration of toluene;  $G_k^\circ$  is the vapor-concentration of toluene at the source; and  $L$  is the length of the column over which the equations are solved. Dirichlet boundary conditions were specified for toluene at both ends of the column (see Chapter 2). At the reservoir end, a constant-concentration of vapor toluene was maintained, and thus the Dirichlet boundary was prescribed. At the other end, air flushed through the soil surface to provide an instantaneous mixing and flushing of toluene such that a zero-concentration boundary was justified.

Next, equations (4.18) and (4.19) were solved numerically in sequence. The initial and boundary conditions associated with equation (4.18) were,

$$G_{O_2}(z,0) = G_{O_2}|_{atm} \quad ; 0 \leq z \leq L \quad (4.24.a)$$

$$\frac{\partial}{\partial z} G_{O_2}|_{(0,t)} = 0 \quad ; t > 0 \quad (4.24.b)$$

$$G_{O_2}(L,t) = G_{O_2}|_{atm} \quad ; t > 0 \quad (4.24.c)$$

Similarly, the initial and boundary conditions associated with equation (4.19) were

$$G_{CO_2}(z,0) = G_{CO_2}|_{atm} \quad ; 0 \leq z \leq L \quad (4.25.a)$$

$$\frac{\partial}{\partial z} G_{CO_2}|_{(0,t)} = 0 \quad ; t > 0 \quad (4.25.b)$$

$$G_{CO_2}(L,t) = G_{CO_2}|_{atm} \quad ; t > 0 \quad (4.25.c)$$

Equations (4.24.a) and (4.25.a) specify the initial values for  $G_{O_2}$  and  $G_{CO_2}$ . Zero boundary fluxes were specified at the reservoir end for both  $O_2$  and  $CO_2$  (equations

4.24.b and 4.25.b). These were good approximations for  $O_2$  due to its low aqueous solubility and for  $CO_2$  in the column experiment with saturated source-concentration. However, in the lower source-concentration columns, the flux-boundary condition was complicated by the dissolution of  $CO_2$  into the aqueous source (see Chapter 2). Dirichlet boundary conditions (equations 4.24.c and 4.25.c) were prescribed for the sweep-air end, implying negligible accumulation of  $CO_2$  or depletion of  $O_2$  at this end.

At each time step, criteria for the availability of organic compound,  $O_2$ , and N were checked, and constraints were imposed to readjust biodegradation rates. If the nodal concentration of hydrocarbon or  $O_2$  was zero, then the reaction rate was zero. After N was depleted, the biodegradation rate was maintained at 0.5% of the rate from the last time step. The reduced rate was set to approximate energy requirements for cell maintenance after microbial growth ceased.

The set of PDE developed above was discretized through space using the Galerkin finite-element method. Nodal variables  $G_k$ ,  $G_{O_2}$ , and  $G_{CO_2}$  were approximated by quadratic bases. Physical coefficients of the porous medium were assigned by nodes and interpolated by quadratic bases. Time discretization was carried out by a variable weighted finite-difference operator. The model can accommodate two types of boundary conditions: Dirichlet and Neuman. Developments of the discrete equations and source codes are compiled in Appendix D and E.

The above set of equations may also apply to a more general setting, in which the spatial domain is bounded by a subsurface region extensively contaminated with residual phase of volatile compounds and the ground surface. In addition, volatilization and dissolution from the residual phase would have to be instantaneous so that equilibrium assumptions apply.

#### 4.2.2 Numerical Verification

The set of PDE developed above did not have an analytical solution. The model was evaluated by comparing diffusion and reaction components separately against

analytical solutions. The accuracy of the diffusion component was verified by setting the reaction to zero, thereafter equation (4.16) was reduced to:

$$\frac{\partial G_k}{\partial t} = D_{eff} \frac{\partial^2 G_k}{\partial Z^2} \quad (4.26)$$

Equation (4.26) is a one-dimensional, transient gas diffusion with phase partitioning, in which an analytical solution exists for a finite system of  $G_k = G_{k0}$  at  $z = 0$ ,  $G_k = 0$  at  $z = L$ , and  $G_k = 0$  at  $t = 0$ .  $D_{eff}$  is the combined diffusion coefficient of both water and air phases over the retardation factor. An analytical solution of equation (4.26) was given by (Crank, 1985) as

$$G = G_1 - G_1 \frac{Z}{L} + \frac{2}{\pi} \sum_1^{\infty} -\frac{G_1}{n} \sin \frac{n\pi Z}{L} \exp\left(-\frac{D_{eff} n^2 \pi^2 t}{L^2}\right) \quad (4.27)$$

A series of numerical experiments was conducted by varying spatial and temporal discretizations. Experimental conditions of Column 2 were used in these simulations (see Table 4.1). Physical and chemical properties of toluene at 15°C are summarized in Table 4.2. All parameters were assigned to be spatially uniform throughout the entire domain.

Propagation of toluene vapor as a function of time is illustrated in Fig. 4.2. A total time of 50 hours was simulated, employing a constant time step ( $\Delta t$ ) of 0.5 hour and a grid size ( $\Delta z$ ) of 5 cm. Solid lines depict analytical solutions. Open and closed symbols represent time-derivative approximations by the backward difference ( $\alpha = 1$ ) and Crank-Nicholson ( $\alpha = 0.5$ ) methods, respectively. Results of numerical modeling were compared to the analytical solutions for each simulation, and the deviations defined by  $L_2$ -norm (Burden and Faires, 1985) were designated as numerical errors. In Fig. 4.3, the  $L_2$ -norm error per node of these simulations was plotted against the number of time steps. As expected, simulations using  $\alpha = 0.5$  converged at a faster rate than those using  $\alpha = 1$ . After 10,000 time steps, the errors of both time schemes were indistinguishable, implying limitations in computer storage of significant digits.

Convergence properties of both time schemes ( $\alpha = 0.5$  and  $\alpha = 1$ ) in space and time were examined. Simulations were conducted by varying either  $\Delta z$  or  $\Delta t$ , and their  $L_2$ -norm error per node are plotted against the corresponding variable. Figure 4.4 illustrates the error reduction due to grid refinement. Results of three grid sizes (2.5, 5, and 10 cm) were compared at a fixed simulation time using same  $\Delta t$  of 0.5 hour. It was apparent that results using smaller grid size gave rise to more accurate solutions than larger grid size. Simulations using  $\alpha = 0.5$  were subject to less error than those using  $\alpha = 1$ . The rate of convergence with respect to  $\Delta z$  for  $\alpha = 0.5$  is faster than that of  $\alpha = 1$ . Solutions for various time-step sizes were compared at a specific time (500 hours) for a fixed nodal spacing ( $\Delta z = 5$  cm). Figure 4.5 shows the effect of a decreasing time step on the accuracy of both time schemes. As in the case of grid refinement, a decrease in  $\Delta t$  reduced the numerical error. Simulations using  $\alpha = 0.5$  offered slightly faster rate of convergence than that of  $\alpha = 1$ .

Likewise, the reaction component of equation (4.16) was tested by setting the diffusivity to zero, yielding

$$[\theta_a + \theta_w H_{wa} + \rho_b K_d H_{wa}] \frac{\partial G}{\partial t} = \theta_w \mu_{\max} X \quad (4.28)$$

Equation (4.28) has an analytical solution of

$$G = G_0 + \frac{\theta_w X_0}{[\theta_a + \theta_w H_{wa} + \rho_b K_d H_{wa}]} [1 - \exp(-\mu_{\max} t)] \quad (4.29)$$

In these simulations, the initial concentrations of toluene vapor were constant throughout the column at 10 mg/L. Model inputs were identical to those used in the diffusion tests except the values of diffusion coefficients. Simulations were conducted using two time-step sizes (0.1 and 0.5 hours) and both time-derivative schemes ( $\alpha = 0.5$  and  $\alpha = 1$ ). These simulations, along with the analytical solution for comparison purpose, are plotted as concentration remaining versus time in Fig. 4.6. The numerical method using  $\alpha = 0.5$  and a time step of 0.1 hour provided a more accurate solution to the reaction equation.

The maximum relative error associated with this numerical method was calculated at the end of the simulation to be 0.04%.

The above numerical experiments showed that the numerical solution developed here was unconditionally stable and convergent. The accuracy of the model was dependent on the choice of nodal spacing and time-step size. Within the span of the conditions analyzed, Crank-Nicholson time scheme ( $\alpha = 0.5$ ) offered a more accurate solution than the backward difference scheme ( $\alpha = 1$ ). Hence, the former scheme will be used in all model simulations discussed below.

### 4.3 MODEL EVALUATION

Overall model performance was evaluated by comparison with laboratory data from column experiments (see Chapter 2). The column experiments were conducted to study toluene diffusion and biodegradation under influences of air-water partitioning and sorption in an unsaturated sandy soil. The column system resembles the unsaturated zone, in which an upward flux of a volatile hydrocarbon from an immobilized source above capillary fringe interacts with a downward flux of  $O_2$  from ground surface, producing  $CO_2$  and biomass. Two cases were simulated: the first case (Column 1) was at  $10^\circ C$  with a saturated-vapor source of toluene (65 mg/L) and the second case (Column 2) was at  $15^\circ C$  with a lower source-concentration of 10 mg/L. Table 4.1 lists the initial and boundary conditions used in simulations of both columns. In both cases, the simulations started at time zero when toluene concentrations at the boundary  $z = 0$  were raised to their source concentrations for  $t > 0$ . Additionally,  $O_2$  and  $CO_2$  concentration gradients were also set equal to zero for no flux-boundary conditions at this boundary. At the opposite boundary from the source, toluene concentration was set equal to zero, whence  $O_2$  and  $CO_2$  concentrations were held constant at 21 and 0%, respectively, as detected in the effluent air. Because soil properties were not measured for Column 1, values similar to field measurements of the same sand were used (MacPherson, 1991). Mean values of measured soil properties of Column 2 were used in the simulations of

the second case (Table 4.1). The required physical and chemical parameters of toluene, O<sub>2</sub>, and CO<sub>2</sub> at both temperatures are summarized in Table 4.2. Parameters associated with microbial processes were obtained from either literature or batch kinetic experiments (Chapter 3). These values are also included in Table 4.1. It was assumed that the microbes were uniformly present at an initial concentration corresponding to the mean value found in batch experiments. Unless stated otherwise, Tables 4.1 and 4.2 contain parameter values used for the simulations discussed below.

#### 4.3.1 Simulation Results

Toluene profiles for the saturated-concentration-source case (Column 1) are plotted in Fig. 4.7. Both computed profiles (solid lines) and measured data (symbols) are shown over a period of 1560 hours. [Because the column was operated at 10°C rather than 15°C,  $\mu_{\max}$  in this simulation was reduced from 0.1 to 0.05 h<sup>-1</sup> (Chang et al., 1985).] Also plotted in the figure are the computed profiles resulting from diffusion only (shown in dotted lines). Overall, the diffusion-only profiles gave an excellent match to the experimental profiles, suggesting that under these conditions biodegradation was not an important process relative to diffusion.

Computed and measured toluene profiles for the lower-concentration-source case (Column 2) are plotted in Fig. 4.8 over a period of 1750 hours. Experimental data are represented by both open and closed symbols. The thin solid lines are model results corresponding to experimental data depicted by open symbols, whereas the thick solid lines correspond to the closed symbols. Considering that all the input parameters were determined independently and that no curve-fitting was used, the model was in excellent agreement with the experimental data.

Prior to initiating the experiment, Column 2 was periodically exposed to toluene at varying toluene concentrations. As a result, the initial microbial concentration determined from the batch experiments would be lower than the population concentration in the column. To account for the pre-exposure, a series of simulations was carried out

at varying source concentrations using an initial microbial concentration obtained from batch experiments. It was the concentration of microbial distribution at the end of the simulation series that was designated as the initial population for the actual simulation (thick solid line shown in Fig. 4.10). The simulation series also showed that microbes consumed all the bioavailable N in the first 50 cm near the source during this pre-exposure period. The large initial population resulting from pre-exposure brought about significant biodegradation more rapidly. Most of the toluene in the column at 43 hours was consumed by 73 hours such that the vapor front moved backward towards the source to a location, where the effects of biodegradation and diffusion processes were balanced. Because N was limited in the region from 0 to 50 cm (see Fig. 4.10 below), most of the biodegradation occurred at the very front of the profile, hereafter referred to as the bioactive zone. Inside the bioactive zone, the rate of toluene consumption was equal to its rate of supply. The microbial concentration within the zone continued to increase until all the N was utilized, after which the biodegradation rate dropped to a level of cell maintenance energy. Consequently, diffusion caused the vapor front to move away from the source into a region where N was not yet limited. In the presence of both substrate and N, biodegradation continued in the new region until N was used up, after which toluene moved further away from the source. The overall result was a slowly moving toluene front away from the source. The time for toluene transport across the column was therefore controlled by diffusion, biodegradation, and N availability. Toluene migration was much slower in the presence of biodegradation than without. Simulations conducted under exactly same conditions except a zero reaction rate yielded a steady-state profile within 1171 hours (plots not shown).

A considerable amount of CO<sub>2</sub> produced by degradation was lost by dissolution into toluene aqueous-source storage. This resulted in a complicated CO<sub>2</sub> boundary condition at  $z = 0$ . In light of the difficulty in simulating CO<sub>2</sub> profiles under such boundary condition, simulations were carried out as if no CO<sub>2</sub> was lost at the source (a zero-flux boundary condition). Model and measured results of CO<sub>2</sub> profiles at various

times are shown in Fig. 4.9(a) and (b). It can be seen that CO<sub>2</sub> loss at the source boundary had a profound effect on the shape of CO<sub>2</sub> profiles.

The change in the microbial distribution over time is presented in Fig. 4.10. The initial population distribution was also included in the figure. Since source concentration was lower than the inhibitory concentration used in the model (21 mg/L of vapor at 15°C), microbial populations proliferated throughout the entire column provided there was enough toluene and N to support growth. According to these model simulations, biodegradation was significant in a small region at the very front of toluene profiles. This can be explained as populations in an upper-gradient location grow to a size that is capable of degrading all the toluene that migrates by. Therefore, no toluene is left for those microorganisms down the column. Hence, a narrow bioactive zone is established. However, the microbial active zone extended with time (Fig. 4.10). The reason was that as toluene diffusive flux became smaller with time, the biodegradation rate was also lower such that the upgradient microbes were not able to completely degrade all the toluene. Hence, there was some toluene available for the microbial population further down the column, causing the active zone to elongate.

In brief, model results agreed well with toluene data from column experiments. Biodegradation was important when toluene concentration was below the inhibitory level, and the factor ultimately affecting the extent of biodegradation was the bioavailability of N in the soil.

### 4.3.2 Sensitivity Analyses

In the following section, sensitivity analyses were carried out to examine how various physical, chemical, and biological parameters affected modeling results. These parameters were examined in the following order:  $\mu_{\max}$ ,  $X_0$ ,  $X_N$ ,  $K_{oc}$ , and  $\theta_a$ . For some parameters, base scenarios of both Column 1 and 2 were tested. For others, only the base scenario of Column 2 was explored. Table 4.3 summarizes the parameter ranges

employed in all the sensitivity tests. All simulations were performed with a spatially uniform initial microbial concentration of 0.011 mg/L.

*Sensitivity analyses with respect to  $\mu_{\max}$*

The equivalent microbial concentration ( $X$ ) and the specific growth rate ( $\mu_{\max}$ ) are two key microbial variables in controlling the utilization rate of toluene. Both conditions of high and low source-concentrations were selected to be base cases. Because toluene utilization rates reflecting maintenance-energy requirements for other growth rates were not known, all simulations were conducted with no maintenance-energy requirement.

Figures 4.11 and 4.12 show the effects of different  $\mu_{\max}$  on toluene profiles under high (Column 1) and low (Column 2) concentration sources, respectively. In both cases, the effect of different  $\mu_{\max}$  was not observed initially due to a small initial population (plots not shown). As time progressed, simulations with higher  $\mu_{\max}$  yielded higher biodegradation rates and affected toluene profiles at earlier times. In the high source-concentration cases, the model was relatively insensitive to  $\mu_{\max}$  due to high diffusive flux and substrate toxicity. As a result, steady-state conditions developed quickly as three profiles collapsed into one (occurred at ~320 hours). For the low source-concentration cases, the model was more sensitive to  $\mu_{\max}$  at early times as populations were growing with no limiting conditions (Fig. 4.12). However, as biodegradation became large, the growth rates, thereby their biodegradation rates corresponding to these  $\mu_{\max}$ , were limited by the supply of toluene. Therefore, the difference in the effect of  $\mu_{\max}$  diminished. Since populations with high  $\mu_{\max}$  exploited the N resource more rapidly than populations with low  $\mu_{\max}$ , the vapor front of high  $\mu_{\max}$  moved ahead that of low  $\mu_{\max}$  eventually. Steady-state profiles in the low-source-concentration case was reached by 3600 hours (plots not shown).

*Sensitivity analyses with respect to  $X_0$*

Indigenous hydrocarbon-degrading populations in subsurface soil typically range from  $10^4$  to  $10^6$  cells per g of aquifer material (Allen-King et al., 1994; Rosenberg, 1992;

Raymond et al., 1976). Considering the uncertainty associated with this variable, simulations were performed using  $X_0$  values that range two orders of magnitude. The influence of different  $X_0$  on toluene migration was analyzed under both conditions of Column 1 and Column 2, and the respective toluene-concentration profiles at various times were compared.

Figures 4.13 and 4.14 illustrate the effects of different  $X_0$  on toluene migration under high (Column 1) and low (Column 2) concentration sources, respectively. In all cases, the overall effect was minimal in the beginning and became more apparent at later times. For the high concentration cases, the effect of  $X_0$  was less dramatic than the low concentration cases due to high diffusive flux, and toluene profiles converged as they approached steady state at a much earlier time (263 vs. 1750 hours). For the low concentration cases, the difference among profiles diminished when biodegradation was limited by the supply of toluene. Clearly, the effect of varying  $X_0$  on toluene profiles was similar to that of varying  $\mu_{\max}$  for both high and low concentration cases, with lesser magnitude of impact by varying  $X_0$ . In addition, higher values of  $X_0$  or  $\mu_{\max}$  had more effect on toluene migration at a much earlier time than their lower values, since growth was exponential.

The above simulations illustrated a relatively small overall effect on toluene migration by varying the initial biomass concentration over 2 orders of magnitude; although, the model was initially sensitive to  $X_0$  for a short period of time. In natural settings, the process of vigorous growth with no limitations imposed would sooner or later level off due to deficiency of one or more of the essential elements for growth. The lack of sensitivity of model performance on values of  $X_0$  used implied that  $X_0$  needs not be known precisely.

#### *Sensitivity analyses with respect to $X_N$*

The extent to which bioavailable N content ( $X_N$ ) influenced the extent at which aerobic biodegradation took place was also examined. N is needed by microbes for the synthesis of cellular material including protein, DNA, and RNA as well as for the

synthesis of ATP. N constitutes about 15% of the dry cell weight, which is more than any other inorganic elements. Figures 4.15 and 4.16 show the effects of  $X_N$  on toluene migration under high (Column 1) and low (Column 2) concentration sources, respectively.

Under high source-concentration conditions (Fig. 4.15), toluene migration for the base case and for a case with ten times as much N were compared. As anticipated, no effect of  $X_N$  was observed initially because N was not limiting. Later, the effect became significant when significant reduction of toluene occurred in the high N case despite strong diffusive flux. This was because high  $X_N$  supported a large microbial population, which resulted in high biodegradation rates that removed toluene faster than it was supplied. Microbial growth in the high  $X_N$  case was eventually limited by the availability of N, and vapor front moved away from the source. However, toluene moved across the column much more slowly in the case of high  $X_N$  than low  $X_N$ . In reality, when N is abundant, growth may continue until some other mineral nutrients besides N become limiting. In addition, as microcolonies grow larger in size, supplies of substrate, nutrients, and growth factors into colony center may become diffusion-limited. This may have an effect on the apparent  $\mu_{max}$ .

No initial effect ( $\leq 73$  hours) was shown in the cases of low source-concentration (Fig. 4.16). (Note that a narrower range of  $X_N$  was used in these analyses.) Similar to the cases above, different  $X_N$  values influenced toluene migration to different degrees. Low  $X_N$  resulted in low extent of biodegradation; as a result, it had a low impact on the advance of the profile. A comparison between profiles at 117 and 1750 hours showed that the difference became more apparent with time. Unlike the cases above, the effect of  $X_N$  was consistent through time. All profiles approached steady-state after 7200 hours without converging into one. This was caused by low diffusive flux and the fact that all three profiles had different maintenance levels (hence different biodegradation rates after growth ceased). Different  $X_N$  sustained different sizes of populations in which their maintenance-energy levels were proportional to their sizes. This effect of  $X_N$  was not

seen in the high-source cases because the effect of biodegradation due to maintenance was not large enough to affect diffusion.

*Sensitivity analyses with respect to  $K_{oc}$*

Among all the physical parameters used,  $K_{oc}$  is generally subject to the most uncertainty. Consequently, simulations were conducted to determine  $K_{oc}$  influence on toluene migration at three different values of  $K_{oc}$  reported for toluene. These values of  $K_{oc}$  are 46 (Chen et al., 1992), 98 (Jury et al., 1984), and 300 (Mabey et al., 1982) ml/g. Higher  $K_{oc}$  values correspond to higher sorption, therefore reducing the mass in the vapor and water phases. Adsorbed compounds are generally thought to be not accessible for microbial utilization (Borden and Bedient, 1986; Widdowson et al., 1988); nonetheless, the microbial degradation affects sorption by reducing compound concentration in the aqueous phase.

Figure 4.17 shows time series of simulated toluene profiles using above  $K_{oc}$  values under the condition of low source-concentration. The dependency of model performance to  $K_{oc}$  was apparent in the two early times when biodegradation was not important. However, the dependency diminished when biodegradation became important as shown by smaller differences among profiles at later times. To confirm that biodegradation was in part responsible for the profiles becoming indistinguishable, simulations were repeated for conditions under no biodegradation. The results are plotted in Fig. 4.18. In the absence of biodegradation, toluene was retarded to different degrees by  $K_{oc}$ . Toluene profiles diverged with time before the boundary effect set in (between 19 and 73 hours), after which the profiles coincided with one another as they reached steady state. These results indicated that  $K_{oc}$  was an important sink in the beginning. As populations grew larger and because sorption was at equilibrium, biodegradation became the major sink, hence controlling transport. In other words, toluene moved much slower in the presence of biodegradation such that a pseudo-steady state was reached, (the time scale of transport was long compared to the time needed to saturate the porous medium with sorbed compounds), and toluene was no longer retarded by the medium.

Under such conditions,  $K_{oc}$  no longer controlled transport, and only a minor effect of partitioning due to different  $K_{oc}$  values was exhibited.

*Sensitivity analyses with respect to  $\theta_a$*

All simulations presented up to this point have not depicted a development of anaerobic conditions due to inadequate  $O_2$  supply. Therefore, a simulation of Column 2 in which the air-filled porosity was reduced to 0.10 from a previous value of 0.31 was conducted. Along with a toluene profile at 300 days, profiles of  $O_2$  and X at the same time are presented in Fig. 4.19. At 75% water saturation,  $O_2$  supply was nearly depleted by metabolism in the vicinity of source boundary. This was because when air-filled porosity was decreased, the rate of  $O_2$  diffusion was also reduced, and anoxic conditions quickly developed as the initial  $O_2$  supply was consumed. [One of the requirements for biodegradation imposed in the model was the presence of  $O_2$  at a dissolved concentration above 2 mg/L (Barker and Mayfield, 1988; Chiang et al., 1989).] Denitrification by dissimilatory reduction of nitrate is commonly found in groundwater when dissolved  $O_2$  levels are below 1 to 2 mg/L (Gillham and Cherry, 1978). As  $O_2$  concentration drops below this critical level, the current model which includes only aerobic respiration assumes microorganisms would stop growing and become dormant. In spite of a continual supply of substrate and ample N left in the source region, microorganisms in the area were unable to respond to additional toluene. Consequently, toluene front advanced further away from the source. However, diffusion of toluene was very slow because the apparent diffusion coefficient was reduced and more toluene partitioned into the water phase. As toluene vapor front moved away from the source,  $O_2$  supply rates were relatively higher, and biodegradation continued until N in the area was exhausted. The advance of toluene was therefore controlled by diffusion of toluene and  $O_2$ , biodegradation, and N limitation. The erratic behavior of the X profile developed in the anoxic region was caused by the inadequacy of microbial kinetics formulation for the  $O_2$ -limiting condition imposed in this simulation. (The microbial kinetics used in the model is applicable to cases of unlimited  $O_2$ , in which a microbial growth rate is dependent on

the concentration of substrate but not  $O_2$ .) Fig. 4.20 shows toluene,  $O_2$ , and X profiles at 300 days from a simulation scenario of  $\theta_a = 0.21$ . It can be seen that at 50% water saturation,  $O_2$  prevailed throughout the column, and no erratic behavior of X was shown. In these simulations, a smaller grid size (0.625 cm) was used in handling sharp front.

#### 4.4 CONCLUSIONS

A model for simulating diffusion and biodegradation of a volatile hydrocarbon compound,  $O_2$ , and  $CO_2$  in unsaturated porous media was developed. The model was used in support of a laboratory study for examining effects of various processes on toluene migration through unsaturated sandy soil. Processes included in the model are diffusion, air-water and water-solid partitionings, and microbial growth/degradation. No effect of temperature was considered, and soil characteristics were invariant with time and space. Biodegradation was formulated in accordance to findings from batch kinetic experiments of toluene. The rate of biodegradation was zero order with respect to both toluene and  $O_2$  concentrations and first order with respect to microbial concentration. Such kinetics reflects the rate of contaminant utilized by a microbial population growing logarithmically under unlimited substrate and  $O_2$  supply. The extent of biodegradation was ultimately limited by the lack of an inorganic nutrient essential for growth (in this case, the limiting nutrient was N). The resultant system of three transport and one microbial growth equations described toluene transport and fate in unsaturated porous media under influences of physical, chemical, and biological processes.

The transport equations were solved through applications of the Galerkin finite-element method and Crank-Nicholson time-weighting scheme for 1-D transport of toluene,  $O_2$ , and  $CO_2$ . The microbial growth function was solved analytically. The model was evaluated against data from column experiments which resembled vapor-phase transport in an unsaturated region bounded by an immobilized source above the capillary fringe and ground surface. All model parameters were obtained from either literature or independent laboratory characterizations. In general, simulations of toluene migration

were in good agreement with column data. Parameter sensitivity analyses were performed with respect to maximum specific growth rates, initial biomass concentrations, bioavailable N contents, sorption coefficients, and air-filled porosities for different source concentrations.

Results of model evaluations and sensitivity tests can be summarized as follows. In an unsaturated sandy environment, diffusion is often the dominant process in the vicinity of a source. The effect of biodegradation may be insignificant due to high diffusive flux and substrate toxicity. Under these conditions, hydrocarbon migration was greatly affected by diffusion and was sensitive to sorption coefficients. However, the effect of sorption disappeared as profiles approached steady state. When environmental conditions are appropriate for growth, biodegradation may have a major effect on contaminant transport. Appropriate conditions include that 1) the contaminant concentration is not inhibitory, 2) there is surplus of toluene and O<sub>2</sub> supply in the system, and 3) the inorganic nutrients such as N are not limiting. Under these circumstances, model performance was dependent highly on microbial parameters, less on N availability, and insensitive to sorption. When the rate of biodegradation was limited by the supply rate of toluene and the availability of N, biodegradation took place within a thin zone, and model sensitivity with respect to all parameters except the bioavailable N was low. Under these conditions, all parameters except the bioavailable N had a secondary effect on toluene migration, implying that they need not be known precisely. Inherent in the model formulation was the assumption that O<sub>2</sub> was present in excess.

The 1-D model applied well in the case of column studies. Simulations of natural *in situ* biodegradation in a polluted unsaturated zone where lateral transport is important would require an increase in model dimensionality. However, there are many "real-world" cases where the areal extent of the source is large relative to the vertical distance from the source to ground surface in which case the 1-D model will be appropriate. Regardless, the concepts presented here can be generalized readily to higher dimensions.

#### 4.5 REFERENCES

- Alexander, M., and K. M. Scow, Kinetics of biodegradation in soil, in *Reactions and Movement of Organic Chemicals in Soils*, edited by B. L. Sawhney and K. Brown, SSSA Special Publication No. 22, Soil Science Society of America, Madison, pp. 243-269, 1989.
- Allen-King, R. M., J. F. Barker, R. W. Gillham, and B. K. Jensen, Substrate- and nutrient-limited toluene biotransformation in sandy soil, *Environ. Toxicol. Chem.*, *13*, 693-705, 1994.
- Angelakis, A. N., and D. E. Rolston, Transient movement and transformation of carbon species in soil during wastewater application, *Water Resour. Res.*, *21*, 1141-1148, 1985.
- Baehr, A. L., Selective transport of hydrocarbons in the unsaturated zone due to aqueous and vapor phase partitioning, *Water Resour. Res.*, *23*, 1926-1938, 1987.
- Baehr, A. L., and M. Y. Corapcioglu, A compositional multiphase model for groundwater contamination by petroleum products, 1, Theoretical considerations, *Water Resour. Res.*, *23*, 201-213, 1987.
- Barker, J. F., and C. I. Mayfield, The persistence of aromatic hydrocarbons in various ground water environments, in *Proceedings of the Conference on Petroleum Hydrocarbons and Organic Chemicals in Groundwater: Prevention, Detection, and Restoration*, National Water Well Association, Dublin, Ohio, pp. 649-667, 1988.
- Barnes, C. J., Solute and water movement in unsaturated soils, *Water Resour. Res.*, *25*, 38-42, 1989.
- Borden, R. C., and P. B. Bedient, Transport of dissolved hydrocarbons influenced by oxygen-limited biodegradation, 1, Theoretical development, *Water Resour. Res.*, *22*, 1973-1982, 1986.
- Borden, R. C., P. B. Bedient, M. D. Lee, C. H. Ward, and J. T. Wilson, Transport of dissolved hydrocarbons influenced by oxygen-limited biodegradation, 2, Field application, *Water Resour. Res.*, *22*, 1983-1990, 1986.
- Bruell, C. J., and G. E. Hoag, The diffusion of gasoline-range hydrocarbon vapors in porous media, experimental methodologies, in *Proceedings of the NWWA/API Conference on Petroleum Hydrocarbons and Organic Chemicals in Groundwater: Prevention, Detection, and Restoration*, National Water Well Association, Dublin, Ohio, pp. 420-443, 1986.

Brunner, W., and D. D. Focht, Deterministic three-half order kinetic model for microbial degradation of added carbon substrates in soil, *Appl. Environ. Microbiol.*, *47*, 167-172, 1984.

Burden, R. L., and J. D. Faires, *Numerical Analysis*, 3rd ed., PWS Publishers, Boston, 1985.

Chang, F. H., M. F. Hult, N. N. Noben, D. Brand, Microbial degradation of crude oil and some model hydrocarbons, in U.S. Geological Survey Program on Toxic Waste--Ground-Water Contamination, Proceedings of the Second Technical Meeting, Cape Cod, Massachusetts, Oct. 21-25, 1985, *U.S. Geol. Surv. Open File Rep. 86-481*, pp. C33-C42, 1988.

Chen, Y., L. M. Abriola, P. J. J. Alvarez, P. J. Anid, and T. M. Vogel, Modeling transport and biodegradation of benzene and toluene in sandy aquifer material: Comparisons with experimental measurements, *Water Resour. Res.*, *28*, 1833-1847, 1992.

Corapcioglu, M. Y., and A. L. Baehr, A compositional multiphase model for groundwater contamination by petroleum products, 1, Theoretical considerations, *Water Resour. Res.*, *23*, 191-200, 1987.

Crank, J., *The Mathematics of Diffusion*, 2nd ed., Oxford University Press, New York, 1985.

De Smedt, F., and P. J. Wierenga, Solute transfer through columns of glass beads, *Water Resour. Res.*, *20*, 225-232, 1984.

Falta, R. W., I. Javandel, K. Pruess, and P. A. Witherspoon, Density-driven flow of gas in the unsaturated zone due to the evaporation of volatile organic compounds, *Water Resour. Res.*, *25*, 2159-2169, 1989.

Farmer, W. J., M. S. Yang, J. Letey, and W. F. Spencer, Hexachlorobenzene: Its vapor pressure and vapor phase diffusion in soil, *Soil Sci. Soc. Am. Proc.*, *44*, 676-680, 1980.

Gillham, R. W., and J. A. Cherry, Field evidence of denitrification in shallow groundwater flow systems, *Water Poll. Res. Canada*, *13*, 53-71, 1978.

Jury, W. A., R. Grover, W. F. Spencer, and W. J. Farmer, Modeling vapor losses of soil-incorporated triallate, *Soil Sci. Soc. Am. J.*, *44*, 445-450, 1980.

Jury, W. A., D. Russo, G. Streile, and H. El. Abd, Evaluation of volatilization by organic chemicals residing below the soil surface, *Water Resour. Res.*, *26*, 13-20, 1990.

Jury, W. A., W. F. Spencer, and W. J. Farmer, Behavior assessment model for trace organics in soil, I. Model description, *J. Environ. Qual.*, 12, 558-564, 1983.

Jury, W. A., W. F. Spencer, and W. J. Farmer, Behavior assessment model for trace organics in soil, III. Application of screening model, *J. Environ. Qual.*, 13, 573-579, 1984.

Karimi, A. A., W. J. Farmer, and M. M. Cliath, Vapor-phase diffusion of benzene in soil, *J. Environ. Qual.*, 16, 38-43, 1987.

Konikow, L. F., and J. D. Bredeheft, Computer model of two-dimensional solute transport and dispersion in groundwater, in *Automated Data Processing and Computations, Techniques of Water Resources Investigations of the U.S.G.S.*, 90 pp., U.S. Geological Survey, Washington, DC, 1978.

Longmuir, I. S., Respiration rate of bacteria as a function of oxygen concentration, *Biochemistry*, 57, 81-87, 1954.

Mabey, W. R., J. H. Smith, R. T. Podoll, H. L. Johnson, T. Mill, T. W. Chou, J. Gates, I. W. Partridge, H. Jaber, and D. Vandenberg, *Aquatic Fates Process Data For Organic Priority Pollutants*, USEPA, Washington D.C., 1982. EPA/440/4-81-014.

MacPherson, J. R. Jr., *Gas Phase Diffusion of Organic Compounds in Porous Media: Physical and Numerical Modeling*, Ph.D. diss., Oregon Graduate Institute of Science & Technology, Department of Environmental Science and Engineering, Beaverton, 1991.

MacQuarrie, K. T. B., and E. A. Sudicky, Simulation of biodegradable organic contaminants in groundwater, 2, Plume behavior in uniform and random flow fields, *Water Resour. Res.*, 26, 223-239, 1990.

MacQuarrie, K. T. B., E. A. Sudicky, and E. O. Frind, Simulation of biodegradable organic contaminants in groundwater, 1, Numerical formulation in principal directions, *Water Resour. Res.*, 26, 207-222, 1990.

Mayer, R., J. Letey, and W. J. Farmer, Models for predicting volatilization of soil-incorporated pesticides, *Soil Sci. Soc. Am. Proc.*, 38, 563-568, 1974.

McCarthy, K. A., and R. L. Johnson, Measurements of TCE diffusion as a function of moisture content in sections of gravity-drained soil columns, *J. Environ. Qual.*, (submitted), 1994.

Millington, R. J., Gas diffusion in porous media, *Science*, 130, 100-102, 1959.

Molz, F. J., M. A. Widdowson, and L. D. Benefield, Simulation of microbial growth dynamics coupled to nutrient and oxygen transport in porous media, *Water Resour. Res.*, 22, 1207-1216, 1986.

Ostendorf, D. W., and D. H. Kampbell, Biodegradation of hydrocarbon vapors in the unsaturated zone, *Water Resour. Res.*, 27, 453-462, 1991.

Patrick, G. C., J. F. Barker, R. W. Gillham, C. I. Mayfield, and D. Major, The behaviour of soluble petroleum product derived hydrocarbons in groundwater. Phase II. PACE Rept. No. 86-1, Petrol. Assoc. for Conservation Can. Environ., Ottawa, 1986.

Pirt, S. J., *Principles of Microbe and Cell Cultivation*, John Wiley, New York, 1975.

Rao, P. S. C., D. E. Rolston, R. E. Jessup, and J. M. Davidson, Solute transport in aggregated porous media: Theoretical and experimental evaluation, *Soil Sci. Soc. Am. J.*, 44, 1139-1146, 1980.

Raymond, R. L., J. O. Hudson Jr., and V. W. Jamison, Oil degradation in soil, *Appl. Environ. Microbiol.*, 31, 522-535, 1976.

Rifai, H. S., and P. B. Bedient, Bioplume II- two dimensional modeling for hydrocarbon biodegradation and in situ Restoration, *Proceedings of NWWA/API Conference on Petroleum Hydrocarbons and Organic Chemicals in Ground Water: Prevention, Detection, and Restoration*, National Water Well Association, Dublin, Ohio, pp. 431-450, 1987.

Rosenberg, E., The hydrocarbon-oxidizing bacteria, *The Prokaryotes*, 2<sup>nd</sup> ed., *A Handbook on the Biology of Bacteria: Ecophysiology, Isolation, Identification, Applications*, edited by Balows A., H. G. Trüper, M. Dworkin, W. Harder, and K. H. Schleifer, Vol. I, Springer Verlag, pp. 446-458, 1992.

Scow, K. M., S. Simkins, and M. Alexander, Kinetics of mineralization of organic compounds at low concentrations in soil, *Appl. Environ. Microbiol.*, 51, 1028-1035, 1986.

Silka, L. R., Simulation of vapor transport through the unsaturated zone-Interpretation of soil-gas surveys, *Ground Water Monitoring Review*, 8, 115-123, 1988.

Simkins, S., and M. Alexander, Models for mineralization kinetics with the variables of substrate concentration and population density, *Appl. Environ. Microbiol.*, 47, 1299-1306, 1984.

Sleep, B. E., and J. F. Sykes, Modeling the transport of volatile organics in variably saturated media, *Water Resour. Res.*, 25, 81-92, 1989.

Striegl, R. G., and A. L. Ishii, Diffusion and consumption of methane in an unsaturated zone in north-central Illinois, U.S.A., *J. of Hydrol.*, *111*, 133-143, 1989.

Sykes, J. F., S. Soyupak, and G. J. Farquhar, Modeling of leachate organic migration and attenuation in groundwaters below sanitary landfills, *Water Resour. Res.*, *18*, 135-145, 1982.

van Genuchten, M. T., G. F. Pinder, and W. P. Saukin, Modelling of leachate and soil interaction in an aquifer, paper presented at the *Symposium on Management of Gas and Leachate in Landfills*, USEPA, St. Louis, Mo., March 1977.

van Genuchten, M. T., and P. J. Wierenga, Mass transfer studies in absorbing porous media, I. Analytical solutions, *Soil Sci. Soc. Am. J.*, *40*, 473-480, 1976.

Wagenet, R. J., and P. S. C. Rao, Basic concepts of modeling pesticide fate in the crop root zone, *Weed Sci.*, *33*(Suppl. 2), 25-32, 1985.

Widdowson, M. A., F. J. Molz, and L. D. Benefield, A numerical transport model for oxygen- and nitrate- based respiration linked to substrate and nutrient availability in porous media, *Water Resour. Res.*, *24*, 1553-1565, 1988.

**Table 4.1. Boundary and initial conditions and other parameter inputs used in majority of modeling.**

	Column 1	Column 2
Temperature (°C)	10	15
Column length (L, cm)	170	160
Boundary conditions: for toluene (mg/L) at Z = 0 at Z = L for O <sub>2</sub> at Z = 0 at Z = L for CO <sub>2</sub> at Z = 0 (%/cm <sup>2</sup> /s) at Z = L (%/cm <sup>2</sup> /s)	65 0 0 21 0 0	10 0 0 21 0 0
Initial conditions: for toluene (mg/L) for O <sub>2</sub> (%) for CO <sub>2</sub> (%) for °X (mg/L)	0 21 <i>a</i> 0.011	0 21 <i>b</i> <i>d</i>
Δt (h)	0.5	0.05
ΔZ (cm)	5.0	2.5
Soil properties: ρ <sub>b</sub> (g/ml) θ <sub>T</sub> (ml/ml) θ <sub>a</sub> (ml/ml)	1.50 0.40 0.35	1.54 0.42 0.31
Microbial parameters: μ <sub>max</sub> (h <sup>-1</sup> ) K <sub>s</sub> (mg/L) °X <sub>N</sub> (mg/L) °C <sub>inh</sub> (mg/L) °M <sub>f</sub>	0.052 <0.003 433 16.4 0.005	0.103 <0.003 739 20.8 0.005

<sup>a</sup> Linear interpolation of CO<sub>2</sub> data on March 27, 1990 (see Appendix-A).

<sup>b</sup> Linear interpolation of CO<sub>2</sub> data on March 16, 1991 (see Appendix-A).

<sup>c</sup> X has a unit of concentration in the aqueous phase.

<sup>d</sup> See text and Figure 4.10.

<sup>e</sup> M<sub>f</sub> ≡ Maintenance factor (Appendix C); C<sub>inh</sub> ≡ Inhibitory concentration.

**Table 4.2. Physical and chemical properties of toluene at 10 and 15°C.**

Compound Properties	10 °C			15 °C		
	Toluene	O <sub>2</sub>	CO <sub>2</sub>	Toluene	O <sub>2</sub>	CO <sub>2</sub>
H <sub>i,wa</sub> (dimensionless)	6.1	0.04	1.2	4.8	0.04	1.1
K <sub>d</sub> (ml/g)	0.14	0.0	0.0	0.14	0.0	0.0
d <sub>iw</sub> × 10 <sup>5</sup> (cm <sup>2</sup> /s)	0.62	1.5	2.3	0.75	1.7	1.6
d <sub>ia</sub> × 10 <sup>1</sup> (cm <sup>2</sup> /s)	0.80	1.9	1.5	0.82	2.0	1.6

**Table 4.3. Parameter ranges used for sensitivity analyses.**

	Column 1	Column 2
$\mu_{\max}$ ( $\text{h}^{-1}$ )	0.01 - 0.10	0.05 - 0.50
$X_0$ (mg/L)	0.0011 - 0.110	0.0011 - 0.110
$X_N$ (mg/L)	433 - 4330	370 - 1109
$K_{oc}$ (ml/g)	N/A	46 - 300
$\theta_a$ (vol/vol)	N/A	0.31 - 0.10

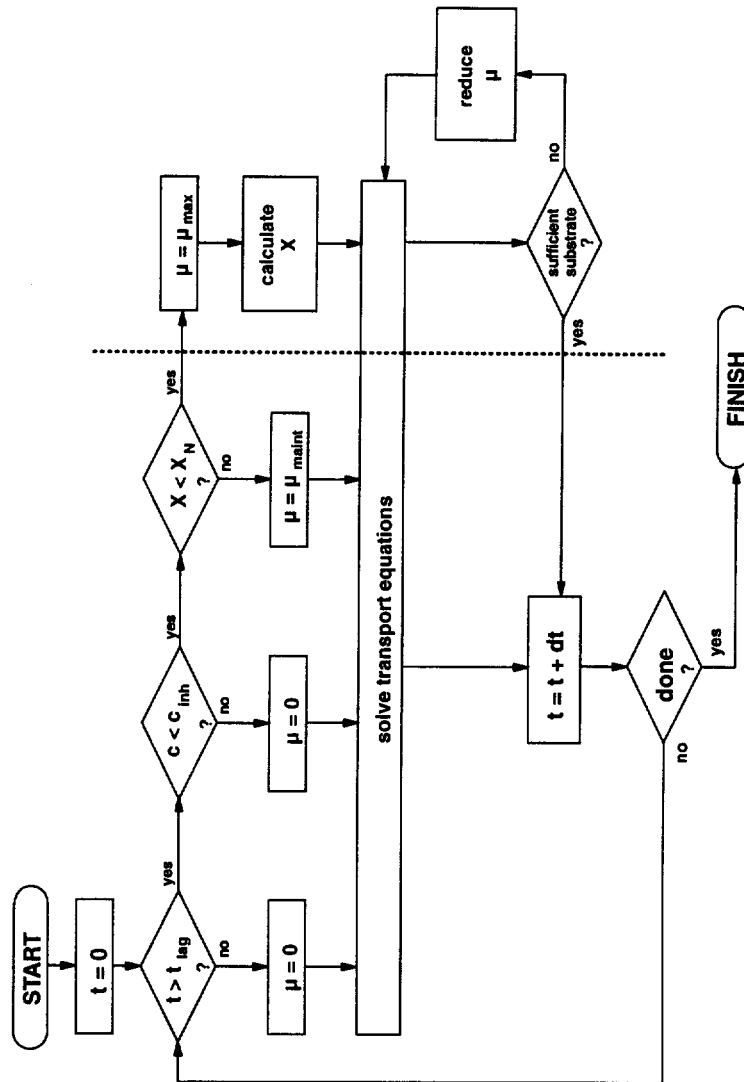
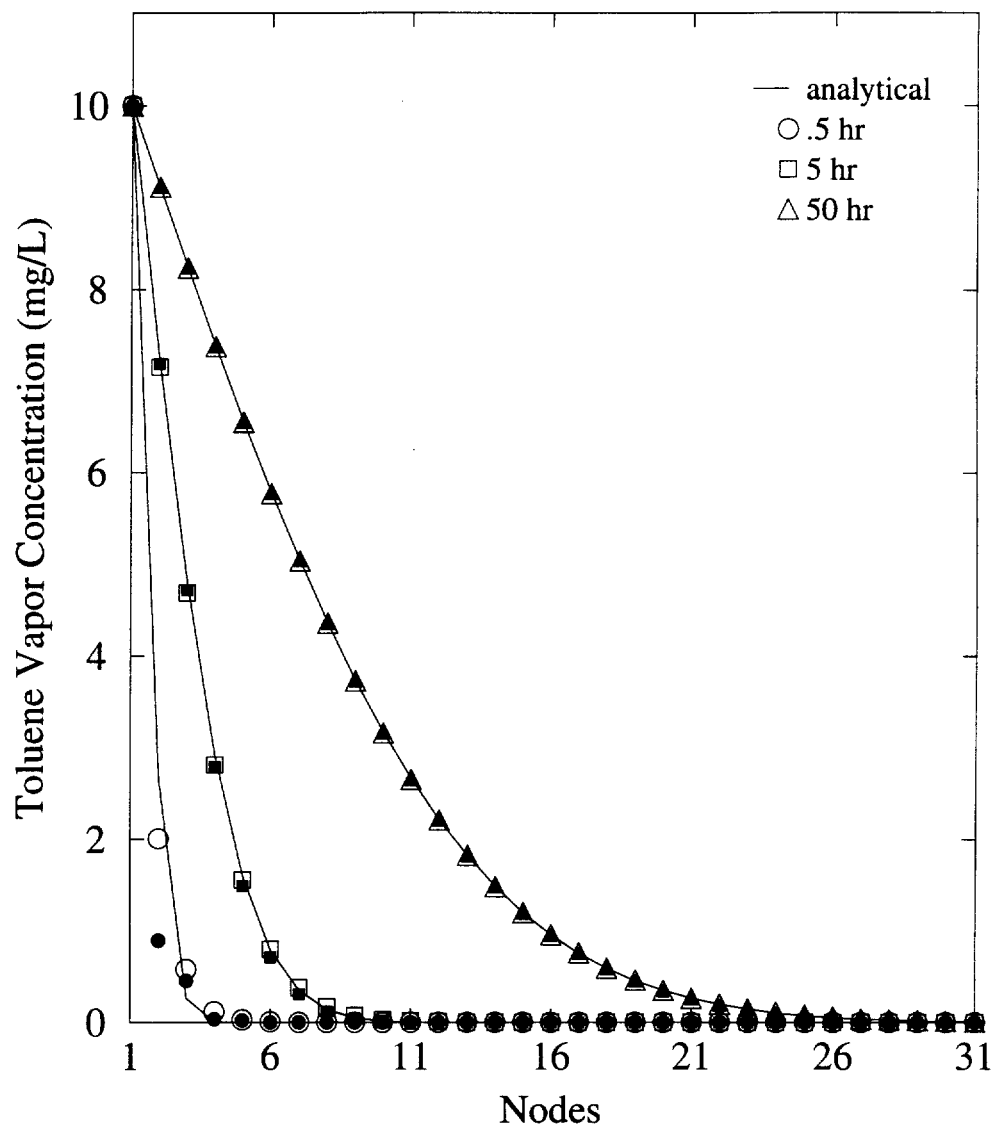
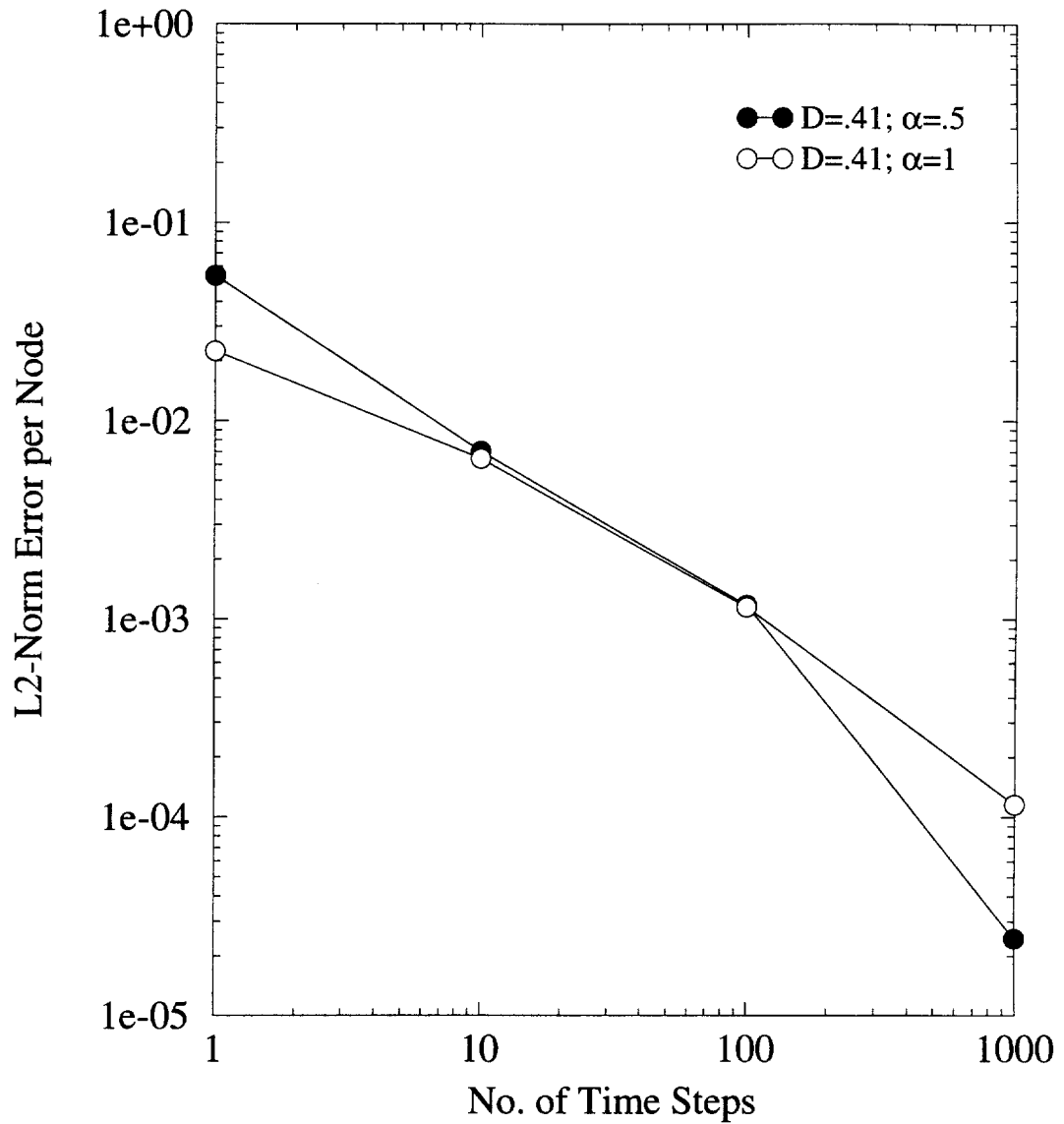


Figure 4.1. Flow chart of numerical scheme.



**Figure 4.2. Diffusion profiles of toluene over time. Solid lines depict analytical solutions. Open ( $\alpha=1$ ) and closed ( $\alpha=0.5$ ) symbols depict model results using  $\Delta z = 5$  cm and  $\Delta t = 0.5$  hour.**



**Figure 4.3.** Decrease in numerical error with time for diffusion solutions with different  $\alpha$  (time-weighting schemes).  $\Delta z = 5$  cm and  $\Delta t = 5$  hour.

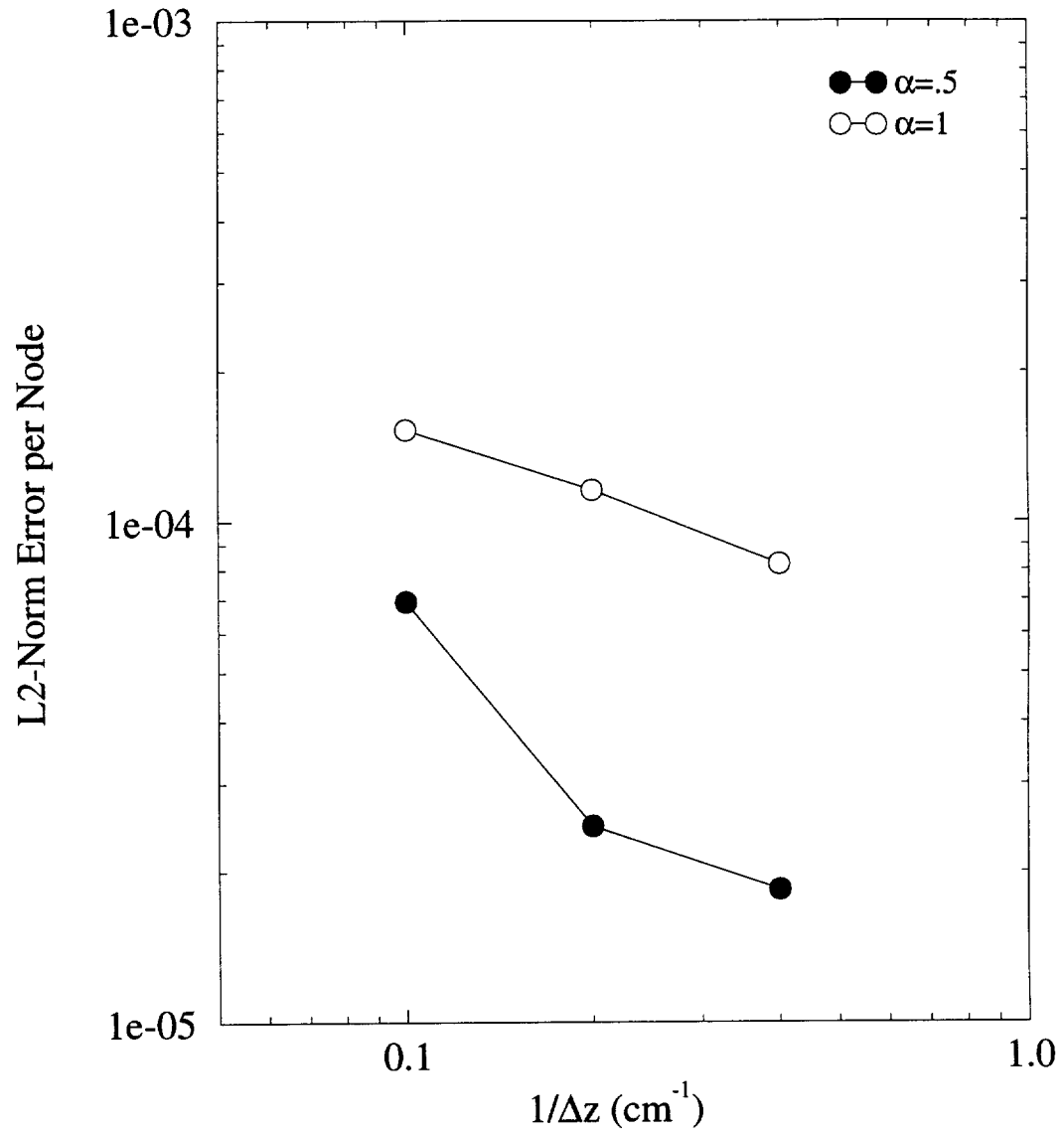
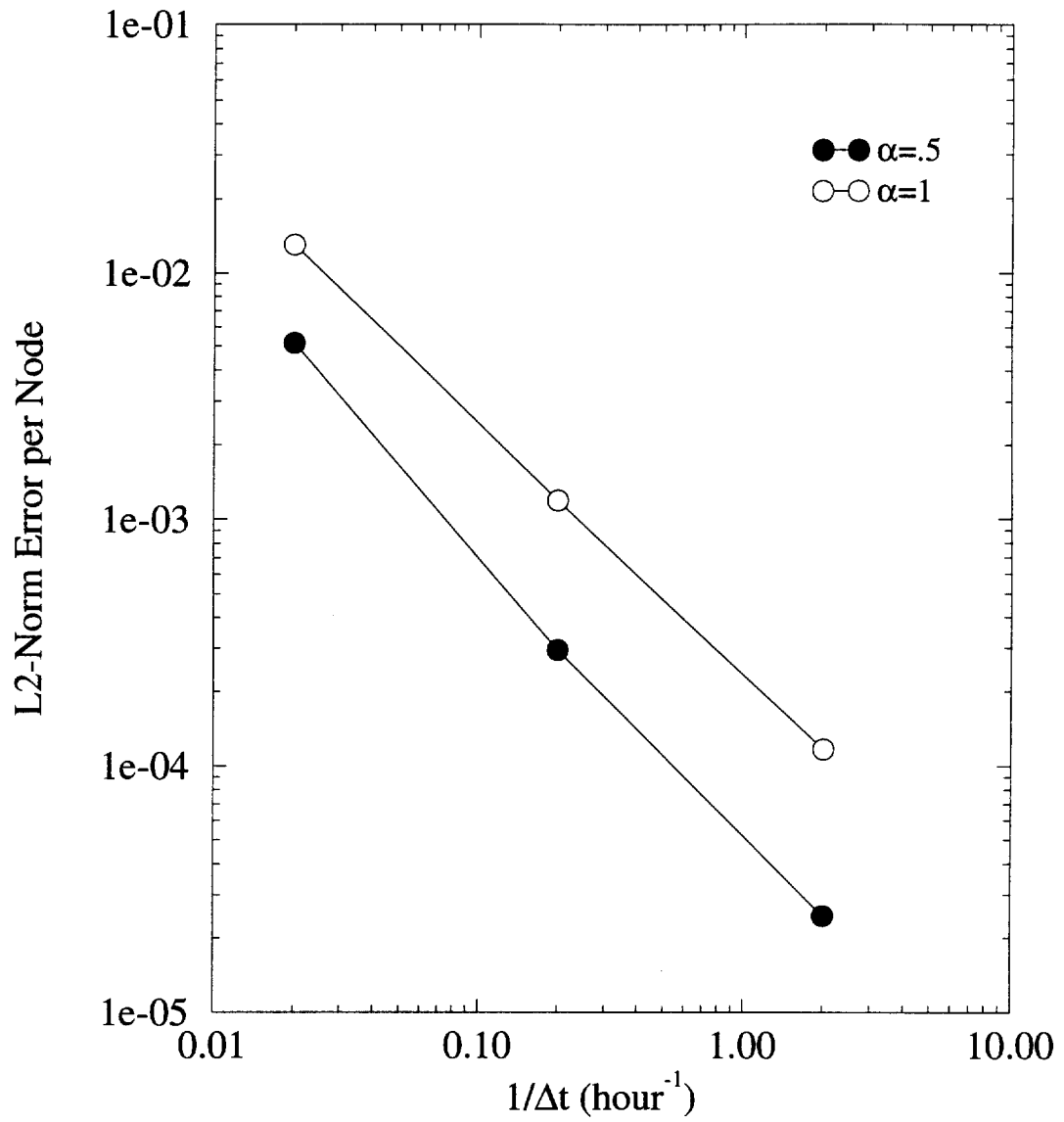


Figure 4.4. Rates of convergence with respect to  $1/\Delta z$  ( $\Delta z = 5$  cm and  $\Delta t = 0.5$  hour).



**Figure 4.5.** Rates of convergence with respect to  $1/\Delta t$  ( $\Delta z = 5$  cm and  $\Delta t = 0.5$  hour). Simulation time = 21 days.

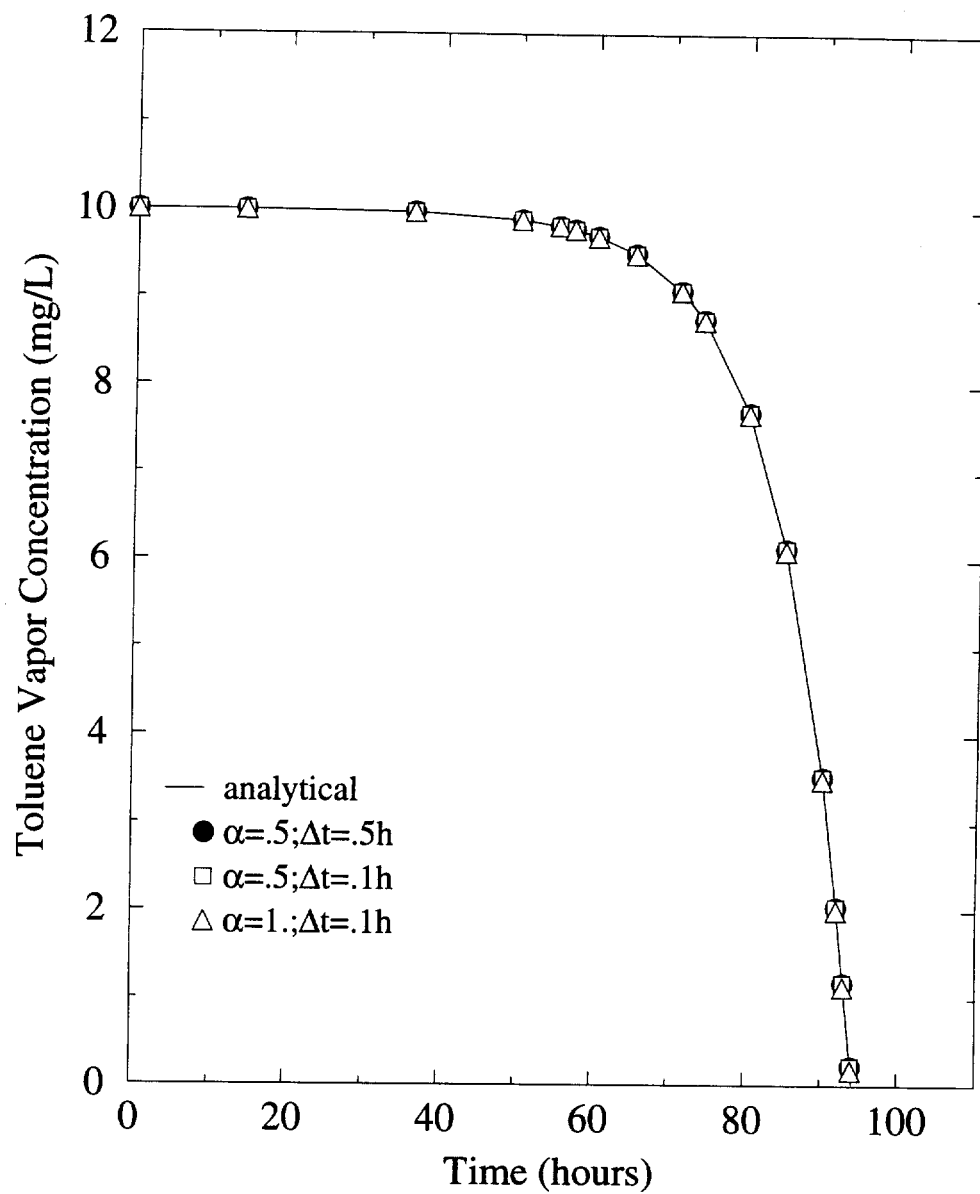
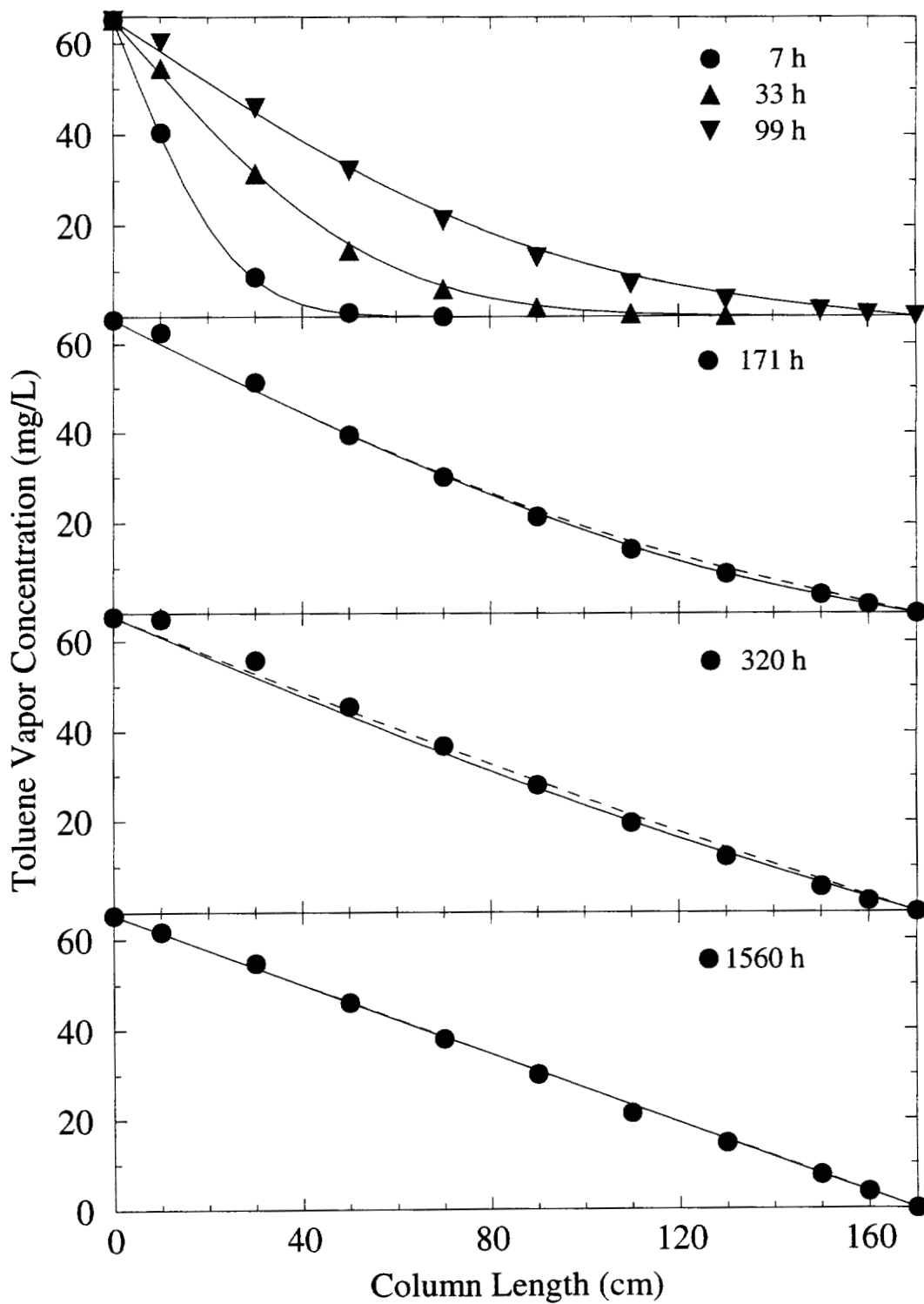


Figure 4.6. Biodegradation of toluene (model and analytical solutions).



**Figure 4.7. Model simulations (solid lines) of toluene migration in Column 1. Symbols are data; dashed lines are diffusion profiles generated by model.**

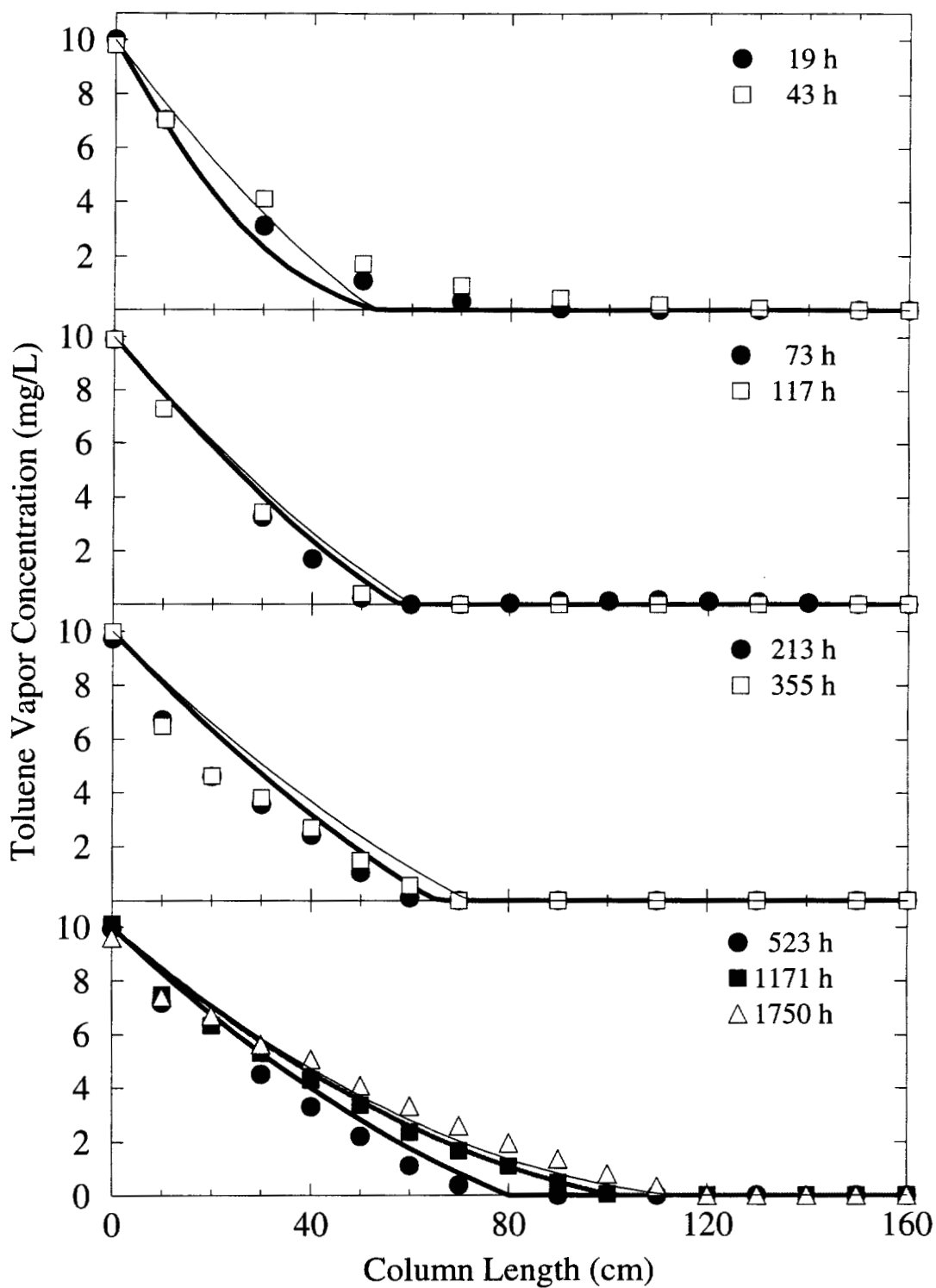


Figure 4.8. Model simulations (solid lines) of toluene migration in Column 2. Symbols are experimental data.

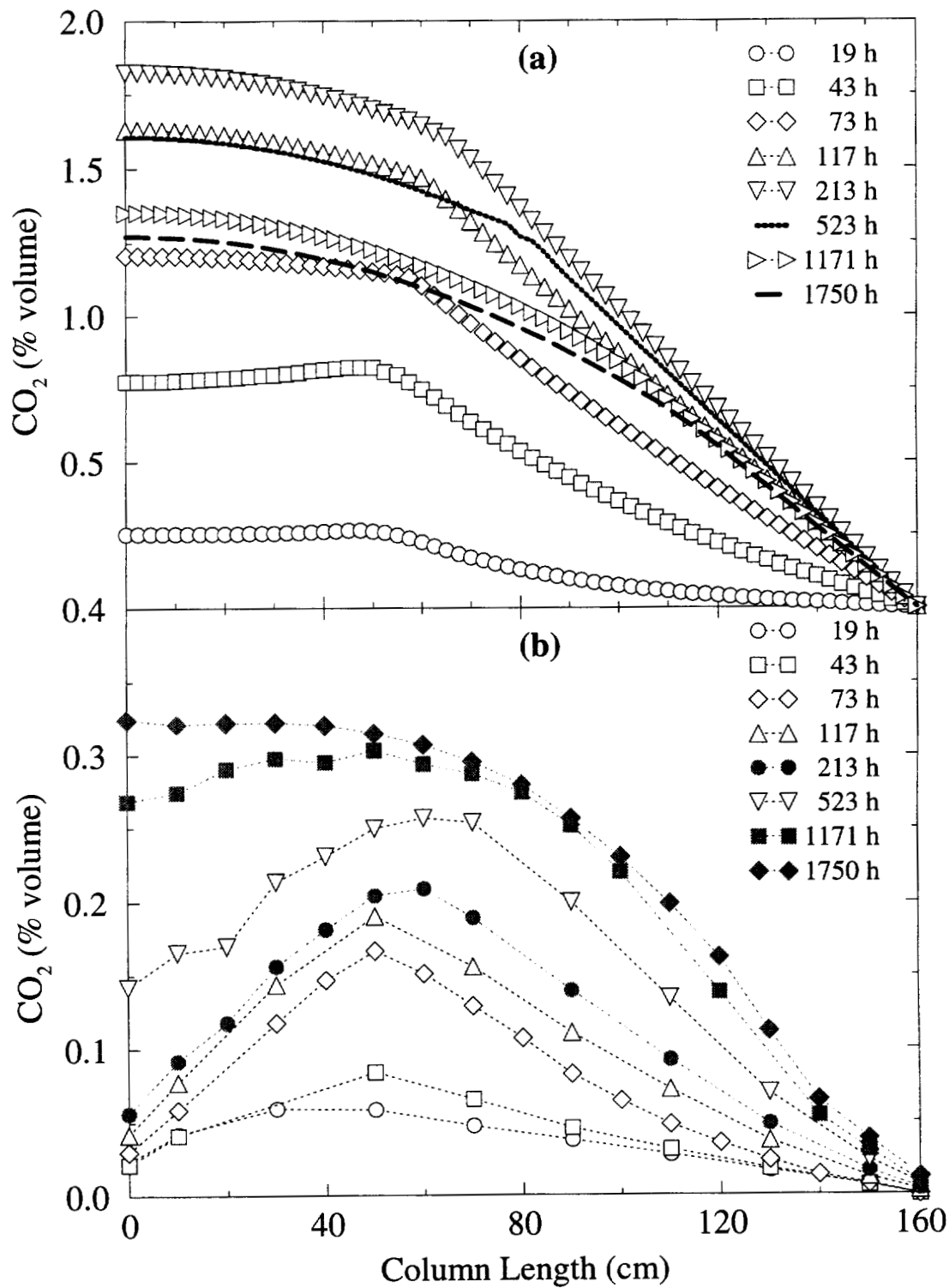


Figure 4.9. Simulated (a) and measured (b) CO<sub>2</sub> profiles in Column 2 as a function of time.

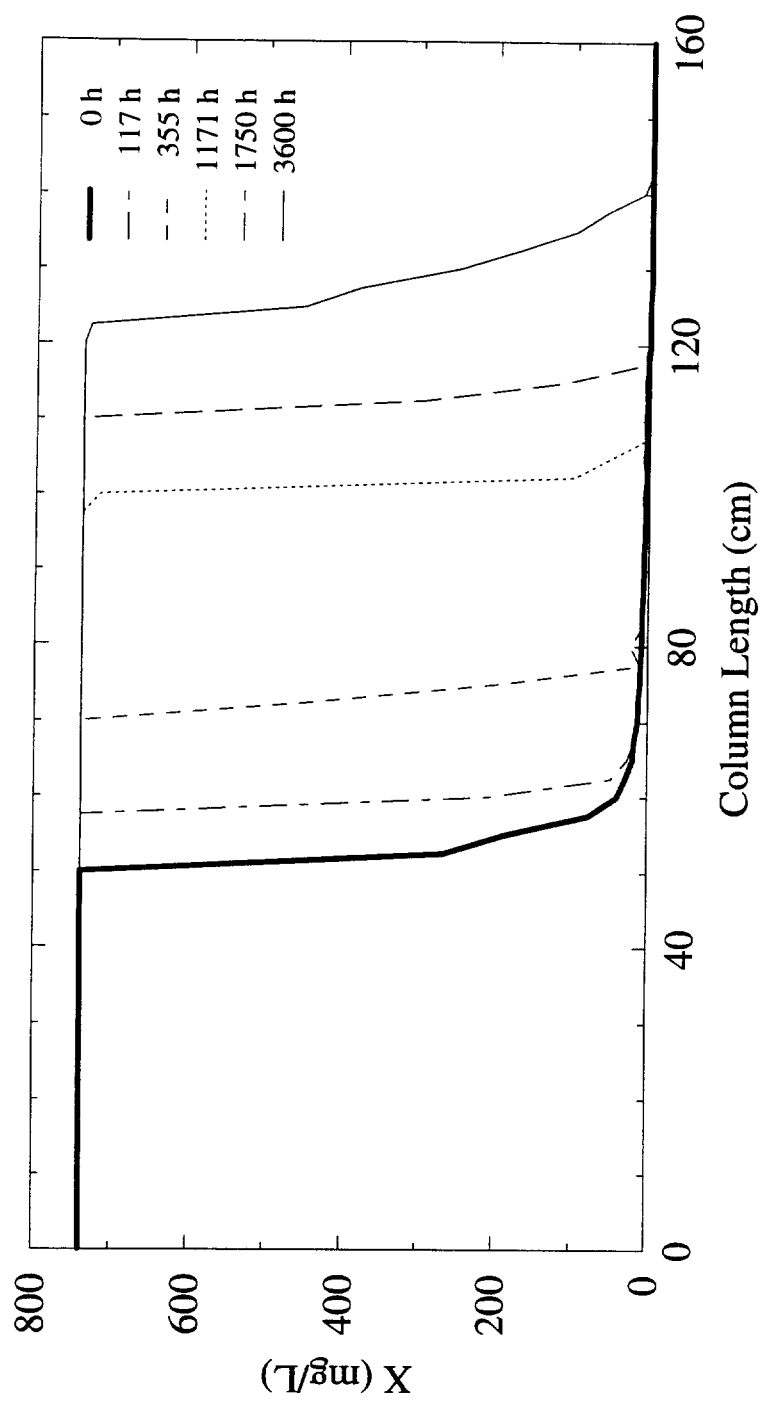


Figure 4.10. Model simulations of cell concentrations in Column 2 over time.

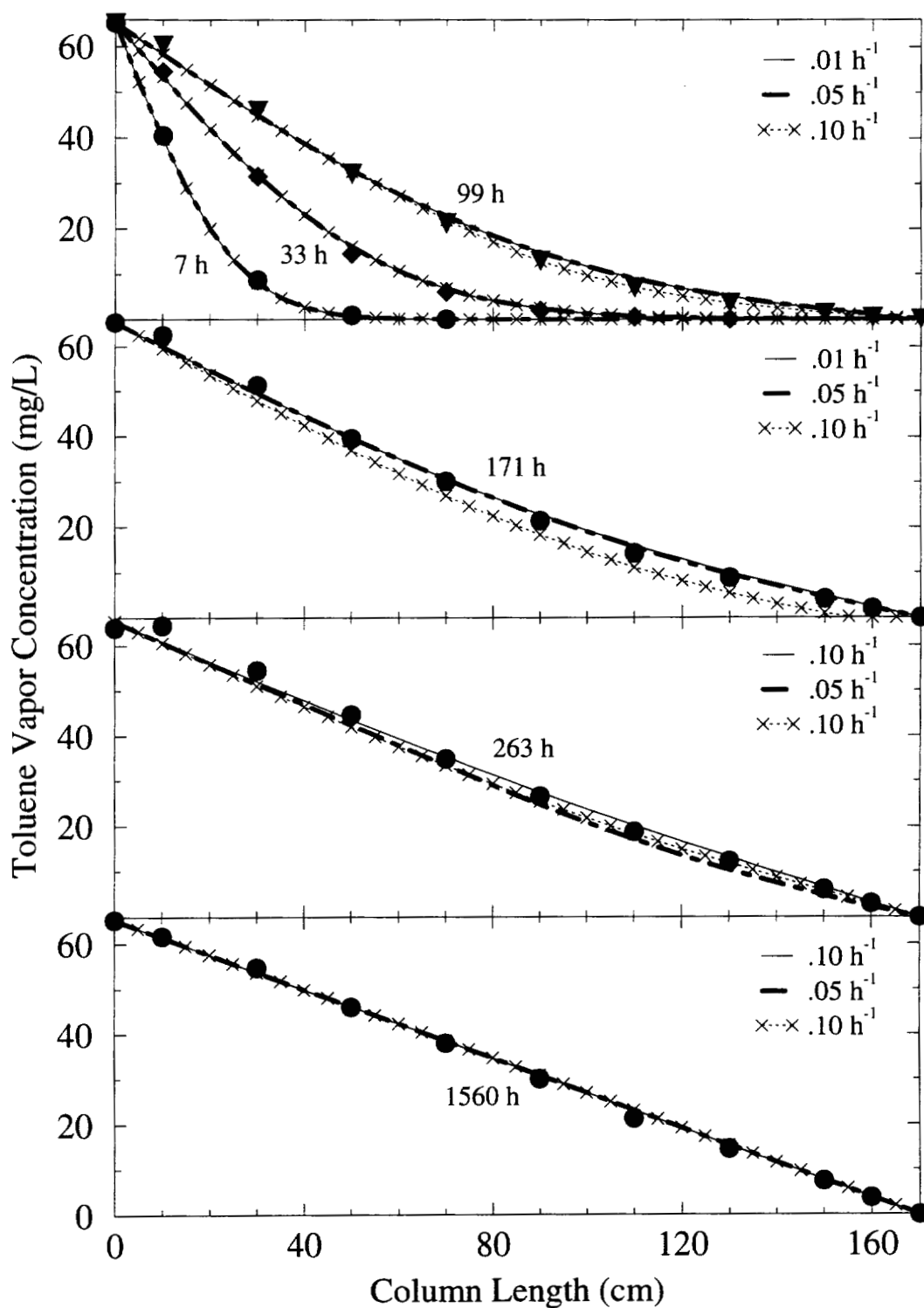


Figure 4.11. Effects of  $\mu_{\max}$  on toluene concentration profiles in Column 1 (model sensitivity analyses).

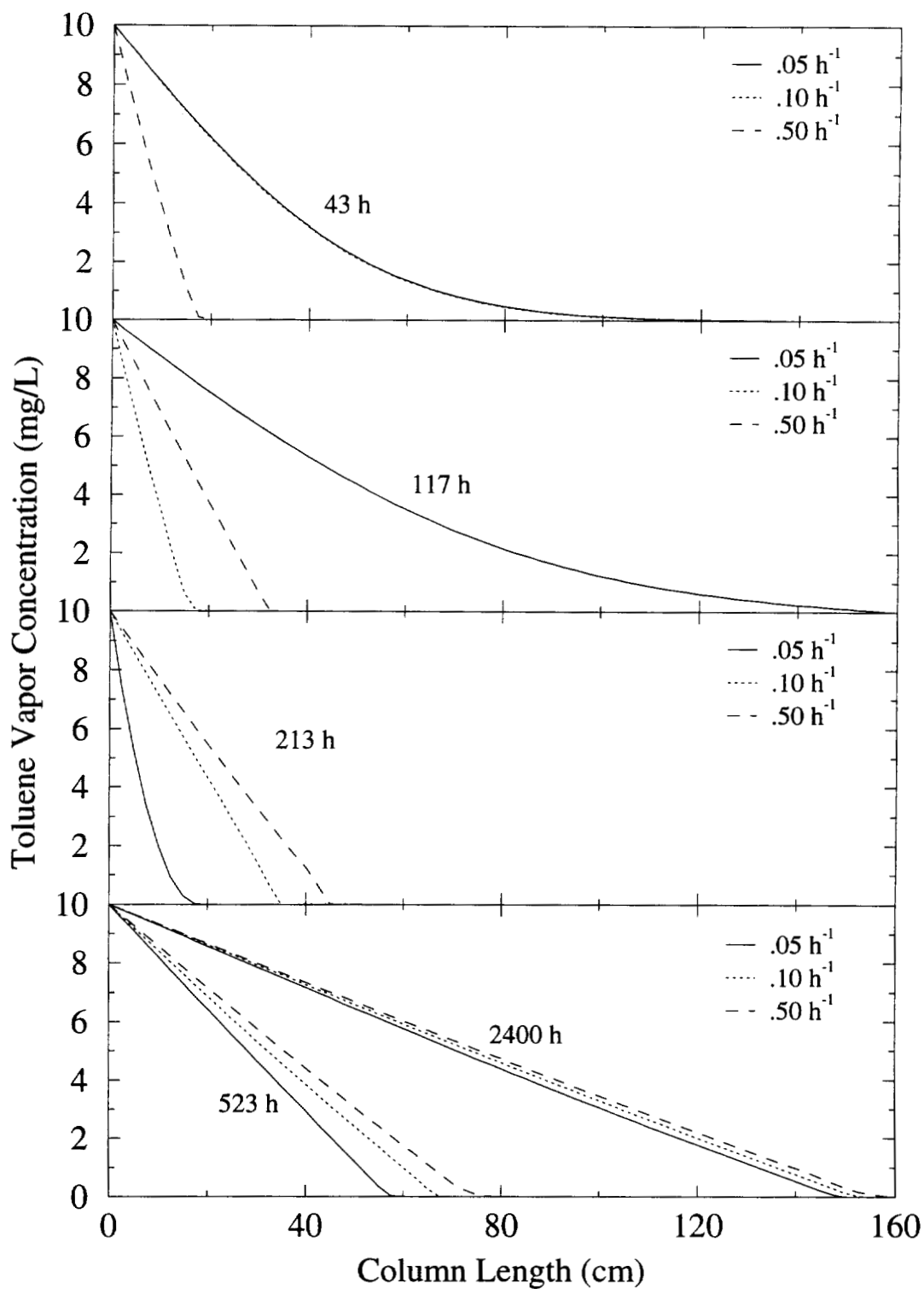


Figure 4.12. Effects of  $\mu_{\max}$  on toluene concentration profiles in Column 2 (model sensitivity analyses).

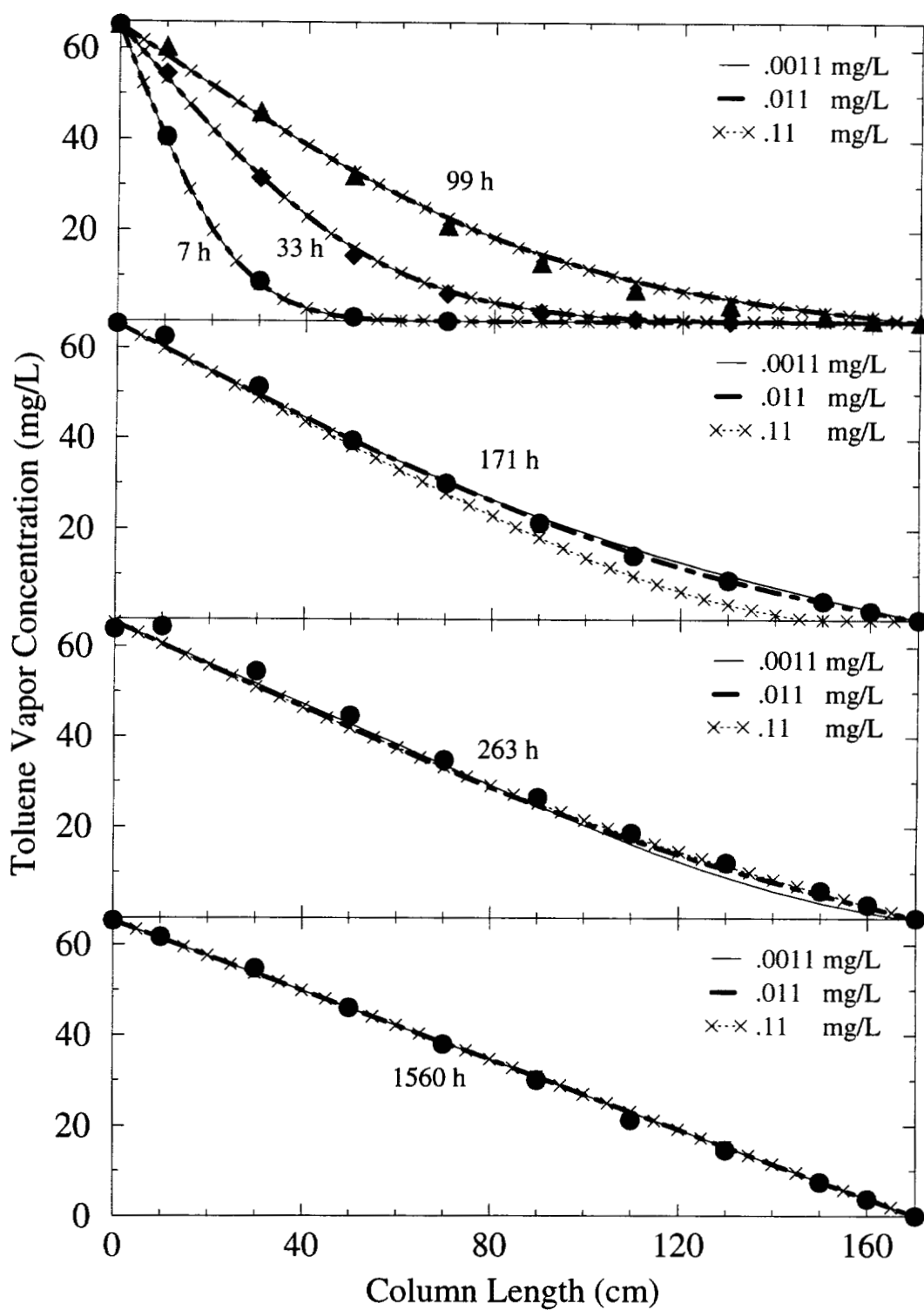
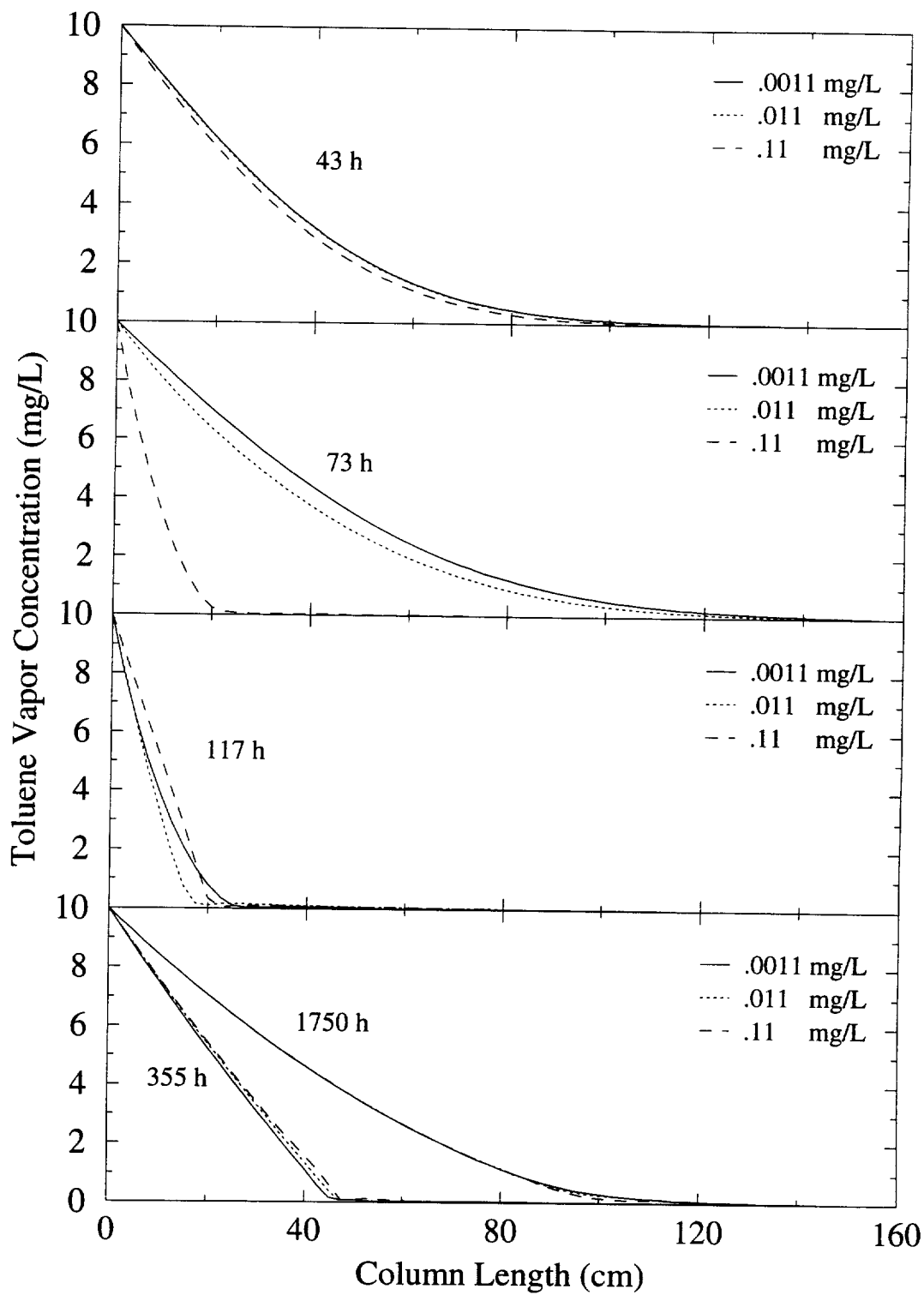


Figure 4.13. Effects of  $X_0$  on toluene concentration profiles in Column 1 (model sensitivity analyses).



**Figure 4.14.** Effects of  $X_0$  on toluene concentration profiles in Column 2 (model sensitivity analyses).

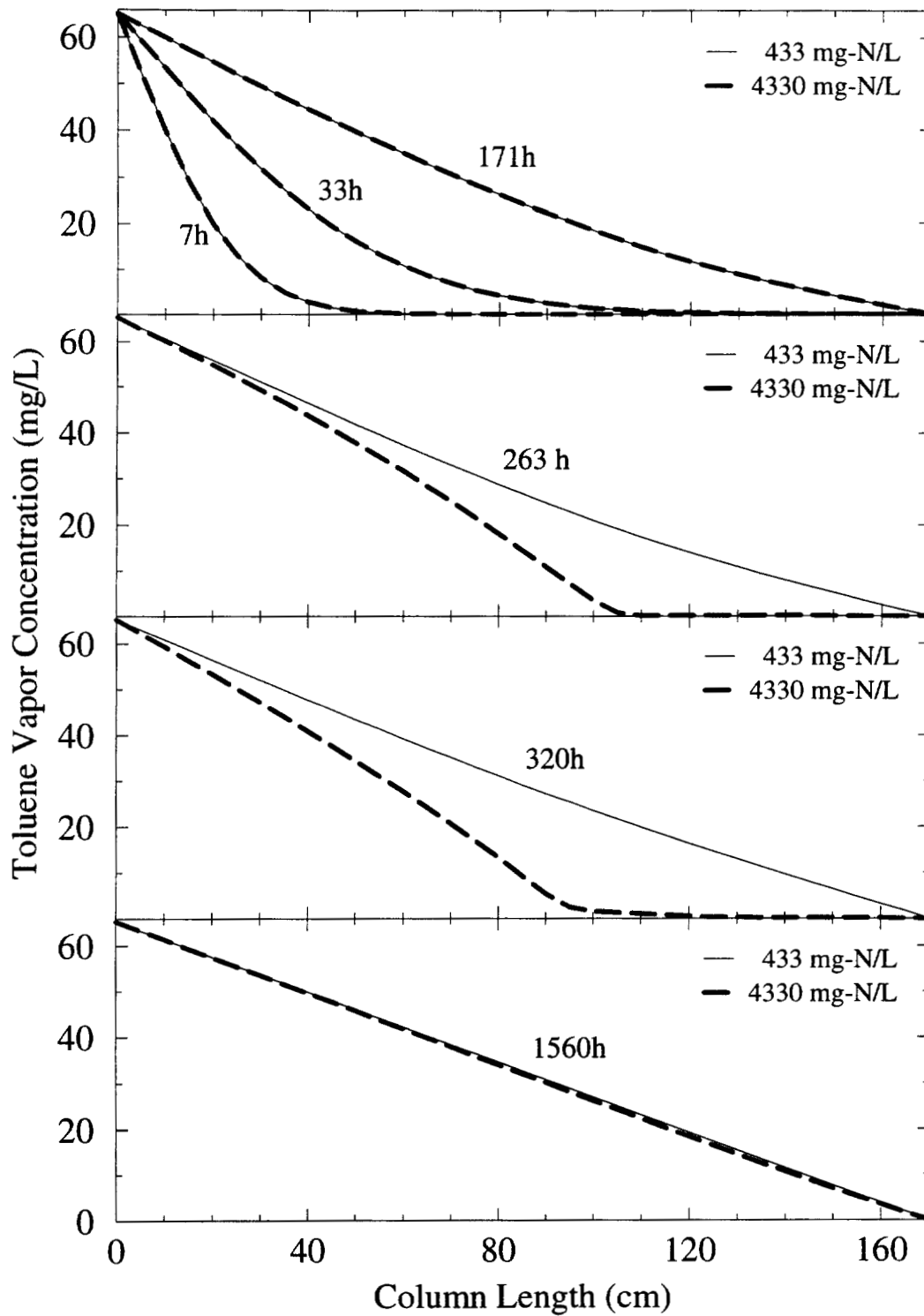


Figure 4.15. Effects of  $X_N$  on toluene concentration profiles in Column 1 (model sensitivity analyses).

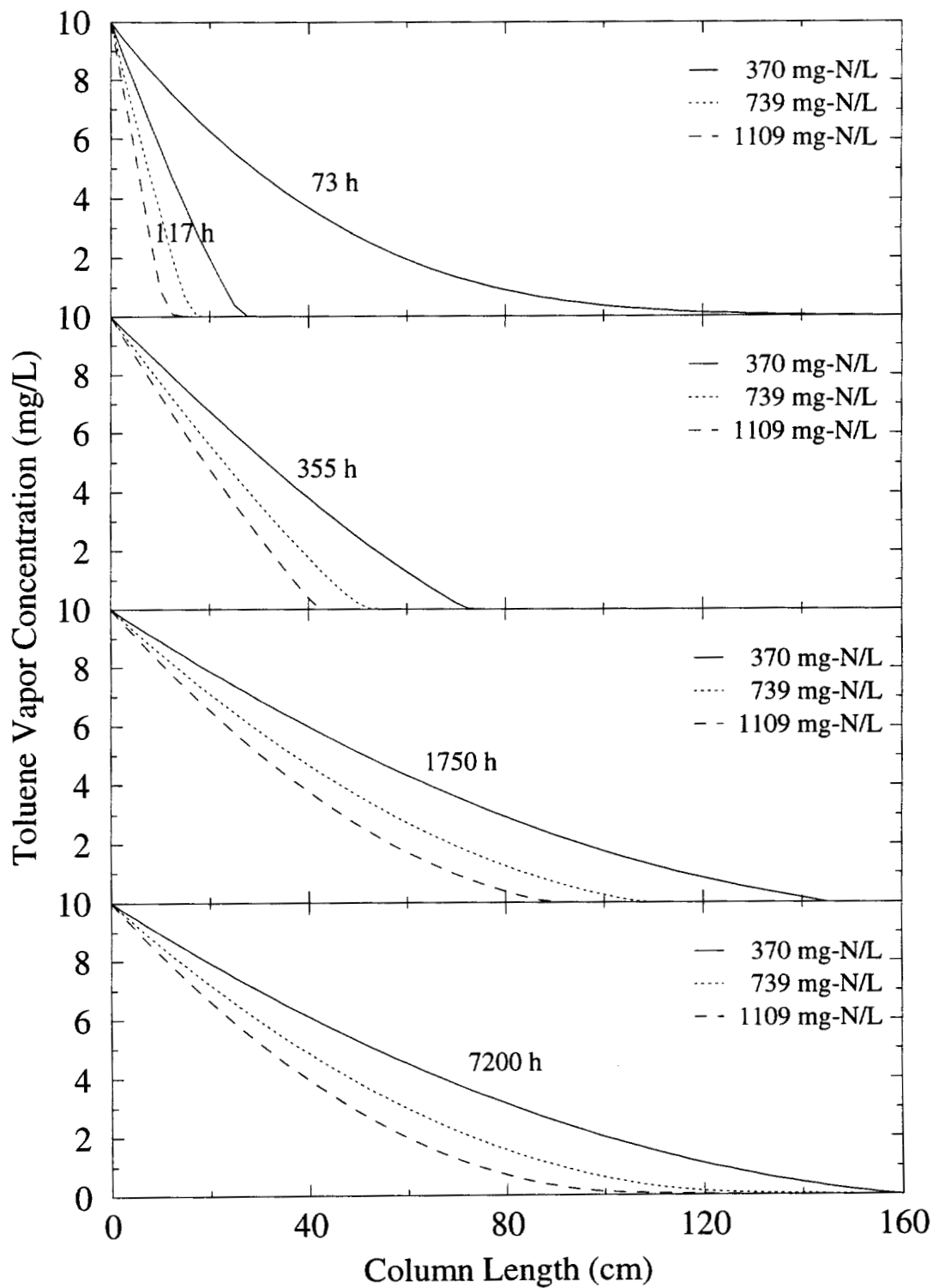


Figure 4.16. Effect of  $X_N$  on toluene concentration profiles in Column 2 (model sensitivity analyses).

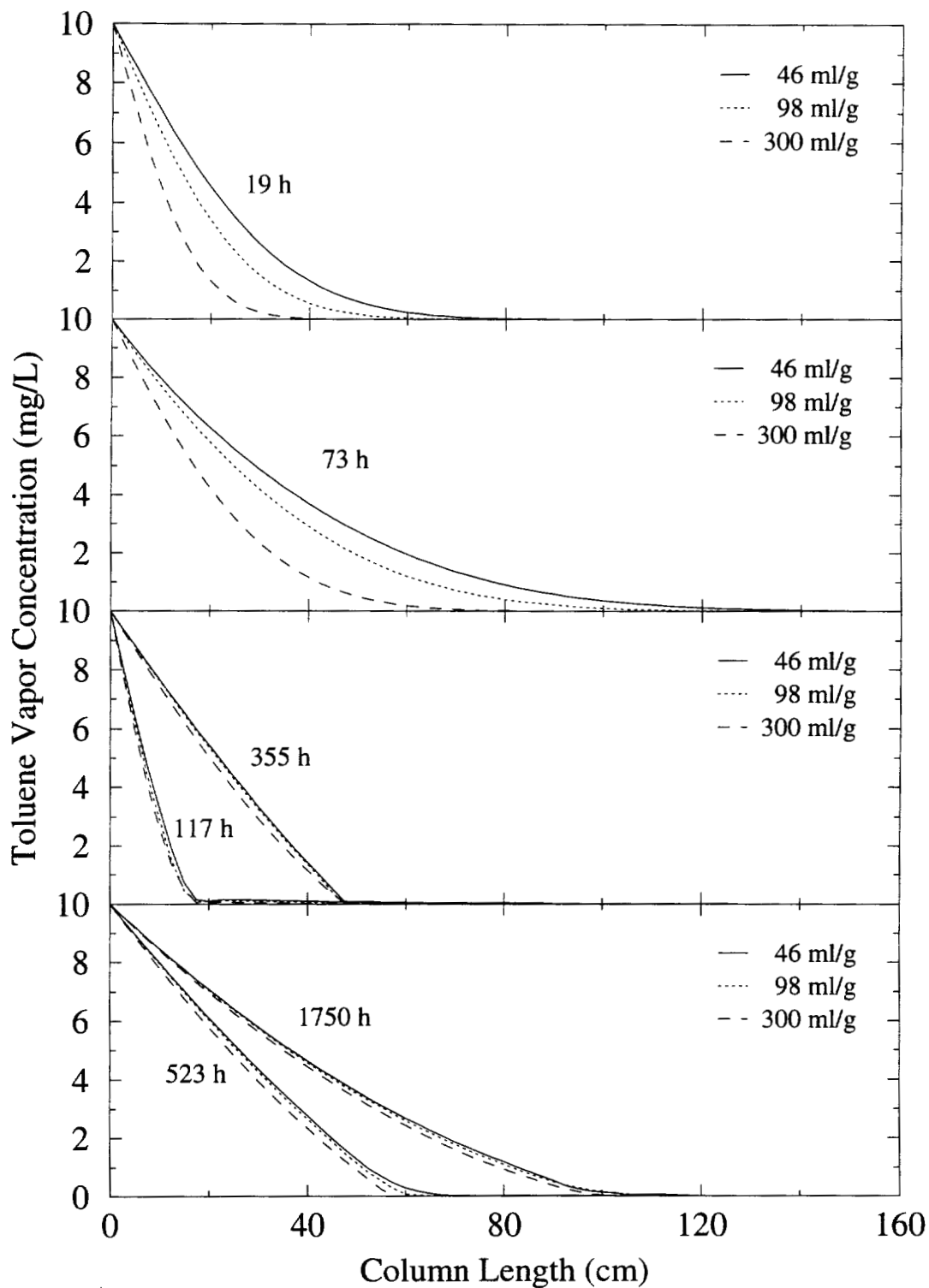


Figure 4.17. Effects of  $K_{oc}$  on toluene concentration profiles in Column 2 (model sensitivity analyses).

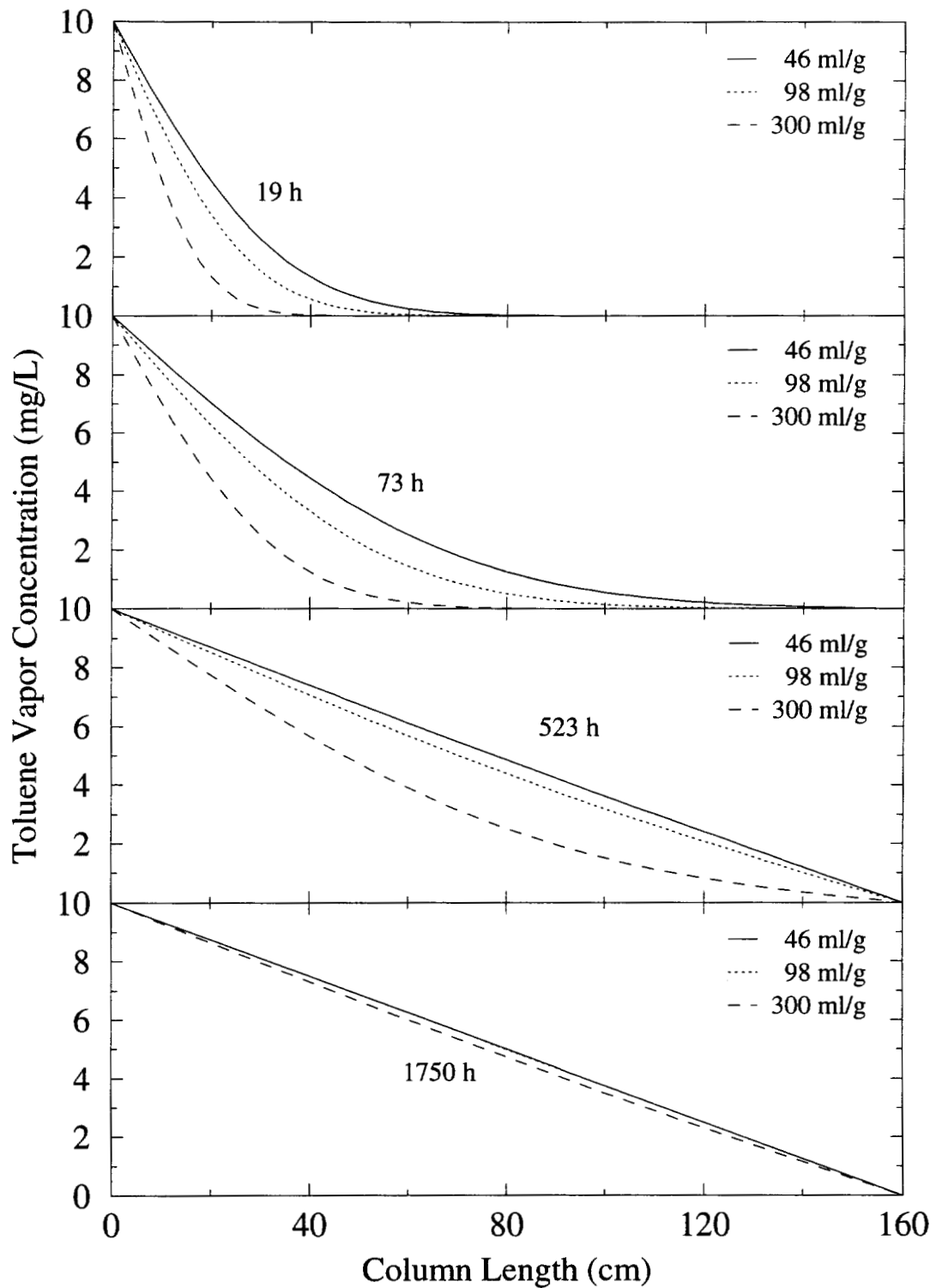
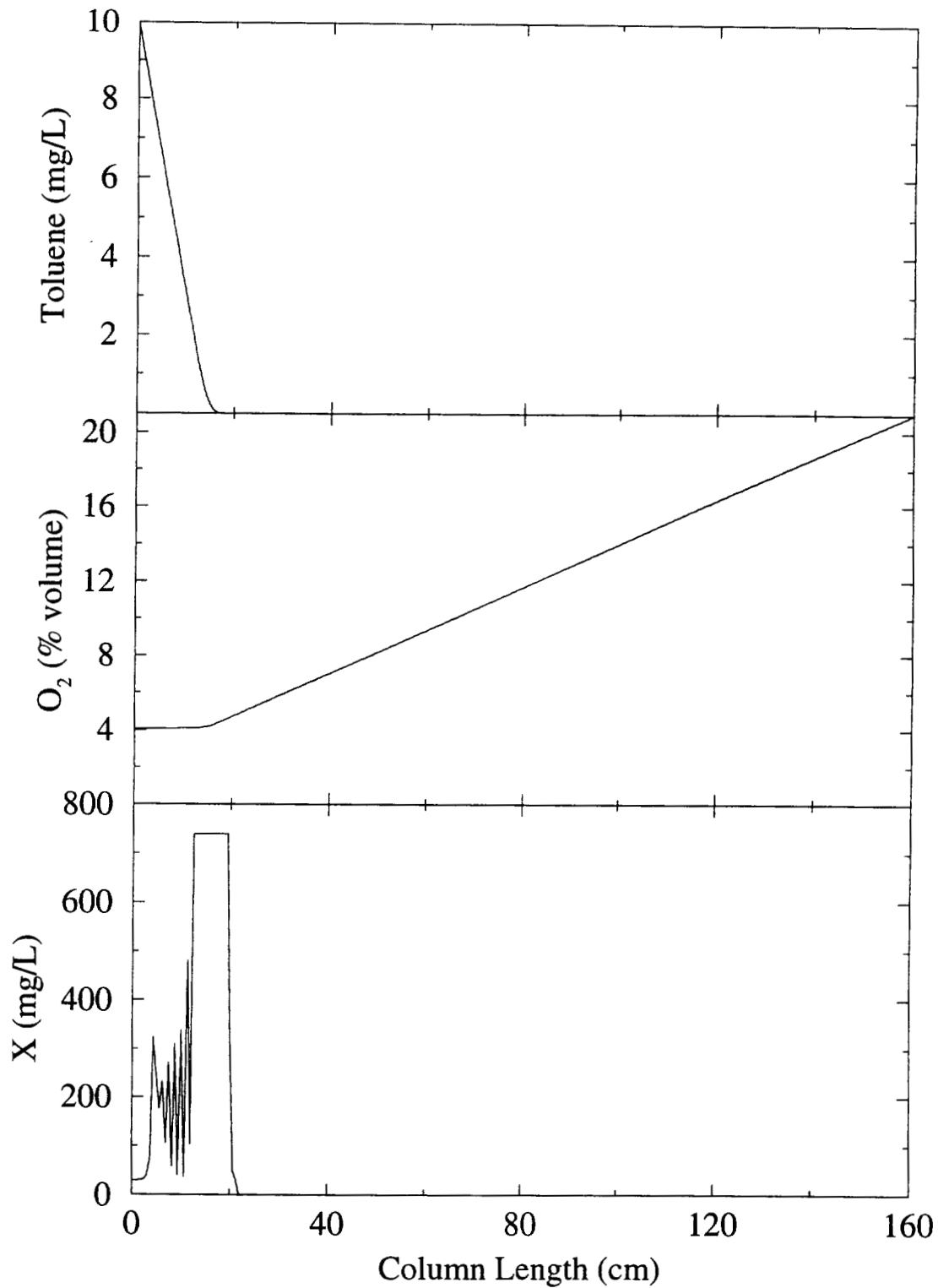
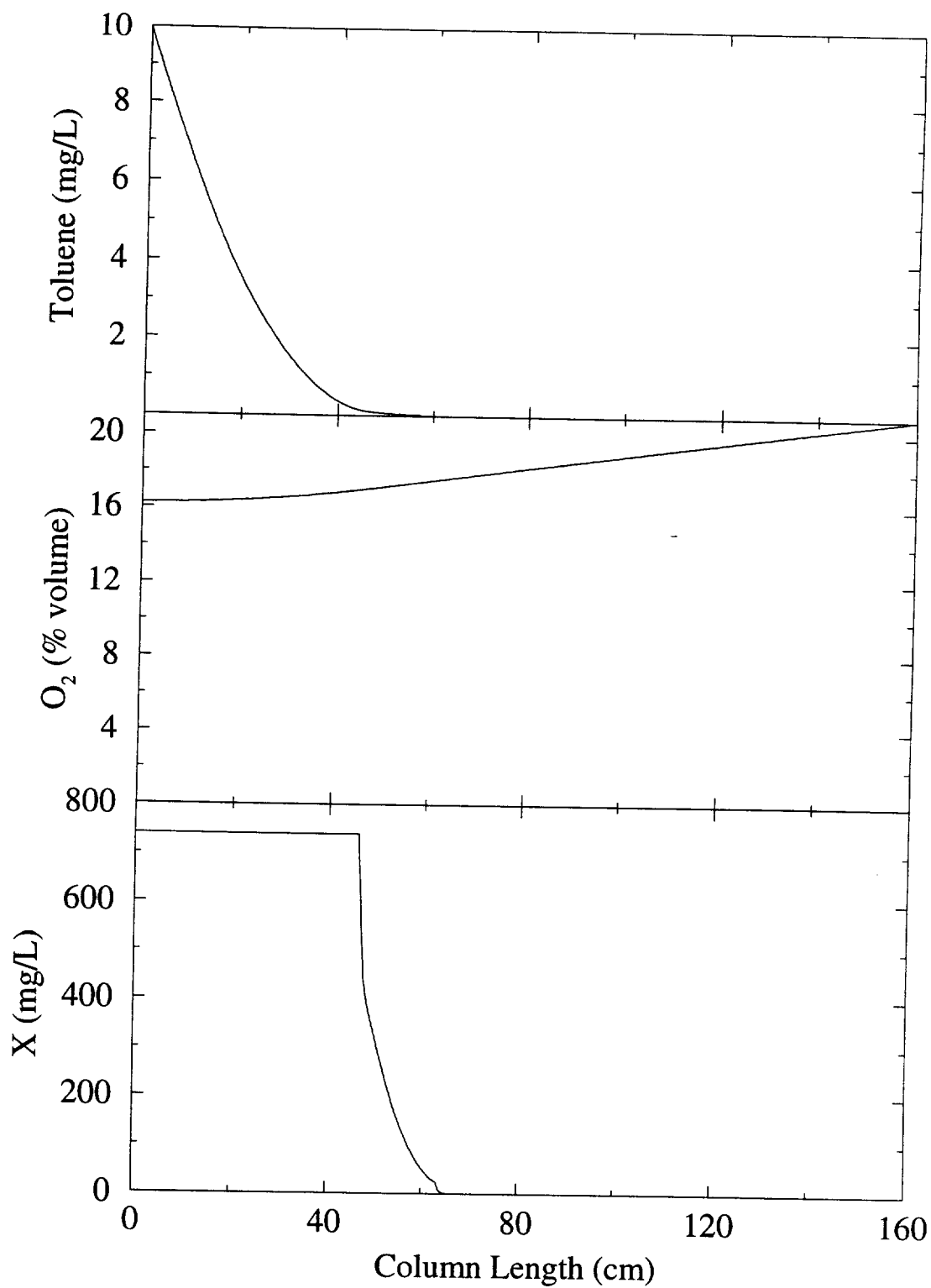


Figure 4.18. Effects of  $K_{oc}$  on toluene diffusion profiles in Column 2 (model sensitivity analyses).



**Figure 4.19.** Model simulations of toluene, O<sub>2</sub>, and X profiles in Column 2 at ~75% water saturation. Simulation time = 300 days.



**Figure 4.20. Model simulations of toluene, O<sub>2</sub>, and X profiles in Column 2 at 50% water saturation. Simulation time = 300 days.**

## **CHAPTER 5**

### **SUMMARY AND CONCLUSIONS**

#### **5.1 OVERALL RESEARCH**

The unsaturated zone plays a significant role as a natural remedial pathway for volatile organic compounds in the subsurface. Hydrocarbon contaminants have been observed to be partially or completely removed by microbially remediated processes before they reached ground surface at a number of sites (Ostendorf and Kampbell, 1991; Chiang et al., 1989; Hult, 1987). These reports confirm the importance of biodegradation in the unsaturated zone. However, the coupled processes of transport and biodegradation are not well understood. Therefore, the purposes of this research were to examine the interaction of these processes and to investigate the factors which control transport and biodegradation in unsaturated porous media.

A series of laboratory experiments and numerical modeling were employed in this study. Toluene and a sandy soil were selected as the study system. Column experiments provided comprehensive data of toluene migration in the unsaturated soil. Batch experiments were conducted to provide information on biodegradation kinetics from which biological parameters could be determined independently of column studies. To compliment the physical studies, a mathematical model was developed based on fundamental principles of multi-phase transport and biodegradation kinetics obtained from the batch experiments. Model simulations of toluene diffusion and biodegradation were conducted under conditions of soil columns using independently derived parameters. Simulation results agreed well with column data. A summary of these principal tasks is presented below.

### 5.1.1 Soil Column Experiments

Diffusion/degradation experiments were conducted in soil columns made of stainless-steel (SS) cylinders that were 0.1-m in diameter and 1.6-m long. The columns were filled with medium sand under a uniform residual water content. At one end of the column, toluene diffused from a source at a constant vapor concentration. Two source concentrations were used in the study: 65 and 10 mg/L. At the other end of the column, 50 ml/min of saturated moist air swept away any toluene that migrated through the column. Concentrations of toluene, O<sub>2</sub>, and CO<sub>2</sub> in soil air were measured along the column length periodically.

Results from the column with a saturated-vapor source (65 mg/L) indicated that vapor diffusion of toluene was the dominant process at all times. CO<sub>2</sub> profiles also confirmed that microbial activity was low initially, presumably due to the coupled effect of high toluene concentration and a small initial population. Under these conditions, the rate of biodegradation was too slow to noticeably affect the advance of toluene front. As a result, toluene vapor moved rapidly across the column and approached steady state approximately at 263 hours. CO<sub>2</sub> concentrations then became slightly elevated near the flushed end where toluene concentration was not inhibitory. However, biodegradation soon declined as a result of N limitation.

Significant biodegradation was observed when the source concentration was at 10 mg/L vapor. Under a small diffusive flux, the effect of biodegradation was such that it delayed the movement of toluene across the column. CO<sub>2</sub> data indicated that the biodegradation rate was initially low due to low microbial activity, and toluene vapor was detected over most parts of the column. However, within 73 hours, the rate of biodegradation increased, as suggested by an increase in CO<sub>2</sub> concentrations. Since the source concentration was below the inhibitory level, biodegradation took place throughout the area where toluene was present. As a result, toluene levels were reduced to zero in most parts of the column except the first 50 cm from the source. Over the next 1750 hours, toluene gradually moved down the column.

The movement of toluene vapor in the column was caused by the counteracting effects of biodegradation and diffusion. Because biodegradation was associated with growth, its rate changed with time, reflecting the energy consumption of a growing population. Biodegradation was initially low due to a small population naturally present in the sand studied, then increased as the population increased in size, and later declined to a minimal energy level when the bioavailable N was utilized. N is required by active microbial communities, and was determined to be the most limiting inorganic nutrient in the sand used in this study. Nitrate analyses of column soils supported the hypothesis. These results were confirmed in a duplicate column conducted using a low concentration source of 10 mg/L. Results from the two columns were consistent.

In all column experiments, O<sub>2</sub> monitoring confirmed that aerobic conditions existed throughout the experiments. In addition, concentration gradients of O<sub>2</sub> over column length were negligible and seldom changed with time.

### **5.1.2 Batch Kinetics Experiments**

Batch studies of toluene biodegradation kinetics were conducted in 0.8-L SS canisters with 55 g of sand containing similar water content as those in the columns. A precalculated amount of liquid toluene was added to each canister, after which it was sealed, shaken, and incubated at 15°C. Toluene concentration in the headspace was monitored closely with time over a range of initial concentrations. In all cases, a measurable decrease of toluene concentration was observed within 2-4 days after toluene injection. Once biodegradation initiated, toluene was completely consumed within 0.5-2 days. Typical substrate disappearance curves showed increasingly rapid toluene removal rate over time, thereby reflecting a biodegradation pattern of microbes growing at a logarithmic rate. Such biodegradation patterns were obtained even at the lowest initial concentration tested, implying the half-saturation constant ( $K_s$ ) of this system was low and environmentally irrelevant. In view of very low  $K_s$  value, Monod kinetics were simplified to zero order. Microbial parameters, such as the maximum specific growth

rate and the initial population concentration, were fitted using nonlinear regression. For batch experiments with initial concentrations above 5 mg/L vapor, degradation ceased before all toluene was exhausted. Addition of  $\text{NH}_4\text{NO}_3$  solution resulted in further breakdown. The dependence of biodegradation on added N confirmed the supposition of N limitation in the column experiments. Autoclaved controls showed no degradation of toluene during a period of 15 days. Controls also indicated that sorption was rapid (equilibrium conditions established within 14 hours).

All batch experiments were conducted in duplicate or triplicate. Measurements of  $\text{O}_2$  ensured that the aerobic condition existed during the entire experiment. In addition to kinetic parameters, stoichiometry of toluene biodegradation was also estimated using a basis of C balance.

### 5.1.3 Numerical Modeling

A 1-D numerical model was developed to describe vapor-phase transport and degradation of toluene in the unsaturated zone. The model accounts for air, water, and solid phases, in which mass partitioning was assumed to be linear and at equilibrium. Furthermore, it assumed physical properties were spatially uniform and invariant with time. Both aqueous- and vapor-phase diffusion were considered, whereas advection and leaching were neglected. Biodegradation followed zero-order Monod kinetics. The effects of substrate toxicity and nutrient limitation on biodegradation were also accounted for. Because the impact of these factors was not characterized quantitatively here, their effects were approximated. The transport model was solved using the Galerkin finite-element method for spatial discretization and a variable weighted time scheme for time discretization. To evaluate the model, simulations were conducted under experimental conditions of the column studies using input parameters derived from batch experiments or literature. Good agreement was achieved between model and experimental results. Parameter sensitivity analyses were also conducted to demonstrate model capability and to give insight into the dynamics of toluene transport and fate in unsaturated porous

media. It should be emphasized that the model developed here was not intended for predictive purposes, and the validity of model was limited to biodegradation/growth under unlimited O<sub>2</sub> supply and low K<sub>s</sub> values.

## 5.2 GENERAL CONCLUSIONS

This work has illustrated the utility of a combination of physical experiments and numerical modeling to provide a comprehensive analysis of contaminant transport and fate in an unsaturated soil. Results of column experiments demonstrated spatial and temporal variations of toluene and CO<sub>2</sub> under major influence of biodegradation and diffusion. Batch data contributed information regarding the kinetics of biodegradation and the rate-limiting factor. The numerical model which was developed by incorporating various processes in relevance to those in the column experiments provided quantitative analyses of column results. Due to the complexity of interactions among various physical, chemical, and biological processes governing the transport, such a model was very useful in support of the physical studies. Attempts to mathematically simulate column experiments were successful. This supported the underlying principles and assumptions used in developing the model. In addition, the model was useful in assessing the relative importance of various processes affecting toluene transport and fate.

General conclusions drawn from this research were as follows:

- a) Near a high-concentration source, vapor diffusion was strong, biodegradation was inhibited, and toluene migration was controlled by diffusion. Thus, a contaminant vapor migrating from a high-concentration source advances quickly and is less subject to biodegradation.
- b) Under low-flux conditions, biodegradation had a substantial impact on the migration of toluene, and the system was under the effects of both biodegradation and diffusion. The transport dynamics observed in the low source-concentration columns can be broken into four stages in which different processes control the rate and extent of degradation: (1) Diffusion was initially important due to low

microbial activity in the beginning; (2) Shortly after, biodegradation became increasingly important due to sufficient toluene, O<sub>2</sub>, and N; (3) However, as the biodegradation rate increased, toluene was consumed faster than supplied, and the overall rate was governed by the transport rate of toluene; and (4) biodegradation rates later became much smaller when soil was depleted with N. Consequently, the movement of toluene at non-inhibitory concentrations is controlled by biodegradation, diffusion, and N bioavailability.

- c) When conditions for microbial growth were not limited, microbial parameters, such as the maximum growth rate and the initial population, were critical in controlling the migration of toluene. However, nutrient-limiting conditions are likely to develop, in which case microbial parameters will be less important. This research has shown that for a shallow unsaturated sandy soil environment, the bioavailability of N instead of O<sub>2</sub> is the limiting factor in the microbial removal of volatile aromatic hydrocarbons.

### 5.3 APPLICATIONS AND FUTURE STUDIES

In efforts to better quantify contaminant transport in subsurface, it is necessary to gain thorough understanding of the effects of various physical, chemical, and biological processes upon the pollutant compound. This study demonstrated that the biological process was important when the environmental conditions were appropriate. However, the extent of biodegradation was ultimately limited by the availability of an inorganic nutrient. Since nutrient limited conditions are likely to exist in the subsurface at most sites, the effect of maintenance-energy requirements on biodegradation rates will be critical. For example, the long term performance of *in situ* bioremediation systems may depend upon the capacity of non-growing microbial populations to metabolize contaminants. Further research is needed in this area.

The effects of substrate toxicity and inorganic nutrients on biodegradation were approximated in this study. In order to better quantify these effects, the dependence of

biodegradation rate upon individual factors should be examined. It should be emphasized that the observed functional dependency would be specific to the type of soil and experimental conditions used. Therefore, caution should be taken in using published values of kinetic parameters. The inclusion of these effects in any model certainly introduces complications towards solving the problem. Therefore, any improvement in model performance should be weighed against additional computation efforts required.

The experimental conditions studied here are likely to be found in the unsaturated zone of a shallow sandy/gravelly aquifer where the rate of O<sub>2</sub> diffusion is usually not limiting the biodegradation. In systems where the depth of the unsaturated zone may be large, where the subsurface formation composes of low permeable materials such as clay, or in the immediate vicinity of a source, O<sub>2</sub> may be limited or absent. Under limited-O<sub>2</sub> supply, the dependence of biodegradation rates on O<sub>2</sub> concentration needs to be investigated. Additional batch studies are needed to quantify a functional relationship between hydrocarbon biodegradation rates and O<sub>2</sub> concentration.

When O<sub>2</sub> is absent, hydrocarbon biodegradation may occur via anaerobic pathways. A prominent mechanism that has been investigated in groundwater systems is denitrification, a dissimatory reduction of nitrate and nitrite to gaseous products. Denitrifiers were found in groundwater and soil samples from aerobic to extremely reduced zones (Barker and Mayfield, 1988). Biodegradation of BTX compounds under denitrifying conditions has been reported (Barbaro et al., 1992; Kuhn et al., 1988; Mayor et al., 1988; Major et al., 1988; Zeyer et al., 1986; Kuhn et al., 1985; Schwarzenbach et al., 1983). Substrate removal rates under denitrifying conditions may be comparable to those by aerobic degradation (Barbaro et al., 1992; Barker and Mayfield, 1988; Major et al., 1988). Therefore, further research efforts are needed to examine the importance of BTX biodegradation via denitrification, and if necessary, to characterize a functional relationship between hydrocarbon degradation rates and nitrate concentration.

At most contaminated field sites, organic compounds are usually present in a mixture. Hence, a logical next step for this study is to extend the single-compound system to a multi-component one. However, the presence of other compounds as

potential multiple substrates adds complications to the study since substrate interactions, such as sequential or simultaneous utilization and competitive inhibition, can possibly occur. The susceptibility to degradation of individual components within a petroleum mixture has been observed by many researchers (Atlas, 1981). Fuel components were found either stimulated, repressed, or not affected by the presence of others (Atlas, 1981; Jamison et al., 1975). The interaction of BTX compounds with respect to degradation of individual compounds was studied in the laboratory (Chang et al., 1992; Alvarez and Vogel, 1991). Catabolic diversities of subsurface microbes precluded generalizations about the effects of individual BTX compounds on biodegradation of other BTX compounds (Alvarez and Vogel, 1991). Schmidt et al. (1985) showed that the kinetics of biodegradation of organic compounds were altered by a supplementary substrate. Further investigations of the interaction of multiple substrates are needed to provide some insight into the biodegradation capabilities of subsurface microbial community. Last but not least, the effect of mixture on chemical properties of each individual components also needs to be defined.

Despite success in simulating column experiments, field data are needed to check the validity of conclusions drawn from laboratory investigations conducted here. In addition, the model needs to be increased to two or three dimensions and includes multiple components for dealing with more general situations. Nonetheless, the 1-D model can be used as guidelines in certain field scenarios. In addition to its application in the environmental field, the model can be applied to problems in soil science with respect to gas transport of pesticides through cover of unconsolidated earthen materials.

## 5.4 REFERENCES

- Alvarez, P. J. J., and T. M. Vogel, Substrate interactions of benzene, toluene, and *para*-xylene during microbial degradation by pure cultures and mixed culture aquifer slurries, *Appl. Environ. Microbiol.*, *57*, 2981-2985, 1991.
- Atlas, R. M., Microbial degradation of petroleum hydrocarbons: An environmental perspective, *Microbiol. Rev.*, *45*, 180-209, 1981.
- Barker, J. F., and C. I. Mayfield, The persistence of aromatic hydrocarbons in various ground water environments, in *Proceedings of the Conference on Petroleum Hydrocarbons and Organic Chemicals in Groundwater*, National Water Well Association, Dublin, Ohio, pp. 649-667, 1988.
- Chang, M., T. C. Voice, and C. S. Criddle, Kinetics of competitive inhibition and cometabolism in the biodegradation of benzene, toluene, and *p*-xylene by two *Pseudomonas* isolates, *Biotechnol. Bioeng.*, *41*, 1057-1065, 1992.
- Chiang, C. Y., J. P. Salanitro., E. Y. Chai, J. D. Colthart, and C. L. Klein, Aerobic biodegradation of benzene, toluene, and xylene in a sandy aquifer - Data analysis and computer modeling, *Ground Water*, *27*, 823-834, 1989.
- Hult, M. F., Microbial oxidation of petroleum vapors in the unsaturated zone, in U.S. Geological Survey Program on Toxic Waste--Ground-Water Contamination, edited by B. J. Franks, Proceedings of the Third Technical Meeting, Pensacola, Florida, March 23-27, 1987, *U.S. Geol. Surv. Open File Rep.*, *87-109*, pp. C25-C26, 1987.
- Jamison, V. W., R. L. Raymond, and J. O. Hudson Jr., Biodegradation of high octane gasoline in groundwater, *Dev. Ind. Microbiol.*, *16*, 305-312, 1975.
- Kuhn E. P., P. J. Colberg, J. L. Schnoor, O. Wanner, A. J. B. Zehnder, and R. P. Schwarzenbach, Microbial transformations of substituted benzenes during infiltration of river water to groundwater: Laboratory column studies, *Environ. Sci. Technol.*, *19*, 961-968, 1985.
- Kuhn E. P., J. Zeyer, P. Eicher, and R. P. Schwarzenbach, Anaerobic degradation of alkylated benzenes in denitrifying laboratory aquifer columns, *Appl. Environ. Microbiol.*, *54*, 490-496, 1988.
- Major, D. W., C. I. Mayfield, and J. F. Barker, Biotransformation of benzene by denitrification in aquifer sand, *Ground Water*, *26*, 8-14, 1988.

Ostendorf, D. W., and D. H. Kampbell, Biodegradation of hydrocarbon vapors in the unsaturated zone, *Water Resour. Res.*, 27, 453-462, 1991.

Schmidt, S. K., S. Simkins, and M. Alexander, Models for the kinetics of biodegradation of organic compounds not supporting growth, *Appl. Environ. Microbiol.*, 50, 323-331, 1985.

Schwarzenbach, R. P., W. Giger, E. Hoehn, and J. K. Schneider, Behavior of organic compounds during infiltration of river water to groundwater. Field studies, *Environ. Sci. Technol.*, 17, 472-479, 1983.

Zeyer, J., E. P. Kuhn, and R. P. Schwarzenbach, Rapid microbial mineralization of toluene and 1,3-dimethylbenzene in the absence of molecular oxygen, *Appl. Environ. Microbiol.*, 52, 944-947, 1986.

**APPENDIX A**

**SELECTED DATA FROM COLUMN EXPERIMENTS**

This appendix consists of two parts: Appendix A.1 and A.2. Appendix A.1 contains gravimetric soil properties from Column 2. Appendix A.2 contains selected experimental data from column experiments discussed in Chapter 2.

**Table A.1. Soil properties of column 2.**

Distance (cm)	Wet sand (g)	dry sand (g)	Volume of core (ml)	Volume of sand (ml)	Porosity (vol/vol)	Volumetric content of		Bulk dry density (g/ml)
						water	air	
0-10	150.6	141.2	93.8	54.3	0.42	0.10	0.32	1.5
10-20	144.1	134.3	90.4	51.7	0.43	0.11	0.32	1.5
20-30	136.6	127.4	90.4	49.0	0.46	0.10	0.36	1.4
30-40	152.7	143.1	95.7	55.0	0.42	0.10	0.32	1.5
40-50	158.5	147.8	95.7	56.9	0.41	0.11	0.30	1.5
50-60	156.8	146.6	96.2	56.4	0.41	0.11	0.31	1.5
60-70	169.7	158.5	97.2	61.0	0.37	0.11	0.26	1.6
70-80	153.7	143.9	94.8	55.4	0.42	0.10	0.31	1.5
80-90	167.1	156.2	96.2	60.1	0.38	0.11	0.26	1.6
90-100	153.4	143.2	96.2	55.1	0.43	0.11	0.32	1.5
100-110	170.2	158.8	96.2	61.1	0.37	0.12	0.25	1.7
110-120	164.3	153.8	94.3	59.2	0.37	0.11	0.26	1.6
120-130	157.1	146.3	96.2	56.3	0.42	0.11	0.30	1.5
130-140	175.8	164.1	97.7	63.1	0.35	0.12	0.23	1.7
140-150	150.5	140.9	94.8	54.2	0.43	0.10	0.33	1.5
150-160	137.7	129.4	92.4	49.8	0.46	0.09	0.37	1.4
				avg	0.41	0.11	0.30	1.5
				std	0.03	0.01	0.04	0.1

**Table A.2. Estimation of N content initially present in column 2.**

Distance (cm)	dry sand (g)	N present in sand (mg N)	bulk wet density (g/ml)	Residual water (ml)	N added (mg N)	Initial N (mg N)
0-10	1112.4	1.5	1.6	74.0	1.6	3.2
10-20	1097.4	1.5	1.6	79.7	1.8	3.3
20-30	1041.2	1.4	1.5	74.7	1.7	3.1
30-40	1104.9	1.5	1.6	74.0	1.6	3.2
40-50	1141.3	1.6	1.7	81.9	1.8	3.4
50-60	1125.8	1.5	1.6	78.2	1.7	3.3
60-70	1205.7	1.7	1.7	84.6	1.9	3.5
70-80	1122.2	1.5	1.6	76.6	1.7	3.2
80-90	1200.1	1.6	1.7	83.3	1.9	3.5
90-100	1099.8	1.5	1.6	78.7	1.7	3.3
100-110	1219.5	1.7	1.8	88.0	2.0	3.6
110-120	1205.4	1.7	1.7	82.0	1.8	3.5
120-130	1123.7	1.5	1.6	83.3	1.9	3.4
130-140	1241.8	1.7	1.8	88.7	2.0	3.7
140-150	1098.6	1.5	1.6	75.0	1.7	3.2
150-160	1035.4	1.4	1.5	66.0	1.5	2.9
sum	18175.1	24.9		1268.6		
avg	1136		1.6			
std	62		0.1			

*Notes: The bioavailable N ( $NO_3-N + NH_4-N$ ) originally present in the soil was measured to be .00137 mg N/g dry sand. The N-amended solution used in flooding the column has a concentration of .022 mg-N/L.*

Appendix A.2 contains experimental data from column experiments as discussed in Chapter 2. The values given here are absolute concentrations of toluene, O<sub>2</sub>, and CO<sub>2</sub> in soil air from selected sampling ports along column length. The reported times are relative to the start of each experiment.

## A.2 Column 1

March 27, 1990

---

	Time (hour)	Toluene (mg/L)	O <sub>2</sub> (%)	CO <sub>2</sub> (%)
reservoir	1h00m	65.	-	-
port1	1h15m	17.	20.8	0.032
port5	1h30m	N/D	21.3	0.024
port3	1h45m	0.4	21.2	0.026
port7	2h00m	N/D	21.4	0.020
reservoir	3h00m	65.	20.8	0.037
port1	3h15m	29.	20.7	0.030
port3	3h30m	2.1	21.0	0.024
port5	3h45m	N/D	21.2	0.021
port7	4h00m	N/D	21.7	0.020
effluent	4h15m	N/D	21.8	N/D

March 28, 1990

---

	Time (hour)	Toluene (mg/L)	O <sub>2</sub> (%)	CO <sub>2</sub> (%)
reservoir	24h00m	65.	21.2	0.028
port1	24h10m	54.	20.9	0.026
port3	24h20m	27.	21.1	0.023
port5	24h30m	11.	21.1	0.019
port7	24h40m	3.5	21.4	0.016
port9	25h00m	0.9	21.8	0.014
port11	25h10m	N/D	21.5	0.011
port13	25h20m	N/D	21.7	0.008
port16	25h30m	N/D	21.8	0.004

March 30, 1990

---

	Time (hour)	Toluene (mg/L)	O <sub>2</sub> (%)	CO <sub>2</sub> (%)
reservoir	75h40m	65.	20.8	0.021
port1	75h50m	62.	20.5	0.020
port3	76h00m	42.	20.8	0.019
port5	76h10m	29.	20.6	0.017
port7	76h20m	17.	20.8	0.014
port9	76h30m	9.7	20.5	0.012
port11	76h35m	4.4	20.7	0.008
port13	76h40m	1.8	20.3	0.006
port15	76h55m	0.2	20.4	0.002
port16	77h00m	0.1	20.2	0.001
effluent	77h06m	N/D	20.2	N/D
influent	77h15m	N/D	20.2	N/D

April 2, 1990

---

	Time (hour)	Toluene (mg/L)	O <sub>2</sub> (%)	CO <sub>2</sub> (%)
effluent	140h15m	N/D	20.8	N/D
port16	140h30m	65.	20.7	0.001
port15	140h45m	61.	20.7	0.002
port13	141h10m	49.	20.5	0.005
port11	141h15m	36.	20.6	0.009
port9	141h20m	26.	20.7	0.012
port7	141h25m	18.	20.8	0.016
port5	141h35m	11.5	20.7	0.016
port3	141h40m	6.9	20.7	0.017
port1	141h45m	3.5	20.7	0.019
reservoir	141h55m	1.8	20.7	0.019

July 11, 1990

---

	Time (hour)	Toluene (mg/L)	O <sub>2</sub> (%)	CO <sub>2</sub> (%)
effluent	2540h45m	N/D	21.1	0.029
port16	2540h55m	2.8	19.2	0.012
port15	2541h05m	6.2	19.3	0.023
port13	2541h15m	13.	19.2	0.040
port11	2541h25m	19.	19.2	0.049
port9	2541h35m	27.	19.1	0.057
port7	2541h45m	33.	19.2	0.060
port5	2541h55m	40.	19.2	0.059
port3	2542h05m	45.	19.1	0.060
port1	2542h15m	54.	19.2	0.060
reservoir	2542h25m	65.	19.1	0.059

July 19, 1990

---

	Time (hour)	Toluene (mg/L)	O <sub>2</sub> (%)	CO <sub>2</sub> (%)
effluent	2734h55m	N/D	21.4	0.048
port16	2735h00m	3.2	19.6	0.022
port15	2735h10m	6.8	19.5	0.032
port13	2735h20m	13.5	19.6	0.047
port11	2735h30m	20.	19.5	0.057
port9	2735h40m	27.	19.5	0.064
port7	2735h50m	34.	19.5	0.069
port5	2736h00m	41.	19.4	0.068
port3	2736h10m	49.	19.4	0.067
port1	2736h20m	55.	19.4	0.067
reservoir	2736h30m	64.	19.4	0.068

## A.3 Column 2

October 15, 1991

---

	Time (hour)	Toluene (mg/L)	O <sub>2</sub> (%)	CO <sub>2</sub> (%)
reservoir	0h00m	0.	20.6	0.070
port1	0h00m	0.	20.7	0.070
port3	0h00m	0.	20.7	0.055
port5	0h00m	0.	20.7	0.044
port7	0h00m	0.	20.7	0.035
port9	0h00m	0.	20.7	0.026
port13	0h00m	0.	20.6	0.012
port15	0h00m	0.	20.7	0.009
effluent	0h00m	0.	20.6	0.006

October 22, 1991

---

	Time (hour)	Toluene (mg/L)	O <sub>2</sub> (%)	CO <sub>2</sub> (%)
effluent	163h55m	N/D	20.6	0.004
port15	164h03m	N/D	20.4	0.015
port13	164h11m	N/D	20.3	0.045
port11	164h19m	N/D	20.2	0.087
port9	164h27m	N/D	20.2	0.133
port7	164h35m	N/D	20.2	0.179
port6	164h43m	N/D	20.1	0.202
port5	164h51m	0.74	20.1	0.202
port4	165h05m	2.2	20.1	0.179
port3	165h13m	3.8	20.2	0.154
port2	165h21m	4.3	20.3	0.116
port1	165h30m	6.8	20.2	0.088
reservoir	165h45m	9.3	20.1	0.051

October 27, 1991

---

	Time (hour)	Toluene (mg/L)	O <sub>2</sub> (%)	CO <sub>2</sub> (%)
effluent	284h55m	N/D	20.4	0.004
port15	284h52m	N/D	20.3	0.017
port13	285h00m	N/D	20.2	0.050
port11	285h08m	N/D	20.2	0.097
port9	285h16m	N/D	20.2	0.148
port7	285h25m	N/D	20.1	0.198
port6	285h33m	0.26	20.1	0.213
port5	285h41m	1.2	20.0	0.208
port4	285h49m	2.3	20.0	0.187
port3	285h57m	3.4	20.1	0.164
port2	286h05m	4.1	20.2	0.124
port1	286h13m	6.5	20.0	0.104
reservoir	286h21m	9.6	20.0	0.069

October 30, 1991

---

	Time (hour)	Toluene (mg/L)	O <sub>2</sub> (%)	CO <sub>2</sub> (%)
effluent	355h06m	N/D	20.1	0.004
port15	355h14m	N/D	20.1	0.018
port13	355h22m	N/D	20.0	0.056
port11	355h30m	N/D	19.9	0.107
port9	355h38m	N/D	19.8	0.161
port7	355h46m	N/D	19.7	0.216
port6	355h54m	0.56	19.7	0.225
port5	356h02m	1.5	19.7	0.215
port4	356h10m	2.7	19.7	0.194
port3	356h18m	3.8	19.7	0.172
port2	356h30m	4.6	19.8	0.134
port1	356h38m	6.5	19.7	0.113
reservoir	356h46m	10.	19.7	0.083

November 14, 1991

---

	Time (hour)	Toluene (mg/L)	O <sub>2</sub> (%)	CO <sub>2</sub> (%)
port1	714h45m	7.0	19.5	0.215
port7	715h02m	0.62	19.6	0.282
port6	715h10m	1.2	19.6	0.287
port5	715h18m	1.8	19.5	0.279
port4	715h27m	2.9	19.6	0.267
port3	715h35m	3.8	19.6	0.254
port2	715h43m	3.7	19.9	0.211
port8	716h00m	0.21	19.6	0.270
port15	716h20m	N/D	19.9	0.027
port14	716h28m	N/D	19.8	0.047
port13	716h36m	N/D	19.8	0.082
port11	716h43m	N/D	19.7	0.158
port9	716h50m	N/D	19.6	0.239
effluent	716h59m	N/D	19.7	0.007

November 26, 1991

---

	Time (hour)	Toluene (mg/L)	O <sub>2</sub> (%)	CO <sub>2</sub> (%)
effluent	1003h17m	N/D	19.6	0.009
port15	1003h25m	N/D	19.5	0.031
port14	1003h33m	N/D	19.5	0.054
port12	1003h41m	N/D	19.4	0.138
port10	1003h49m	N/D	19.3	0.220
port9	1003h57m	0.25	19.3	0.256
port8	1004h05m	0.85	19.3	0.280
port7	1004h13m	1.5	19.3	0.291
port6	1004h21m	2.3	19.3	0.296
port5	1004h29m	3.3	19.2	0.302
port4	1004h37m	4.4	19.4	0.290
port3	1004h45m	5.3	19.4	0.284
port2	1004h53m	6.6	19.5	0.271
port1	1005h01m	7.9	19.3	0.256
reservoir	1005h09m	10.	19.4	0.244

December 09, 1991

---

	Time (hour)	Toluene (mg/L)	O <sub>2</sub> (%)	CO <sub>2</sub> (%)
effluent	1315h40m	N/D	19.9	0.006
port15	1315h48m	N/D	19.8	0.030
port14	1315h58m	N/D	19.8	0.053
port12	1316h07m	N/D	19.7	0.138
port10	1316h16m	0.18	19.7	0.219
port9	1316h24m	0.63	19.6	0.247
port8	1316h32m	1.3	19.5	0.272
port7	1316h40m	1.9	19.5	0.286
port6	1316h49m	2.5	19.6	0.295
port5	1316h57m	3.6	19.5	0.302
port4	1317h06m	4.6	19.6	0.303
port3	1317h14m	5.3	19.6	0.298
port2	1317h22m	6.5	19.5	0.296
port1	1317h30m	7.7	19.5	0.291
reservoir	1317h39m	10.	19.4	0.288

December 12, 1991

---

	Time (hour)	Toluene (mg/L)	O <sub>2</sub> (%)	CO <sub>2</sub> (%)
effluent	1386h25m	N/D	19.9	0.011
port15	1386h33m	N/D	19.7	0.035
port14	1386h47m	N/D	19.8	0.059
port13	1386h55m	N/D	19.7	0.101
port12	1387h05m	N/D	19.6	0.148
port11	1387h13m	N/D	19.6	0.192
port10	1387h21m	0.30	19.9	0.228
port9	1387h29m	0.82	19.8	0.254
port8	1387h38m	1.5	19.7	0.278
port7	1387h46m	2.2	19.7	0.291
port6	1387h54m	3.0	19.8	0.302
port5	1388h02m	3.8	19.7	0.306
port4	1388h10m	5.0	19.8	0.308

## December 12, 1991 (continued)

---

	Time (hour)	Toluene (mg/L)	O <sub>2</sub> (%)	CO <sub>2</sub> (%)
port3	1388h18m	5.7	19.7	0.306
port2	1388h26m	6.8	19.7	0.313
port1	1388h34m	7.9	19.7	0.298
reservoir	1388h42m	10.	19.7	0.294

## December 16, 1991

---

	Time (hour)	Toluene (mg/L)	O <sub>2</sub> (%)	CO <sub>2</sub> (%)
effluent	1482h52m	N/D	19.8	0.010
port15	1483h00m	N/D	19.8	0.035
port14	1483h08m	N/D	19.8	0.061
port13	1483h16m	N/D	19.7	0.105
port12	1483h24m	N/D	19.7	0.155
port11	1483h32m	0.04	19.6	0.199
port10	1483h40m	0.43	19.6	0.232
port9	1483h48m	0.94	19.6	0.257
port8	1483h56m	1.6	19.6	0.281
port7	1484h04m	2.3	19.6	0.295
port6	1484h12m	3.0	19.6	0.305
port5	1484h20m	3.8	19.8	0.311
port4	1484h28m	4.8	19.7	0.313
port3	1484h36m	5.5	19.8	0.313
port2	1484h44m	6.6	19.7	0.311
port1	1484h52m	7.3	19.7	0.306
reservoir	1485h00m	9.7	19.7	0.307

December 20, 1991

---

	Time (hour)	Toluene (mg/L)	O <sub>2</sub> (%)	CO <sub>2</sub> (%)
port15	1583h30m	N/D	19.7	0.033
port14	1583h38m	N/D	19.7	0.055
port13	1583h46m	N/D	19.7	0.095
port12	1583h54m	N/D	19.6	0.140
port11	1584h02m	0.12	19.6	0.176
port10	1584h15m	0.49	19.6	0.209
reservoir	1584h28m	10.	19.4	0.304
port9	1585h02m	0.98	19.5	0.236
port8	1585h10m	1.6	19.5	0.260
port7	1585h18m	2.2	19.5	0.276
port6	1585h26m	2.9	19.5	0.291
port5	1585h34m	3.6	19.5	0.300
port4	1585h42m	4.7	19.5	0.308
port3	1585h50m	5.6	19.5	0.311
port2	1585h58m	6.6	19.5	0.313
port1	1586h06m	8.1	19.5	0.310
effluent	1586h50m	N/D	19.9	0.010

December 24, 1991

---

	Time (hour)	Toluene (mg/L)	O <sub>2</sub> (%)	CO <sub>2</sub> (%)
effluent	1675h20m	N/D	19.8	0.011
port15	1675h28m	N/D	19.7	0.036
port2	1675h44m	6.7	19.4	0.316
port1	1675h52m	7.8	19.4	0.313
reservoir	1676h00m	10.	19.4	0.317
port14	1676h15m	N/D	19.7	0.062
port13	1676h23m	N/D	19.7	0.107
port12	1676h31m	N/D	19.6	0.157
port11	1676h39m	0.22	19.6	0.194
port10	1676h49m	0.67	19.6	0.226
port9	1676h57m	1.2	19.5	0.253

December 24, 1991

---

	Time (hour)	Toluene (mg/L)	O <sub>2</sub> (%)	CO <sub>2</sub> (%)
port8	1677h05m	1.9	19.5	0.276
port7	1677h13m	2.5	19.4	0.291
port6	1677h21m	3.1	19.5	0.302
port5	1677h36m	4.1	19.7	0.309
port4	1677h44m	5.2	19.5	0.315
port3	1677h52m	5.9	19.7	0.325

January 2, 1992

---

	Time (hour)	Toluene (mg/L)	O <sub>2</sub> (%)	CO <sub>2</sub> (%)
effluent	1895h34m	N/D	19.6	0.011
port15	1895h42m	N/D	19.5	0.036
port14	1895h50m	N/D	19.5	0.061
port13	1895h58m	N/D	19.4	0.105
port12	1896h06m	0.12	19.4	0.152
port11	1896h15m	0.46	19.3	0.181
port10	1896h24m	0.91	19.4	0.211
port9	1896h32m	1.4	19.3	0.236
port8	1896h40m	2.0	19.3	0.260
port7	1896h48m	2.6	19.3	0.276
port6	1896h56m	3.2	19.3	0.288
port5	1897h02m	4.1	19.3	0.300
port4	1897h10m	5.0	19.3	0.306
port3	1897h18m	5.7	19.3	0.309
port2	1897h26m	6.4	19.2	0.311
port1	1897h34m	7.6	19.2	0.311
reservoir	1897h42m	9.8	19.2	0.316

January 17, 1992

---

	Time (hour)	Toluene (mg/L)	O <sub>2</sub> (%)	CO <sub>2</sub> (%)
effluent	2254h53m	N/D	19.6	0.014
port15	2255h04m	N/D	19.5	0.049
port14	2255h12m	0.05	19.4	0.082
port13	2255h20m	0.56	19.4	0.119
port12	2255h28m	1.3	19.3	0.151
port11	2255h36m	2.0	19.3	0.175
port10	2255h44m	2.8	19.3	0.197
port9	2255h52m	3.7	19.3	0.217
port8	2256h00m	4.6	19.2	0.231
port7	2256h08m	5.6	19.3	0.243
port6	2256h16m	6.6	19.3	0.251
port5	2256h24m	7.6	19.2	0.256
port4	2256h32m	8.8	19.2	0.259
port3	2256h40m	9.4	19.2	0.259
port2	2256h48m	11.	19.2	0.255
port1	2257h06m	12.	19.3	0.250
reservoir	2257h14m	16.	19.1	0.250

January 18, 1992

---

	Time (hour)	Toluene (mg/L)	O <sub>2</sub> (%)	CO <sub>2</sub> (%)
effluent	2276h23m	N/D	19.6	0.016
port15	2276h31m	0.03	19.5	0.051
port14	2276h39m	0.26	19.5	0.078
port13	2276h59m	0.85	19.4	0.111
port12	2277h07m	1.6	19.3	0.141
port11	2277h15m	2.4	19.3	0.166
port10	2277h23m	3.1	19.3	0.188
port9	2277h31m	4.1	19.2	0.208
port8	2277h39m	4.9	19.3	0.223
port7	2277h47m	5.8	19.2	0.233
port6	2277h55m	6.9	19.3	0.243

## January 18, 1992 (continued)

---

	Time (hour)	Toluene (mg/L)	O <sub>2</sub> (%)	CO <sub>2</sub> (%)
port5	2278h03m	7.6	19.2	0.248
port4	2278h12m	8.9	19.2	0.252
port3	2278h20m	9.7	19.2	0.253
port2	2278h28m	11.	19.2	0.253
port1	2278h36m	12.	19.2	0.252
reservoir	2278h44m	15.	19.1	0.253

## January 29, 1992

---

	Time (hour)	Toluene (mg/L)	O <sub>2</sub> (%)	CO <sub>2</sub> (%)
port15	2418h51m	0.14	19.7	0.047
port14	2418h59m	0.42	19.8	0.070
port13	2419h07m	1.1	19.7	0.101
port12	2419h15m	1.9	19.7	0.131
port11	2419h31m	2.6	19.6	0.155
port10	2419h39m	3.4	19.6	0.177
port9	2419h47m	4.2	19.5	0.195
port8	2420h03m	5.3	19.5	0.213
port7	2420h11m	6.2	19.5	0.224
port6	2420h19m	7.0	19.5	0.232
port5	2420h27m	8.1	19.4	0.240
port4	2420h35m	9.1	19.5	0.244
port3	2420h43m	10.	19.5	0.247
port2	2420h51m	11.	19.5	0.247
port1	2420h59m	13.	19.4	0.246
reservoir	2421h07m	15.	19.4	0.250
effluent	2421h23m	N/D	19.9	0.016

February 7, 1992

---

	Time (hour)	Toluene (mg/L)	O <sub>2</sub> (%)	CO <sub>2</sub> (%)
effluent	2638h01m	0.06	19.6	0.014
port15	2638h09m	0.33	19.4	0.039
port14	2638h20m	0.67	19.4	0.062
port13	2638h28m	1.3	19.3	0.093
port12	2638h36m	2.2	19.3	0.123
port11	2638h44m	2.9	19.3	0.147
port10	2638h52m	3.7	19.3	0.171
port9	2639h00m	4.6	19.2	0.191
port8	2639h08m	5.6	19.2	0.208
port7	2639h16m	6.3	19.2	0.218
port6	2639h24m	7.2	19.2	0.228
port5	2639h32m	8.3	19.2	0.235
port4	2639h40m	9.4	19.2	0.240
port3	2639h48m	10.	19.2	0.246
port2	2639h56m	11.	19.2	0.250
port1	2640h04m	12.	19.1	0.247
reservoir	2640h24m	15.	19.1	0.254

February 13, 1992

---

	Time (hour)	Toluene (mg/L)	O <sub>2</sub> (%)	CO <sub>2</sub> (%)
reservoir	2782h39m	16.	19.2	0.255
port1	2782h47m	13.	19.2	0.250
effluent	2783h20m	0.06	19.6	0.012
port15	2783h28m	0.35	19.5	0.037
port14	2783h37m	0.73	19.4	0.058
port13	2783h45m	1.4	19.4	0.087
port12	2783h53m	2.2	19.2	0.117
port11	2784h01m	3.0	19.4	0.140
port10	2784h09m	3.8	19.4	0.164
port9	2784h17m	4.8	19.3	0.185
port8	2784h25m	5.9	19.2	0.202

## February 13, 1992 (continued)

---

	Time (hour)	Toluene (mg/L)	O <sub>2</sub> (%)	CO <sub>2</sub> (%)
port7	2784h33m	6.5	19.3	0.212
port6	2784h41m	7.5	19.3	0.222
port5	2784h49m	8.3	19.2	0.230
port4	2784h57m	9.6	19.2	0.238
port3	2785h05m	11.	19.3	0.242
port2	2785h14m	12.	19.2	0.246

## February 20, 1992

---

	Time (hour)	Toluene (mg/L)	O <sub>2</sub> (%)	CO <sub>2</sub> (%)
effluent	2950h11m	0.06	19.6	0.011
port15	2950h19m	0.35	19.5	0.034
port14	2950h27m	0.69	19.5	0.054
port13	2950h35m	1.4	19.4	0.082
port12	2950h59m	2.2	19.4	0.111
port11	2951h07m	3.0	19.4	0.136
port10	2951h15m	3.9	19.4	0.158
port9	2951h29m	4.6	19.4	0.176
port8	2951h37m	5.7	19.4	0.195
port7	2951h54m	6.3	19.3	0.206
port6	2952h02m	7.3	19.4	0.217
port5	2952h10m	8.4	19.3	0.226
port4	2952h18m	9.6	19.3	0.233
port3	2952h26m	11.	19.3	0.238
port2	2952h34m	12.	19.3	0.244
port1	2952h42m	13.	19.3	0.247
reservoir	2952h52m	15.	19.3	0.251

## A.4 Column 3

March 13, 1992

---

	Time (hour)	Toluene (mg/L)	O <sub>2</sub> (%)	CO <sub>2</sub> (%)
effluent	0h00m	N/D	20.1	0.012
port15	0h00m	N/D	19.8	0.066
port14	0h00m	N/D	19.7	0.112
port13	0h00m	N/D	19.9	0.116
port12	0h00m	N/D	20.2	0.114
port11	0h00m	N/D	20.2	0.174
port10	0h00m	N/D	20.3	0.172
port9	0h00m	N/D	19.9	0.176
port8	0h00m	N/D	20.0	0.175
port7	0h00m	N/D	19.8	0.117
port6	0h00m	N/D	20.0	0.197
port5	0h00m	N/D	20.1	0.181
port4	0h00m	N/D	20.1	0.179
port3	0h00m	N/D	20.6	0.057
port2	0h00m	N/D	20.8	0.143
port1	0h00m	N/D	20.7	0.149
reservoir	0h00m	0.03	20.7	0.163

March 17, 1992

---

	Time (hour)	Toluene (mg/L)	O <sub>2</sub> (%)	CO <sub>2</sub> (%)
effluent	90h58m	N/D	20.1	0.015
port15	91h06m	N/D	20.0	0.053
port14	91h14m	N/D	20.0	0.079
port13	91h22m	N/D	19.9	0.107
port12	91h29m	N/D	19.7	0.142
port11	91h37m	N/D	19.6	0.189
port10	91h45m	N/D	19.6	0.215
port9	91h53m	N/D	19.5	0.255

## March 17, 1992 (continued)

---

	Time (hour)	Toluene (mg/L)	O <sub>2</sub> (%)	CO <sub>2</sub> (%)
port8	92h00m	N/D	19.3	0.294
port6	92h14m	N/D	19.2	0.376
port5	92h23m	N/D	19.1	0.410
port4	92h29m	N/D	19.0	0.466
port7	93h02m	N/D	19.2	0.343
port3	93h10m	0.22	19.0	0.482
port2	93h48m	1.3	18.8	0.493
port1	93h55m	2.0	18.8	0.440
reservoir	94h24m	9.4	18.6	0.370

## March 19, 1992

---

	Time (hour)	Toluene (mg/L)	O <sub>2</sub> (%)	CO <sub>2</sub> (%)
effluent	139h05m	N/D	20.2	0.010
port15	139h12m	N/D	20.1	0.037
port14	139h20m	N/D	20.1	0.056
port13	139h28m	N/D	20.0	0.077
port11	139h36m	N/D	19.9	0.133
port9	139h52m	N/D	20.0	0.194
port7	140h09m	N/D	19.8	0.245
port5	140h18m	N/D	19.7	0.327
port4	140h26m	N/D	19.5	0.385
port3	141h48m	0.23	19.5	0.454
port2	141h57m	1.1	19.3	0.475
port1	142h36m	2.6	19.3	0.435
reservoir	142h44m	9.8	19.3	0.400

March 21, 1992

---

	Time (hour)	Toluene (mg/L)	O <sub>2</sub> (%)	CO <sub>2</sub> (%)
effluent	187h00m	N/D	20.3	0.013
port15	187h07m	N/D	20.3	0.048
port14	187h15m	N/D	20.2	0.073
port13	187h23m	N/D	20.2	0.100
port4	188h13m	0.17	19.4	0.485
port11	188h21m	N/D	19.9	0.171
port9	188h29m	N/D	19.9	0.252
port7	188h38m	N/D	19.6	0.342
port5	188h45m	N/D	19.6	0.434
port3	189h28m	1.3	19.4	0.512
port2	189h36m	2.5	19.3	0.496
port1	189h44m	4.3	19.3	0.461
reservoir	189h52m	10.	19.2	0.414

March 31, 1992

---

	Time (hour)	Toluene (mg/L)	O <sub>2</sub> (%)	CO <sub>2</sub> (%)
effluent	427h03m	N/D	19.9	0.018
port15	427h10m	N/D	19.8	0.067
port14	427h18m	N/D	19.8	0.101
port13	427h25m	N/D	19.7	0.138
port11	427h33m	N/D	19.5	0.235
port9	427h48m	N/D	19.4	0.330
port7	427h56m	N/D	19.3	0.441
port5	428h03m	0.29	19.1	0.551
port6	428h11m	N/D	19.1	0.501
port4	428h58m	1.3	19.0	0.575
port3	429h15m	2.2	19.0	0.584
port2	429h42m	4.2	19.0	0.579
port1	429h58m	5.7	19.0	0.559
reservoir	430h06m	10.	18.9	0.534

April 7, 1992

---

	Time (hour)	Toluene (mg/L)	O <sub>2</sub> (%)	CO <sub>2</sub> (%)
port15	595h10m	N/D	20.0	0.037
port14	595h23m	N/D	20.0	0.056
port13	595h30m	N/D	19.9	0.079
port11	595h38m	N/D	19.9	0.135
effluent	595h45m	N/D	20.1	0.013
port9	595h52m	N/D	19.8	0.209
port7	596h07m	N/D	19.7	0.297
port6	596h14m	N/D	19.7	0.342
port5	596h21m	0.06	19.6	0.393
port4	596h29m	0.42	19.6	0.437
port3	596h37m	1.2	19.6	0.471
port2	597h18m	2.5	19.5	0.512
port1	597h26m	4.0	19.5	0.531
reservoir	597h50m	10.	19.4	0.544

April 16, 1992

---

	Time (hour)	Toluene (mg/L)	O <sub>2</sub> (%)	CO <sub>2</sub> (%)
effluent	812h00m	N/D	20.0	0.022
port15	812h15m	N/D	19.9	0.083
port14	812h22m	N/D	19.8	0.124
port13	812h29m	N/D	19.8	0.169
port11	812h36m	N/D	19.6	0.280
port9	812h43m	N/D	19.4	0.387
port7	812h50m	0.09	19.3	0.515
port6	812h58m	0.52	19.3	0.552
port5	813h06m	1.0	19.2	0.576
port4	813h14m	2.2	19.2	0.597
port3	813h22m	3.1	19.2	0.607
port2	813h30m	4.3	19.1	0.610
port1	813h38m	5.5	19.1	0.602
reservoir	813h46m	9.8	19.0	0.593

April 17, 1992

---

	Time (hour)	Toluene (mg/L)	O <sub>2</sub> (%)	CO <sub>2</sub> (%)
effluent	830h03m	N/D	19.9	0.023
port15	830h10m	N/D	19.8	0.086
port14	830h17m	N/D	19.7	0.130
port13	830h24m	N/D	19.7	0.176
port11	830h31m	N/D	19.6	0.293
port9	830h38m	N/D	19.4	0.403
reservoir	831h48m	10.	18.9	0.601
port7	834h52m	0.12	19.2	0.525
port6	835h00m	0.51	19.2	0.558
port5	835h16m	1.3	19.1	0.587
port4	835h24m	2.2	19.1	0.603
port3	835h32m	3.3	19.0	0.614
port2	835h40m	4.5	19.0	0.618
port1	835h48m	5.7	19.0	0.609

May 19, 1992

---

	Time (hour)	Toluene (mg/L)	O <sub>2</sub> (%)	CO <sub>2</sub> (%)
effluent	1602h59m	N/D	20.1	0.030
port15	1603h06m	N/D	19.9	0.107
port14	1603h13m	N/D	19.1	0.159
port13	1603h20m	N/D	19.7	0.222
port11	1603h27m	N/D	18.9	0.346
port10	1603h34m	0.11	18.8	0.403
port9	1603h42m	0.37	19.5	0.452
port8	1603h50m	0.83	19.4	0.497
port7	1603h58m	1.8	19.4	0.539
port6	1604h06m	2.1	19.3	0.568
port4	1604h22m	3.6	19.2	0.614
port3	1604h30m	4.4	19.2	0.640
port2	1604h38m	5.4	19.2	0.648
port1	1604h46m	6.5	19.2	0.653
reservoir	1604h54m	10.	19.1	0.660

May 26, 1992

---

	Time (hour)	Toluene (mg/L)	O <sub>2</sub> (%)	CO <sub>2</sub> (%)
effluent	1772h25m	N/D	19.8	0.033
port15	1772h32m	N/D	19.8	0.105
port14	1772h40m	N/D	19.8	0.155
port13	1772h47m	N/D	19.7	0.218
port12	1772h54m	N/D	19.6	0.282
port11	1773h01m	0.03	19.5	0.340
port9	1773h19m	0.54	19.4	0.438
port7	1773h35m	1.9	19.3	0.525
port6	1773h44m	2.2	19.2	0.556
port10	1774h00m	0.28	19.5	0.393
port8	1774h08m	1.1	19.3	0.483
port4	1774h24m	3.6	19.2	0.611
port3	1774h32m	4.4	19.2	0.637
port2	1774h40m	5.1	19.2	0.645
port1	1774h48m	5.9	19.2	0.654
reservoir	1774h56m	10.	19.0	0.663

June 9, 1992

---

	Time (hour)	Toluene (mg/L)	O <sub>2</sub> (%)	CO <sub>2</sub> (%)
effluent	2107h53m	N/D	20.0	0.030
port15	2108h00m	N/D	19.9	0.110
port14	2108h07m	N/D	19.8	0.170
port13	2108h14m	N/D	19.8	0.228
port12	2108h21m	0.07	19.7	0.289
port11	2108h29m	0.27	19.6	0.337
port10	2108h37m	0.67	19.6	0.384
port9	2108h45m	0.94	19.5	0.426
port8	2108h53m	1.4	19.5	0.469
port7	2109h03m	2.6	19.3	0.506
port4	2109h35m	4.3	19.4	0.593
port6	2109h48m	2.8	19.3	0.540

## June 9, 1992 (continued)

---

	Time (hour)	Toluene (mg/L)	O <sub>2</sub> (%)	CO <sub>2</sub> (%)
port5	2109h56m	3.4	19.4	0.569
port3	2110h04m	4.5	19.4	0.611
port2	2110h12m	5.7	19.3	0.630
port1	2110h20m	6.3	19.3	0.639
reservoir	2110h28m	10.	19.2	0.650

## June 24, 1992

---

	Time (hour)	Toluene (mg/L)	O <sub>2</sub> (%)	CO <sub>2</sub> (%)
effluent	2468h21m	N/D	20.1	0.032
port15	2468h28m	N/D	20.0	0.112
port14	2468h35m	N/D	19.9	0.165
port13	2468h42m	0.07	19.9	0.228
port12	2468h50m	0.28	19.9	0.279
port11	2468h58m	0.52	19.8	0.325
port10	2469h06m	1.0	19.8	0.366
port9	2469h14m	1.3	19.7	0.405
port8	2469h22m	1.8	19.7	0.446
port7	2469h30m	2.8	19.7	0.483
port6	2469h38m	2.9	19.6	0.513
port5	2469h46m	3.3	19.6	0.543
port4	2469h54m	4.2	19.5	0.566
port3	2470h02m	4.9	19.5	0.599
port2	2470h10m	5.6	19.5	0.617
port1	2470h18m	6.4	19.5	0.627
reservoir	2470h26m	10.	19.3	0.637

July 7, 1992

---

	Time (hour)	Toluene (mg/L)	O <sub>2</sub> (%)	CO <sub>2</sub> (%)
effluent	2781h45m	N/D	21.0	0.029
port15	2781h52m	N/D	20.0	0.109
port14	2781h59m	0.02	20.0	0.167
port13	2782h06m	0.19	19.9	0.214
port12	2782h13m	0.43	19.9	0.261
port11	2782h20m	0.66	19.9	0.300
port10	2782h27m	1.2	19.7	0.341
port9	2782h34m	1.5	19.7	0.381
port8	2782h41m	2.0	19.7	0.417
port7	2782h48m	3.0	19.6	0.452
port6	2783h01m	3.2	19.5	0.482
port5	2783h09m	3.6	19.6	0.511
port4	2783h17m	4.5	19.5	0.539
port2	2783h33m	5.9	19.5	0.581
port1	2783h41m	7.0	19.5	0.593
reservoir	2783h49m	10.	19.4	0.594

August 11, 1992

---

	Time (hour)	Toluene (mg/L)	O <sub>2</sub> (%)	CO <sub>2</sub> (%)
effluent	3618h00m	N/D	19.9	0.029
port15	3618h07m	0.15	20.1	0.100
port14	3618h14m	0.32	20.0	0.139
port12	3618h30m	0.90	19.9	0.227
port11	3618h38m	1.3	19.7	0.249
port9	3618h54m	1.9	19.6	0.334
port8	3619h02m	2.5	19.6	0.369
port6	3619h20m	3.9	19.4	0.429
port5	3619h28m	4.1	19.5	0.458
port3	3619h44m	5.8	19.5	0.494
reservoir	3620h08m	10.	19.5	0.544

## **APPENDIX B**

### **BIODEGRADATION KINETICS FORMULATION**

This appendix contains the derivation of a kinetic function describing biodegradation in a multi-phase system under the influence of logarithmic growth.

Monod kinetics adequately describe the relation between the specific growth rate and the substrate concentration in a system of aqueous phase

$$\frac{1}{B} \frac{dB}{dt} = \mu_{\max} \frac{C}{C + K_s} \quad (\text{B-1})$$

where B is the population density (cell mass per unit volume of the aqueous phase); C is the aqueous concentration of the chemical (chemical mass per unit volume of aqueous phase),  $\mu_{\max}$  is the maximum specific growth rate ( $\text{time}^{-1}$ ), and  $K_s$  is the half-saturation constant for growth (chemical mass per unit volume of aqueous phase). In a single phase system, the following equation relates the change of the population density to the corresponding change in the substrate concentration

$$C_0 + \frac{B_0}{Y} = C + \frac{B}{Y} \quad (\text{B-2})$$

where Y is the biomass yield (the amount of substrate required to produce one unit of cell mass). The subscript denotes the conditions at time zero. Y can be treated as invariant with time when the substrate is a C source (Simkins and Alexander, 1984). When only the substrate disappearance is of interest, B/Y can be replaced with X, and equation (B-1) becomes

$$\frac{dX}{dt} = X \mu_{\max} \frac{C}{C + K_s} \quad (\text{B-3})$$

where X is the aqueous concentration of the substrate required to produce a population of density B (chemical mass per unit volume of the aqueous phase). In addition, by combining equation (B-1) and the derivative of equation (B-2), one obtains an equation describing the rate of substrate disappearance reflecting Monod kinetics for a single-phase system

$$-\frac{dC}{dt} = X \mu_{\max} \frac{C}{C + K_s} \quad (\text{B-4})$$

In a multi-phase system, a mass balance of the chemical can be written by summing the compound mass over all phases

$$\theta_a G_0 + \theta_w C_0 + \rho_b S_0 + \theta_w X_0 = \theta_a G + \theta_w C + \rho_b S + \theta_w X \quad (\text{B-5})$$

where  $\theta_a$  and  $\theta_w$  are the volumetric air (volume of air phase per total volume) and water content (volume of aqueous phase per total volume), respectively;  $\rho_b$  is the bulk soil density (mass of solids per total volume);  $G$  (chemical mass per unit volume of the air phase) and  $S$  (chemical mass per solid mass) are the concentrations of the chemical in the vapor and solid phases, respectively. Take the derivative of equation (B-5) with respect to time and substitute the left hand side of equation (B-4),

$$-\left(\theta_a \frac{dG}{dt} + \theta_w \frac{dC}{dt} + \rho_b \frac{dS}{dt}\right) = X \mu_{\max} \frac{C}{C + K_s} \quad (\text{B-6})$$

Employing equilibrium relationships (discussed in Chapter 2) for describing the interphase partitioning of the chemical, equation (B-6) can be written in terms of air phase concentration as

$$-(\theta_a + \theta_w H_{wa} + \rho_b K_d H_{wa}) \frac{dG}{dt} = \theta_w X \mu_{\max} \frac{G}{G + K_s/H_{wa}} \quad (\text{B-7})$$

In the case of very small  $K_s$  ( $K_s \ll G_0$ ), equation (B-6) is reduced to

$$-\frac{dG}{dt} = \frac{\theta_w \mu_{\max}}{a} X \quad ; \quad (\text{B-8})$$

$$a = \theta_a + \theta_w H_{wa} + \rho_b K_d H_{wa}$$

From equation (B-5),

$$X = \frac{R(G_0 - G)}{\theta_w} + X_0 \quad (\text{B-9})$$

Substituting equation (B-9) into equation (B-8),

$$-\frac{dG}{dt} = \mu_{\max} \left( G_0 + \frac{\theta_w X_0}{a} - G \right) \quad (\text{B-10})$$

Integrating equation (B-10), one obtains the integral form

$$G = G_0 + \frac{X_0 \theta_w}{R} (1 - e^{-\mu_{\max} t}) \quad (\text{B-11})$$

Equation (B-11) was used in the parameter determination.

**APPENDIX C**  
**SELECTED EXPERIMENTAL DATA AND CALCULATIONS**  
**FROM BATCH EXPERIMENTS**

This appendix consists of 2 parts. The first part contains samples of calculations of those numbers reported in Chapter 3. The second part contains selected data of toluene measurements from batch respiked experiments.

## C.1 Sample of Calculations

### C.1.1 Mass partitioning of toluene in the batch experiments

Toluene mass loss due to biodegradation in batch experiments can be calculated using the following mass balance equation,

$$\begin{aligned}
 M_k &= G_k V_g + C_k V_w + S_k W_s \\
 &= G_k V_g + H_k G_k V_w + K_p C_k W_s \\
 &= G_k (V_g + H_k V_w + K_p H_k W_s)
 \end{aligned}
 \tag{C-1}$$

where  $H_k$  = water-air partitioning coefficient of toluene

$G_k$  = gas phase concentration

$C_k$  = aqueous phase concentration

$V_g$  = volume of gaseous phase

$V_w$  = volume of the aqueous phase

$S_k$  = solid phase concentration

$W_s$  = mass of solid phase

$K_p$  = sorption coefficient of toluene

Assumptions inherent in equation (C-1) are mass partitioning between phases (i.e., air/water and water/solid) is linear and  $H_k$  and  $K_p$  are the respective equilibrium constants. The table below lists various parameters of equation (C-1) at three temperatures.

T (°C)	$p^*$ (atm)	$p_k^*$ (atm)	$p_{avg}$ (atm)	$G_k$ (mg/L)	*Henry's Constant (atm/M)	$H_k$ (dimension- less)
10	0.0163	0.0166	0.0165	64.19	0.00381	6.0977
15	0.0218	0.0220	0.0219	85.28	0.00492	4.8029
25	0.0374	0.0374	0.0374	145.8	0.00642	3.6807

\* T. E. Jordan, *Vapor pressure of organic compounds*, 266 p., Interscience publishers, New York, 1954.

# Clausius-Clapeyron equation.

+ Ashworth, R. A., G. B. Howe, M. E. Mullins, and T. N. Rogers, Air-water partitioning coefficients of organics in dilute aqueous solutions, *J. Hazard. Mat.*, 18, 25-36, 1988.

Parameter Calculation:

$$G_k = \frac{P_{avg}}{RT} \quad (C-2)$$

$$H_k = \frac{RT}{h_k} \quad (C-3)$$

where R = universal gas constant

T = temperature

$h_k$  = Henry's constant

By substituting toluene concentration into equation (C-1), toluene mass present initially and remaining was calculated. The amount of toluene being degraded was determined by subtracting toluene mass remaining from that present initially. These results are compiled in Tables C.1, C.2, and C.3 for various batch experiments.

#### C.1.2 Mass partitioning of O<sub>2</sub> in batch experiments

Similarly, initial and final O<sub>2</sub> concentrations can be used to calculate the total O<sub>2</sub> mass being utilized in the biodegradation experiments using equation (C-1). Because oxygen is not sorbed to soil, therefore equation (C-1) is reduced to

$$M_{O_2} = G_{O_2}(V_g + H_{O_2}V_w) \quad (C-4)$$

where  $H_{O_2}$  = water-air partitioning coefficient of O<sub>2</sub>. Values of dimensionless  $H_{O_2}$  are .039 and .036 at 10 and 15°C, respectively (Perry and Green, 1984).

#### C.1.3 Mass partitioning of CO<sub>2</sub> in batch experiments

Total CO<sub>2</sub> production can be calculated from batch experiment data. CO<sub>2</sub> in the gas phase was measured before and after the experiments. In addition, the initial and final pH of the soil were measured to be 6.56 and 6.55 respectively. The small change

in pH is an indicative of either small amount of CO<sub>2</sub> evolved or buffer capacity of soil. Since the pH was around pK<sub>1</sub> (6.3), approximately half of the dissolved CO<sub>2</sub> is in the form of bicarbonate, and little CO<sub>2</sub> could possibly precipitated as carbonates. A mass balance equation for CO<sub>2</sub> in the aqueous phase is written as

$$(1 - \alpha_1 - \alpha_2) C_T = H_{CO_2} p_{CO_2} \quad (C-5)$$

where C<sub>T</sub> is the total mass of dissolved CO<sub>2</sub> species (dissolved CO<sub>2</sub> + CO<sub>3</sub><sup>2-</sup> + HCO<sub>3</sub><sup>-</sup>); α<sub>1</sub> and α<sub>2</sub> are the degree of dissociation of protons (see definition in Stumm and Morgan, 1981); p<sub>CO<sub>2</sub></sub> is the partial pressure of CO<sub>2</sub> in equilibrium with dissolved CO<sub>2</sub>. Because pH did not change, α<sub>1</sub> and α<sub>2</sub> remained constant throughout the experiment. The following values were used in the calculations: {H<sup>+</sup>} = 2.82E-07, α<sub>1</sub> = 0.574, α<sub>2</sub> = 7.57E-05, and H<sub>CO<sub>2</sub></sub> = 0.0479 M/atm (Pankow, 1991). Because α<sub>2</sub> is insignificant when compared to α<sub>1</sub>, it was neglected. The mass balance equation was rearranged and solved for C<sub>T</sub>

$$C_T = \frac{p_{CO_2} H_{CO_2}}{1 - \alpha_1} \quad (C-6)$$

To calculate the amount of CO<sub>2</sub> being produced, the difference of C<sub>T</sub> is calculated

$$\Delta C_T = \frac{\Delta p_{CO_2} H_{CO_2}}{1 - \alpha_1} \quad (C-7)$$

Because CO<sub>2</sub> concentration was measured in percent, unit conversion was done by dividing the measured values with 100 to get ΔP<sub>CO<sub>2</sub></sub> in atm. The amount of CO<sub>2</sub> produced and dissolved into the solution (dissolved CO<sub>2</sub> + CO<sub>3</sub><sup>2-</sup> + HCO<sub>3</sub><sup>-</sup>) is equal to ΔC<sub>T</sub> times the volume of water in the canister. The amount of gas phase CO<sub>2</sub> was calculated by ideal gas law and the volume of the gas phase, and the total CO<sub>2</sub> produced was the sum in the two phases,

$$\Delta M_{CO_2} = \Delta C_T V_w + \frac{\Delta p_{CO_2} V_g}{RT} \quad (C-8)$$

The above calculation method of CO<sub>2</sub> will be referred to as method (a).

A simpler way to calculate the amount of CO<sub>2</sub> evolved is to neglect HCO<sub>3</sub><sup>-1</sup> in the solution,  $\alpha_1 \rightarrow 0$ , and equation (5) reduces to

$$\Delta C_T = \Delta p_{CO_2} H_{CO_2}$$

The total CO<sub>2</sub> calculated by equations (6) and (7) will be referred to as method (b). CO<sub>2</sub> calculated by both methods for various batches are also compiled in Tables C.1, C.2, and C.3. It can be seen that Method (a) which accounts for HCO<sub>3</sub><sup>-</sup> gives slightly higher values than Method (b) which does not account for HCO<sub>3</sub><sup>-</sup> because there was very little amount of water in the system.

**Table C.1 Batch Experiment #6 (October 8, 1992).**

	10/9/92 $C_i$ (mg/L)	10/13/92 $C_f$ (mg/L)	toluene (moles) $\times 10^5$	<sup>(c)</sup> $O_{2,i}$ (%)	10/13/92 $O_{2,f}$ (%)	$O_2$ (moles) $\times 10^5$	<sup>(c)</sup> $CO_{2,i}$ (%)	10/13/92 $CO_{2,f}$ (%)	$CO_2$ <sup>(a)</sup> (moles) $\times 10^5$	$CO_2$ <sup>(b)</sup> (moles) $\times 10^5$	$CO_2$ <sup>(b)</sup> /toluene ratio
can#1	0.71	N/D	0.6	20.6	20.5	3.2	0.021	0.072	1.70	1.72	2.7
can#2	0.61	N/D	0.5	20.6	20.9	-11.	0.021	0.061	1.33	1.34	2.4
can#3	0.82	N/D	0.7	20.6	20.5	3.9	0.021	0.129	3.59	3.63	4.9
can#6	2.5	0.046	2.2	20.6	20.3	8.6	0.021	0.179	5.25	5.3	2.4
can#11	1.4	N/D	1.3	20.6	20.7	-5.	0.021	0.100	2.63	2.7	2.1
can#12	1.2	0.037	1.1	20.6	20.5	2.8	0.021	0.108	2.89	2.92	2.7
can#13	1.3	N/D	1.2	20.6	20.4	7.4	0.021	0.114	3.08	3.11	2.6
can#16	2.7	N/D	2.4	20.6	20.4	5.1	0.021	0.184	5.39	5.4	2.3
control	2.3	0.029	2.1	20.6	20.3	10.2	0.021	0.176	5.14	5.2	2.5
										avg	2.7
										std	0.83

<sup>(a)</sup>  $CO_2$  calculated using Method A.

<sup>(b)</sup>  $CO_2$  calculated using Method B which accounts for  $HCO_3^-$ , and gives slightly higher total  $CO_2$  production than Method A.

<sup>(c)</sup> No measurements were made. Numbers are the average values from Batch Experiment #5 (see Table C.2).

*Other information for batch experiment #6*

Each batch has approximately	55.0	g of wet sand
The moisture content of sand	0.10	ml H <sub>2</sub> O/g wet sand
The amount of water in each batch	5.55	ml
The weight of dry sand in these batches	49.45	g of dry sand
The volume of solid phase	19.02	ml
The volume of air phase	775.43	ml
The concentration of NH <sub>4</sub> NO <sub>3</sub> solution	0.0222	mg-N/ml
The amount of N added by the solution	0.123	mg-N
The original available N in leap sand	0.00137	mg-N/g of dry sand
The available N in the original sand	0.0677	mg-N
The sum of N in each batch	0.191	mg-N
	1.36E-05	gmole NO <sub>3</sub>
	6.81E-06	gmole NH <sub>4</sub> NO <sub>3</sub>

Table C.2 Batch Experiment #5 (October 5, 1992).

	10/6/92	10/13/92	10/6/92	10/13/92	10/6/92	10/13/92	O <sub>2</sub>	10/6/92	10/13/92	CO <sub>2</sub> <sup>(a)</sup>	CO <sub>2</sub> <sup>(b)</sup>	CO <sub>2</sub> <sup>(b)</sup>
	C <sub>i</sub>	C <sub>f</sub>	toluene	O <sub>2,i</sub>	O <sub>2,f</sub>	O <sub>2,f</sub>	(moles)	CO <sub>2,i</sub>	CO <sub>2,f</sub>	(moles)	(moles)	/toluene
	(mg/L)	(mg/L)	x10 <sup>5</sup>	(%)	(%)	(%)	x10 <sup>5</sup>	(%)	(%)	x10 <sup>5</sup>	x10 <sup>5</sup>	ratio
can#4	3.0	N/D	2.7	20.5	20.6	20.6	-1.0	0.021	0.229	6.89	7.0	2.5
can#5	2.6	N/D	2.3	20.8	20.7	20.7	1.0	0.024	0.219	6.47	6.5	2.8
can#7	3.3	N/D	3.0	20.5	20.4	20.4	0.2	0.021	0.231	6.95	7.0	2.3
can#14	3.0	N/D	2.7	20.5	20.4	20.4	4.7	0.019	0.260	7.99	8.1	3.0
can#8	4.3	N/D	3.9	20.4	20.3	20.3	5.4	0.020	0.301	9.30	9.4	2.4
can#9	4.5	N/D	4.1	20.5	20.4	20.4	4.0	0.021	0.300	9.20	9.3	2.3
can#10	5.1	N/D	4.6	20.6	20.6	20.6	-0.54	0.019	0.287	8.87	9.0	1.9
can#15	4.2	N/D	3.8	20.9	20.6	20.6	7.0	0.020	0.294	9.06	9.2	2.4
			avg	20.6	20.6	20.6	avg	0.021		avg	avg	2.5
											std	0.33

Note: The first four cans (#4, 5, 7, and 14) are not N-limited. The last four cans (#8, 9, 10, and 15) may be N-limited.

<sup>(a)</sup> CO<sub>2</sub> calculated using Method A.

<sup>(b)</sup> CO<sub>2</sub> calculated using Method B which accounts for HCO<sub>3</sub><sup>-</sup>, and gives slightly higher total CO<sub>2</sub> production than Method A.

*Other information for batch experiment #5*

Each batch has approximately	55.0	g of wet sand
The moisture content of sand	0.093	ml H <sub>2</sub> O/g wet sand
The amount of water in each batch	5.10	ml
The weight of dry sand in these batches	49.90	g of dry sand
The volume of solid phase	19.19	ml
The volume of air phase	775.71	ml
The concentration of NH <sub>4</sub> NO <sub>3</sub> solution	0.0222	mg-N/ml
The amount of N added by the solution	0.113	mg-N
The available N in the original sand	0.0684	mg-N
The sum of N in each batch	0.182	mg-N
	1.30E-05	gmole NO <sub>3</sub>
	6.48E-06	gmole NH <sub>4</sub> NO <sub>3</sub>

**Table C.3 Batch Experiment #4 (August 12,1992).**

	8/13/92 C <sub>i</sub> (mg/L)	8/19/92 C <sub>f</sub> (mg/L)	toluene (moles) x10 <sup>5</sup>	8/13/92 O <sub>2,i</sub> (%)	8/19/92 O <sub>2,f</sub> (%)	O <sub>2</sub> (moles) x10 <sup>5</sup>	8/13/92 CO <sub>2,i</sub> (%)	8/19/92 CO <sub>2,f</sub> (%)	CO <sub>2</sub> <sup>(a)</sup> (moles) x10 <sup>5</sup>	CO <sub>2</sub> <sup>(b)</sup> (moles) x10 <sup>5</sup>	CO <sub>2</sub> <sup>(b)</sup> /toluene ratio
can#1	6.3	0.027	5.7	20.6	20.4	5.6	0.032	0.349	10.5	10.6	1.9
can#2	5.7	0.50	4.7	20.3	20.2	2.7	0.026	0.346	10.6	10.7	2.3
can#3	6.4	0.36	5.4	20.3	20.1	5.6	0.021	0.338	10.5	10.6	2.0
can#7	8.0	3.0	4.5	20.3	20.3	-1.0	0.020	0.314	9.67	9.8	2.1
can#8	7.8	3.6	3.8	20.0	19.8	4.9	0.023	0.312	9.53	9.6	2.5
can#9	7.2	1.8	4.9	20.3	20.1	7.9	0.028	0.362	11.1	11.2	2.3
can#11	7.2	0.37	6.2	20.3	20.4	-2.0	0.063	0.405	11.3	11.4	1.9
can#12	6.1	1.4	4.2	20.5	20.4	2.9	0.022	0.319	9.81	9.9	2.3
can#13	6.4	1.8	4.1	20.6	20.6	-0.55	0.022	0.311	9.57	9.7	2.3
										average	2.2
										standard deviation	0.21

*Note:* All cans in this experiment are N-limited.

<sup>(a)</sup> CO<sub>2</sub> calculated using Method A.

<sup>(b)</sup> CO<sub>2</sub> calculated using Method B which accounts for HCO<sub>3</sub><sup>-</sup>, and gives slightly higher total CO<sub>2</sub> production than Method A.

*Other information for batch experiment #4*

Each can has approximately	55.0	g of wet sand
The moisture content of sand	0.085	ml H <sub>2</sub> O/g wet sand
The amount of water in each batch	4.69	ml
The weight of dry sand in these batches	50.31	g of dry sand
The volume of solid phase	19.35	ml
The volume of air phase	775.96	ml
The concentration of NH <sub>4</sub> NO <sub>3</sub> solution	0.0222	mgN/ml
The amount of N added by the solution	0.104	mg-N
The available N in the original sand	0.069	mg-N
The total N in the can is	0.173	mg-N
	1.24E-05	gmole NO <sub>3</sub>
	6.18E-06	gmole NH <sub>4</sub> NO <sub>3</sub>

**Table C.4. Nitrogen Assimilation and Mineralization.**

	Can #	C (mole-atom)		mineralization (%)	assimilation (%)
		$C_{\text{tol}}$ $\times 10^5$	$C_{\text{CO}_2}$ $\times 10^5$		
Batch Expt. #5 (10/5/92)	4	19.2	6.96	36	64
	5	16.2	6.53	40	60
	7	21.1	7.02	33	67
	14	18.8	8.07	43	57
average					62
Batch Expt. #6 (10.6.92)	1	4.48	1.72	38	62
	2	3.84	1.34	35	65
	3	5.21	3.63	70	30
	6	15.6	5.31	34	66
	11	9.04	2.66	29	71
	12	7.65	2.92	38	62
	13	8.33	3.11	37	63
	16	16.8	5.45	32	68
	"c"	14.7	5.19	35	65
average					61

## C.2 Estimation of stoichiometric coefficients (mol/mol) of $\text{NH}_4\text{NO}_3$ :toluene

**Table C.5 Batch Experiment #4 (8/12/92)<sup>a</sup>**

Can#	$\Delta G_{\text{tol}}$ mg/L	Toluene $\times 10^5$ mol	$\text{NH}_4\text{NO}_3$ : toluene	$\Delta C$ mg	C:N g/g	Toluene:N (mg/mg)
1	4.7	4.3	0.14	3.6	20.8	22.8
11	5.9	5.3	0.12	4.4	25.8	28.3
12	3.8	3.4	0.18	2.9	16.5	18.1
13	3.9	3.5	0.17	2.9	17.0	18.6
2	4.1	3.7	0.17	3.1	18.0	19.7
3	5.1	4.6	0.14	3.8	22.2	24.3
7	4.3	3.9	0.16	3.2	18.6	20.4
8	3.4	3.1	0.20	2.6	15.1	16.5
9	4.5	4.1	0.15	3.4	19.8	21.6
Average			0.16		19.3	21.2

<sup>a</sup>Calculations made by using batches that had become N-limited.  $\Delta G_{\text{tol}}$  is the difference between the toluene concentration at which biodegradation ceased due to N limitation and the initial concentration.

**Table C.6 Batch Experiment #5 (10/5/92)<sup>b</sup>**

Can#	$\Delta G_{\text{tol}}$ mg/L	Toluene $\times 10^5$ mol	$\text{NH}_4\text{NO}_3$ : toluene	$\Delta C$ mg	C:N g/g	Toluene:N (mg/mg)
8	4.3	3.9	0.16	3.3	18.2	19.9
9	4.5	4.1	0.16	3.4	18.8	20.6
10	5.1	4.6	0.14	3.8	21.3	23.3
15	4.2	3.8	0.17	3.1	17.6	19.3
Average			0.16		19.0	20.8

<sup>b</sup>Only batches with initial concentrations greater than 4.0 mg/L were used in these calculations. Batches with lower initial concentrations did not consume all the bioavailable N after first amendment of toluene.

This part of appendix-C contains selected experimental data from biodegradation experiments discussed in Chapter 3. The values given here are time series of headspace toluene concentrations measured in those batches used in the kinetic parameter determination, and later used in the respire experiments. The reported times are relative to the start of each experiment.

## C.3 Respike experiment I

## Canister #14

Sampling Date	Time (hour)	Toluene (mg/L)	Remark
10/05/92	02:22 pm	0	(a)
10/06/92	12:52 pm	22.50	2.96
10/07/92	11:10 pm	56.80	3.03
10/08/92	07:17 am	64.92	2.99
10/08/92	02:48 pm	72.43	2.84
10/08/92	09:30 pm	79.13	2.64
10/08/92	10:19 pm	79.95	2.60
10/09/92	07:11 am	88.82	1.83 *
10/09/92	03:06 pm	96.73	0.28 *
10/09/92	11:31 pm	105.15	0.17
10/10/92	11:04 pm	128.70	0.12
10/14/92	09:37 am	211.25	(a)
10/14/92	03:18 pm	216.93	3.03
10/14/92	06:10 pm	219.80	3.13
10/14/92	10:24 pm	224.03	3.12
10/15/92	10:35 am	236.22	2.91
10/15/92	01:08 pm	238.77	2.88
10/15/92	06:06 pm	243.73	2.88
10/16/92	10:38 am	260.27	2.76
10/16/92	05:13 pm	266.85	2.73
10/19/92	12:21 pm	333.98	2.35 *
10/20/92	11:21 am	356.98	2.33 *
10/21/92	11:11 am	380.82	2.21
10/22/92	07:31 am	401.15	2.15
10/22/92	07:58 am	401.60	(b)
10/22/92	08:43 am	402.35	2.20
10/22/92	09:58 am	403.60	2.12
10/22/92	11:38 am	405.27	2.14
10/22/92	01:38 pm	407.27	2.19
10/22/92	04:41 pm	410.32	2.12
10/23/92	07:14 am	424.87	2.17
10/23/92	09:50 am	427.47	2.07
10/23/92	05:38 pm	435.27	2.09
10/26/92	04:05 pm	505.72	1.94

<sup>(a)</sup>Addition of liquid toluene; <sup>(b)</sup>Addition of 0.5 ml of NaCl solution;

<sup>(c)</sup>Addition of 0.5 ml of NaNO<sub>3</sub> solution; \* used for calculating M<sub>r</sub>.

## Canister #4

Sampling Date	Time (hour)	Toluene (mg/L)	Remark
10/05/92	01:45 pm	0	(a)
10/06/92	12:30 pm	22.75	
10/07/92	10:59 pm	57.23	
10/08/92	07:48 am	66.05	
10/08/92	02:44 pm	72.98	
10/08/92	09:25 pm	79.67	
10/08/92	10:04 pm	80.32	
10/09/92	06:57 am	89.20	
10/09/92	03:25 pm	97.67	
10/09/92	11:47 pm	106.03	
10/10/92	11:25 pm	129.67	0
10/14/92	09:37 am	211.87	(a)
10/14/92	03:12 pm	217.45	2.74
10/14/92	06:06 pm	220.35	2.86
10/14/92	10:19 pm	224.57	2.80
10/15/92	10:31 am	236.77	2.64
10/15/92	01:04 pm	239.32	2.62
10/15/92	06:02 pm	244.28	2.60
10/16/92	10:31 am	260.77	2.51
10/16/92	05:07 pm	267.37	2.46
10/19/92	12:17 pm	334.53	2.24
10/20/92	11:15 am	357.50	2.19
10/21/92	11:06 am	381.35	2.04
10/22/92	07:26 am	401.68	2.06
10/22/92	07:55 am	402.17	(b)
10/22/92	08:37 am	402.87	2.07
10/22/92	09:53 am	404.13	2.01
10/22/92	11:33 am	405.80	2.04
10/22/92	01:32 pm	407.78	2.08
10/22/92	04:36 pm	410.85	1.98
10/23/92	07:09 am	425.40	2.07
10/23/92	09:45 am	428.00	2.04
10/23/92	05:33 pm	435.80	2.02
10/26/92	04:00 pm	506.25	1.87

## Canister #7

Sampling Date	Time (hour)	Toluene (mg/L)	Remark
10/05/92	01:50 pm	0	(a)
10/06/92	12:44 pm	22.90	
10/07/92	11:04 pm	57.23	
10/08/92	07:53 am	66.05	
10/08/92	02:39 pm	72.82	
10/08/92	09:15 pm	79.42	
10/08/92	10:00 pm	80.17	
10/14/92	09:37 am	211.78	(a)
10/14/92	03:06 pm	217.27	
10/14/92	06:01 pm	220.18	
10/14/92	10:14 pm	224.40	
10/15/92	10:26 am	236.60	
10/15/92	01:00 pm	239.17	
10/15/92	05:57 pm	244.12	
10/16/92	10:25 am	260.58	
10/16/92	05:03 pm	267.22	
10/19/92	12:12 pm	334.37	
10/19/92	12:35 pm	334.75	
10/20/92	11:10 am	357.33	
10/21/92	11:01 am	381.18	
10/22/92	07:21 am	401.52	
10/22/92	08:04 am	402.23	(c)
10/22/92	08:54 am	403.07	
10/22/92	10:07 am	404.28	
10/22/92	11:47 am	405.95	
10/22/92	01:49 pm	407.98	
10/22/92	04:50 pm	411.00	
10/23/92	06:59 am	425.15	
10/23/92	07:26 am	425.60	
10/23/92	08:29 am	426.65	
10/23/92	09:00 am	427.17	
10/23/92	09:35 am	427.75	
10/23/92	10:06 am	428.27	

## Canister #8

Sampling Date	Time (hour)	Toluene (mg/L)	Remark
10/05/92	01:55 pm	0	(a)
10/06/92	01:06 pm	23.18	
10/07/92	11:22 pm	57.45	
10/08/92	07:27 am	65.53	
10/08/92	02:58 pm	73.05	
10/08/92	09:40 pm	79.75	
10/08/92	10:14 pm	80.32	
10/09/92	07:07 am	89.20	
10/09/92	03:35 pm	97.67	
10/09/92	11:58 pm	106.05	
10/10/92	11:20 pm	129.42	
10/14/92	09:37 am	211.70	(a)
10/14/92	03:23 pm	217.47	
10/14/92	06:14 pm	220.32	
10/14/92	10:28 pm	224.55	
10/15/92	10:39 am	236.73	
10/15/92	01:13 pm	239.30	
10/15/92	06:11 pm	244.27	
10/16/92	10:44 am	260.82	
10/16/92	05:18 pm	267.38	
10/19/92	12:27 pm	334.53	
10/20/92	11:30 am	357.58	
10/21/92	11:16 am	381.35	
10/22/92	07:36 am	401.68	
10/22/92	08:07 am	402.20	(c)
10/22/92	09:00 am	403.08	
10/22/92	10:11 am	404.27	
10/22/92	11:52 am	405.95	
10/22/92	01:54 pm	407.98	
10/22/92	04:54 pm	410.98	
10/23/92	07:04 am	425.15	
10/23/92	08:18 am	426.38	
10/23/92	08:25 am	426.50	
10/23/92	09:40 am	427.75	
10/23/92	11:45 am	429.83	
10/23/92	01:47 pm	431.87	
10/23/92	03:24 pm	433.48	
10/23/92	05:22 pm	435.45	

## Canister #9

Sampling Date	Time (hour)	Toluene (mg/L)	Remark
10/05/92	02:00 pm	0	(a)
10/06/92	01:14 pm	23.23	
10/07/92	11:27 pm	57.45	
10/08/92	07:32 am	65.53	
10/08/92	03:03 pm	73.05	
10/08/92	09:45 pm	79.75	
10/09/92	07:21 am	89.35	
10/09/92	03:16 pm	97.27	
10/09/92	11:36 pm	105.60	
10/10/92	11:09 pm	129.15	
10/14/92	09:37 am	211.62	(a)
10/14/92	03:28 pm	217.47	
10/14/92	06:19 pm	220.32	
10/14/92	10:32 pm	224.53	
10/15/92	10:45 am	236.75	
10/15/92	01:18 pm	239.30	
10/15/92	06:15 pm	244.25	
10/16/92	10:49 am	260.82	
10/16/92	05:25 pm	267.42	
10/19/92	12:31 pm	334.52	
10/20/92	11:35 am	357.58	
10/21/92	11:21 am	381.35	
10/22/92	07:40 am	401.67	
10/22/92	08:01 am	402.02	(b)
10/22/92	08:48 am	402.80	
10/22/92	10:02 am	404.03	
10/22/92	11:43 am	405.72	
10/22/92	01:43 pm	407.72	
10/22/92	04:45 pm	410.75	
10/23/92	07:18 am	425.30	
10/23/92	09:55 am	427.92	
10/23/92	05:44 pm	435.73	
10/26/92	04:10 pm	506.17	

## C.4 Respike Experiment II

Canister #1			
Sampling Date	Time (hour)	Toluene (mg/L)	Remark
10/08/92	05:03 pm	0	(a)
10/09/92	07:29 am	14.43	
10/09/92	02:38 pm	21.58	
10/09/92	11:14 pm	30.18	
10/10/92	07:23 am	38.33	
10/10/92	01:33 pm	44.50	
10/10/92	07:11 pm	50.13	
10/10/92	10:09 pm	53.10	
10/11/92	12:24 am	55.35	
10/11/92	12:29 am	55.43	
10/11/92	04:07 am	59.07	
10/11/92	08:40 am	63.62	
10/11/92	12:18 pm	67.25	
10/11/92	04:20 pm	71.28	
10/11/92	08:29 pm	75.43	
10/12/92	02:04 am	81.02	
10/12/92	04:02 am	82.98	
10/12/92	06:33 am	85.50	
10/12/92	09:09 am	88.10	
10/12/92	12:01 pm	90.97	
10/19/92	06:10 pm	265.12	(a)
10/20/92	10:58 am	281.92	3.39
10/20/92	01:29 pm	284.43	2.98
10/20/92	01:34 pm	284.52	3.01
10/20/92	03:37 pm	286.57	2.64
10/20/92	05:39 pm	288.60	2.18
10/20/92	08:02 pm	290.98	1.40
10/21/92	09:42 am	304.65	0
10/21/92	10:24 am	305.35	0
10/23/92	01:18 pm	356.25	(a)
10/23/92	05:48 pm	360.75	4.99
10/24/92	11:42 am	378.65	4.51
10/25/92	04:20 pm	407.28	4.04
10/26/92	03:30 pm	430.45	3.75
10/27/92	01:31 pm	452.47	3.46
10/31/92	12:25 pm	547.37	3.09
11/01/92	09:56 pm	580.88	2.93

## Canister #1 (continued)

Sampling Date	Time (hour)	Toluene (mg/L)	Remark
11/01/92	10:40 pm	581.62	(c)
11/01/92	11:04 pm	582.02	2.95
11/02/92	07:15 am	590.20	2.79
11/02/92	09:09 am	592.10	2.64
11/02/92	11:05 am	594.03	2.41
11/02/92	01:02 pm	595.98	2.13
11/02/92	03:11 pm	598.13	1.71
11/02/92	05:23 pm	600.33	1.23
11/02/92	05:51 pm	600.80	1.12
11/02/92	10:09 pm	605.10	0.06
11/02/92	10:39 pm	605.60	0
11/02/92	10:44 pm	605.68	0

## Canister #11

Sampling Date	Time (hour)	Toluene (mg/L)	Remark
10/08/92	05:14 pm	0	(a)
10/09/92	07:44 am	14.50	1.42
10/09/92	02:52 pm	21.63	1.48
10/09/92	10:49 pm	29.58	1.44
10/10/92	07:38 am	38.40	1.39
10/10/92	01:17 pm	44.05	1.39
10/10/92	06:57 pm	49.72	1.40
10/10/92	10:14 pm	53.00	1.38
10/11/92	12:08 am	54.90	1.38
10/11/92	04:20 am	59.10	1.36
10/11/92	08:23 am	63.15	1.35
10/11/92	12:01 pm	66.78	1.33
10/11/92	04:05 pm	70.85	1.34
10/11/92	08:13 pm	74.98	1.28
10/12/92	02:18 am	81.07	1.20
10/12/92	04:15 am	83.02	1.16
10/12/92	06:12 am	84.97	1.12

## Canister #11 (continued)

Sampling Date	Time (hour)	Toluene (mg/L)	Remark
10/12/92	09:22 am	88.13	
10/12/92	12:16 pm	91.03	
10/12/92	02:21 pm	93.12	
10/12/92	05:16 pm	96.03	
10/12/92	08:26 pm	99.20	
10/12/92	11:26 pm	102.20	
10/12/92	11:45 pm	102.52	
10/19/92	05:35 pm	264.35	(a)
10/20/92	10:47 am	281.55	1.14
10/20/92	01:19 pm	284.08	0.64
10/20/92	03:27 pm	286.22	0.39
10/20/92	05:30 pm	288.27	0.23
10/20/92	08:21 pm	291.12	0.09
10/21/92	10:37 am	305.38	0
10/23/92	02:15 pm	357.02	(a)
10/23/92	06:10 pm	360.93	5.04
10/24/92	12:01 pm	378.78	4.71
10/25/92	04:40 pm	407.43	4.34
10/26/92	03:47 pm	430.55	4.14
10/27/92	01:50 pm	452.60	4.02
10/31/92	12:46 pm	547.53	3.64
11/01/92	10:16 pm	581.03	3.51
11/01/92	10:50 pm	581.60	(c)
11/01/92	11:13 pm	581.98	3.49
11/02/92	07:19 am	590.08	3.37
11/02/92	09:19 am	592.08	3.25
11/02/92	11:14 am	594.00	3.07
11/02/92	01:11 pm	595.95	2.86
11/02/92	03:21 pm	598.12	2.54
11/02/92	05:33 pm	600.32	2.16
11/02/92	10:17 pm	605.05	0.98
11/02/92	10:57 pm	605.72	0.76

## Canister #12

Sampling Date	Time (hour)	Toluene (mg/L)	Remark
10/08/92	05:16 pm	0	(a)
10/09/92	07:49 am	14.55	
10/09/92	02:56 pm	21.67	
10/09/92	10:54 pm	29.63	
10/10/92	07:49 am	38.55	
10/10/92	01:22 pm	44.10	
10/10/92	07:01 pm	49.75	
10/10/92	10:18 pm	53.03	
10/11/92	12:12 am	54.93	
10/11/92	04:25 am	59.15	
10/11/92	08:28 am	63.20	
10/11/92	12:06 pm	66.83	
10/11/92	04:10 pm	70.90	
10/11/92	08:17 pm	75.02	
10/12/92	02:23 am	81.12	
10/12/92	04:19 am	83.05	
10/12/92	06:46 am	85.50	
10/12/92	09:27 am	88.18	
10/12/92	12:24 pm	91.13	
10/12/92	02:25 pm	93.15	
10/12/92	05:20 pm	96.07	
10/12/92	08:04 pm	98.80	
10/12/92	11:36 pm	102.33	
10/13/92	02:21 am	105.08	
10/14/92	09:37 am	136.35	(a)
10/14/92	03:02 pm	141.77	
10/14/92	05:55 pm	144.65	
10/14/92	10:10 pm	148.90	
10/15/92	10:21 am	161.08	
10/15/92	12:55 pm	163.65	
10/15/92	05:52 pm	168.60	
10/16/92	10:17 am	185.02	
10/16/92	04:54 pm	191.63	
10/16/92	04:59 pm	191.72	

## Canister #13

Sampling Date	Time (hour)	Toluene (mg/L)	Remark
10/08/92	05:19 pm	0	(a)
10/09/92	08:13 am	14.90	
10/09/92	03:01 pm	21.70	
10/09/92	10:59 pm	29.67	
10/10/92	07:43 am	38.40	
10/10/92	01:27 pm	44.13	
10/10/92	07:06 pm	49.78	
10/10/92	10:23 pm	53.07	
10/11/92	12:17 am	54.97	
10/11/92	04:29 am	59.17	
10/11/92	08:32 am	63.22	
10/11/92	12:10 pm	66.85	
10/11/92	04:15 pm	70.93	
10/11/92	08:22 pm	75.05	
10/12/92	02:28 am	81.15	
10/12/92	04:24 am	83.08	
10/12/92	06:51 am	85.53	
10/12/92	09:31 am	88.20	
10/12/92	12:29 pm	91.17	
10/12/92	02:29 pm	93.17	
10/12/92	05:25 pm	96.10	
10/12/92	08:21 pm	99.03	
10/12/92	11:31 pm	102.20	
10/13/92	02:17 am	104.97	
10/19/92	05:48 pm	264.48	(a)
10/20/92	10:53 am	281.57	
10/20/92	01:24 pm	284.08	
10/20/92	03:32 pm	286.22	
10/20/92	05:35 pm	288.27	
10/20/92	08:26 pm	291.12	
10/21/92	10:42 am	305.38	
10/23/92	02:27 pm	357.13	(a)
10/23/92	06:17 pm	360.97	
10/24/92	12:05 pm	378.77	
10/25/92	04:44 pm	407.42	
10/26/92	03:52 pm	430.55	
10/27/92	01:54 pm	452.58	
10/31/92	12:51 pm	547.53	

## Canister #13 (continued)

Sampling Date	Time (hour)	Toluene (mg/L)	Remark
11/01/92	10:20 pm	581.02	
11/01/92	10:35 pm	581.27	(b)
11/01/92	11:00 pm	581.68	
11/02/92	07:33 am	590.23	
11/02/92	09:34 am	592.25	
11/02/92	11:30 am	594.18	
11/02/92	05:46 pm	600.45	
11/02/92	10:32 pm	605.22	

## Canister #16

Sampling Date	Time (hour)	Toluene (mg/L)	Remark
10/08/92	05:35 pm	0	(a)
10/09/92	08:34 am	14.98	
10/09/92	12:13 pm	18.63	
10/09/92	03:51 pm	22.27	
10/10/92	08:04 am	38.48	
10/10/92	01:59 pm	44.40	
10/10/92	07:36 pm	50.02	
10/11/92	12:43 am	55.13	
10/11/92	08:58 am	63.38	
10/11/92	12:43 pm	67.13	
10/11/92	04:43 pm	71.13	
10/11/92	08:54 pm	75.32	
10/12/92	02:42 am	81.12	
10/12/92	06:26 am	84.85	
10/12/92	09:38 am	88.05	
10/12/92	12:34 pm	90.98	
10/12/92	02:16 pm	92.68	
10/12/92	05:29 pm	95.90	
10/12/92	07:59 pm	98.40	
10/19/92	06:47 pm	265.20	(a)
10/20/92	10:41 am	281.10	

## Canister #16 (continued)

Sampling Date	Time (hour)	Toluene (mg/L)	Remark
10/20/92	01:14 pm	283.65	
10/20/92	03:15 pm	285.67	
10/20/92	05:21 pm	287.77	
10/20/92	08:16 pm	290.68	
10/21/92	10:46 am	305.18	
10/23/92	02:02 pm	356.45	(a)
10/23/92	06:04 pm	360.48	
10/24/92	11:56 am	378.35	
10/25/92	04:35 pm	407.00	
10/26/92	03:43 pm	430.13	
10/27/92	01:46 pm	452.18	
10/31/92	12:41 pm	547.10	
11/01/92	10:12 pm	580.62	
11/01/92	10:30 pm	580.92	(b)
11/01/92	10:55 pm	581.33	
11/02/92	07:29 am	589.90	
11/02/92	09:29 am	591.90	
11/02/92	11:25 am	593.83	
11/02/92	05:42 pm	600.12	
11/02/92	10:27 pm	604.87	

## Canister #2

Sampling Date	Time (hour)	Toluene (mg/L)	Remark
10/08/92	05:07 pm	0	(a)
10/09/92	07:34 am	14.45	
10/09/92	02:43 pm	21.60	
10/09/92	11:20 pm	30.22	
10/10/92	07:28 am	38.35	
10/10/92	01:38 pm	44.52	
10/10/92	07:16 pm	50.15	
10/11/92	12:33 am	55.43	
10/11/92	04:11 am	59.07	

## Canister #2 (continued)

Sampling Date	Time (hour)	Toluene (mg/L)	Remark
10/11/92	08:44 am	63.62	
10/11/92	12:24 pm	67.28	
10/11/92	04:24 pm	71.28	
10/11/92	08:35 pm	75.47	
10/12/92	02:09 am	81.03	
10/12/92	04:06 am	82.98	
10/12/92	06:37 am	85.50	
10/12/92	09:13 am	88.10	
10/12/92	12:06 pm	90.98	
10/14/92	09:37 am	136.50	(a)
10/14/92	02:57 pm	141.83	
10/14/92	05:51 pm	144.73	
10/14/92	10:06 pm	148.98	
10/15/92	10:18 am	161.18	
10/19/92	06:20 pm	265.22	(a)
10/20/92	10:23 am	281.27	
10/20/92	01:01 pm	283.90	
10/20/92	03:05 pm	285.97	
10/20/92	05:11 pm	288.07	
10/20/92	07:53 pm	290.77	
10/21/92	10:14 am	305.12	
10/21/92	10:28 am	305.35	

## Canister #3

Sampling Date	Time (hour)	Toluene (mg/L)	Remark
10/08/92	05:10 pm	0	(a)
10/09/92	07:39 am	14.48	
10/09/92	02:48 pm	21.63	
10/09/92	11:26 pm	30.27	
10/10/92	07:33 am	38.38	
10/10/92	01:43 pm	44.55	
10/10/92	07:21 pm	50.18	

## Canister #3 (continued)

Sampling Date	Time (hour)	Toluene (mg/L)	Remark
10/11/92	04:16 am	59.10	
10/11/92	08:48 am	63.63	
10/11/92	12:29 pm	67.32	
10/11/92	04:29 pm	71.32	
10/11/92	08:40 pm	75.50	
10/12/92	02:13 am	81.05	
10/12/92	04:11 am	83.02	
10/12/92	06:42 am	85.53	
10/12/92	09:18 am	88.13	
10/12/92	12:10 pm	91.00	
10/19/92	06:01 pm	264.85	(a)
10/20/92	11:04 am	281.90	
10/20/92	01:38 pm	284.47	
10/20/92	03:42 pm	286.53	
10/20/92	05:44 pm	288.57	
10/20/92	05:48 pm	288.63	
10/20/92	08:07 pm	290.95	
10/21/92	09:47 am	304.62	
10/21/92	10:32 am	305.37	
10/23/92	01:29 pm	356.32	(a)
10/23/92	05:53 pm	360.72	
10/24/92	11:46 am	378.60	
10/25/92	04:25 pm	407.25	
10/26/92	03:34 pm	430.40	
10/27/92	01:35 pm	452.42	
10/31/92	12:31 pm	547.35	
11/01/92	10:01 pm	580.85	
11/01/92	10:25 pm	581.25	(b)
11/01/92	10:51 pm	581.68	
11/02/92	07:24 am	590.23	
11/02/92	07:37 am	590.45	
11/02/92	09:24 am	592.23	
11/02/92	11:19 am	594.15	
11/02/92	05:36 pm	600.45	
11/02/92	10:22 pm	605.20	

## Canister #6

Sampling Date	Time (hour)	Toluene (mg/L)	Remark
10/08/92	05:32 pm	0	(a)
10/09/92	08:29 am	14.95	2.50
10/09/92	12:08 pm	18.60	2.55
10/09/92	03:45 pm	22.22	2.58
10/10/92	07:59 am	38.45	2.48
10/10/92	01:53 pm	44.35	2.50
10/10/92	07:31 pm	49.98	2.48
10/10/92	10:29 pm	52.95	2.44
10/11/92	12:38 am	55.10	2.45
10/11/92	04:38 am	59.10	2.43
10/11/92	12:38 pm	67.10	2.40
10/11/92	04:39 pm	71.12	2.43
10/11/92	08:49 pm	75.28	2.34
10/12/92	02:37 am	81.08	2.25
10/12/92	06:21 am	84.82	2.10
10/12/92	10:02 am	88.50	1.92
10/12/92	12:42 pm	91.17	1.74
10/12/92	02:38 pm	93.10	1.59
10/12/92	05:39 pm	96.12	1.29
10/12/92	08:13 pm	98.68	0.95
10/12/92	11:14 pm	101.70	0.45
10/12/92	11:19 pm	101.78	0.44
10/13/92	02:12 am	104.67	0.05
10/19/92	06:39 pm	265.12	(a)
10/20/92	10:34 am	281.03	1.17
10/20/92	01:10 pm	283.63	1.04
10/20/92	03:21 pm	285.83	0.99
10/20/92	05:25 pm	287.88	0.92
10/20/92	08:31 pm	290.98	0.83
10/21/92	10:00 am	304.47	0.49
10/21/92	11:25 am	305.88	0.46

## Canister "c"

Sampling Date	Time (hour)	Toluene (mg/L)	Remark
10/08/92	05:28 pm	0	(a)
10/09/92	08:23 am	14.92	2.35
10/09/92	12:03 pm	18.58	2.40
10/09/92	03:40 pm	22.20	2.45
10/10/92	07:54 am	38.43	2.33
10/10/92	01:48 pm	44.33	2.36
10/10/92	07:26 pm	49.97	2.36
10/10/92	10:35 pm	53.12	2.34
10/11/92	12:47 am	55.32	2.33
10/11/92	04:34 am	59.10	2.32
10/11/92	08:53 am	63.42	2.31
10/11/92	12:34 pm	67.10	2.28
10/11/92	04:34 pm	71.10	2.30
10/11/92	08:45 pm	75.28	2.22
10/12/92	02:32 am	81.07	2.12
10/12/92	06:17 am	84.82	2.00
10/12/92	09:58 am	88.50	1.81
10/12/92	12:38 pm	91.17	1.59
10/12/92	02:34 pm	93.10	1.44
10/12/92	05:33 pm	96.08	1.14
10/12/92	08:09 pm	98.68	0.79
10/12/92	11:09 pm	101.68	0.33
10/13/92	02:07 am	104.65	0.03
10/19/92	06:28 pm	265.00	(a)
10/20/92	10:29 am	281.02	0.61
10/20/92	01:05 pm	283.62	0.43
10/20/92	03:10 pm	285.70	0.34
10/20/92	05:16 pm	287.80	0.26
10/20/92	07:57 pm	290.48	0.18
10/21/92	10:51 am	305.38	0
10/23/92	01:43 pm	356.25	(a)
10/23/92	05:59 pm	360.52	4.87
10/24/92	11:51 am	378.38	4.50
10/25/92	04:31 pm	407.05	4.16
10/26/92	03:38 pm	430.17	3.93
10/27/92	01:41 pm	452.22	3.78
10/31/92	12:36 pm	547.13	3.39
11/01/92	10:05 pm	580.62	3.29

## Canister "c" (continued)

Sampling Date	Time (hour)	Toluene (mg/L)	Remark
11/01/92	10:45 pm	581.28	(c)
11/01/92	11:09 pm	581.68	3.27
11/02/92	07:11 am	589.72	3.15
11/02/92	09:14 am	591.77	3.01
11/02/92	11:09 am	593.68	2.82
11/02/92	01:06 pm	595.65	2.58
11/02/92	03:16 pm	597.80	2.17
11/02/92	05:27 pm	599.98	1.69
11/02/92	10:13 pm	604.75	0.22
11/02/92	10:48 pm	605.33	0.08
11/02/92	10:53 pm	605.42	0.06

## **APPENDIX D**

### **NUMERICAL SOLUTIONS TO 1-D TRANSPORT EQUATIONS**

This appendix contains the development of numerical solutions to 1-D transport equations of a volatile hydrocarbon,  $O_2$ , and  $CO_2$ . These compounds move in a multi-phase system under influences of liquid- and air-phase diffusion, air/water partitioning, linear sorption, and growth-related biodegradation. The equations were solved through the Galerkin finite-element method. Since the transport/biodegradation equations of all three compounds were solved in an analogous manner, only the discrete formulation of hydrocarbon equation will be presented.

### Numerical Solutions for Transport/Degradation Equations

In a homogeneous hydrogeologic medium, the transport equation of a hydrocarbon compound may be simplified to

$$a_k \frac{\partial G_k}{\partial t} - b_k \frac{\partial^2 G_k}{\partial z^2} = -\theta_w \mu_{\max} X \quad (\text{D-1})$$

$$\begin{aligned} a_k &= \theta_a + \theta_w H_{wa} + \rho_b K_d H_{wa} \\ b_k &= D_{ka} + D_{kw} H_{wa} \end{aligned}$$

where  $G$  is the air-phase concentration of hydrocarbons; the subscript  $k$  denotes hydrocarbon compounds;  $\theta_a$  and  $\theta_w$  are the air- and water- volumetric contents, respectively;  $H_{wa}$  is the water-air partitioning coefficient;  $\rho_b$  is the bulk density of the soil;  $K_d$  is the distribution coefficient between soil and water phases;  $D_{ka}$  and  $D_{kw}$  are the effective diffusion coefficients in air and water phases, respectively;  $\mu_{\max}$  is the maximum specific growth rate;  $X$  is the aqueous-phase concentration of the contaminant compound required in producing a population of density  $B$ ;  $t$  is time and  $z$  is the domain axis. Equation (D-1) is solved using a Galerkin finite-element method in conjunction with the following boundary conditions.

$$G_k = G_k^0 \quad ; (z=0) \quad (\text{D-2})$$

and

$$G_k = 0 \quad ; (z=L) \quad (\text{D-3})$$

A quadratic basis function is employed throughout the whole domain. For any element, the air-phase concentration at any point within an element was approximated in terms of nodal concentrations of that element by

$$G \approx \hat{G} = \sum_{i=1}^3 G_i \phi_i(z) \quad (\text{D-4})$$

where  $\hat{G}$  is the approximated solution;  $G_i$  are the nodal concentrations of the element;  $\phi_i$  are basis functions defined over the element. A weak formulation of weighted residual statement is written for equation (D-1) over the entire domain

$$W = \sum_{e=1}^n W^e + \langle (0-\hat{G}), w \rangle_L + \langle (G^0-\hat{G}), w \rangle_0 \quad (D-5)$$

where  $W^e$  is the weighted residual statement over each element and the boundary conditions were essentially enforced.  $W^e$  can be written as follows

$$W^e = \int_e w^T \frac{\partial \hat{G}}{\partial t} dz - \frac{b}{a} \left[ w^T \frac{\partial \hat{G}}{\partial z} \right]_0^L + \frac{b}{a} \int_e \frac{\partial w^T}{\partial z} \frac{\partial \hat{G}}{\partial z} dz - \frac{\theta_w}{a} \int_e w^T \mu dz \quad (D-6)$$

where  $\mu = \mu_{\max} X$ . In Galerkin method, the same basis functions are used as weighting functions. Therefore, by substituting equation (D-4) into equation (D-3), and assembling the elements over the domain length (L), the hydrocarbon transport equation becomes

$$\frac{\partial G}{\partial t} \int_e \phi^T \phi dz + \frac{b}{a} G \int_e \frac{\partial \phi^T}{\partial z} \frac{\partial \phi}{\partial z} dz + \frac{\theta_w}{a} \int_e \phi^T \mu dz = 0 \quad (D-7)$$

The time-derivative term is solved by using a variably weighted finite difference approximation, and equation (D-7) can be written in the matrix form as

$$\begin{aligned} [GPP] \left[ \frac{\{G(t)\}^n - \{G(t)\}^{n-1}}{\Delta t} \right] + \alpha \left[ \frac{b}{a} \{G(t)\}^n [GDD] + \frac{\theta_w}{a} [GX]^n \right] \\ + (1-\alpha) \left[ \frac{b}{a} \{G(t)\}^{n-1} [GDD] + \frac{\theta_w}{a} [GX]^{n-1} \right] = 0 \end{aligned} \quad (D-8)$$

where  $\alpha$  is the time weighting term and [GPP], [GDD], and [GX] are defined as follows.

$$\begin{aligned} [GPP] &= \int \phi(z)^T \phi(z) dz \\ [GDD] &= \int \frac{d}{dz} \phi(z)^T \frac{d}{dz} \phi(z) dz \\ [GX] &= \int \phi(z)^T \mu dz \quad ; \quad \mu = \sum_{j=1}^3 \mu_j \phi(z)_j \end{aligned} \quad (D-9)$$

## **APPENDIX E**

### **ONE-DIMENSIONAL NUMERICAL-MODEL CODE**

This appendix contains the Fortran code for the one-dimensional Galerkin finite-element diffusion/biodegradation numerical model discussed in Chapter 4.

```

CCCCCCCCCCCCCCCCCCCCCCCCCCCCCCCCCCCCCCCCCCCCCCCCCCCCCCCCCCCC
CC                                                                    CC
CC                          BIODIFFUSION                             CC
CC                                                                    CC
CC                          A ONE-DIMENSIONAL MULTI-PHASE TRANSIENT  CC
CC                          DIFFUSION/BIODEGRADATION MODEL          CC
CC                          USING GALERKIN FINITE-ELEMENT TECHNIQUE CC
CC                                                                    CC
CC                          by Lianna Sa                             CC
CC                          March 31, 1994                           CC
CC                                                                    CC
CCCCCCCCCCCCCCCCCCCCCCCCCCCCCCCCCCCCCCCCCCCCCCCCCCCCCCCCCCCC
C
C--THIS MODEL IS 1-D TRANSIENT TRANSPORT THROUGH UNSATURATED
C HOMOGENEOUS MEDIUM OF ONE HYDROCARBON COMPOUND UNDER THE
C INFLUENCE OF AIR-WATER PARTITIONING, LINEAR SORPTION, AND
C BIODEGRADATION
C--SOURCE IS TREATED AS A BOUNDARY CONDITION
C--TWO BOUNDARY TYPES:  NEWMAN OR DIRICHLET
C--NO IMMISCIBLE PHASE IS PRESENT INSIDE THE DOMAIN
C
C--BIODEGRADATION KINETICS REFLECT MONOD WITH LOGARITHMIC GROWTH
C  RATE = UmaxX
C  Umax is the maximum maximum growth rate
C  X - population concentration which increases with time at
C      logarithmic rate
C
C--BIODEGRADATION IS LIMITED BY THE AVAILABILITY OF NUTRIENT
C AND SUBSTRATE TOXICITY
C
C--PHYSICAL & MICROBIAL PROPERTIES OF SOIL ARE SPECIFIED BY NODES
C
C--QUADRATIC BASES FUNCTIONS
C  NEN (NUMBER OF NODES PER ELEMENT) = 3
C--LINEAR MAPPING
C  IT CAN HANDLE NON-UNIFORM ELEMENT SIZE BUT THE MIDDLE NODE
C  NEEDS TO BE IN THE MIDDLE OF THE ELEMENT
C  THE NUMBERING OF ELEMENTAL NODES:  1, 2, 3.
C
C--TIME IS DISCRETIZED BY ALPHA METHOD
C
C--ARRAY DIMENSIONS CAN BE DEFINED IN THE INCLUDE FILE
C  'parametr.inc'
C          MNN = MAXIMUM NUMBER OF NODES
C          MNE = MAXIMUM NUMBER OF ELEMENTS

```

```

C*****DEFINE TYPE AND DIMENSION OF*****

      INCLUDE 'parametr.inc'

C--GENERAL INFORMATION

C..a flag letting the program know if it is working on
C  a brand new task or a sequal
      INTEGER FLAG1
C..a flag telling the program to write out special output
C  to be used as the input of a sequal run
      INTEGER FLAG2
C..a flag telling the program to recalculate the concentrations
      INTEGER FLAG3
C..a flag telling the program to make an xmgr file
      INTEGER FLAG4
C..a flag telling the program to make an output file
      INTEGER FLAG5
C..nodal type for HC, oxygen, and co2
      INTEGER ITYPE(MNN,3)
C..initial and boundary flux vectors for hydrocarbons and oxygen
C  for zero-flux and zero-concentration boundary types, flux = 0.

      REAL*8 FLUX(MNN,3), CONSTC(MNN,3)
C..nodal coordinates,
      REAL*8 Z(MNN)
C..nodal concentrations
      REAL*8 CONC(MNN,3)
C..concentrations at previous time step
      REAL*8 LASTC(MNN)
      REAL*8 LASTX(MNN)
C..time
      REAL*8 TIME

C
C--PHYSICOCHEMICAL PROPERTIES

C..phase-equilibrium constants (water-air and soil-air) of n
C  hydrocarbons and oxygen
      REAL*8 EQUIWA(3), EQUISA(3)
C..molecular diffusion coefficients for n hydrocarbons and oxygen

C  in water and air phases
      REAL*8 WDIFF(3), ADIFF(3)
C..volumetric contents of air, water, and porosity
      REAL*8 VOLAIR(MNN), VOLWAT(MNN), POROSITY(MNN)

```

C..bulk density of the medium  
     REAL\*8    DENSITY(MNN)  
 C..dummy variables for calculating effective diffusion  
 coefficients  
 C  in water and air phases of any compounds  
     REAL\*8    WEFFDIFF(MNN), AEFFDIFF(MNN)  
 C..retardation factor of any compound  
     REAL\*8    RETARD(MNN,3)  
 C..diffusion coefficients of n hydrocarbons, O2 and CO2  
     REAL\*8    DCOEFF(MNN,3)

C  
 C--MICROBIAL PARAMETERS

C..the equivalent aqueous concentrations of microorganisms  
 C  expressed in terms of HC concentrations at time t  
     REAL\*8    X(MNN)  
 C..adaptation time for nk hydrocarbon compounds  
     REAL\*8    adaptime  
 C..the critical concentration of X to deplete all the N  
     REAL\*8    Xcrit  
 C..the initial nodal concentration of X  
     REAL\*8    Xo(MNN)  
 C..the quantity of X increment at every time step  
     REAL\*8    DELX(MNN)  
 C..reaction rates of oxygen consumption and CO2 production  
     REAL\*8    PGRATE(MNN,2)  
 C..molecular weights  
     REAL\*8    WEIGHT(3)  
 C..stoichiometric ratios of oxygen/HCs and CO2/HCs  
     REAL\*8    RATIO(2)  
 C..Umax of hydrocarbon compounds (The nature of Umax is  
 C  compound-specific). However, because the nutrient  
 C  limitation, Umax is assigned to an elementary variable,  
 C  Rcoeff, for variation in the reaction rate due to nutrient  
 C  limitation  
     REAL\*8    Umax, Rcoeff(MNN)  
 C..inhibition concentration of nk hydrocarbon compounds  
     REAL\*8    CINHIB  
 C..maintenance energy level  
     REAL\*8    MAINTENA

C  
 C--FINITE ELEMENT PARAMETERS

C..nodes that contains in each element  
     INTEGER    IN(MNE,3), NODE(3)

```

C..guass points for numerical integration, number of time step
    INTEGER  NG, NSTEP
C..number of nodes per element, number of element
    INTEGER  NEN, NE
C..total number of nodes, types of element length
    INTEGER  NN, LENGTH
C..time interval
    REAL*8   DT, alpha
C..jacobian operator for each element
    REAL*8   RJACOB(MNE)
C..dimensions for elemental matrices EBP, EB, and ED
    REAL*8   EBP(3,3), ED(3,3,3), EB(3)
C..dimensions of global matrices for time-derivative term, GBP,
C and the diffusion term, GD,
    REAL*8   GBP(MNN,MNN), GD(MNN,MNN,3)
C..dimension of column vector for zero order term
C it is used by oxygen and CO2
    REAL*8   GB(MNN)
C..dimension of column vector for zero order with interpolation
C it is used by all hydrocarbon components
    REAL*8   GBInew(MNN), GBIOld(MNN)

C
C--INTERPOLATION VARIABLES
C..a flag to turn on the option of USER's acquired nodal
C concentration at user's specified location
    INTEGER  iuser
C..Gauss quadrature points at which the concentrations are
C interpolated for use in calculating massloss
    REAL*8   r(10)
C..nodal concentrations of gas phase in each element
    REAL*8   NODALCON(3)
C..return variables of subroutine INTERPOL to interpolate
C concentrations at distance other than nodes
    REAL*8   INTPC(10)
C..user's specified points in global scale at which
concentrations
C are acquired
    REAL*8   zuser(10)

C
C--COMMENTS & NAMES
    CHARACTER*70 COMMENT
C..names of hydrocarbon compounds, input and output files
    CHARACTER*25 NAME(3), INFILE, OUTFILE
C..names of special input and output files
    CHARACTER*25 INFILE2, OUTFILE2

```

C

C--COMMON STATEMENT

```

COMMON /smatrix0/GBInew,GB
COMMON /smatrix/EBP,RETARD,X,VOLWAT,RJACOB,IN,NODE
COMMON /sprint/FLAG4,FLAG5,NAME
COMMON /ssolver/GD,GBP,GBIold,DT,alpha,ML,MU,NN
COMMON IDO2,IDCO2

```

C

C\*\*\*\*\* READ FILE NAMES AND OPEN FILES: \*\*\*\*\*

```

WRITE (*,5000)
5000 FORMAT (' ', 'NAME OF DATA INPUT FILE:')
READ (*,1) INFILE
WRITE (*,5010)
5010 FORMAT (' ', 'NAME OF OUTPUT FILE:')
READ (*,1) OUTFILE

```

```

OPEN (15,FILE=INFILE)
OPEN (16,FILE=OUTFILE)

```

C\*\*\*\*\* open xmgr files \*\*\*\*\*

```

open (17,file='lian.grf')
open (84, file='neg')

```

C\*\*\*\*\* write header for graph file \*\*\*\*\*

```

WRITE(17,701) '@with g0'
WRITE(17,701) '@view 0.10, 0.15, 0.35, 0.85'
WRITE(17,701) '@world 0, -160, 20, 0'
WRITE(17,701) '@yaxis tick major 20.'
WRITE(17,701) '@yaxis LABEL "Elevation relative to land
& surf. (cm) "'
WRITE(17,701) '@xaxis LABEL "Toluene (mg/L) "'
WRITE(17,701) '@xaxis tick major 10'
WRITE(17,701) '@yaxis tick minor 10.'
WRITE(17,701) '@xaxis tick minor 5'
WRITE(17,701) '@xaxis ticklabel prec 0'
WRITE(17,701) '@with g1'
WRITE(17,701) '@g1 on'
WRITE(17,701) '@view 0.40, 0.15, 0.65, 0.85'
WRITE(17,701) '@world 0, -160, 10, 0'
WRITE(17,701) '@yaxis tick major off'
WRITE(17,701) '@xaxis tick major 2.'
WRITE(17,701) '@xaxis LABEL "CO2 concentration (%) "'
WRITE(17,701) '@yaxis tick minor off'
WRITE(17,701) '@yaxis ticklabel off'
WRITE(17,701) '@xaxis ticklabel prec 0'

```

```

WRITE(17,701) '@xaxis tick minor 1.'
WRITE(17,701) '@with g2'
WRITE(17,701) '@g2 on'
WRITE(17,701) '@view 0.70, 0.15, 0.95, 0.85'
WRITE(17,701) '@world 0, -160, 50, 0'
WRITE(17,701) '@yaxis tick major off'
WRITE(17,701) '@yaxis ticklabel off'
WRITE(17,701) '@xaxis tick major 10'
WRITE(17,701) '@xaxis LABEL "Reaction (mg/L/step) "'
WRITE(17,701) '@yaxis tick minor off'
WRITE(17,701) '@xaxis ticklabel prec 0'
WRITE(17,701) '@xaxis tick minor 10'
WRITE(17,701) '@focus off'
WRITE(17,701) '@doublebuffer true'
WRITE(17,701) '@kill S0'
WRITE(17,701) '@redraw'
701  FORMAT(A)
WRITE(17,701) '@with g0'
WRITE(17,701) '@kill s0'
WRITE(17,701) '@s0 symbol 0'
WRITE(17,701) '@s0 linestyle 1'

C***** READ/WRITE DATA INPUT *****
C--FINITE-ELEMENT PARAMETERS
C..comment
   READ(15,1) COMMENT
   WRITE(16,1) COMMENT

C..system temperature
   READ(15,*) temp
   WRITE(16,56) temp

C..no. of compounds (maximum 3)
   READ(15,*) NK

C..the order of compounds - HC always the first compound,
C followed by O2 or CO2 or both
C the program needs to know the order of CO2 (your
C choice is 2 or 3 or 0, if CO2 is not included)
   READ(15,*) IDCO2
   READ(15,*) ITIME
   READ(15,*) ISTEP
   READ(15,*) Kmod
   READ(15,*) LASTP
C..compound names
   READ(15,1) (NAME(I), I=1, NK)

```

```

C..# of nodes, elements, and elemental nodes
  READ(15,*) NN,NE
  NEN = 3
  WRITE(16,3) NN,NE,NEN

C..element length (1=equal / any other no. = unequal)
  READ(15,*) LENGTH
  if (length .eq. 1) then
    WRITE(16,52)
52 FORMAT(' EQUAL ELEMENT LENGTH IS BEING USED'//)
  else
    WRITE(16,36)
36 FORMAT(' NONUNIFORM ELEMENT LENGTH IS BEING USED'//)
  endif

C..nodes, nodal coordinates, nodal types for all hydrocarbons
C and oxygen
  READ(15,*) (Z(I), (ITYPE(I,K),K=1,NK),
1          (FLUX(I,K),K=1,NK),I=1,NN)
  WRITE(16,4)
  WRITE(16,34) (NAME(I),I=1,NK), (NAME(I),I=1,NK)

  if (NK .eq. 2) then
    WRITE(16,7) (I,Z(I), (ITYPE(I,K),K=1,NK), (FLUX(I,K),K=1,NK),
1          I=1,NN)
7  FORMAT (' ',I3,3x,f10.3,5x,I5,9x,I5,10x,f5.2,10x,f5.2)
  else
    WRITE(16,20) (I, Z(I), (ITYPE(I,K),K=1,NK),
1          (FLUX(I,K),K=1,NK),I=1,NN)
20 FORMAT (' ',I3,3x,f10.3,5x,I5,9x,I5,9x,I5,12x,f5.2,9x,
1          f5.2,9x,f5.2)
  endif

C..# of time steps, time increment
  READ (15,*) NSTEP,DT,alpha
  WRITE(16,8) NSTEP,DT,alpha

C..# of Gauss points
  READ(15,*) NG
  WRITE(16,9) NG

C..table of elemental data
  READ(15,*) ((IN(I,J),J=1,NEN),I=1,NE)
  WRITE(16,10)
  WRITE(16,11) (I, (IN(I,J),J=1,NEN),I=1,NE)

```

C..# of diagonals below and above the main diagonals, ML, and MU.

```

      READ(15,*) ML,MU
      WRITE(16,12) ML,MU

```

C..a flag to request a print out of the coefficients of global  
C matrices (1=Yes / any other no.=No)

```

      READ (15,*) MATRIX

```

C

C--PHYSICOCHEMICAL PROPERTIES OF HYDROCARBON COMPONENT AND OXYGEN

C..molecular weights

```

      READ(15,*) (WEIGHT(I),I=1,NK)

```

C..stoichiometric ratios of oxygen/HCs and CO2/HCs

```

      READ(15,*) (RATIO(I),I=1,NK-1)

```

C..phase-equilibrium constants: water-air and soil-air phases

```

      READ(15,*) (EQUIWA(I),EQUISA(I),I=1,NK)

```

C..molecular diffusion coefficients in water and air phases

```

      READ(15,*) (WDIFF(I),ADIFF(I),I=1,NK)

```

```

      WRITE(16,80)

```

```

      WRITE(16,18) (NAME(I), EQUIWA(I), EQUISA(I),
&                WDIFF(I),ADIFF(I),I=1,NK)

```

C

C--MICROBIAL CONSTANTS FOR NK HYDROCARBON COMPONENTS

C..max specific growth rates

```

      READ(15,*) Umax

```

C..inhibition concentrations of nk hydrocarbon compounds

```

      READ(15,*) CINHIB

```

C..maintenance energy level

```

      READ(15,*) maintena

```

C..the reasonable magnitude of zero

```

      READ(15,*) zero

```

C the concentration of X that will deplete N-nutrient

C the lag time for the hydrocarbon compound

```

      READ(15,*) Xcrit, adaptime

```

```

      WRITE(16,14)

```

```

      WRITE(16,41) NAME(1),WEIGHT(1)

```

```

      WRITE(16,41) (NAME(I),WEIGHT(I),RATIO(I-1),I=2,NK)

```

```

      WRITE(16,50) Umax, adaptime, CINHIB, maintena

```

C--SOIL PARAMETERS (VARY WITH ELEMENT)  
 C..volumetric contents for air and water phases, bulk density,  
 C and total porosity

```

      READ(15,*) (VOLAIR(I),DENSITY(I),POROSITY(I),I=1,NN)
      DO 48 I = 1, NN
      VOLWAT(I) = POROSITY(I) - VOLAIR(I)
48 CONTINUE
      WRITE(16,13)
      WRITE(16,47) (I,VOLAIR(I),DENSITY(I),POROSITY(I),I=1,NN)

```

C  
 C--BOUNDARY AND CONSTANT NODAL CONCENTRATIONS  
 C..for all compounds

```

      READ(15,*) ((CONSTC(J,I),J=1,NN),I=1,NK)

```

C  
 C--INITIAL NODAL CONCENTRATIONS for HC, oxygen and CO2

C read in the flag telling the program either it's performing  
 C a one-step simulation (set FLAG1=0) OR a step-task of a  
 C multi-step simulation (set FLAG=any number)

```

      READ(15,*) FLAG1

      if (FLAG1 .eq. 0) then
      READ(15,*) tinit
      READ(15,*) ((CONC(J,I),J=1,NN),I=1,NK)
      else
      READ (15,1) infile2
      OPEN (99,file=infile2)
      READ (99,*) tinit
      do 70 i = 1, nk
      READ(99,*) (CONC(J,I),J=1,NN)
70 continue
      endif

```

C read in the flag telling the program to print xmgr files  
 C 1=yes, any number = no

```

      READ(15,*) FLAG4

```

C read in a flag telling the program to print output files  
 C 1=yes, any other number = no

```

      READ(15,*) FLAG5

```

```

C   for microorganisms
      READ(15,*) (Xo(I),I=1,NN)

      WRITE(16,45)
      CALL PRINT (CONC,MNN,3,Z,X,Xo,DELX,time,NN,NK)

C
C--unit conversion for O2 and CO2

      DO 58 I = 2, NK
      CALL UNITS (CONSTC(1,I),WEIGHT(I),temp,nn)
      CALL UNITS (CONC(1,I),WEIGHT(I),temp,nn)
58  CONTINUE

C
C***** DETERMINATIONS OF MODEL PARAMETERS *****
C
C--CALCULATE DIFFERENTIAL-EQUATION COEFFICIENTS
C  water- and air-phase effective diffusion coefficients, and
C  retardation factors

      DO 19 I = 1, NK
      DO 46 J = 1, NN
      WEFDDIFF(J) = WDIFF(I)*VOLWAT(J)**(10./3.)/POROSITY(J)**2
      AEFDDIFF(J) = ADIFF(I)*VOLAIR(J)**(10./3.)/POROSITY(J)**2
C..retardation factors for nk hydrocarbon compounds and oxygen
      RETARD(J,I) = VOLAIR(J) + EQUIWA(I)*VOLWAT(J) + EQUISA(I)*
      &              DENSITY(J)
C..coefficients of the diffusion term for hydrocarbons and oxygen
      DCOEFF(J,I) = (WEFDDIFF(J)*EQUIWA(I) +
      AEFDDIFF(J))/RETARD(J,I)
      46  CONTINUE
C..print water- and air- phase effective diffusion coefficients,
C  diffusion coefficient, and retardation factor
      WRITE(16,1) NAME(I)
      WRITE(16,40)
      WRITE(16,42) (J,WEFDDIFF(J),AEFDDIFF(J),DCOEFF(J,I),
      &              RETARD(J,I),J=1,NN)
      19  CONTINUE

C
C***** DEFINE ELEMENTAL MATRIX *****
C..the elemental matrix for each element is the same because
C  linear transformation has a jacobian operator that

```

C is a constant (not depend on the coordinates of the element).  
 C--COMPUTE ELEMENTAL MATRICES: EB(NEN),EBP(NENxNEN),ED(NENxNENx3)

```
CALL BASESPRO (NG,EBP)
CALL DBDZ (NG,ED)
```

C--COMPUTE JACOBIAN OPERATOR OF EACH ELEMENT FOR EBP, EB, AND ED  
 C..IJM are nodes containing in each element

```
DO 22 I = 1, NE
DO 23 J = 1, NEN
  IJM = IN(I,J)
  IF (J .EQ. 1) Z1 = Z(IJM)
  IF (J .EQ. 3) Z2 = Z(IJM)
23 CONTINUE
  RJACOB(I) = 0.5 * (Z2 - Z1)
```

C..check elemental length! if uniform length is used, then skip  
 C the rest of the DO loop

```
  IF (LENGTH .EQ. 1) GO TO 24
22 CONTINUE
  GO TO 26
24 DO 25 J = 1, NE
  RJACOB(J) = RJACOB(1)
25 CONTINUE
```

C..PRINT OUT JACOBIAN OPERATOR FOR EACH ELEMENT

```
26 WRITE(16,101)
  WRITE(16,102) (J,RJACOB(J),J=1,NE)
```

C--INITIALIZE GLOBAL MATRIX COEFFICIENTS:

C GBP(NNxNN),GD(NNxNN),GB(NN)

```
DO 882 K = 1, NK
DO 880 I = 1, NN
DO 490 J = 1, NN
  GBP(I,J) = 0.
  GD(I,J,K) = 0.
490 CONTINUE
880 CONTINUE
882 CONTINUE
```

C--ASSEMBLY ELEMENTAL MATRIX ONTO GLOBAL MATRIX  
 C..GBP(NN×NN) and GD(NN×NN)

```

DO 310 L= 1, NE

DO 320 I = 1, 3
  NODE(I) = IN(L,I)
320 CONTINUE

```

```

  II = NODE(1)
  JJ = NODE(2)
  MM = NODE(3)

```

```

DO 329 K = 1, 3

```

```

  NR = NODE(K)

```

C..GBP(NN,NN)

C the matrix coefficient of the rate accumulation term

```

  GBP(NR,II) = GBP(NR,II) + EBP(K,1)*RJACOB(L)
  GBP(NR,JJ) = GBP(NR,JJ) + EBP(K,2)*RJACOB(L)
  GBP(NR,MM) = GBP(NR,MM) + EBP(K,3)*RJACOB(L)

```

C..GD(NN,NN,NK+1)

C the matrix coefficient of the diffusion term

```

DO 328 J = 1, NK
  GD(NR,II,J) = GD(NR,II,J) + 1./RJACOB(L)*(DCOEFF(II,J)*
& ED(1,1,K)+DCOEFF(JJ,J)*ED(1,2,K)+DCOEFF(MM,J)*ED(1,3,K))
  GD(NR,JJ,J) = GD(NR,JJ,J) + 1./RJACOB(L)*(DCOEFF(II,J)*
& ED(2,1,K)+DCOEFF(JJ,J)*ED(2,2,K)+DCOEFF(MM,J)*ED(2,3,K))
  GD(NR,MM,J) = GD(NR,MM,J) + 1./RJACOB(L)*(DCOEFF(II,J)*
& ED(3,1,K)+DCOEFF(JJ,J)*ED(3,2,K)+DCOEFF(MM,J)*ED(3,3,K))
328 CONTINUE

```

```

329 CONTINUE

```

```

310 CONTINUE

```

C

C..PRINT OUT THE GLOBAL MATRIX COEFFICIENTS

```

  IF (MATRIX .EQ. 1) THEN
    WRITE(16,27)
    WRITE(16,28) ((GBP(I,J),J=1,11),I=1,11)
    DO 32 K = 1, NK
      WRITE(16,1) NAME(K)
      WRITE(16,29)
      WRITE(16,30) ((GD(I,J,K),J=1,11),I=1,11)
    32 CONTINUE

```

```
        ELSE
        WRITE(16,122)
        ENDIF

C
C--TIME DISCRETIZATION

C..initialize arrays
C  array Rcoeff(MNN)
C  array GBInew(MNN)
C  array X(MNN)
C  array LASTX(MNN)

C  read the starting time of the run

        if (FLAG1 .eq. 0) then
            DO 38 I = 1, NN
                Rcoeff(I) = 0.
                GBInew(I) = 0.
                LASTX(I) = 0.
38          CONTINUE
            else
                DO 69 I = 1, NN
                    Rcoeff(I) = 0.
69          CONTINUE
                READ (99,*) (GBInew(I),I=1,NN)
                READ (99,*) (X(I),I=1,NN)
                CLOSE (UNIT=99)
            endif

C  initialize FLAG3
        FLAG3 = 0

C..identify the order of OXYGEN

        IF (IDCO2 .eq. 2) THEN
            IDO2 = 3
        ELSE
            IDO2 = 2
        ENDIF
        write(*,*) IDO2,IDCO2

C--STEPPING THROUGH TIME

        TIME = tinit
```

```
DO 350 K = 1, NSTEP

TIME = DT*K + tinit

C
C--HYDROCARBON COMPOUND

C..update reaction matrix coefficient at last time step for HC
C equation

DO 51 I = 1, NN
  GBIold(I) = GBInew(I)
51 CONTINUE

C..biodegradation is zero prior to some lag time
C the if condition was set as .lt. over .le. because .lt. works
C in the case of no adaptation time

IF (time .lt. adapttime) THEN

DO 43 J = 1, NN
  Rcoeff(J) = 0.
  X(J) = Xo(J)
43 CONTINUE

C call subroutine RXNMATRX to assemble the reaction matrices
C for hydrocarbon equation

CALL RXNMATRX (Rcoeff,1,nn,ne,2)

C call subroutine SOLVER to solve hydrocarbon equation

CALL SOLVER (ITYPE,FLUX,CONSTC,CONC,1)

GO TO 39

ENDIF

C initialize X for simulations w/o any adaptation

IF (tinit .eq. 0. .and. K .eq. 1) THEN
  DO 82 J = 1, NN
    X(J) = Xo(J)
82 CONTINUE
ENDIF
```

```

C  store X and CONC(J,1) from last time step

      DO 83 J = 1, NN
          LASTC(J) = CONC(J,1)
          LASTX(J) = X(J)
83  CONTINUE

C
C..initiate biodegradation
C  update reaction coefficients at each node via all kinds
C  of conditions

      DO 53 J = 1, NN

C  1)  biodegradation is zero when HC concentration is in the
C      inhibition range

          IF (CONC(J,1) .ge. CINHIB) THEN
              Rcoeff(J) = 0.
              GO TO 53
          ENDIF

C  2)  biodegradation is at maintenance level when N-nutrients is
C      depleted, i.e., if the accumulation of toluene utilized
C      from last time step exceeds X critical, the reaction
C      ceases for that node

          IF (X(J) .ge. Xcrit) THEN
              Rcoeff(J) = maintena*Umax
              GO TO 53
          ENDIF

C  3)  biodegradation is zero if hydrocarbon concentration is
C      zero or if hydrocarbon concentration is 0. at the boundary
C      or if the dissolved oxygen concentration is below 2 mg/L

          IF (CONC(J,1) .lt. zero
&          .or. ITYPE(J,1) .eq. 1 .and. CONC(J,1) .eq. 0.
&          .or. CONC(J,2) .le. 55.55) THEN
              Rcoeff(J) = 0.
          ELSE
              Rcoeff(J) = Umax
          ENDIF

53  CONTINUE

```

```

C SOLVE the biomass equation at each node analytically

      DO 55 J = 1, NN

      IF (X(J) .ge. Xcrit .or. CONC(J,1) .ge. CINHIB) THEN
        GO TO 55
      ELSE
        X(J) = LASTX(J)*EXP(Rcoeff(J)*dt)
        If (X(J) .ge. Xcrit) X(J) = Xcrit
      ENDIF

55 CONTINUE

C readjust the concentrations to the original concentrations

911 IF (FLAG3 .eq. 1) THEN
      DO 73 J = 1, NN
        CONC(J,1) = LASTC(J)
73 CONTINUE
      ENDIF

C
C call subroutine RXNMATRX to assemble the reaction matrices
C for hydrocarbon equation

      CALL RXNMATRX (Rcoeff,1,nn,ne,2)

C call subroutine SOLVER to solve hydrocarbon equation

      CALL SOLVER (ITYPE,FLUX,CONSTC,CONC,1)

C check if there was enough mass to react

      FLAG3 = 0

      DO 74 J = 1, NN
      IF (X(J) .gt. LASTX(J) .and. Rcoeff(J) .eq. Umax
&          .and. CONC(J,1) .lt. 0.) THEN
        FLAG3 = 1
        Rcoeff(J) = Umax*LASTC(J)/(.003+LASTC(J))
        X(J) = LASTX(J)*EXP(Rcoeff(J)*dt)
        if (X(J) .ge. Xcrit) X(J) = Xcrit
      If (X(J) .lt. LASTX(J)) THEN
        X(J) = LASTX(J)
        Rcoeff(J) = 0.
      Endif

```

```

        GO TO 74
    ENDIF
    IF (Rcoeff(J) .lt. Umax .and. Rcoeff(J) .gt. 0.
    &                                     .and. CONC(J,1) .lt. 0.) THEN
        X(J) = LASTX(J)
        Rcoeff(J) = 0.
        FLAG3 = 1
    ENDIF
74  CONTINUE

    IF (FLAG3 .eq. 1) GO TO 911

C  the quantity of HC being degraded

    DO 81 J = 1, NN
        DELX(J) = X(J)-LASTX(J)
81  CONTINUE

39  DO 75 J = 1, NN
        if (conc(j,1) .lt. 0.) then
            write(84,*) time, z(j), conc(J,1)
        endif
        IF (CONC(J,1) .lt. 0.) CONC(J,1) = 0.
75  CONTINUE

C
C--OXYGEN & CO2

C..calculate consumption rates of O2 and CO2 at each node

    DO 44 I = 2, NK
        DO 49 J = 1, NN
            PGRATE(J,I-1) = VOLWAT(J)/RETARD(J,I)*X(J)*Rcoeff(J)*
    &                                     RATIO(I-1)/weight(1)*weight(I)
49  CONTINUE
44  CONTINUE

    IF (IDCO2 .ne. 0) THEN
        DO 54 i = 1, NN
            PGRATE(i,IDCO2-1) = -PGRATE(i,IDCO2-1)
54  CONTINUE
        ENDIF

    IF (K .eq. nstep .and. NK .eq. 2) THEN
        write (16,'(a)') 'rxnrates for all compounds'

```

```

      write(16,88) (j,Rcoeff(j),(pgrate(j,1)),j=1,nn)
88  format (1x,i5,2e12.5)
      ENDIF
      IF (K .eq. nstep .and. NK .eq. 3) THEN
      write (16,'(a)') 'rxnrates for all compounds'
      write(16,89) (j,Rcoeff(j),(pgrate(j,i),i=1,nk-1),j=1,nn)
89  format (1x,i5,3e12.5)
      ENDIF

```

C..call RXNMATRX to assembly the reaction matrices of oxygen or CO2

C..then call SOLVER to solve for its concentrations

```

      CALL RXNMATRX (PGRATE(1,IDO2-1),IDO2,NN,NE,0)
      CALL SOLVER (ITYPE(1,IDO2),FLUX(1,IDO2),CONSTC(1,IDO2),
&                CONC(1,IDO2),IDO2)

c      DO 77 J = 1, NN
c      if (CONC(j,IDO2) .lt. 0) CONC(j,IDO2) = 0.
c 77 CONTINUE

      if (IDCO2 .ne. 0) then
      CALL RXNMATRX (PGRATE(1,IDCO2-1),IDCO2,NN,NE,0)
      CALL SOLVER (ITYPE(1,IDCO2),FLUX(1,IDCO2),CONSTC(1,IDCO2),
&                CONC(1,IDCO2),IDCO2)
      endif

```

C

C--PRINT OUTPUT at intermediate steps

C..print time and concentrations at each time step OR

```

      IF (ITIME .EQ. 1 .and. lastp .ne. 1) THEN
      GO TO 444

```

C at steps of every ten or multiple of ten

```

      ELSEIF (ISTEP .eq. 1 .and. mod(K,kmod) .eq. 0) THEN
      GO TO 444

```

```

      ELSE

```

C..print output at last time step only

```

      GO TO 350

```

```

ENDIF

444 WRITE(16,37) TIME

C convert the units of permgases back to % using the storage of
C DCOEFF
  DO 57 I = 2, NK
  DO 59 J = 1, NN
    DCOEFF(J,I) = CONC(J,I)/WEIGHT(I)/1.e6*82.05*temp*100.
  59 CONTINUE
  57 CONTINUE

C copy concentration of HC into DCOEFF(J,1)
  DO 60 J = 1, NN
    DCOEFF(J,1) = CONC(J,1)
  60 CONTINUE

  CALL PRINT (DCOEFF,MNN,3,Z,X,Xo,DELX,time,NN,NK)

350 CONTINUE

  if (lastp .eq. 1) then
    WRITE(16,'(a)') 'microbial mass'
    WRITE(16,'(3e12.6)') (X(I),I=1,NN)
    WRITE(16,33)
    WRITE(16,37) TIME
  C convert the units of permgases to %
    DO 62 I = 2, NK
    DO 61 J = 1, NN
      CONC(J,I) = CONC(J,I)/WEIGHT(I)/1.e6*82.05*temp*100.
    61 CONTINUE
    62 CONTINUE
    CALL PRINT (CONC,MNN,3,Z,X,Xo,DELX,time,NN,NK)

  else

    WRITE(16,'(a)') 'NO OUTPUT IS PRINTED'
    GO TO 123

  endif

C--a flag telling program to print out input file to be used
C next in the case of a multi-step simulation
C set FLAG2=1 when creating the special input file

```

```

READ(15,*) FLAG2
IF (FLAG2 .eq. 1) THEN
  read (15,1) outfile2
  open (98,file=outfile2)
  write(98,*) time
  do 71 i = 1, nk
    write(98,*) (CONC(J,I),J=1,NN)
71  continue
    write(98,*) (GBInew(I),I=1,NN)
    write(98,*) (X(I),I=1,NN)
  close (unit=98)
ENDIF

C--CONCENTRATIONS AT USER'S SPECIFIED LOCATIONS

READ (15,*) iuser
IF (iuser .eq. 1) THEN

  read (15,*) nz
  do 65 j = 1, nz
    read(15,*) zuser(j)
65  continue

C  locate the element that x lies in

  do 63 k = 1, nz

    do 64 i = 1, ne
      ii = in(i,1)
      jj = in(i,2)
      kk = in(i,3)
      if (zuser(k) .ge. z(ii) .and. zuser(k) .le. z(kk))then
        nodalcon(1) = conc(II,1)
        nodalcon(2) = conc(JJ,1)
        nodalcon(3) = conc(KK,1)
        go to 66
      endif
64  continue

C  calculate the corresponding local coordinates for X
C
66  write(16,*) zuser(k)
    write(16,*) z(ii),z(jj),z(kk)

    b = 2./(Z(kk)-Z(ii))*zuser(k)
    c = 2.*Z(jj)/(Z(kk)-Z(ii))

```

```

      zuser(k) = b-c

C   only one location is being calculated at each call

      write(16,*) 'r'
      write(16,*) zuser(k)

      call INTPOL (1,zuser(k),nodalcon,intpc(k))

63   continue

      write(16,68)
      do 67 k = 1, nz
      write(16,*) zuser(k),intpc(k)
67   continue

      ENDIF

      CLOSE (UNIT=15)
      CLOSE (UNIT=16)
123  STOP

C
C*****          FORMAT STATEMENTS          *****
C
1   FORMAT (A)
2   FORMAT (' ELEMENT# ',5x,A15,5x,A15)
56  FORMAT (' system temperature (Kelvin) = ',f5.1)
3   FORMAT (1x,'NUMBER OF NODES = ',I5/' NUMBER OF ELEMENTS',
&
&      ' = ',I5/' NUMBER OF NODES PER ELEMENT = ',I5)
4   FORMAT (1x,'NODE',5x,'DISTANCE',15x,'NODAL TYPE FOR',
1     28x,'FLUXES FOR')
34  FORMAT (23x,6A15)
8   FORMAT ('/ NO. OF TIME STEP = ',I10/' TIME INCREMENT =
1     ',f10.0 /' alpha = ',f5.2)
50  FORMAT ('/MAX GROWTH RATE = ',e12.5/'LAG TIME = ',f12.0/
1     'INHIBITORY CONC. = ',e12.5/'MAINTENANCE ENERGY
2     LEVEL = ',f4.3)
9   FORMAT (1x,'NO. OF GUASS POINTS = ',I5)
10  FORMAT (1x,'ELEMENTAL DATA',/5x,' ELEMENT',10x,'INCIDENCE')
11  FORMAT (5x,I4,5x,3I8)
12  FORMAT (' NUMBER OF DIAGONALS BELOW THE MAIN DIAGONAL =
1     ',I5/' NUMBER OF DIAGONALS ABOVE THE MAIN DIAGONAL
2     = ',I5/)

```

```

13  FORMAT (' NODAL NO.',3x,' AIR VOLUMETRIC CONTENT ',5x,
1      ' BULK DENSITY OF MEDIUM ',5x,' TOTAL POROSITY')
47  FORMAT (1x,I7,11x,f8.5,18x,e12.5,15x,f8.5)
80  FORMAT (6x,'COMPOUND',10x,'WATER-AIR EQUIL',3x,'SOIL-AIR
1      EQUIL',3x,'MOL. DIFF COE(L).',3x,'MOL. DIFF COE(G).')
18  FORMAT (1x,A21,3x,e12.5,3x,e12.5,6x,e12.5,8x,e12.5)
14  FORMAT (6x,'COMPOUND',16x,'MOL. WT.',10x,'STOI. RATIO')
41  FORMAT (1x,A21,7x,f8.3,9x,e12.5)
45  FORMAT (/1x,' INITIAL CONCENTRATIONS')
101 FORMAT (/ ' JACOBIAN OPERATOR FOR EACH ELEMENT')
102 FORMAT (1x,I5,10x,f8.5)
27  FORMAT (1x,'GLOBAL COEFFICIENT MATRIX, GBP')
28  FORMAT (1x,11f8.5)
29  FORMAT (1x,'GLOBAL COEFFICIENT MATRIX, GD')
30  FORMAT (1x,11f11.7)
31  FORMAT (1x,'GLOBAL COEFFICIENT MATRIX, GB')
33  FORMAT (/ ' NODAL CONCENTRATIONS')
37  FORMAT (1x,/'TIME = ',f10.0,'s')
40  FORMAT (' NODAL #',5x,' EFF. DIFF. COEFF(L).',5x,
1      ' EFF. DIFF. COEFF(G).',5x,' COMBINED DIFF COEFF.',
2      2x,' RETARDATION FACTOR')
42  FORMAT (1x,i7,4x,e12.5,13x,e12.5,14x,e12.5,14x,e12.5)
122 FORMAT (/ ' NO COEFFICIENT MATRICES WILL BE PRINTED')
68  FORMAT (/ 'CONCENTRATIONS AT LOCATIONS DEFINED BY USER')

```

END

CC

C\*\*\*\*\* SUBROUTINE FOR PRINT \*\*\*\*\*

```

SUBROUTINE PRINT (CONC,NR,NC,Z,X,Xo,DELX,time,NN,NK)
INTEGER          NR,NC,NN,NK,FLAG4,FLAG5
REAL*8          CONC(NR,NC),Z(NR),DELX(NR),time
REAL*8          X(NR),Xo(NR)
CHARACTER*25    NAME(3)
COMMON          /sprint/FLAG4,FLAG5,NAME

```

```

IF (FLAG5 .eq. 1) THEN
  if (NK .eq. 3) then
    WRITE(16,1) (NAME(I),I=1,NK)
1  FORMAT (' DISTANCE          ',3A17,'HC utilized/step')
  else

```

```

WRITE(16,2) (NAME(I),I=1,NK)
2  FORMAT (' DISTANCE          ',2A17,'HC utilized/step')
   endif

   DO 3 J = 1, NN
WRITE(16,17) Z(J), (CONC(J,I),I=1,NK), DELX(J)
3  CONTINUE
17  FORMAT (' ',f8.2,4(5x,e12.5))
   ENDIF

   IF (FLAG4 .eq. 1) THEN
do 8 j=1,nn
write (17,18) conc(j,1),z(j)-z(nn)
18  FORMAT (e12.5,1x,f7.1)
8   continue
1009 FORMAT('&')
WRITE(17,1009)
WRITE(17,701) '@with g1'
WRITE(17,701) '@kill s0'
WRITE(17,701) '@s0 symbol 0'
WRITE(17,701) '@s0 linestyle 1'
701 Format (a)
do 10 j=1,nn
write (17,18) conc(j,3),z(j)-z(nn)
10  continue
WRITE(17,1009)
WRITE(17,701) '@with g2'
WRITE(17,701) '@kill s0'
WRITE(17,701) '@s0 symbol 0'
WRITE(17,701) '@s0 linestyle 1'
do 12 j=1,nn
write (17,18) delx(j),z(j)-z(nn)
12  continue
WRITE(17,1009)
DTIME=time/86400.
WRITE(17,702) DTIME
702 FORMAT('@subtitle "Time: ',F7.3,' days" ')
WRITE(17,701) '@redraw'
WRITE(17,701) '@kill s0'
WRITE(17,701) '@with g0'
WRITE(17,701) '@kill s0'
WRITE(17,701) '@with g2'
WRITE(17,701) '@kill s0'
WRITE(17,701) '@with g0'
   ENDIF

```

```

RETURN
END

```

```

C*****SUBROUTINE TO CONVERT PERMGAS UNITS

```

```

SUBROUTINE UNITS (perm,MW,temp,nn)
INTEGER NN
REAL*8 perm(1)
REAL*8 temp,MW

DO 1 I = 1, NN
perm(I) = perm(I)/100./82.05/temp*1.e6*MW
1 CONTINUE

RETURN
END

```

```

C*****SUBROUTINE FOR GAUSS POINT*****

```

```

SUBROUTINE GAUSS (U,W)
REAL*8 U(3), W(3)

U(1) = .0000000000000000
U(2) = .774596669241483
U(3) = -.774596669241483
W(1) = .8888888888888889
W(2) = .5555555555555556
W(3) = .5555555555555556

RETURN
END

```

```

C--SUBROUTINE TO CALCULATE THE INTEGRAL OF A QUADRATIC BASES
FUNCTION

```

```

SUBROUTINE BASES (N,SUMB)
IMPLICIT REAL*8 (A-H,O-Z)
REAL*8 SUMB(3), RT(3), WGT(3)

CALL GAUSS (RT,WGT)
SUM1 = 0.
SUM2 = 0.
SUM3 = 0.
DO 1 K = 1, N

```

```

PHE1 = WGT(K)*0.5*(RT(K)**2 - RT(K))
PHE2 = (1.- RT(K)**2)*WGT(K)
PHE3 = 0.5*(RT(K)**2 + RT(K))*WGT(K)
SUM1 = SUM1 + PHE1
SUM2 = SUM2 + PHE2
SUM3 = SUM3 + PHE3
1 CONTINUE
SUMB(1) = SUM1
SUMB(2) = SUM2
SUMB(3) = SUM3
RETURN
END

```

C\*\*\*\*\*SUBROUTINE TO CALCULATE THE INTEGRAL OF THE PRODUCT OF  
C TWO QUADRATIC BASES FUNCTIONS

```

SUBROUTINE BASESPRO (N,SUMBB)
IMPLICIT REAL*8 (A-H,O-Z)
REAL*8      SUMBB(3,3), RT(3), WGT(3)

CALL GAUSS (RT, WGT)
SUM11 = 0.
SUM12 = 0.
SUM13 = 0.
SUM22 = 0.
SUM23 = 0.
SUM33 = 0.
DO 1 K = 1, N
PHE11 = WGT(K)*(0.5*(RT(K)**2 - RT(K)))**2
PHE12 = 0.5*(RT(K)**2 - RT(K))*(1.- RT(K)**2)*WGT(K)
PHE13 = 0.25*(RT(K)**2 - RT(K))*(RT(K)**2 + RT(K))*WGT(K)
PHE22 = (1.- RT(K)**2)**2*WGT(K)
PHE23 = (1.-RT(K)**2)*0.5*(RT(K)**2 + RT(K))*WGT(K)
PHE33 = (0.5*(RT(K) + RT(K)**2))**2*WGT(K)
SUM11 = PHE11 + SUM11
SUM12 = PHE12 + SUM12
SUM13 = PHE13 + SUM13
SUM22 = PHE22 + SUM22
SUM23 = PHE23 + SUM23
SUM33 = PHE33 + SUM33
1 CONTINUE
SUMBB(1,1) = SUM11
SUMBB(1,2) = SUM12
SUMBB(1,3) = SUM13
SUMBB(2,1) = SUM12
SUMBB(2,2) = SUM22

```

```

SUMBB(2,3) = SUM23
SUMBB(3,1) = SUM13
SUMBB(3,2) = SUM23
SUMBB(3,3) = SUM33
RETURN
END

```

```

C*****SUBROUTINE TO CALCULATE THE INTEGRAL OF THE PRODUCT OF
C TWO DERIVATIVES OF QUADRATIC BASES FUNCTION

```

```

SUBROUTINE DBDZ (N,SUM)
IMPLICIT REAL*8 (A-H,O-Z)
REAL*8 SUM(3,3,3), RT(3), WGT(3)

CALL GAUSS (RT, WGT)

DO 2 K = 1, 3
DO 3 J = 1, 3
DO 4 I = 1, 3
SUM(I,J,K) = 0.
4 CONTINUE
3 CONTINUE
2 CONTINUE

DO 10 J = 1, N
SUM(1,1,1) = SUM(1,1,1) +
1 (RT(J) - 0.5)**2*0.5*(RT(J)**2 - RT(J))*WGT(J)
SUM(1,2,1) = SUM(1,2,1) +
1 (RT(J) - 0.5)**2*(1.- RT(J)**2)*WGT(J)
SUM(1,3,1) = SUM(1,3,1) +
1 (RT(J) - 0.5)**2*0.5*(RT(J)**2 + RT(J))*WGT(J)
SUM(2,1,1) = SUM(2,1,1)
1 -RT(J)*(RT(J) - 0.5)*(RT(J)**2 - RT(J))*WGT(J)
SUM(2,2,1) = SUM(2,2,1)
1 -2.*RT(J)*(RT(J) - 0.5)*(1.- RT(J)**2)*WGT(J)
SUM(2,3,1) = SUM(2,3,1)
1 -RT(J)*(RT(J) - 0.5)*(RT(J)**2 + RT(J))*WGT(J)
SUM(3,1,1) = SUM(3,1,1) +
1 (RT(J)**2 - 0.25)*0.5*(RT(J)**2 - RT(J))*WGT(J)
SUM(3,2,1) = SUM(3,2,1) +
1 (RT(J)**2 - 0.25)*(1.- RT(J)**2)*WGT(J)
SUM(3,3,1) = SUM(3,3,1) +
1 (RT(J)**2 - 0.25)*0.5*(RT(J)**2 + RT(J))*WGT(J)
SUM(2,1,2) = SUM(2,1,2) +
1 2.*RT(J)**2*(RT(J)**2 - RT(J))*WGT(J)

```

```

SUM(2,2,2) = SUM(2,2,2) +
1      4.*RT(J)**2*(1.- RT(J)**2)*WGT(J)
SUM(2,3,2) = SUM(2,3,2) +
1      2.*RT(J)**2*(RT(J)**2 + RT(J))*WGT(J)
SUM(3,1,2) = SUM(3,1,2)
1      -RT(J)*(RT(J) + 0.5)*(RT(J)**2 - RT(J))*WGT(J)
SUM(3,2,2) = SUM(3,2,2)
1      -2.*RT(J)*(RT(J) + 0.5)*(1.- RT(J)**2)*WGT(J)
SUM(3,3,2) = SUM(3,3,2)
1      -RT(J)*(RT(J) + 0.5)*(RT(J)**2 + RT(J))*WGT(J)
SUM(3,1,3) = SUM(3,1,3) +
1      (RT(J) + 0.5)**2*0.5*(RT(J)**2 - RT(J))*WGT(J)
SUM(3,2,3) = SUM(3,2,3) +
1      (RT(J) + 0.5)**2*(1.- RT(J)**2)*WGT(J)
SUM(3,3,3) = SUM(3,3,3) +
1      (RT(J) + 0.5)**2*0.5*(RT(J)**2 + RT(J))*WGT(J)
10 CONTINUE

```

```

SUM(1,1,2) = SUM(2,1,1)
SUM(1,2,2) = SUM(2,2,1)
SUM(1,3,2) = SUM(2,3,1)
SUM(1,1,3) = SUM(3,1,1)
SUM(1,2,3) = SUM(3,2,1)
SUM(1,3,3) = SUM(3,3,1)
SUM(2,1,3) = SUM(3,1,2)
SUM(2,2,3) = SUM(3,2,2)
SUM(2,3,3) = SUM(3,3,2)
RETURN
END

```

C\*\*\*\*\*SUBROUTINE CALCULATES MATRICES FOR REACTION TERMS\*\*\*\*\*

```

SUBROUTINE RXNMATRX (rxn,NC,nn,ne,index)
INCLUDE 'parametr.inc'
INTEGER IN(MNE,3),NODE(3),NN,NE
REAL*8 RXN(1)
REAL*8 RETARD(MNN,3),VOLWAT(MNN)
REAL*8 X(MNN)
REAL*8 EBP(3,3),RJACOB(MNE)
REAL*8 GBInew(MNN),GB(MNN)
COMMON /smatrix0/GBInew,GB
COMMON /smatrix/EBP,RETARD,X,VOLWAT,RJACOB,IN,NODE
DATA NUM/1/
SAVE NUM

```

```

C..GB(NN)
C the column vector of the zero order reaction term for O2 & CO2

```

```

      IF (index .eq. 0) THEN

```

```

C initialize the matrices
C everytime the subroutine is called

```

```

      DO 83 I = 1, NN
        GB(I) = 0.
83 CONTINUE

```

```

C

```

```

C..ASSEMBLY GLOBAL MATRICES: GB

```

```

      DO 40 L = 1, NE

```

```

        II = IN(L,1)
        JJ = IN(L,2)
        MM = IN(L,3)

```

```

      DO 50 K = 1, 3

```

```

        NR = IN(L,K)

```

```

        GB(NR) = GB(NR) + RJACOB(L) *
1          (RXN(II)/RETARD(II,NC)*EBP(K,1)+
2          RXN(JJ)/RETARD(JJ,NC)*EBP(K,2)+
3          RXN(MM)/RETARD(MM,NC)*EBP(K,3))

```

```

50 CONTINUE

```

```

40 CONTINUE

```

```

      GOTO 555

```

```

      ENDIF

```

```

C

```

```

C..GBI(NN)

```

```

C the column vector of the zero order term with interpolation
C among the elemental nodes

```

```

      IF (index .eq. 2) THEN

```

```

C initialize the matrices
C everytime the subroutine is called

```

```

      DO 84 I = 1, MN
        GBInew(I) = 0.
84  CONTINUE

```

C

C..ASSEMBLY GLOBAL MATRICES: GBI

```

      DO 60 L= 1, NE

      DO 70 I = 1, 3
        NODE(I) = IN(L,I)
70  CONTINUE

      II = NODE(1)
      JJ = NODE(2)
      MM = NODE(3)

      DO 80 K = 1, 3

      NR = NODE(K)

      GBInew(NR) = GBInew(NR) + RJACOB(L) *
1      (RXN(II) /RETARD(II,NC) *VOLWAT(II) *X(II) *EBP(K,1) +
2      RXN(JJ) /RETARD(JJ,NC) *VOLWAT(JJ) *X(JJ) *EBP(K,2) +
3      RXN(MM) /RETARD(MM,NC) *VOLWAT(MM) *X(MM) *EBP(K,3) )
80  CONTINUE
60  CONTINUE

      ENDIF

555  RETURN
      END

```

C\*\*\*\*SUBROUTINE FOR DETERMINING CONCENTRATIONS BETWEEN NODES

C

C r is the interpolated point in the local distance

C FINTER is the function being interpolated at r

C X is the location of r in the global system

C N is the no. of interpolated points

```

      SUBROUTINE  INTPOL (N,r,ELEHYDRO,FINTER)
      INTEGER    N
      REAL*8     FINTER(1),r(1),ELEHYDRO(3)

```

```

      DO 1 J = 1, N

```

C calculate the bases functions in local coordinates

```

bases1 = (r(J)**2-r(J))/2.
bases2 = (1.-r(J)**2)
bases3 = (r(J)**2+r(J))/2.

```

C interpolate function "FINTER" at r

```

FINTER(J) = ELEHYDRO(1)*bases1 + ELEHYDRO(2)*bases2 +
&          ELEHYDRO(3)*bases3

```

1 CONTINUE

```

RETURN
END

```

C\*\* SUBROUTINE TO SOLVE FOR CONCENTRATIONS AT EACH TIME STEP \*\*

```

SUBROUTINE SOLVER (ITYPE,FLUX,CCON,CONC,KC)
INCLUDE      'parametr.inc'
INTEGER     ITYPE(1),IPVT(MNN),LDA,flag
REAL*8     F(MNN),CCON(1),CONC(1),Z(MNN),FLUX(1)
REAL*8     GB(MNN),fload(MNN)
REAL*8     GBInew(MNN),GBIold(MNN)
REAL*8     GBP(MNN,MNN),GD(MNN,MNN,3)
REAL*8     COM(MNN,MNN)
REAL*8     ABD(7,MNN)

COMMON      /smatrix0/GBInew,GB
COMMON      /ssolver/GD,GBP,GBIold,DT,alpha,ML,MU,NN
COMMON      IDO2,IDCO2

```

C..initialize load vector with boundary fluxes

```

DO 1 I = 1, NN
F(I) = FLUX(I)
1 CONTINUE

```

C

C--COMBINE MATRICES: GBP, & GD

```

DO 12 I = 1, NN

```

C set fixed boundary concentrations on the matrix

```
IF (ITYPE(I) .EQ. 1) THEN
```

```
DO 47 J = 1, NN
  IF (I .EQ. J) THEN
    COM(I,J) = 1.
  ELSE
    COM(I,J) = 0.
  ENDIF
```

```
47 CONTINUE
```

```
ELSE
```

C

C..LHS matrix coefficient

```
DO 13 J = 1, NN
  COM(I,J) = GBP(I,J) + alpha*dt*GD(I,J,KC)
```

```
13 CONTINUE
```

```
ENDIF
```

```
12 CONTINUE
```

C

C--CONSTRUCT LOAD VECTOR (KNOWN QUANTITIES ON RHS)

C the reason FLUX is not passed to F because the values of F  
C is being modified in the subroutine, therefore the value of  
C flux boundary will change and this is not desired

C

C..for hydrocarbon equations

```
IF (KC .eq. IDO2 .or. KC .eq. IDCO2) THEN
```

```
DO 38 I = 1, NN
  IF (ITYPE(I) .EQ. 1) THEN
    F(i) = CCON(i)
  ELSE
    DO 35 J = 1, NN
      F(i) = F(i) + (GBP(i,j) -
& (1.-alpha)*dt*GD(i,j,KC))*CONC(j)
```

```
35 CONTINUE
```

```
F(i) = F(i) - dt*GB(i)
```

```

      ENDIF
38      CONTINUE

      ELSE

          DO 39 I = 1, NN
              IF (ITYPE(I) .EQ. 1) THEN
                  F(i) = CCON(i)
              ELSE
                  DO 37 J = 1, NN
                      F(i) = F(i) + (GBP(i,j) -
&                                (1.-alpha)*dt*GD(i,j,KC))*CONC(J)
37      CONTINUE
                      F(i) = F(i) - dt*(GBInew(i)*alpha +
&                                (1.-alpha)*GBIold(i))
                  ENDIF
39      CONTINUE

          ENDIF

      ENDIF

C
C*** PROGRAM TO CONVERT THE BANDED MATRIX TO BANDED STORAGE ***
C
C          IF A IS A BAND MATRIX, FOR EXAMPLE,
C
C          11 12 13  0  0  0
C          21 22 23 24  0  0
C           0 32 33 34 35  0
C           0  0 43 44 45 46
C           0  0  0 54 55 56
C           0  0  0  0 65 66          BANDED MATRIX
C
C          THEN NN=6, ML=1, MU=2, LDA .GE. 5 (LDA = 2*ML+MU+1)
C          AND ABD SHOULD CONTAIN
C
C          * * * + + + , * = NOT USED
C          * * 13 24 35 46 , + = USED FOR PIVOTING
C          * 12 23 34 45 56
C          11 22 33 44 55 66
C          21 32 43 54 65 *
C
C          THE FOLLOWING PROGRAM WILL SET UP THE INPUT (ABD)
C
C          ML = (BAND WIDTH BELOW THE DIAGONAL)
C          MU = (BAND WIDTH ABOVE THE DIAGONAL)

```

```
      M = ML + MU + 1
      DO 20 J = 1, NN
        I1 = MAX0(1, J-MU)
        I2 = MIN0(NN, J+ML)
        DO 10 I = I1, I2
          K = I - J + M
          ABD(K,J) = COM(I,J)
10      CONTINUE
20 CONTINUE

C          THIS USES ROWS ML+1 THROUGH 2*ML+MU+1 OF ABD .
C          IN ADDITION, THE FIRST ML ROWS IN ABD ARE USED
C          FOR ELEMENTS GENERATED DURING THE TRIANGULARIZATION.
C          THE TOTAL NUMBER OF ROWS NEEDED IN ABD IS
C          2*ML+MU+1 .
C          THE ML+MU BY ML+MU UPPER LEFT TRIANGLE AND THE
C          ML BY ML LOWER RIGHT TRIANGLE ARE NOT REFERENCED.

      LDA = 2*ML + MU + 1

C
C--call subroutines DGBCO to factor the banded matrix, and DBGSL
C to solve the equations

      CALL DGBCO (ABD,LDA,NN,ML,MU,IPVT,RCOND,Z)
      CALL DGBSL (ABD,LDA,NN,ML,MU,IPVT,F,JOB)

      DO 33 I = 1, NN
        CONC(I) = F(I)
33 CONTINUE

      RETURN
      END
```

## VITA

The author was born on January, 1959 in Taipei, Taiwan to Mr. and Mrs. Chun Hsuan Sa. She was a fourth grader when her family moved to Bangkok, Thailand in 1968. In this new foreign land where the language and cultures were unfamiliar, she had to re-start her education from kindergarten. With lots of nights tutoring by the school master, she quickly moved up to the level where she belonged. In 1978, she passed the entrance examination and entered Chulalongkorn University. Following her father's footsteps, she received her bachelor degree in chemical engineering in 1982. For the next 15 months, she worked as an assistant engineer in a small textile resin plant, prepared for TOEFL and GRE tests, and applied for graduate schools in the United States. In 1983, she went to Louisiana State University in pursuit of her master degree in chemical engineering. It was her first time away from her family, but studies kept her busy. In 1986, she was granted her degree. Upon graduation, she realized that she had crossed thousands of miles of ocean and had not gained the expertise she desired. She then applied for and was accepted into the Ph.D. program at OGI in 1987. There, she met her husband, Don Buchholz, and they have been married since 1989. The author became a U.S. citizen in 1993, and cast the first vote in her life in that same year. In the following year, the author completed her degree.

The author believes that her life totally fits the saying that "life is full of learning experiences". Yet, for all the learning she has done, she still wonders why there is life. Her near future plan is to put into practice what she has learned. However, some time in the future, she would like to transfer her knowledge and work experience to people in Thailand.

**PUBLICATION:** Sa, L., Focht, G. D., Ranade, P. D., and Harrison, D. P. (1989)  
"High-temperature desulfurization using Zince-ferrite: solid structural changes", *Chem. Eng. Sci.*, 44(2), 215-224.